Effects of Forest Cover Change on Streamflow in Low Relief Glaciated Catchments

A DISSERTATION
SUBMITTED TO THE FACULTY OF THE
UNIVERSITY OF MINNESOTA
BY

Zachary P. McEachran

IN PARTIAL FULFILLMENT OF THE REQUIREMENTS
FOR THE DEGREE OF
DOCTOR OF PHILOSOPHY

Advised by Diana Karwan

AUGUST 2020

© Zachary P. McEachran 2020

Acknowledgements

I acknowledge my committee and particular collaborators for making valuable contributions to each chapter: Chapter 1 (Diana and Rob), Chapter 2 (Diana, Steve, Rob, and Crystal in particular to the methods section), and Chapter 3 (Diana and Rob). Thank you to Harsh Anurag for alerting me to the USGS SSEBop ET data product.

I would like to acknowledge my committee and in particular my advisor Diana, for patiently guiding me to a new way of thinking about the natural world that recognizes the innumerable complexity, yet clear intelligibility, of the objects of everyday experience. I acknowledge the Karwan Lab – Ethan, Lucy, Will, Hudson, Mark, Kevin, and Nicole – for listening to countless practice presentations and for always improving my thinking about whatever I am working on. I acknowledge my wife Meg for supporting me through this Ph.D. and for offering always helpful conversation and insight about my projects, scientific thinking, the broader context of things, and what it all could mean for our family. And finally, I acknowledge in humble gratitude to God for the privilege of a truly liberal education and my many blessings.

All men by nature desire to know.

This thesis is dedicated to Margaret, Theresa Joy, and Tiny #2.

Abstract

Forest cover disturbance, climate change, and their interaction can alter how catchments store and process water, which has ramifications for all aspects of the hydrologic cycle, including flood risk, channel geomorphology, and water quality. Catchments in the boreal-temperate transition zone may be especially vulnerable to these factors. While streams in this glaciated region have low-topographic relief and may originate from expansive wetlands, much of the past research on forest disturbance-streamflow relationships comes from regions where landscape characteristics and subsequent hydrological function is substantially different, e.g. mountainous regions with bedrock close to the soil surface. Further, most work investigating the forest-streamflow relationship occurs at small spatial scales (< 10 km^2). I seek to fill a knowledge gap by 1) creating a new conceptual model for how forest cover change affects sediment yield in managed temperate forested catchments that accounts for how sediment yield responds to altered catchment hydrology, 2) developing a new approach to peak-flow analysis using paired catchment experiments at the Marcell Experimental Forest (MEF) in north-central Minnesota, and 3) investigating how forest cover change and climate affect peak flows and water yield in large (> 10 km^2) catchments in Minnesota. My results indicate that in low-relief glaciated regions, glacial geology controls sediment yield response to forest harvesting; forest harvesting may affect large peak flows by altering the occurrence probabilities of large peaks at the small catchment scale; and streamflow in larger catchments is largely controlled by climate variation, with land cover a minor yet discernable driver of peak flows and water yield. These results are framed within a new forest harvesting/water quality framework that holistically accounts for all sources of increased sediment yield after forest harvesting in diverse landscapes. Please note that multiple of these chapters are under peer review in scientific journals as of August 2020, and those versions will supersede this dissertation for purposes of citations.

TABLE OF CONTENTS

LIST OF TABLES

LIST OF FIGURES

LIST OF ABBREVIATIONS

MEF = Marcell Experimental Forest

GEV = Generalized Extreme Value distribution

ANCOVA = Analysis of Covariance

ET = Evapotranspiration

GW = Groundwater

McMC = Markov chain Monte Carlo

USGS = United States Geological Survey

AMS = Annual maximum (streamflow) series

AMO = Atlantic Multidecadal Oscillation

PDO = Pacific Decadal Oscillation

NAO = North Atlantic Oscillation

ENSO MEI = El Nino Southern Oscillation, Multivariate ENSO index

INTRODUCTION

Forest cover change and forest harvesting effects on watershed processes have been an area of concern and research for decades, particularly high flows and flooding (Alila et al., 2009; Andréassian, 2004; Hornbeck, 1973; Verry, 1986; Zon, 1927), and water yield (Bosch and Hewlett, 1982; Zhang et al., 2017). Alterations in peak flows can have serious ramifications for channel geomorphology as well as stream ecology and sediment dynamics (Auerswald and Geist, 2018; Poff, 2002; Poff et al., 2006, 1997; Van Steeter and Pitlick, 1998), and floods can be devastating for local communities (Bradshaw et al., 2007). Forests are generally thought to offer some level of flood protection (Andréassian, 2004), although the extent of that protection is unclear and even contentious (Alila et al., 2009; Calder et al., 2007; Laurance, 2007; Lewis et al., 2010; Mogollón et al., 2016; Rogger et al., 2017; van Dijk et al., 2009). Increases in water yield after forest harvesting are well-established at the small basin scale (Bosch and Hewlett, 1982; Brown et al., 2005; Stednick, 1996), but emergence of new processes of streamflow generation at larger scales (Tiwari et al., 2017) and cumulative interactions of forest disturbance throughout the landscape (MacDonald, 2005) make the effect of forest disturbance on streamflow at larger scales unclear.

A changing climate and a growing demand for wood products may threaten forest ecosystems and extent (Angel et al., 2018; Buongiorno et al., 2012; Buras and Menzel, 2018). Thus, it is necessary to understand how changes in forest cover affect peak flow generation in varied landscapes. However, much of the literature examining how forest harvesting and forest cover change affect hydrological function in the USA is sourced from high-relief regions with bedrock close to the soil surface (Alila et al., 2009; Jones and Grant, 1996; Kuraś et al., 2012; Stednick, 1996; Thomas and Megahan, 1998). It is unclear how findings in these landscapes apply to those found in low-relief glaciated regions common along the temperate to boreal transition zone such as those found in central North America, Russia, and Scandinavia. Further, catchments at these northern latitudes are expected to be especially sensitive to climate change due to their highly climate-dependent and seasonal hydrologic cycle (Tetzlaff et al., 2015, 2013).

Managed forests generally produce high-quality surface water, but water quality can decrease if proper management practices are not implemented during harvesting. Sediment concerns, such as increased sediment delivery and yield, provide the primary water quality effects associated with forest harvest. To address these, it is necessary to recognize and understand all contributing processes. However, forest harvesting Best Management Practices (BMPs) focus almost exclusively on overland sediment sources, while in-and-near stream sources including legacy sediments in the stream channel go unaddressed even while being major contributors to sediment yield in some areas. To support the development of a more comprehensive management paradigm, I propose a new framework to classify forest harvesting effects on surface water sediment yield into direct and indirect effects based on their contributing processes. Direct effects are those caused by erosion and sediment delivery to surface water from overland sources: i.e., sediment and surface hydrologic connectivity are contemporaneous in space and time. Indirect effects are those caused by a process alteration in the water cycle due to tree removal that accounts for increases in subsurface as well as surface flows to the stream such that alterations in water quality are not predicated upon overland sediment delivery to the stream. For indirect effects, streamflow increases can mobilize sediments in and immediately connected to the channel network. Although the direct/indirect distinction is often implicit in forest hydrology studies, the primary drivers of sediment yield due to forest harvesting are unclear in varied geologic, management, vegetative, and legacy circumstances.

A critical driver of in-stream erosion and channel adjustment is peak flows. The general paradigm for the effect of forest harvesting on peak flows is decreasing effect size with increasing peak flow return interval, and thus a greater proportional impact for frequent, low-discharge peak flows (Andréassian, 2004; Bathurst et al., 2011; Thomas and Megahan, 1998). This paradigm has been supported with numerous paired-catchment studies at a spatial scale of < 10 km^2 (Andréassian, 2004). However, some studies, especially from snowmelt-dominated watersheds, have found sizeable effects for large peak flows, and even an increasing effect size with increasing return interval (Green and Alila, 2012; Kuraś et al., 2012). Due to unique changes in hydrology in snowmelt-dominated catchments after harvesting (increased catchment saturation and snow accumulation, faster melt compared to forested conditions, etc. (Murray and Buttle, 2003; Pomeroy et al., 1994)), there is a new peak flow generating system that may increase peak flows even for infrequent, large peak flows.

Small (< 10 km^2) paired-catchment studies have provided the foundation for much of the current knowledge in forest hydrology, including about peak flows and flooding (Andréassian, 2004). However, methods traditionally used to quantify changes in peak flows from paired-catchment experiments rarely account for changes in peak flow probability of occurence in addition to the magnitude (Alila et al., 2009). Further, many methods assume statistical stationarity in which distributions of peak flows and the parameters that describe them remain constant through time, but this assumption may be dubious due to land use and climate changes (Milly et al., 2008). Thus, the integration of nonstationary and probabilistic analysis methods offers an increasingly detailed framework compared to previously used methods, and allows inferences about how peak flow magnitudes *and* probabilities of occurrence change in response to forest cover and climatic changes through time at the small catchment scale.

Even with increasingly robust inferences about changes in peak flows at the small catchment scale through time as a result of the application of nonstationary and probabilistic analysis frameworks, it is unclear how changes in streamflow generation due to forest cover change scale spatially due to a lack of forest hydrology literature that incorporates spatial scaling effects. I broaden the scope of previous work in small catchments through conducting analyses directed towards understanding hydrological processes at larger spatial scales and emergent scaling dynamics. Further, water resource management is often informed by process-based knowledge gained at the small catchment scale; understanding how these dynamics operate across multiple scales, including larger scales such as those commonly used in management schemes (e.g., HUC-08), is critical for optimized water resource management in the face of a changing climate and land use conditions (Slesak et al., 2018).

Objectives and Hypotheses

The overarching goal of my dissertation was to quantify the mechanisms by which forest cover change affects how catchments process water and sediments to generate streamflow, with a focus in low-relief glaciated landscapes. This investigation was structured by three objectives, and two hypotheses. Each objective corresponds to a chapter of this dissertation, numbered respectively. At the time of dissertation publication, Chapter1 and Chapter 2 have been submitted for consideration to scholarly journals.

Objective 1: Develop a new conceptual model for the mechanisms by which forest cover change increases stream sediment yield.

Objective 2: Quantify the effect of forest cover change on peak flow magnitudes and probabilities of occurrence at the small watershed scale for low-relief glaciated catchments.

Hypothesis 1. Clearcutting the entire upland of a small upland-peatland watershed will increase annual peak flows across all return intervals compared to preharvest mature forest conditions. Forest regrowth of the upland will decrease annual peak flows across all return intervals compared to the initial increase.

Objective 3: Quantify the effect of forest cover disturbance on the way that low-relief glaciated catchments process water and generate streamflow, aggregated as water yield and peak flows, at spatial scales larger than the traditional small catchment study.

Hypothesis 2. A spatial threshold exists in low-relief glaciated catchments below which forest disturbance effects are detectable on surface water hydrology (e.g. annual water yield and peak flow). Above this spatial threshold, land cover effects are negligible among signals of regional groundwater, climate, and water storage.

Approach

In Chapter 1, I developed a novel conceptual model for how forest harvesting affects sediment yield in United States temperate catchments, including the low-relief catchments of the western Lake States. Chapter 1 reviewed the general mechanisms by which forest harvesting affects the water budget, and how these changes may induce water quality degradation through in-stream erosion, in addition to upland landscape erosion. In Chapter 2, I proposed and implemented a new method for analyzing peak flows in small, paired catchments at the Marcell Experimental Forest (Minnesota, USA) utilizing a nonstationary probabilistic extreme-value analysis technique. Finally, in Chapter 3, I used a case study approach to investigate how long-term climate trends interact with forest disturbance to drive water yield and peak flow in a boreal Canadian Shield catchment at a large spatial scale (650 km^2). This included a discussion of how hydrological function varies across scales, and at which scales forest management is relevant for influencing streamflow in low-relief glaciated landscapes.

CHAPTER 1:

Direct and indirect effects of forest harvesting on sediment yield in United States forested temperate watersheds

1.1: INTRODUCTION

Managed forests generally produce high-quality surface water (Neary et al., 2009), providing nearly two-thirds of the drinking water supply in the United States (National Research Council (NRC), 2008). Because of this, forest harvesting effects on water quality have been an area of concern for decades (Binkley and Brown, 1993; Cristan et al., 2016; Megahan, 1972), with sedimentation often identified as the greatest water quality threat (Binkley and Brown, 1993). There has been a tremendous amount of work developing and evaluating water quality Best Management Practices (BMPs) to address this concern, and it is generally concluded that BMPs are very effective at reducing overland sediment delivery when properly implemented (Binkley and Brown 1993, Aust and Blinn 2004, Cristan et al. 2016). However, overland sources of sediment delivery forms only a portion of the watershed's sediment yield over a given time interval. Sediment yield, the mass of sediment flowing out of a watershed outlet per year, incorporates sediment delivery from the entire watershed above the outlet as well as fluvial transport processes and (re)mobilization of sediments within and connected to the channel network. In-and-near-stream sources of sediment yield (e.g., bank erosion, remobilization of stored or "legacy" sediments) are often not considered in forestry water quality assessments, but have been identified as important contributors to sediment yield that can change in response to forest harvest and disturbance (Beasley and Granillo, 1988; Ensign and Mallin, 2001; Fraser et al., 2012; Gomi et al., 2005; Hassan et al., 2006; Hewlett and Doss, 1984; Karwan et al., 2007; Klein et al., 2012; McBroom et al., 2008; Moore and Wondzell, 2005; Terrell et al., 2011). For example, Fraser et al. (2012)

attributed the majority of sediment yield after forest harvesting to in-stream sources eroding due to altered hydrology in the Georgia (USA) Piedmont.

Here, I propose a new framework to holistically classify forest harvesting effects on surface water variables according to their direct and indirect process and contribution to watershed sediment yield. I demonstrate its utility in the context of sediment yield with a review of the existing literature for several regions containing managed temperate forests in the contiguous United States (and adjacent ecoregions in Canada) grouped by physiographic and management conditions (Figure 1.1) to explore direct and indirect effects drivers in different landscape settings and themes in the regional literature. I also identify future research directions on the effects of forest harvesting on surface water sediment yield. I then discuss spatial and temporal scaling considerations and how these are modulated by management intensity and extent, harvesting interactions with non-harvest disturbances, and discuss management implications for sediment yield via direct or indirect processes.

1.1.1: Direct/Indirect Framework

Forest harvesting can have both direct and indirect effects on water quality variables, including sediment and nutrient yields. I define direct effects as those caused by overland hydrologic delivery of sediments or nutrients to surface water (i.e., connected by overland flow), including those sourced from site infrastructure such as the forest road network, and general harvesting area. Such sediments are rapidly delivered and exported from the channel due to high hydrologic connectivity that carries recent surface erosion with it – i.e., sediment and hydrologic connectivity occur along the same pathways and on the same timescale (Figure 1.2). Indirect effects result from a post-harvest shift in hydrologic processes, due to a reduction in watershed evapotranspiration, that delivers more water to the stream via subsurface and surface pathways. This increase in streamflow leads to an increase in sediment yield from river corridor sources that are not predicated upon overland sediment delivery to the stream. Indirect effects encompass increases in subsurface and surface hydrologic connectivity that don't precisely overlap in space and time with sediment connectivity (Figure 1.2). In these cases, the hydrologic connectivity extends well into the upslope contributing areas, but the sediment connectivity to the channel remains in and very near the fluvial network. Indirect effects are invariant to the path by which water arrives at the stream. Thus, the hydrologic connectivity causing increased flows via surface and subsurface pathways throughout a watershed is not spatially and temporally aligned with the sediment connectivity. Direct effects, in contrast, occur such that sediment and water are delivered along the same paths (i.e., overland flow), so can be traced via the contemporaneity of sediment influxes to the stream with overland flow influxes to the stream in time and space.

Both direct and indirect mechanisms could cause a change in sediment yield following forest harvest, however, most BMPs only address the former (Fraser et al., 2012) with some exceptions (e.g., green up rules). The distinction between "direct" versus "indirect" effects may be applied to many different water quality variables, but I focus exclusively on sediment because it is the water quality variable of highest concern related to forest harvesting (Binkley and Brown, 1993). The distinction between direct and indirect effects has been alluded to previously (Anderson and Lockaby, 2011; Hassan et al., 2006; Varanka et al., 2015), and even termed as such (Hassan et al., 2006), but these effects have not been formally defined, nor have the drivers of these effects and their relative importance been identified. Sediment yield increases after forest harvesting derived from paired-catchment studies integrate direct and indirect effects. Some paired watershed studies have indicated that contemporary harvest practices can have little effect on stream sediment yield (Hatten et al., 2018); others, however, have shown sediment yield increases (Fraser et al., 2012). It is critical to define the direct and indirect processes by which sediment yield increases may occur to gain physical insight into sediment yield and water quality management. Drivers of direct and indirect effects include management intensity and extent, basin geology and physiography, disturbance history and disturbance interactions with management, legacy effects, cover type, geomorphic variables and stream stability, and hydrologic regime. The most important variables and relative importance of direct versus indirect effects depend on the unique local combination of these factors.

1.2: DIRECT AND INDIRECT EFFECTS

1.2.1: Direct Effects

Direct effects of forest harvesting on sediment yield are dependent on the hillslope-scale processes of erosion and sediment delivery via overland pathways (Croke and Hairsine, 2006). For direct effects, recent surface erosion is transported quickly through overland flow by infiltration-excess and/or saturation-excess flow pathways. Erosion on forest harvest sites in temperate regions is generally hydrologically controlled through sheet, rill, and gully processes (i.e., "water erosion"), or through landslide events induced by altered hillslope hydrology (Rice and Lewis, 1991); detached sediment is then transported to streams through pathways of hydrologic connectivity (Bracken et al., 2015; Croke and Hairsine, 2006). Factors influencing sheet and rill water erosion and delivery are widely studied, and include slope grade, length, and roughness, vegetative ground coverage and root structure, soil texture, compaction, and erodibility, and rainfall amount and intensity (Luce and Black, 1999; Wischmeier and Smith, 1978). Hydrologically-induced landslide events, a primary detachment process in steep terrain, occur naturally but are exacerbated by forest harvesting – by the interruption and concentration of road runoff, over-steepening of slopes by side-cast roads, valley fill failures, high subsurface water levels often caused by increased soil saturation of bare hillslopes, non-cohesive slope materials, and loss of soil strength due to decay of roots (Beschta, 1978; Collins, 2008; Durgin et al., 1988; Gomi et al., 2005; Johnson et al., 2007; Madej, 2001; Montgomery, 1994; Neary et al., 2009; O'Loughlin, 1985; Rice and Lewis, 1991; Roberts and Church, 1986; Wemple et al., 2001, 1996). Which erosion factors are dominant depends on local biophysical and management factors (e.g., climate, topography, soils, tectonics, silvicultural treatment, etc.).

High intensity management is associated with increased risk for both erosion and delivery aspects of direct effects due to increased soil disturbance and altered vegetation growth due to competition release, for example, compared to low-intensity managed sites (Grigal, 2000; Hayes et al., 2005; McBroom et al., 2008). Intensive silvicultural practices and management include slash removal and utilization, site preparation, and vegetation control, in contrast to low-intensity practices, as discussed by Grigal (2000). BMPs are designed to address direct effects of intensive management, and are highly effective when utilized, and properly installed and employed (Aust and Blinn, 2004; Cristan et al., 2016). Thus, although actual direct effects on intensively managed sites are low where BMPs are (properly) implemented, the risk of direct effect occurrence via erosion and sediment delivery is higher on these sites if BMPs are not (properly) implemented.

The road and skid trail network on any harvest site disproportionately influences both erosion and sediment delivery, especially where this network is near or intersects stream channels (Croke and Hairsine, 2006; Lang et al., 2015). Forest roads influence sediment detachment via landslide processes, as discussed above, but also can serve as a significant source of sediment themselves (Luce and Black, 1999; Megahan et al., 2001; Megahan and Kidd, 1972). The degree to which roads are sediment sources varies greatly by soil texture and road material (Luce and Black, 1999). In steep terrain, forest roads intercept subsurface flow in hillslopes and redirect this flow to ditches, delivering water to streams more quickly; the hydrologic effects of forest roads are dependent on hillslope length, soil depth, and cutbank depth (Wemple and Jones, 2003). Sediment production from roads also depends on how frequently the road is used (Reid and Dunne, 1984). Gully initiation can occur where overland flow from forest roads is discharged onto hillslopes, particularly where slopes are steep and road contributing area is high (Croke and Mockler, 2001; Madej, 2001). Connection of forest road drainage directly to streams via gullies is a high risk scenario for direct effects, as a sediment source (forest road) becomes connected via overland flow directly to the stream (Croke and Hairsine, 2006). Many of the BMPs developed for reducing sediment yield effects of forest harvesting thus focus on reducing risks from forest roads, such as constructing water bars to slow overland flow, drainage control, and road removal (Madej, 2001; Reid et al., 2010). In summary, direct effects occur in temperate watersheds via sediment sources eroding by water, delivered to the stream channel via pathways of overland hydrologic connectivity, and subsequently exit the watershed as suspended sediment. In undisturbed temperate forests, the primary mechanism for overland flow is saturation excess flow, but infiltration excess flow is common on forest roads and can become common after forest harvesting due to soil compaction and exposure in the general harvesting area (Buttle, 2011; Chanasyk et al., 2003).

1.2.2: Indirect Effects

Indirect effects of forest harvesting on sediment yield are those caused by increased in-and-near-stream erosion due to increased flows. Such changes are predicted based on channel evolution models in alluvial rivers (e.g., Simon and Hupp 1987), but are an effect of channel processes propagating from an increase in streamflow rather than an increase in surface erosion delivered to the stream network. Hydrologic alterations themselves are directly related to decreases in evapotranspiration (ET) after forest harvesting and changes in catchment flowpaths associated with disturbance (Buttle, 2011). Although these hydrologic changes directly result from forest harvesting, the subsequent sediment yield response of streams is associated with increased flow, thus being a mediated process and an indirect result of harvest. In connectivity parlance, the hydrologic and sediment connectivity are not coincident in both space and time (Figure 1.2). Hydrological effects of forest harvesting on streamflow vary widely due to regional and watershed conditions, but post-harvest increases in streamflow are well-established (Bosch and Hewlett, 1982; Brown et al., 2005; Sahin and Hall, 1996; Stednick, 1996; Zhang et al., 2017). Forest harvesting can affect the entire spectrum of flow regimes from baseflow (Price, 2011) to peak flows (Guillemette et al., 2005). Although indirect effects have been alluded to and discussed in many studies, they are often not quantified and compared to direct effects (Table 1.1). For example, Table 1.1 references key studies relating hydrologic change to sediment yield change for the regions reviewed, including primary paired-watershed studies and reviews focused on paired-watershed results that could causally attribute the effects of forest harvesting on stream sediment.

Indirect effects depend on catchment-and-reach-scale variables such as watershed size, climate characteristics (e.g., hydrologic regime, energy regime: Zhang et al., 2017), watershed geologic and physiographic characteristics, cover type, and stream geomorphic characteristics (e.g., stability, bank material, floodplain storage, etc.). Further, forest management may influence indirect effects via changing catchment flowpaths through road construction and altering vegetation composition post-harvest (e.g., through control of competing vegetation or other actions that reduce total leaf area). For this review of indirect effects processes, I will focus on the small spatial (< 10 km^2) watershed scale because the majority of the forest hydrology literature occurs at this scale (Andréassian, 2004).

Changes in high and peak flows are particularly important for channel form and instream erosional dynamics, changing channel dimensions and mobilizing bank and floodplain sediments (Phillips and Jerolmack, 2016; Wolman and Miller, 1960). It is generally agreed upon that forest harvesting affects *at least* small, frequently occurring, peak flows important for channel formation and erosional dynamics in many streams (Andréassian, 2004; Beschta et al., 2000; Buttle, 2011; Guillemette et al., 2005). Infrequent high-discharge events can be important for channel form and structure in certain regions (e.g., where large materials form parts of important channel units: Grant et al., 1990), highlighting the importance of understanding how forest harvesting affects flows across a range of high flow regimes. In addition to peak discharge increases, streams can spend a longer time of the year at elevated discharge, thereby mobilizing more sediment within the channel compared to the pre-harvest condition. Further, increases in baseflow can be important for indirect effects: e.g., for headwater catchments where active channel length can be highly variable (Godsey and Kirchner, 2014), channels may expand and activate new sources of instream erosion, and for longer periods of time during the year (Gomi et al., 2005).

Sediment yield generated within the fluvial network is based on complex feedbacks including discharge, channel geomorphic characteristics and history, sediment storage reservoirs, and sediment grain sizes and their distribution (Pizzuto et al., 2014). Channel characteristics and stability antecedent to disturbance can influence the sensitivity of streams to indirect effects, with unstable streams more sensitive to changes (Harvey, 2007; Heede, 1991; Mukundan et al., 2011). Further, alterations to the flow regime can force streams across geomorphic thresholds and induce instability, dependent on pre-disturbance stream condition (Church, 2002). Consideration of both the preharvest conditions of the stream as well as its disturbance history is important where streams are unstable or include large sources of erodible sediment. Some examples include where legacy sediments have dramatically altered stream morphology and comprise large sediment storage reservoirs (Jackson et al., 2005; James, 2013), streams are incising due to crustal rebound after glaciation (Riedel et al., 2005), or where streams are adjusting to a sudden base level change (Gran et al., 2011). Legacy sediment deposited as a result of anthropogenic land use (such as clearcutting or grazing), and channel alterations due to historic anthropogenic activities (e.g., log drives, beaver trapping, and placer mining) will also influence the potential for indirect effects to occur (Noe et al., 2020; Wohl and Merritts, 2007). For example, where legacy sediments are pervasive in the mid-Atlantic Chesapeake Bay watershed, implementation of traditional agricultural and upland BMPs is expected to decrease sediment yields eventually, but reworking of legacy sediments within the channel may confound and mask the effect of these BMPs for years to come (Noe et al., 2020).

Undisturbed streams have historically been modeled in a state of quasi-equilibrium, wherein sediment transport rate equals sediment supply rate. When a disturbance in this equilibrium condition occurs, either in transport capacity (i.e., increased streamflow), or increased sediment supply, then streams adjust their grade and/or width depending on bank and bed grain size and cohesion, and catchment characteristics such as presence of bedrock controls (Simon, 1992). Thus, indirect effects of forest harvesting on sediment yield of streams follows directly from these energy and adjustment considerations from fluvial geomorphology (Langbein and Leopold, 1964;

Phillips and Jerolmack, 2019; Simon and Rinaldi, 2006). Perturbations to this equilibrium will tend to re-approach equilibrium through processes of degradation, channel widening, and aggradation, with channel incision an archetypal behavior of a stream in disequilibrium (Phillips, 1992a; Simon and Hupp, 1987; Simon and Rinaldi, 2006). However, there has been widespread debate about the validity and exact definition of equilibrium concepts, and the need for conceptual frameworks that can support disequilibrium, nonlinear processes, and multiple equilibria (Bracken and Wainwright, 2006; Phillips, 1992b; Trimble, 1977). Further, there continues to be debate about the primary drivers of channel form even in well-studied gravel bed systems (Pfeiffer et al., 2017; Pfeiffer and Finnegan, 2018; Phillips and Jerolmack, 2016). Streams are hypothesized to be in a state of disequilibrium in large areas of the US, such as areas of the Southeast Piedmont that store large amounts of legacy sediment in floodplains (Trimble, 1977). Further, it is unclear how equilibrium concepts, developed for application to alluvial rivers with relatively coarse-grained sediment, apply in regions with ubiquitous wetland rivers and/or regions recently glaciated, which have patterns of channel evolution considerably different than alluvial or bedrock rivers (Jurmu and Andrle, 1997; Watters and Stanley, 2007). Thus, when considering indirect effects, local geomorphic variables and fluvial characteristics need to be considered, such as possible non-equilibrium conditions, to understand the full geomorphic ramifications of altered discharge regimes after forest harvesting.

Cover type also determines hydrologic response to harvesting and potential for indirect effects, as cover type exerts a strong influence on the ET of the regenerating forest. For example, harvesting conifers often increases streamflow more than harvesting deciduous trees because of the higher water use of conifer species (Brown et al., 2005; Mao and Cherkauer, 2009; Sebestyen et al., 2011c). A conversion from deciduous to coniferous species at the Coweeta Hydrologic Laboratory in North Carolina, USA (Southern Blue Ridge section) caused water yield decreases compared to pre-harvest deciduous species within 10 years after conifer planting, with marked differences during the dormant season (Swank and Douglass, 1974; Swank and Miner, 1968). Evergreen conifer species have higher leaf area and maintain an evaporative flux throughout the year through transpiration longer into the deciduous dormant season and by maintaining their leaf area as an interception surface even while dormant (Hornbeck et al., 1993; Pomeroy and Granger, 1997; Sebestyen et al., 2011c; Sun et al., 2008). Bosch and Hewlett (1982) found water yield increases were highest from pine and eucalypt species, followed by deciduous, and finally brush/scrub cover, but also note that yield increases depend on annual precipitation of the study basin: more wet catchments have greater yield increases after forest harvesting, but drier catchments have more persistent increases due to slower regeneration and recovery. Annual water yield is only one metric of how forest cover and species assemblage affects streamflow; species assemblage can affect the whole range of flows, including geomorphically significant flows. For example, conversion from deciduous hardwood to evergreen conifer species reduces incidence of extreme wet years because of increased soil storage, potentially reducing peak flows in these years, but may exacerbate dry years and drought (Ford et al., 2011).

The hydrologic effects of species selection and assemblages depend not only on conifer versus deciduous, but rather on the particular species being compared and under consideration for unique regional conditions. For example, deciduous sweetgum plantations in the Southeast USA have nearly 70% less water yield than evergreen loblolly pine: although ET was higher for loblolly pine in the dormant season, growing season ET was ~90% higher for sweetgum (Caldwell et al., 2018). Further, understory vegetation can significantly impact catchment wetness and water yield, including offsetting ET losses from forest canopies lost through disease or drought through increased growth of understory shrub species (Ford et al., 2012; Guardiola-Claramonte et al., 2011). Further, partial catchment harvesting can cause remaining trees to increase transpiration rates and partially offset increases in streamflow after forest harvesting (Boggs et al., 2015). Finally, long-term effects of climate change can alter species assemblages even in reference conditions, in turn causing changes in water yield (Caldwell et al., 2016). In this case, altered sediment yield regimes may prevail in the absence of any watershed harvesting because of gradual changes in forest composition and their respective resulting hydrologic regimes.

Forest management and silvicultural system used can influence indirect effects by introducing changes in vegetation composition, either via cover type conversion or through use of practices that further reduce post-harvest leaf area and ET such as competing vegetation control. Thus, similar to intensively managed sites posing greater risk of direct effects, certain intensive management practices such as competing vegetation control also may increase the risk of indirect effects by altering the recovery time of ET to pre-harvest levels. In addition to the type and intensity of silvicultural practices, the spatial extent of harvesting is critically important via its influence on overall change in ET at the catchment scale. Effects of management intensity and extent will be addressed in the context of spatial and temporal scaling effects in the "scaling" section for both direct and indirect effects. I also discuss how forest management can influence disturbance regimes a site may eventually experience in the long run in the "Non-Harvest Disturbances" section.

Direct and indirect effects are not always clear and distinct – there are some cases for which it is unclear whether elevated sediment yield should be attributed to direct or indirect effects, or both. Some uncertainty will persist in partitioning direct and indirect effects, along with background sediment yield expected in the absence of harvesting. However, it is important to recognize direct and indirect effects as distinct contributors to sediment yield that act by different processes, distinguishable through indirect effects' mediation through alterations to the hydrologic cycle, and the distinction of how sediment and hydrologic connectivity overlap in space and time.

1.3: REGIONAL REVIEW

To facilitate management of direct and indirect effects specific to local and regional conditions and explore their drivers, I have structured my review by region to highlight how differences in physical hydrology and geomorphic variables, different cover types, and management affect direct and indirect effects. The regions highlighted are those in the United States where temperate working forests are common, and include the Pacific Mountain System, Intermountain West, Southeast, Northeast, and Western Lake States (Figure 1.1; Fenneman and Johnson, 1946). Regions are broad and contain much internal variation. Rather than serve as a comprehensive review, the regional review highlights pertinent literature and explores how sensitive different biophysical systems may be to direct or indirect affects based on their characteristics, and are not necessarily applicable within each subset of the regions reviewed. I stress how broad differences between regions can affect direct and indirect effects drivers, such as presence of mountains, glacially deposited material, precipitation trends, and anthropogenic landscape history to further elucidate and explore direct and indirect effects.

1.3.1: Pacific Mountain System

The Pacific Mountain System, defined by the northern portion of the eponymous physiographic division (Fenneman and Johnson, 1946), includes areas west of the Cascade range in the U.S. states of Washington and Oregon, areas of northern coastal California, and extends north to western British Columbia in Canada. This region has a complex geologic history influenced by tectonic, volcanic, and glacial activity, but glacial effects were generally localized to that of mountain glaciers not physically connected to the Laurentide Ice Sheet in the United States (Orr and Orr, 2002). Landscape variables such as slope, soils, and geomorphology are strongly dependent on recency of tectonic activity and bedrock geology (Swanson et al., 1987). Precipitation amount is high compared to other regions in the U.S. The rainfall erosivity variable associated with the USLE, average annual rainfall erosivity factor R, goes from 1% of the coterminous USA maximum value east of the Cascades, to nearly 50% of the maximum value for the USA in the Cascades and Olympic Peninsula (Renard, 1997; Wieczorek and LaMotte, 2010). Generally, this region experiences wet winters and dry summers. Hydrologic regime varies widely in space depending on altitude (Dettinger and Cayan, 1995). Many lower-altitude catchments are rainfall-dominated, higher-altitude catchments snowmelt-dominated, and a mixed regime at mid-altitudes. However, the altitude at which these changes occur may increase due to climate warming (Klos et al., 2014). Intensive silvicultural practices (e.g., vegetation control, fertilization) are commonly used in the Pacific Mountain System, with coniferous Douglas-Fir being the primary commercial species (Moores et al., 2007). Areas of the Pacific Mountain System have relatively large harvest extent compared to other regions reviewed, including areas where 2-3% of the regional land area is clearcut each year compared to an annual coterminous U.S. average of 0.9% (Masek et al., 2008). However, recent work on the Alsea watershed study has indicated that when contemporary BMPs are used, suspended sediment can be unaffected by forest harvesting, indicating low potential for direct and indirect effects (Hatten et al. 2018: Oregon Coast Range).

Direct Effects. In the Pacific Mountain System region, many of the direct effects after forest harvesting are the result of hydrologically-induced landslides and mass failures on a small minority of forest harvest sites (Grant and Wolff, 1991; Rice and Lewis, 1991). Attributes in the Pacific Mountain System that influence direct effects are high slope grades and hillslope position (Litschert and MacDonald, 2009; Luce and Black, 1999; Madej, 2001), mountain and coastal driven precipitation patterns (Bywater-Reyes et al., 2017; Madej, 2001; Rashin et al., 2006), catchment geology and sediment supply (Bywater-Reyes et al., 2017), and intensive management (Hayes et al., 2005).

Bedrock type is highly correlated with slope and soil characteristics, influencing areas in which landslide risk factors are present such as cohesiveness of slope materials. Further, precipitation patterns in mountainous catchments are highly heterogeneous, especially during the wet winters in the Pacific Northwest (Beschta, 1999), influencing patterns of rainfall erosivity. Although landslide risk is comparatively high in this region, sheet and rill erosion are uncommon due to low precipitation intensity and high infiltration rate of hillslopes (Swanson et al., 1987). The connectivity of landslide-eroded sediment to streams, however, is determined by basin morphology; sediment eroded via landslide processes is more likely to be delivered in steep-sloped basins with narrow stream valleys in contrast to basins with broad valley floors formed via glaciation and less strong hillslope-stream connectivity (Swanson et al., 1987). Further, although silvicultural management is generally intensive in the region, skyline logging is common in steep terrain, which in general can limit soil disturbance and risks for direct effects (Worrell et al., 2011). When roads are used, their interruption of hillslope drainage creates increased risk for landslide events, in addition to gullying where road runoff drains onto hillslopes through concentrated pathways (e.g., culverts) (Madej, 2001; Wemple et al., 2001).

Indirect Effects. The Pacific Mountain System includes two of the only identified key studies that have directly quantified indirect effects (Table 1.1), where one study found that both direct and indirect effects contribute to sediment yield, but direct effects were substantially more important (Safeeq et al. 2020: Middle Cascade Mountains). However, studies in the California Coast Ranges have attributed increases in storm sediment loads to increased streamflow volume and drainage network expansion (Lewis et al., 2001; Reid et al., 2010). Yet another study, in the Oregon Coast Range, indicated little effect of harvesting on suspended sediment concentration or yields (Hatten et al. 2018). These varied responses between physiographic sections within the Pacific Mountain System illustrate the high diversity of hydrologic and sediment response within a region, and the difficulty with generalizing without accounting for local landscape factors.

The risk for indirect effects in the Pacific Mountain System varies with basin geology and hydrologic regime. Basin geology exerts a primary control on sediment dynamics, and possibly the potential for indirect effects, for Pacific Mountain System streams by determining sediment supply in forested headwater catchments (Bywater-Reyes et al., 2017; Gomi et al., 2005). In this region, suspended sediment depends on sediment source, with friable bedrock and/or presence of unconsolidated glacial material providing a greater source of sediment than erosion-resistant bedrock; this has been supported both in the Cascades and the Oregon Coast Range (Bywater-Reyes et al., 2017; Gomi et al., 2005; Reiter et al., 2009). It is not overall catchment sediment supply *per se* that controls indirect effects, but rather how sediment is connected to and suspended within streams throughout time and space. In steep headwaters, streams will have high unit stream power and high transport/flushing capacity, versus gradual streams with depositional floodplains further downstream (Hassan et al., 2006). Increased discharge increases shear stress, but indirect effects require the increased discharge to overcome the mobilization threshold which varies based on sediment grain size, channel material and bed substrate, etc. Bedrock geology and presence of glaciation, altitude, and stream order may serve as an initial indication of hillslope-floodplain-channel connectivity of streams, stream power, and sediment characteristics such as grain size (i.e., steep bedrock headwaters versus alluvial downstream valleys). The pathways of hydrologic connectivity after forest harvesting, dependent on catchment geology, topography, etc., and how they align with sources of sediment in time and space, will indicate whether direct or indirect effects will be dominant.

Debris jams can be important drivers of stream sediment in all regions, but are especially important for indirect effects in small, steep forested Pacific Mountain System catchments where hillslopes and streams are highly connected, and steep high-energy streams have the energy to export even large debris from channels. This is in contrast to small low-gradient streams such as lowland tributaries, and even those at high elevations such as mountain meadows, where there is less transport energy for woody debris (Hassan et al. 2006). Sediment supply and abundance of woody debris are the primary drivers of sediment travel distance for small, steep Pacific Mountain System streams, and woody debris tends to control the amount of sediment stored in the channel and impact stream stability (Hassan et al., 2006). Changes in large woody debris recruitment to streams after harvest for these catchments (i.e., decreases with harvest of large trees), may cause large changes to stream and reach morphology over time as well as change the pulse dynamics of sediment impoundment and release associated with downstream movement of debris jams and debris flows (Hassan et al., 2006; Jakob et al., 2005; Moore and Wondzell, 2005).

Recent work in the Pacific Northwest (Middle Cascade Mountains), intermountain West (Lower Rocky Mountains), and British Columbia (Okanagan Highlands and Columbia Mountains: Church and Ryder 2010) indicate that forest harvesting may have a large effect on high flow and channel-forming events, particularly in snowmelt-dominated catchments (Alila et al., 2009; Green and Alila, 2012; Kuraś et al., 2012; Schnorbus and Alila, 2013; Yu and Alila, 2019). After harvesting in snowmelt-dominated catchments, large changes in snowmelt peaks are possible due to increased soil moisture caused by decreases in evapotranspiration, increased snow accumulation due to the absence of long-wave radiation and sublimation from tree canopies, and more uniform snowmelt due to lack of heterogeneities in shading (Green and Alila, 2012; Kuraś et al., 2012; Murray and Buttle, 2003; Pomeroy et al., 1994; Schnorbus and Alila, 2013). Rain-on-snow events cause some of the largest peak flow events (Jones and Perkins, 2010; Marks et al., 1998), and are expected to increase in some mid-to-high elevation basins currently dominated by snowmelt as climate warms (Surfleet and Tullos, 2013). Thus, basins in the mid-to-upper-elevation range that experience rain-on-snow and widespread harvesting may be most susceptible to increases in large peak discharge events that influence channel morphology and evolution in the region. However, the results of these recent studies contrast with other work in the region that has shown a diminishing effect of forest harvesting for large discharge events (e.g., Thomas & Megahan, 1998: Middle Cascade Mountains). Thus, more research is needed on how forest harvesting affects peak flows across the whole range of occurrence probabilities.

1.3.2: Intermountain West

The intermountain West, defined as the Rocky Mountain System physiographic division (Figure 1.1), is defined by heterogeneous geologic characteristics created by tectonic activity (Kluth and Coney, 1981; Thompson and Burke, 1974) and climate regimes heavily influenced by elevation gradient (Cowie et al., 2017; Seyfried et al., 2018). Although slope steepness and stream power is similar compared to the Pacific Mountain System, slope characteristics such as erodibility, vegetative communities, and climate are significantly different. The climate varies across the region, but generally has wet winters in which much of the precipitation for the year falls as snow, but also includes erosive, high-intensity summer storms (Clayton and Megahan 1997: Idaho Batholith). Forests dominate at higher elevations where there is sufficient water, but lower elevations are generally too dry to support forest cover (Wondzell and King 2003: Northern Rocky Mountains). Fire is an important driver of intermountain West ecosystems, and is more common in water-limited regions of the western United States compared to the eastern United States (Southeast, Northeast, and western Lake States) (Finney et al., 2011). However, fire is an important ecosystem driver in nearly all ecosystems. The interactions between forest harvesting and large-scale disturbance such as fire is discussed in the "Non-Harvest Disturbances" section. Fire suppression in the intermountain West has changed the composition of fire-dependent forests (Arno et al., 1995; Gavin et al., 2007), and promoted spread of woody species into areas once dominated by shrub and grass species (Pierson et al., 2007). Forest management in the intermountain West, primarily for conifer species, can be intensive in areas, but intensive practices and harvest extent are less widespread than in the Pacific Mountain System or Southeast.

Direct Effects. Direct effects in the intermountain West are influenced by hillslope and geologic factors, including basin parent material (Northern Rocky Mountains: Sugden and Woods 2007; Megahan, Wilson, and Monsen 2001), and precipitation characteristics. Slopes tend to be high and soils thin in headwater reaches, and level out to drier alluvial valleys (Northern Rocky Mountains: Seyfried et al. 2018; Southern Rocky Mountains: Wicherski, Dethier, and Ouimet 2017). Overland flow in arid to semiarid lower elevation catchments can be common following high intensity summer storms (Wondzell and King, 2003), but rainfall erosivity is on average generally lower than the rest of the United States, with the highest R-factor for the Rocky Mountain System division 7% of the national maximum for the coterminous USA (Renard, 1997; Wieczorek and LaMotte, 2010). However, it should be noted that this is an expression of average rainfall erosivity in the long run, applied to low-precipitation intermountain West watersheds, and it is important to account for the fact that some convective summer storms may be much more erosive than the mean conditions (Fletcher et al., 1981).

Further, mass slope failure is an important process in high-slope areas and can detach large amounts of sediment (Megahan, Wilson, and Monsen 2001: Idaho Batholith). Unlike the Pacific Mountain System where mass slope failure is almost always initiated as debris flows due to loss of slope stability, etc., mass slope failure can be initiated via overland flow in the intermountain West region (Wondzell and King, 2003). Further, wind erosion can be a major driver of erosion in semiarid to arid regions (Whicker et al., 2006).

Similar to the Pacific Mountain System, unconsolidated glaciated basins produce a higher sediment supply to streams than unglaciated basins (Sugden and Woods, 2007). Compared to the Pacific Mountain System where forested slopes are relatively more wet and often have high infiltration capacity, the relatively drier slopes combined with intense summer storms in the intermountain West facilitate different erosional processes (i.e., overland-flow induced mass failure versus loss of hillslope stability due to increased saturation: Wondzell and King 2003). Compared to the coast ranges of California, Oregon, and Washington in the Pacific Mountain System, there is generally a lower risk of mass failure in the more arid Northern Rocky Mountains, with localized areas of high landslide risk still occurring (Megahan and King, 2004). Surface erosion by sheet, rill, and gully processes is also important, especially for dry slopes that support less vegetation (Clayton and Megahan, 1997). As with other regions, forest roads tend to be the primary source of direct effects in the intermountain West (Megahan and King, 2004; Schnackenberg and MacDonald, 1998).

Indirect Effects. Drivers of indirect effects in the intermountain West include basin geology and hydrologic/climatic regime. Travel time for fine sediments in mountain streams tends to be fairly quick, with single-event transport distances for fine particles in high flow events on the order of tens of kilometers (Northern Rocky Mountains/Idaho Batholith: Bonniwell, Matisoff, and Whiting 1999). However, landscape position influences exchange with the banks and floodplains (and thus indirect effects), as lower-gradient alluvial reaches at lower elevations tend to have more exchange than high-energy mountain headwaters (Bonniwell et al., 1999). This indicates that, like the Pacific Mountain System, basin sediment supply, geology, and stream characteristics such as stream order and channel material (alluvial versus bedrock) will explain sub-regional differences and drive indirect effect response. Elevation and geology are highly correlated with surface and subsurface hydrologic behavior and regimes, and conditions are heterogeneous in western basins (Seyfried et al., 2018). Woody debris can be an important sediment driver, but wood supply to streams in the interior West has been hypothesized to be generally lower than in the Pacific Mountain System based on results seen in Colorado (Wohl and Goode, 2008). This relatively lower wood supply to streams in Colorado may be a legacy effect of late 19th century forest harvesting and relatively slow forest regeneration (Wohl and Goode, 2008). Relatively slow forest regeneration in water-limited environments have been shown to have more persistent hydrological changes following forest cover change than humid or water-rich areas (Bosch and Hewlett, 1982).

Indirect effects have been identified as potentially important in the intermountain West region (Karwan et al., 2007), but have not been directly quantified (e.g., Alexander et al. 1985). Despite proximity to the Pacific Mountain System region and many similarities (e.g., bedrock close to the soil surface, recent tectonic activity), there are important landscape and climate differences that influence indirect effects response and variation throughout the intermountain West. In particular, the intermountain West includes many catchments that are water-limited at lower elevations. Streamflow in semi-arid areas are more sensitive to changes in forest cover (Zhang et al., 2017), including a lower threshold of basin area cut that will induce a change in annual water yield (Stednick, 1996). Forest harvesting also increases the geomorphic adjustment rate of ephemeral streams, which are common in water-limited environments, but particularly in the southern portion of the intermountain West and Great Basin (Bull, 1997; Heede, 1991). Similar to the Pacific Mountain System, the rain-snow transition is increasing in elevation as a result of climate change (Klos et al., 2014; Seyfried et al., 2018). This is important for forested catchments at mixed-regime elevations: rain-on-snow is often the driver of the annual maximum discharge in the region at mixed hydrologic regimes (MacDonald and Hoffman, 1995). As discussed in the Pacific Mountain System section, recent findings have indicated that even high flow events in snowmelt-dominated basins may increase due to forest harvesting, but the effect of forest harvesting on the highest flows remains contentious (Bathurst, 2014; Birkinshaw, 2014; Green and Alila, 2012).

Legacy sediment deposits from widespread mining activity, much of which is highly erodible, is common in floodplains in some areas such as the Colorado Mineral Belt (Wicherski et al., 2017). Other legacy impacts include channel clearing for log and tie drives that have increased flow erosivity, but also decreased presence of woody debris and sediment storage (southeastern Wyoming: Young, Haire, and Bozek 1994). These are two examples where legacy effects on stream geomorphology may affect indirect effects – the former by offering an ample supply of erodible mining legacy sediment, and the latter by increasing the erosivity of streamflow but not necessarily the supply of sediment. This illustrates that local knowledge of the anthropogenic history and geomorphic condition of streams is necessary to adequately characterize the risk of indirect effects in a catchment. Further, episodic events that produce large amounts of sediment such as wildfire and debris flows dominate long-term sediment yields, and can produce influxes of sediment mobilized for indirect effects for up to centuries (Kirchner et al., 2001; Moody and Martin, 2001). Thus, in previously burned catchments, geomorphic assessments and consideration of increased near-stream sediment supply for increased streamflows to erode may be a dominant legacy affect.

1.3.3: Southeast

The Southeast is defined by several distinct physiographic zones, including the Appalachians (mountainous, bedrock close to the soil surface), Piedmont (foothills, rolling and sometimes steep hills with erodible soils), and Coastal Plain (very low relief, erodible soils), south of Maryland (Figure 1.1). The hydrologic regime is rainfall-dominated, with large peak discharges in Coastal areas possible due to extreme events such as tropical cyclones and hurricanes (Villarini and Smith, 2010). Compared to other regions, the Southeast has high precipitation amount and intensity, most prominently in the Coastal Plain (Hershfield, 1961), which includes the highest R-values in the coterminous United States (Renard, 1997; Wieczorek and LaMotte, 2010). Intensive silvicultural management and relatively large harvest extent of conifer forests and plantation forestry is common in the Southeast (Eisenbies et al., 2009; Grace, 2005; Masek et al., 2008). Compared to the rest of the United States, the Southeast (and Northeast) have relatively long land-use and forest management history, with many forests second growth or more and in abandoned agricultural areas (Rivenbark and Jackson, 2004).

Direct Effects. In the Southeast, direct effects are affected by the legacy of agricultural land use (Jefferson and Mcgee, 2013; Lang et al., 2015; Rivenbark and Jackson, 2004), geologic and hillslope factors (Aust et al., 2015; Lang et al., 2018; Rivenbark and Jackson, 2004; Vinson et al., 2017a, 2017b), relatively high precipitation amount and intensity compared to the rest of the United States (Beasley and Granillo, 1988; Hershfield, 1961; Terrell et al., 2011), and intensive management (Grace, 2005). Flat areas of the Coastal Plain exhibit very little direct effects due to the combination of low slope (McBroom et al., 2008; Terrell et al., 2011) and rapid revegetation which helps to reduce the risk of erosion and direct effects soon after harvest (Beasley and Granillo, 1988; Ensign and Mallin, 2001). However, where slopes are higher in the Piedmont and Appalachian regions, direct effects are more likely to occur compared to the Coastal Plain (Rivenbark and Jackson, 2004; Vinson et al., 2017a).

Historical land use influences direct effects, particularly sediment delivery, in the Southeast Piedmont (Lang et al., 2015; Rivenbark and Jackson, 2004). In that area, the most important of these legacy effects for direct effects are gullies that formed during post-European settlement agriculture that are a major delivery pathway for eroded sediment, bypassing riparian areas and directly connecting uplands and streams (Jefferson and Mcgee, 2013; Lang et al., 2015; Rivenbark and Jackson, 2004). Direct effects occur where sediment sources and delivery pathways are connected spatially and temporally (i.e., sediment eroding and being flushed down an abandoned gully within the timeframe of a single storm). Thus, it is not surprising that direct effects have been found to be most common where harvest operations occur within streamside management zones, and/or are connected to abandoned agricultural gullies that drain directly to streams and bypass riparian buffers (Lang et al., 2015).

Intensive silvicultural practices in the Southeast are associated with increased potential for water quality effects (Grace, 2005). The areas with the highest potential for direct effects in the Southeast are those with high slope and erodible soils. In many of these areas, bladed skid trails (graded by a bulldozer) are often used to extract timber, increasing the likelihood of erosion compared to overland skid trails (wherein equipment simply drives over the soil surface) (Lang et al., 2018; Vinson et al., 2017a, 2017b) or skyline systems used in the Pacific Mountain System. Implementation of BMPs, however, are proven to mitigate direct effect impacts of intensive practices (Griffiths et al., 2017).

Indirect Effects. In much of the Southeast, a key driver of indirect effects is the widespread distribution of legacy sediments in banks and floodplains. Legacy sediments are deposited primarily in Piedmont and Coastal Plain streams as a result of historical landscape erosion and subsequent deposition in river valleys in the post-European settlement agricultural era, and constitute a large source of in-and-near-stream erosion (Balascio et al., 2019; Hupp, 2000; Lang et al., 2015; McCarney-Castle et al., 2017; Mckinley et al., 2013; Pizzuto and O'Neal, 2009; Rivenbark and Jackson, 2004; Trimble, 2008, 1977; Walter and Merritts, 2008). Stored legacy sediments in the banks and floodplains of streams cause channel instability, and may cause sediment yield to be particularly sensitive to flow increases (Donovan et al., 2015; Jackson et al., 2005; Mukundan et al., 2011). Piedmont streams in particular commonly have unstable banks, mobile streambeds, and are high in turbidity (Jackson et al., 2005). Additionally, freeze-thaw has been found to be a crucial destabilizing force for mid-Atlantic Piedmont streambanks when followed by rainfall events (Inamdar et al., 2018).

In the Piedmont and Appalachian regions, flow increases are associated with increases in sediment and nutrients, contributing sediment through channel extension and/or channel scour (Aubertin and Patric, 1974; Hewlett et al., 1984; Kochenderfer and Hornbeck, 1999). Studies in the Appalachians have found increases in peak flows due to forest harvesting that vary with basin responsiveness to precipitation as well as the magnitude of logging and road disturbance (Hewlett and Helvey, 1970; Swank et al., 2001). In one Appalachian study, most of the increased sediment yield in the harvested catchment was sourced from forest roads (i.e., direct effects), but indirect effects were not quantified (Swank et al., 2001). Further, Appalachian streams tend to have higher water quality than those in the Piedmont region (Price and Leigh, 2006). As land use changes from forest to agriculture downstream from the Appalachians, however, water quality can degrade especially during stormflow, highlighting the importance of peak flows in determining sediment and nutrient yields (Bolstad and Swank, 1997).

In the Coastal Plain, indirect effects can be important contributors to observed increases in sediment yield after forest harvesting, with deeply incised channels in erodible parent material (McBroom et al., 2008; Terrell et al., 2011). Flat, wet watersheds in the Coastal Plain can experience high saturation excess flow due to channel expansion during wet conditions (Beasley and Granillo, 1988), and many streams in the Coastal Plain exhibit a majority of their runoff due to infrequent storm events (McBroom et al., 2008, 2003). Because direct effects are often limited on Coastal Plain sites due to low slope and rapid revegetation, indirect effects may be more important in that region. For example, high precipitation and low slope can increase the spatial area of hydrologic connectivity rapidly throughout a watershed, and can connect new sources of sediment through channel expansion. The importance of indirect effects in flat, wet watersheds in the Coastal Plain follows from the increased and spatially pervasive hydrologic connectivity, much of which is subsurface, that cause increased flows and erosion of ample sediment supply of legacy sediments in streambanks. Further, surface flowpaths and channel network expansion that are caused by increased catchment connectivity and saturation create new sources of sediment to contribute to sediment yield.

1.3.4: Northeast

The Northeast, grouped roughly by physiographic characteristics and silvicultural management, includes the northern reaches of the Appalachian, Piedmont, and Coastal Plain physiographic provinces north of Maryland, and New England (Figure 1.1). With average forestland ownership dispersed among a large number of small land owners, forest management is generally not intensive and with small harvest extent (Butler et al., 2016). Further, the hydroclimatic regime transitions from rainfall-dominated to snowmelt-dominated on a northward gradient, as does the importance of freeze-thaw for streambank erosion (Inamdar et al., 2018). The average annual R-factor varies from about 5-25% of the coterminous USA maximum, highest on the coast and lowest in inland New England (Renard, 1997; Wieczorek and LaMotte, 2010). Although non-intensive management is most common throughout the Northeast, it can be intensive in localized areas (e.g., areas of Maine: Czapowskyj and Safford, 1993; Masek et al., 2008). Harvested species often consist of northern hardwoods (Hornbeck and Leak, 1992). Precipitation through the year is relatively evenly distributed, with large rainfall and snowmelt peaks possible (Hodgkins et al., 2003; Huntington et al., 2009); further, large peak flows are possible from extreme events such as tropical storms (Vidon et al., 2018; Villarini and Smith, 2010).

Direct Effects. In general, adverse effects of forest harvesting on sediment yield in the Northeast are thought to be low (Patric, 1976), and BMPs have been documented as highly effective in reducing direct effects (Briggs et al., 1998; Hornbeck and Leak, 1992; Maine Forest Service, 2013; Martin et al., 2000; Schuler and Briggs, 2000; Wilkerson et al., 2010). The southern states of the Northeast include some of the same physiographic regions as the Southeast, (e.g., Appalachian and Piedmont provinces), but the New England states also include areas recently glaciated (Figure 1.1; Dyke et al. 2002). In areas of the Northeast that experience soil freezing in the winter, harvesting on frozen soils is recommended (e.g., Advisory Committee for Vermont FPR, 2015), which reduces many of the risk factors for direct effects (Kolka et al., 2012). Similar to other landscape regions, the potential for direct effects are expected to be high where slope grade is high, soils are erodible, erosion sources are connected to streams (e.g., where skid trails are located close to streams or cross streams), and soils are poorly drained (increased risk of rutting; associated with hillslope position) (Briggs et al., 1998; Schuler and Briggs, 2000).

Indirect Effects. History of land use and glaciation influence indirect effects in the Northeast. In the Northeast, increases in water yield after harvesting are mostly augmentations to low flows, with some peak flows increased (Bent, 2001; Hornbeck et al., 1997, 1993). Conversion of intermittent streams to perennial due to baseflow increases have been observed and may contribute to a longer period of connected flow that carries sediments (Lynch and Corbett, 1990). However, peak flow increases are thought to be small and of only minor importance for stream and channel scour (Martin et al., 2000).

Legacy sediments deposited in-and-near-stream are pervasive in the mid-Atlantic region, where they constitute fine-grained erodible streambanks (Balascio et al., 2019; Hupp, 2000; Pizzuto et al., 2014; Pizzuto and O'Neal, 2009; Schenk and Hupp, 2009; Walter and Merritts, 2008). The presence of these sediments has been attributed to post-European settlement land clearing and agricultural practices, as well as the widespread construction of milldams that altered channel morphology and caused accretion of sediments in floodplains all throughout the eastern United States but especially in the mid-Atlantic region (Walter and Merritts, 2008). Freeze-thaw dynamics, when followed by intense winter rainfall events, destabilize banks and cause high levels of bank erosion (Inamdar et al., 2018). I would hypothesize that streams with these large legacy sediment deposits, such as in the mid-Atlantic Piedmont and Coastal Plain, are most susceptible to indirect effects. Farther north, in the glaciated region of New England, I hypothesize streams have less of a sediment source in the immediate channel area due to less sustained and widespread legacy effects. However, legacy sediments in floodplains have been documented in formerly glaciated New England catchments, but with similar intensity of agricultural and milldam activity as the mid-Atlantic. These legacy deposits varied based on presence of lake and wetland sinks, and the thickness of glacial deposit available for a sediment source, indicating legacy sediment presence and distribution is modulated by glacial history (Johnson et al., 2019).

The Northeast has both glaciated and unglaciated areas with respect to the last glaciation (Figure 1.1; Dyke et al. 2002). Glacial deposits, and their interaction with bedrock forms, are first-order controls on flowpaths in glaciated catchments of the Northeast (Shanley et al., 2015). Thus, the distinction between areas that were recently glaciated versus those that were not serves as a boundary between different drivers of hydrologic response and indirect effects. In glaciated regions, where landscape features are highly heterogeneous, glacial landforms and sediment deposits will determine the critical zone development that influence sensitivity to indirect effects, such as dominant soils and runoff flowpaths. For example, streams in glacial outwash areas will have a higher baseflow component and sustained flows, as well as have more moderate stormflow peaks due to high infiltration in coarse sands compared to till or lacustrine areas (Urie, 1977; Winter, 2001).

1.3.5: Western Lake States

The western Lake States, including primarily the Laurentian Uplands physiographic division in the US states of Minnesota, Wisconsin, and Michigan (Figure 1.1), are unique compared to the other regions because they were heavily glaciated during the last glaciation (Dyke et al., 2002; Jennings and Johnson, 2011; Larson, 2011; Syverson and Colgan, 2011). Here, relief is low, and groundwater-surface water connection via wetlands widespread. Forest management is common but generally not intensive, with practices such as site preparation, short rotations, and vegetation control uncommon; further, harvesting often occurs in the winter on frozen soils (D'Amato et al., 2009; Slesak et al., 2018). Mean rainfall erosivity (R-factor) ranges from about 0.10 to 0.20 of the coterminous USA maximum within the Laurentian Uplands (Renard, 1997; Wieczorek and LaMotte, 2010). Dominant species harvested include northern hardwoods, with some conifer harvesting, including wetland species such as black spruce during winter while the ground is frozen. The largest streamflow of the year is driven mostly by snowmelt or early-spring rain (on saturated catchments after snowmelt), but large summer rainfall peaks can occur (Sebestyen et al., 2011a; Villarini et al., 2011).

Direct Effects. Given the low relief and high amount of winter harvesting, direct effects in the western Lake States are generally very low (McEachran et al., 2018; Verry, 1986, 1972). There are localized regions where mass slope failure is a risk, especially in the Glacial Lake Duluth clay plain and where slopes are greater than 30% in river valleys (Merten et al., 2010; Radbruch-Hall et al., 1982; Riedel et al., 2005), but most erosion occurs via sheet or rill processes due to the low relief. Where direct effects do occur, vegetative cover is the dominant factor controlling erosion where slopes are slight; both erosion and vegetative cover levels are influenced heavily by surficial geology and glacial landform (McEachran et al., 2018). However, slope is an important driver where it is steep relative to within-region conditions. The importance of vegetation in low-relief areas is similar to the findings from the low-relief Coastal Plain in the Southeast, where rapid post-harvest revegetation helps reduce the risk of direct effects soon after harvest (McBroom et al., 2008; Terrell et al., 2011). The risk of direct effects is also reduced by widespread winter harvesting on frozen soils (Kolka et al., 2012; McEachran et al., 2018; Minnesota Forest Resources Council, 2012).

Indirect Effects. Indirect effects in the western Lake States are uniquely influenced by glacial geology and its influence on sediment deposits and wetland extent. Studies on peak flow effects of forest harvesting in the western Lake States have generally found small increases for low-discharge, frequently occurring peak flows, with potential increases in discharge response to large rainfall-caused events (Sebestyen et al., 2011c; Verry et al., 1983). After loss of mature forest cover, there may be more variation between base and peak flows (Detenbeck et al., 2005), which can be an important geomorphic driver that varies with land use (Richards, 1990). Increases in unstable banks and sedimentation have been observed in response to riparian thinning on glacial moraines, pointing to potential indirect effects (Merten et al., 2010). In other glaciated boreal regions similar to the western Lake States, there was little effect of clearcutting on watershed peak flows, but low flows were significantly increased, similar to findings from the Northeast USA (Sørensen et al., 2009).

Unlike the glaciated mountainous Northeast, where bedrock is still relatively close to the land surface, the western Lake States include many areas with a greater depth of glacial deposits (commonly >100m, Jennings and Johnson, 2011), and thus catchment flowpaths are more strongly controlled by glacial landform. Studies in the western Lake States have shown that glacial geology is a dominant control on watershed hydrology, and influences the sensitivity of hydrologic and indirect effect response to changes in land use and land cover (Belmont et al., 2011; Foufoula-Georgiou et al., 2015; Gran et al., 2011; Schomberg et al., 2005; Stoner et al., 1993; Vaughan et al., 2017). Glacial deposits control geomorphic attributes and affect physical stream characteristics (Phillips and Desloges, 2015, 2014), and influence partitioning of water and peak flow generation. For example, high-infiltration outwash and morainal watersheds have a higher groundwater component to flow than "flashier" low-infiltration lacustrine watersheds (Naylor et al., 2016; Richards et al., 1996; Richards, 1990; Urie, 1977). Where fine-grained lacustrine deposits occur in the repeatedly-glaciated western Lake States, layering of heterogeneous deposits with abrupt changes in hydrologic conductivity between layers cause preferential flowpaths, bank slumping, and small mass wasting events (Magner and Brooks, 2008), processes that may be exacerbated by increases in discharge (Riedel et al., 2005). Thus, streams developed in lacustrine sediments may be more sensitive to indirect effects than outwash, moraine, or coarse-grained till deposits.

Wetlands are common and relatively large in spatial extent compared to the other regions reviewed, and influence catchment response to forest harvesting. Wetlands have a "buffering" effect on hydrological response to harvesting (Detenbeck et al., 2005; Verry et al., 1983), and peak flows are smaller in watersheds with more storage (i.e., wetlands and lakes); however, when storage dips below ~10% of watershed area, peak flows can increase rapidly (Detenbeck et al., 2005). Wetlands are also hydrologically important areas for runoff generation (Verry and Kolka, 2003), but it is unclear how their spatial distribution and effects on stream geomorphic variables influence flow in mixed upland-wetland watersheds common in western Lake States conditions. The location of wetlands are often glacially determined, making this driver of indirect effects inextricable from the driver of glacial geology (Richards, 1990; Verry and Janssens, 2011).

Although there is much literature on alluvial and bedrock stream geomorphology response to flow alterations (e.g., Phillips and Jerolmack, 2016), there is less understanding about wetland streams, which can exhibit significantly different geomorphic characteristics (Jurmu and Andrle, 1997; Watters and Stanley, 2007). Wetland stream morphology in peatlands, for example, is governed by biological processes such as peat decomposition and accumulation, as well as groundwater controls, compared to the alluvial channels that are primarily shaped by sediment load and discharge (Watters and Stanley, 2007). Sediment loads in wetland streams tend to be low in general, and bank materials tend to be resistant to erosion (Watters and Stanley, 2007). Further, wetlands can act as a sink for sediments, removing them from flow and transport (Hupp et al., 1993; Zierholz et al., 2001). Because of this, indirect effects on sediment yield within wetland streams are likely low, but changes in wetland hydrology can affect sediment yield downstream because of their disproportionate influence on discharge to downstream alluvial reaches. This may cause indirect effects depending on local glacial geology and the properties of the wetland-alluvial stream reach interaction.

1.3.6: Future Directions

Although each region exhibits different biophysical and management characteristics, and exhibits vast diversity of landscape structure within each region, literature from all regions identifies basin geology as a critical driver of variables that influence both direct and indirect effects. Thus, basin geology may serve as a unifying framework to discuss direct and indirect effects. Basin geologic factors are important drivers of direct and indirect effects in diverse landscapes, from the mountainous western states to the low-relief western Lake States (McEachran et al., 2018; Seibert and

McDonnell, 2010; Sugden and Woods, 2007; Vinson et al., 2017a). The importance of basin geology is not surprising since basin geology is a predictor of many interrelated factors known to influence both direct and indirect effects including soil development and erodibility, native vegetation communities, sediment supply, dominant flowpaths and hydrology, and slope factors. Future regional-level studies could encapsulate sub-regional variability in landscape characteristics using proxies for basin geology and map out high-risk areas for direct and indirect effects. However, some process drivers of direct and indirect effects warrant further investigation.

Direct Effects. Although the drivers of erosion are relatively well understood, sediment delivery is often less understood (Croke and Hairsine, 2006). Identifying primary delivery pathways through identification of areas that are hydrologically connected via overland flow, the time over which the connection takes place, and an understanding of internal watershed sediment storage factors within regional conditions is critical for making the leap from erosion sources to sediment delivery in temperate forested watersheds (Bracken et al., 2015; Croke and Hairsine, 2006). The role of BMPs at preventing sediment delivery is a topic of ongoing investigation, especially how BMPs influence water quality and cumulative effects at the watershed outlet (Klein et al., 2012; Slesak et al., 2018).

Indirect Effects. Because many studies do not quantify indirect effects alongside direct effects (Table 1.1), their importance relative to direct effects is unclear. Sediment fingerprinting techniques are a promising tool that can discriminate between sediment sourced from direct and indirect effects (Belmont et al., 2011) and have been utilized in the context of forest harvesting studies before (Motha et al., 2003). Pairing measurements of stream geomorphology with discharge, landscape erosion, and suspended sediment records from experimental catchments, and utilizing more methods based in concepts from fluvial geomorphology such as the analysis of sediment rating curves, also could help determine the relative importance of direct and indirect effects (Fraser et al., 2012; Reid et al., 2010; Safeeq et al., 2020).

Peak and high flows are critically important in shaping channels as well as mobilizing and transporting sediment (Blom et al., 2017; Wolman and Miller, 1960). There is still much debate about how forest harvesting affects peak flows across the range of peak flow frequencies (Alila et al., 2009; Alila and Green, 2014; Bathurst, 2014; Birkinshaw, 2014; Green and Alila, 2012; Lewis et al., 2010), and more research is needed to understand the full behavior of peak flow response to forest harvesting for large magnitude, infrequently occurring flows. This is important for basins where flows important for channel morphology and instream grade-control elements (e.g., large woody debris) are associated with large, infrequent discharge events.

Despite the importance of the peak and high flow regime, understanding other regimes of the flow duration curve and their associated sediment supply changes are necessary to fully consider indirect effects. For example, a change in the sediment supply to streams (such as introduction of legacy sediments into banks and floodplains) can change the effective discharge necessary to mobilize sediments, causing instream erosion even in the absence of a change in discharge. Variable channel length and increases in connectivity of sediment sources due to increased baseflow after forest harvesting is also necessary to consider, particularly for headwater catchments (Godsey and Kirchner, 2014). Thus, consideration of changes in peak flows only (despite their importance) does not encapsulate the full range of indirect effects drivers, pointing to the necessity of quantifying indirect effects instead of utilizing peak flows as a proxy for changes in sediment transport.

The role of cover type and species harvested on indirect effects also warrants further investigation. There are large inter-species differences between regions; for example, conifer regeneration in subalpine conditions in the intermountain West (Alila et al., 2009) will utilize water differently than short-rotation loblolly pine in the Southeast (McBroom et al., 2008). Of particular interest is the concept of hydrological recovery, i.e., the time after harvest it takes for the water and energy budget terms associated with vegetation cover to re-converge to an approximation of the pre-harvest time period

(Stednick, 2008). Recovery time will vary with the growth rate of the recovering species, management interventions (e.g., competition release), climate, and watershed physiographic conditions. Management designed to decrease recovery times may decrease the potential for indirect effects.

1.4: SPATIOTEMPORAL SCALING OF DIRECT AND INDIRECT EFFECTS

Although the presence and severity of direct and indirect effects rely on many different biophysical and management factors that vary by region, the consideration of spatial and temporal scaling is a common and important research need for both. For direct effects, there are questions about how impacts may vary across spatial and temporal scales (Grace, 2005; Slesak et al., 2018). The fundamental processes for direct effects (i.e., erosion and delivery) can occur at the hillslope scale in the timespan of a single storm or season, and thus direct effects generally occur and are observed at a localized scale (Figure 1.3). However, with increasing disturbance extent within watersheds, direct effects can become dominant drivers of sediment yield at larger spatial scales (i.e, cumulative effects; MacDonald, 2000). Further, with increasing disturbance severity and management intensity, direct effects can persist for a relatively longer amount of time (e.g., severely compacted soil can take many years to recover: Croke et al., 2001; Zenner et al., 2007). Because direct effects are more often studied at the local spatial scale, and event to seasonal temporal scales, it is unclear how the above processes and drivers scale with space and time.

Indirect effects are defined in relation to a watershed-level change in hydrologic flowpaths, and occur at larger spatial scales than direct effects (Figure 1.3). Forest harvesting can promote changes in forest species composition at large spatial scales (Wang et al., 2015), introducing potential for long-term changes to watershed hydrology at multiple scales (Mao and Cherkauer, 2009). However, much of the literature about hydrologic changes as a result of forest harvesting and indirect effects occur at the small watershed scale (~ headwater; < 10 km^2) (Andréassian, 2004), and it is unclear how effects at the small watershed scale propagate to larger watersheds. The effect size of land use and land cover changes on hydrologic variables is widely hypothesized to decrease with increasing spatial scale (Blöschl et al., 2007; Viglione et al., 2016), as variation in climate becomes the dominant factor influencing hydrologic variables (Rogger et al., 2017). The point at which land-use becomes insignificant is unclear and likely depends on regional conditions, but has been generally hypothesized to occur at the level of 1 to 100 square kilometers (Andréassian, 2004; Bathurst et al., 2011; Blöschl et al., 2007; Viglione et al., 2016). Disturbance spatial extent and severity also influence indirect effects, including their magnitude and temporal persistence (Figure 1.3). For example, harvesting that *increases* flows in clearcut sub-basins can *decrease* snowmelt peaks in its larger associated basin due to snowmelt desynchronization depending on harvesting extent (Sebestyen et al., 2011b; Verry et al., 1983). If disturbance is widespread, indirect effects would likely occur at larger spatial scales than if it were limited in extent, but threshold disturbance levels for the occurrence of indirect effects is unknown. Similarly, hydrological changes and watershed recovery depend on biophysical watershed conditions such as forest regeneration and recovery from disturbance. For example, in northern catchments, pine regeneration would allow indirect effects to persist for longer temporal scales compared to rapidly regenerating aspen (*Populous* spp.) because of differences in ET at early growth stages (Thompson et al., 2018).

1.5: NON-HARVEST DISTURBANCE

Particularly important for both direct and indirect effects is the role of forest harvesting in affecting disturbance regimes that are important sources of sediment yield in temperate basins. For example, a significant source of stream sediments can be sourced from overturned root balls of trees that fall in the riparian zone and on streambanks, caused by post-harvest windthrow and elevated water table levels (Bahuguna et al., 2010; Boggs et al., 2016; Grizzel and Wolff, 1995; Jackson et al., 2007; Terrell et al., 2011). Subsequent sediment mobilization and deposition from the rootwad and/or the channel banks can result, particularly if the tree remains in the channel as woody debris (Pizzuto et al., 2010). The ultimate attribution of riparian windthrow sediment detachment and sediment delivery to the stream into a direct or indirect effect is dependent on spatiotemporal contemporaneity of the pathways of sediment and hydrologic connectivity for the situation in question (Figure 1.2). If the particular influx of sediment in question is following a path of overland hydrologic connectivity, synchronizing sediment and hydrologic connectivity, the event can be considered a direct effect. If these are disjoint, the sediment yield effect is an indirect effect. This "indirect effect" portion of sediment yield is the result of a process mediated through altered hydrology based on a decrease in watershed evapotranspiration and flowpaths.

The risks of direct *and* indirect effects, and the effectiveness of BMPs designed to prevent them, should also be weighed against how forest management influences the non-harvesting disturbances a site will eventually experience, particularly in the face of climate change. For example, forest management can decrease the risk of wildfire (Starrs et al., 2018). Wildfire is known to produce large amounts of sediment via exposure of the soil surface and connection of overland flow pathways to the stream over hydrophobic soils, and by altering stream geomorphology and the partitioning of water in catchments. Fire increases peak flows that change channel dimensions and sediment yield (Helvey, 1980; Moody and Martin, 2001), and can alter channel dimensions through loss of bank stability associated with riparian forests (Eaton et al., 2010). Further, there may be large-scale interactions with forest management and climate. Climate change has been attributed as increasing the risk of wildfire (Flannigan et al., 2000), and forest management can be used to mitigate fire risk. Large-scale wildfires in the intermountain West, for example, are increasing in magnitude and frequency due to multiple factors including climate change and historical fire suppression (Cannon and Degraff, 2009). Post-fire debris flows can be a large source of sediment in the area (Cannon et al., 2010; Cannon and Degraff, 2009), and post-fire surface erosion is also high (Shakesby and Doerr, 2006).

The interactions between insect infestation, fire risk, salvage logging, and long-term species composition illustrates another long-term disturbance regime. For example, in the intermountain West of the USA and Canada, mountain pine beetle outbreaks exacerbated by climate change (Kurz et al., 2008) have caused large-scale tree die-offs that increase the risk of wildfire (Negron et al., 2012). In Colorado, salvage logging can change the species composition of regenerating forests compared to beetle-killed stands that are unharvested, promoting lower fire-risk species that are more tolerant to drought die-off and with a canopy structure that decreases the risk of ground fires to transfer to the canopy. This species change after salvage logging could alter fire risk for more than a century (Collins et al., 2012). Although this review has focused on post-harvest sediment yield effects of incremental processes such as land surface denudation and in-stream erosion and deposition, episodic catastrophic events can dominate as long-term sediment sources, such as debris flows and landslides caused by fire (Goode et al., 2012; Wicherski et al., 2017). In fact, the small paired catchment studies that I have used to form the foundation of my review may greatly underestimate long-term erosion rates because they often do not capture catastrophic and rare events that deliver amounts of sediment to streams that dwarf both sheet and rill erosion and delivery, and in-channel erosion (Kirchner et al., 2001).

Very rare, extreme precipitation events can have also long-term effects on stream sediment, alter reference conditions, and affect channel morphology. For example, the sequence of Hurricane Irene and Tropical Storm Lee in 2011 have had large and persistent impacts on water quality in the Northeast (Vidon et al., 2018). Increases in erosion associated with extreme rainfall led to suspended sediment concentrations remaining elevated for years after the event (Dethier et al., 2016). Further, long-term alterations among forest species composition, watershed hydrology, incremental changes in sediment yield, and forest harvesting should also be considered. For example, Swiss needle cast in the Oregon Coast Range, a chronic canopy disturbance, has been found to increase water yields (Bladon et al., 2019). Although a chronic foliage pathogen with gradual spread through time, and not a large-scale and catastrophic disturbance such as wildfire or hurricane, streamflow increases through time may affect stream geomorphology and increase sediment yields even in the absence of harvest. The examples of extreme precipitation events and gradual chronic foliage pathogen are not indirect effects because any in-stream sediment response to these events are not caused by forest harvesting. However, disturbances such as these illustrate the importance of assessing what the "baseline" conditions in a watershed are – in particular, geomorphic and near-stream variables that may be gradually changing through time.

In summary, any sediment yield increases caused by forest harvesting via direct or indirect effects should be weighed against the potential long-term sediment yield risks and benefits that silvicultural management may offer, such as risk reduction for wildfire or altering species composition to offset or manage other drivers of long-term changes in streamflow. Further, watershed disturbance though incremental changes to forest composition, wildfire, or extreme flooding, even when not indirect effects of forest harvesting themselves, affect the geomorphic conditions that influence the probability of indirect effects occurrence, and are critical to account for in assessing the risk of indirect effects.

1.6: MANAGEMENT IMPLICATIONS

The direct/indirect effects framework expands the scope of water quality management traditionally used with respect to forest harvesting practices that focuses primarily on direct effects at small spatial and temporal scales (Aust and Blinn, 2004; Slesak et al., 2018). Often when BMP effectiveness is discussed, all sediment yield above a control level is assumed to be due to direct effects alone (e.g., as implicitly assumed by some calculations of "sediment delivery ratios"). The direct/indirect framework I have presented provides a conceptual framework in which to holistically consider potential sediment yield effects of forest harvesting in a given region of practice. Further, this review has important ramifications to guide future development of BMPs used to prevent increased sediment yield due to forest harvesting, such as promoting further management discussions centered on legacy sediments in watersheds with managed forests.

Contemporary forest harvesting BMPs focus almost exclusively on direct effects, either through preventing erosion (e.g., scattered slash, revegetating exposed soil), or preventing sediment delivery (e.g., riparian corridors, silt fences) (Aust and Blinn, 2004). Often, these BMPs are implemented at the plot scale and have high effectiveness at that scale for at least several years after harvest (Cristan et al., 2016). Further, some direct effects BMPs can also influence indirect effects. For example, forest road runoff can deliver large amounts of flow during the rising limb of hydrographs and increase peak flows (Buttle, 2011; Wemple and Jones, 2003), increasing the risk for indirect effects, while also forming a connected overland flowpath for delivery of surface erosion (increasing the risk for direct effects). BMPs aimed at decreasing connectedness of forest road runoff (e.g., water bars, etc.) thus can decrease direct effects *and* indirect effects. Riparian management zones and equipment exclusion zones near streams protect streambanks from mechanical destabilization that would render them more likely to erode with streamflow increases. Finally, watershed-scale harvest limits and green-up adjacency rules may limit cumulative impacts and indirect effects downstream (Azevedo et al., 2005). However, the impacts of these practices on indirect effects, tailored to regional conditions, are unclear and lack the widespread evaluation that direct effects BMPs have garnered in the forest hydrology literature (e.g., Edwards and Williard 2010). There is potential to further develop and optimize indirect effects BMPs at the watershed-scale to mitigate increased instream erosion. Indirect effects BMPs may include several approaches to limit indirect effects, similar to direct effects BMPs. Starting with harvest planning, managers could identify basins where indirect effects are likely to occur for their particular landscape situation, such as widespread legacy sediments and unstable streams, and plan tailored harvesting schedules that remain below a threshold level of harvest where indirect effects degrade water quality. Process-based hydrologic models may help identify where channel-forming flows could increase with differing levels of harvest in a given basin. Where forest harvesting is identified as a driver of indirect effects, more active measures to buffer increases in peak discharges may need to be explored, such as the construction of wetlands or retention basins. For example, reconstruction of wetlands and watershed storage in the headwaters of the agricultural Le Sueur River watershed in southern Minnesota, USA, is expected to decrease high peak flows and streamflow erosivity resulting from climate and land use/land cover change in the basin and decrease sediment yield (Mitchell et al., 2018). However, it will be difficult to specify where indirect effects BMPs are warranted in the context of forest management activity without detailed study of local hydrology and geomorphology, including process-based models parameterized for local conditions. Thus, it is necessary to increase understanding of the physical and spatial conditions for which indirect effects are a significant contributor to sediment yield.

In some regions, analysis of sediment rating curves and hysteresis during individual events may be helpful to determine sensitivity to indirect effects. In particular, the presence of sediment hysteresis can indicate probable sediment supply, source, and/or depletion within an event or sequence of events (Gellis, 2013; Rose et al., 2018; Smith and Dragovich, 2009), which could give managers more information about the hydrogeomorphic context of a particular watershed. When additional information is available about watershed flowpaths (i.e., through chemical tracers, etc.), sediment influxes that are concurrent with overland flow pathways could be attributed to upslope erosion and sediment delivery, and in-channel sediment mobilization attributed to the remainder. This partitioning of sediment yield may be compared to a baseline scenario to find the level of direct and indirect effects occurring in the watershed after harvest. However, information on sediment rating curves and sediment hysteresis in watersheds of various sizes relevant for forest management can have limited data availability. Sediment rating curve analysis is not uniquely diagnostic of underlying physical conditions (Warrick, 2015). Sediment hysteresis has been found susceptible to dependencies that vary across watersheds and events (e.g. grain size, event sequence, hydrogeomorphic context) in their interpretation (Malutta et al., 2020). Thus, while analysis of sediment hysteresis and rating curves to determine sensitivity to indirect effects might be possible with sufficient data in a local or regional context, this technique requires further development.

1.7: CONCLUSION

My conceptual model of direct and indirect effects, and my exploration of these effects in various hydrogeomorphic contexts based on a review of regional literature where temperate working forests are common in the USA, provides a foundation for managers and for further research to determine the relative importance of different regional drivers. This includes information to facilitate identification of harvest sites and watersheds within regions where increased sediment yield is most likely to occur due to direct and indirect processes that is critical for targeted and optimized management of water quality. To identify these "high risk" areas, it is necessary to account for potential direct and indirect effects, including distinguishing which process is most likely to cause increased sediment yield given the unique local situation. Research directed towards increasing process-based knowledge and the scope of water quality management in forested watersheds to account for spatial and temporal changes in direct and indirect effects, quantification of indirect effects, and the development of more specifically indirect effect BMPs will create a more holistic paradigm in which to account for sediment yield effects of forest harvesting. This review forms the foundation for identifying basins where direct and indirect effects are likely to occur; however, there are few studies that quantify indirect effects alongside direct effects (Table 1.1). Thus, development and efficacy of indirect effects BMPs will depend also on further research.

CHAPTER 2:

Nonstationary flood-frequency analysis to assess effects of harvest and cover type conversion on peak flows at the Marcell Experimental Forest, Minnesota, USA

2.1: INTRODUCTION

Forest cover change and forest harvesting effects on catchment processes, especially on the high flow regime and flooding, have been an area of concern for decades (Andréassian, 2004; Yu and Alila, 2019; Zon, 1927). Alterations in peak flows can have serious ramifications for channel geomorphology, stream ecology, as well as water quality and sediment dynamics (Auerswald and Geist, 2018; Poff et al., 2006). Furthermore, floods can be devastating for local communities (Bradshaw et al., 2007). Forests are generally thought to offer some level of flood protection (Andréassian, 2004), which can be influenced by disturbance such as forest harvesting (Alila and Green, 2014; Birkinshaw, 2014; Green and Alila, 2012). Moving forward, changing climate and a growing demand for wood products may increase forest disturbance (Angel et al., 2018; Buongiorno et al., 2012; Buras and Menzel, 2018), emphasizing the ecological and societal importance to understand the relationship between forests and peak stream flows.

In North America, forest harvesting and forest cover change effects on peak flows are predominantly examined in high-relief regions with bedrock close to the soil surface (Alila et al., 2009; Jones and Grant, 1996; Kuraś et al., 2012; Thomas and Megahan, 1998). Small (< 10 km^2) paired-catchment studies have provided the foundation for much of the current knowledge in forest hydrology, including peak flows and flooding (Andréassian, 2004). However, there is still widespread disagreement that often stems from interpretation of the statistical method used to analyze paired-catchment data (Buttle, 2011). Historical methods used to address the relationship between forest cover change and peak discharges in paired-catchment experiments have typically relied on linear statistical models (e.g., ANOVA, ANCOVA: Hewlett, 1982; Jones and Grant, 1996; Thomas and Megahan, 1998) that utilize traditional frequentist approaches designed to test for differences in mean values and rely on chronological pairing, such that differences between catchments are compared for the same precipitation event (Alila et al., 2009). Such methods have given rise to the general paradigm that the effect of forest harvesting on peak flows exhibits a decreasing effect size with increasing peak flow, and thus a greater proportional impact associated with frequent, low-discharge peak flows (Andréassian, 2004; Bathurst et al., 2011; Thomas and Megahan, 1998). The historic, chronologically paired approach does not account for both event magnitude *and* frequency, which has been found to be critical in the context of peak discharges (e.g., as reviewed by Alilia et al 2009). Analyses accounting for frequency of peak flows, mostly conducted in mountainous, snowmelt-dominated catchments, have found sizable effects for large peak flows, and even an increasing effect size with increasing return interval (Alila et al., 2009; Green and Alila, 2012; Kuraś et al., 2012; Yu and Alila, 2019). It is unclear how findings in these landscapes apply to those found in low-relief glaciated regions such as those found in central North America, Russia, and Scandinavia. Further, catchments at these northern latitudes are expected to be especially sensitive to climate change due to their highly climate-dependent and seasonal hydrologic cycle (Tetzlaff et al., 2015, 2013).

When examining peak flows, changes between control and treatment catchments may manifest in several ways, such as changes in flood magnitude, probability of occurrence, or a change in the type of precipitation event associated with the largest flow events (e.g. rainfall vs snowmelt). A shift in the driving precipitation event has important ramifications for understanding flood generation and catchment processes producing high flows, as these may be different for snowmelt versus rainfall events. For example, post-harvest changes in hydrology in snowmelt-dominated and snowmelt-influenced catchments have the potential to increase peak flows even for large, infrequent events due to catchment hydrologic processes (e.g., increased catchment saturation, alterations in soil thermodynamics, freezing, and infiltration at the time of snowmelt, increased snowpack snow-water equivalent, etc. (Murray and Buttle, 2003; Pomeroy et al., 1994)).

Possible shifts in catchment processes in response to harvest highlight the need for statistical methods that offer flexibility to evaluate the temporal structure of the statistical model of peak discharges. The integration of nonstationary and flood-frequency analysis methods offers a more detailed framework compared to previously used methods, allowing inference about how peak flow magnitudes *and* frequencies change in response to forest cover and climatic changes through time at the small catchment scale (Yu and Alila, 2019). Further, use of Bayesian methods to frame peak flow analysis in a probabilistic framework, allows for uncertainty to be easily calculated in context of the models fitted to observations and my background (or "prior") knowledge about the system.

In this chapter, I quantified the effect of forest cover change on flood and peak flows in two sets of paired catchments at the Marcell Experimental Forest (MEF) in north-central Minnesota, USA in order to test the hypotheses that clearcutting will increase annual peak flows across all return intervals compared to pre-harvest mature forest conditions, and that annual peak flows will decrease with time since harvest as the forest regrows. Additionally, I examined consistency of results and implications for the effects of harvesting on floods by comparing my non-stationary flood frequency analysis with traditional paired-catchment ANCOVA methods.

2.2. METHODS

2.2.1: Study Sites

The MEF catchment studies were established by the U.S. Forest Service in 1961 to investigate the hydrologic and ecological role of peatlands in the boreal-temperate transition zone (Figure 2.1a). Each of six small (<100 ha) upland-peatland experimental catchments, named S1 – S6, consists of an upland forest surrounding a central peatland, from which drains a first-order stream (Figure 2.1b). Aspen (*Populus* spp.) and northern hardwoods dominate the uplands, while black spruce (*Picea mariana*) and tamarack (*Larix laricina*) dominate the central peatlands. The MEF is located on a moraine where multiple ice sub-lobes terminated over the course of the last glaciation (26-12 ka BP)

(Verry and Janssens, 2011). Upland soils are Alfisols or Entisols and generally have a clay loam texture, with Histosols in the peatlands (Nyberg, 1987). The climate is continental, with moist, warm summers and dry, cold winters (Sebestyen et al., 2011b). The mean annual precipitation from 1961 to 2009 was 78 cm (± 11 cm, standard deviation), and the annual mean temperature was 3.4°C (±13°C) (Sebestyen et al., 2011b). About one-third of annual precipitation falls as snow between November and March.

Previous work has quantified some effects of clearcutting and forest regrowth on peak discharges at the MEF from two different long-term paired-catchment experiments, however the full distribution of annual maximum discharge in response to forest harvesting and recovery has not been analyzed. These previous studies, largely summarized by Sebestyen et al. (2011b) and Verry et al. (1983), have included: (1) ANCOVA analyses to separately analyze rainfall and snowmelt-derived peaks (Sebesteyen et al., 2011b; Verry et al., 1983), (2) a frequency comparison up to the 10-year return interval discharge for rainfall-generated peaks only (Verry et al., 1983), and (3) physically based modeling of catchment response to harvest using the Peatland Hydrologic Impact Model (PHIM – see Guertin et al. (1987)) (Lu, 1994). The PHIM modeling study by Lu (1994) used flood-frequency analysis of simulated values for the S4/S5 MEF clearcutting experiment (see below for detail), with results supporting the paradigm of decreasing effect size with increasing return interval. However, when the frequency analysis of rainfall-related peaks was employed in Verry et al. (1983), the 10-year recurrence interval peak discharge after clearcut increased more than the 2-year peak discharge. The response across the entire range of recurrence intervals was not included. Complementing previous work, I examined nonstationary probability distributions of floods for rainfall and snowmelt generated peaks considered together, and compared the results to traditional linear models, using long-term data from two paired-catchment experiments at the MEF.

S4/S5 Experiment. The S4/S5 experiment began with the instrumentation of catchments S4 and S5 in 1962. The control catchment, S5, is 52.6 ha in size, and includes uplands and five small satellite wetlands draining into the 6.1 ha central peatland. The treatment catchment, S4, is 34.0 ha in size, with an 8.1 ha central peatland. Clearcut harvest of merchantable timber in the uplands took place over two sequential fall-winter seasons (1970-71, 1971-72), with final removal of non-merchantable timber in summer 1972. Aspen regenerated on the upland harvest areas and received fertilizer application, according to an intentional study design, in 1978 (Sebestyen et al 2011a).

The S4 catchment straddles the Laurentian Divide. Approximately 70% of its annual water yield drains north to the Hudson Bay (outlet S4N) and 30% drains south to the Mississippi (outlet S4S) (Sebestyen et al., 2011c). Streamflow data collection methods at both outlets have utilized several gaging structures since 1962, including flumes and weirs. All stage data were recorded on stripcharts, which were then digitized and converted to streamflow using stage-discharge relationships (Verry et al. 2018; Appendix A). Previous analyses of peak flows from the S4 catchment have only included the S4N outlet. For this analysis, I used the combined discharge values (S4S + S4N) to identify the total annual maximum peak flow from the S4 catchment. Annual maximum flow series were derived by taking the highest discharge value within each water year, which was defined as March 1 – February 28/29.

S2/S6 Experiment. The pretreatment period in the S2/S6 experiment began in 1976 with a four-year calibration period between catchments. The control catchment, S2, is 9.7 ha in size, which includes a 3.2 ha central peatland. The treatment catchment, S6, is 8.9 ha in size, with a 2.0 ha central peatland. In March-June of 1980, the aspen uplands in the treatment catchment were clearcut-harvested, with 77% of the catchment area harvested. During the summers from June of 1980 to 1982, the catchment was grazed to suppress aspen generation. In May of 1983, red pine (*Pinus resinosa*) and white spruce (*Picea glauca*) were planted in the clearcut area, with ~70% of the upland area in red pine and ~30% in white spruce. The same water year definition as in the S4/S5 experiment was used to determine the annual maximum flow series.

2.2.2: General Approach

Three statistical methods were used to detect differences in annual maximum flows due to forest harvesting and regrowth, utilizing the two paired-catchment experiments. The first method consisted of traditional linear regression to extend previous approaches at the MEF (e.g., Sebestyen et al., 2011b) that facilitate inferences about differences in expected magnitudes of annual maximum flows. The second method utilized logistic regression analysis, with parameters estimated using a Bayesian method, to determine the probability that the annual maximum flow in any given year was generated by the same precipitation event on the control and treatment catchments, which I termed a "coupling analysis". Finally, I utilized nonstationary flood-frequency models of the annual maximum streamflow series fit to observed data using a Bayesian technique to explore differences in the entire probability distribution of annual maximum peak flow magnitudes across return intervals. This analysis supports inferences about how flood magnitude and probability of occurrence change due to forest harvesting and regrowth. Thus, these three statistical approaches offer complementary insights into how forest cover change affects the magnitude, occurrence probability, and timing of peak discharges.

2.2.3: Linear Regression

The effect of different catchment treatments compared to the control catchment conditions were assessed using least squares ANCOVA regression analysis, in which the treatment catchment annual maximum discharge series was assumed to be related to the control catchment annual maximum discharge series through a linear relationship, with slope effects and intercept effects determined for pre- and post-treatment time periods (Table 2.1), following Sebestyen et al. (2011b). Four decades after harvesting on the S4 catchment reflects commercial maturity for the regenerating aspen forest in Lake States conditions, where rotations are typically ~40 years, depending on site quality (Bradford and Kastendick, 2010). Finally, following standard ANCOVA methods, this included a normally distributed error term with a constant residual variance.

For both the S4/S5 and S2/S6 experiments, I detected outliers through standardized residual and residual-versus-leverage plots and used a generalized least squares approach (GLS) to prevent the disproportionate influence of those outliers. The generalized least squares approach was identical to the least-squares ANCOVA, except it introduced a residual variance that linearly increases with the observed control catchment annual maximum flow, which allowed for a looser relationship between the control and treatment catchments during higher flow events, thus reducing the influence of high-flow outliers. ANCOVA analyses were conducted using R Version 3.6.2 (R Core Team, 2019) using the base ordinary least squares regression function (lm) and the generalized least squares regression function (gls) found in the nlme package (Pinheiro et al., 2019).

2.2.4: Coupling Analysis

Control and treatment catchment annual maximum discharges may be generated due to different precipitation events or even precipitation mechanisms (snow or rain), and thus become "decoupled" in any given year. To generate observed binary time series of the occurrence of event-decoupling versus no-event-decoupling, I used a minimum threshold of seven-day separation between annual maximum flow in the treatment catchment and the control catchment. Years in which the catchments had annual maximum flows occurring greater than seven days apart were considered to have "event-decoupled" annual maximum flows (i.e., the annual maximum flow was due to different events on each catchment). The seven-day threshold between catchments was chosen from a visual inspection of discharge records that showed between successive peaks within a single catchment that occured greater than seven days apart, discharge generally decayed to approximately pre-event discharge, indicating the relative independence of peaks occurring greater than seven days apart. When the annual maximum flows on the control and treatment catchments were created by different streamflow generating processes in a given year (snowmelt defined as occurring in March or April versus rainfall defined as occurring in June or beyond), I termed this "process-decoupling," and created binary process decoupling series in addition to the binary event decoupling series.

To determine the probability of event and process decoupling, I analyzed the observed binary decoupling series within pretreatment and multiple post-treatment time periods (Table 2.1) for both catchment experiments using logistic regression with parameters estimated through a Bayesian technique, shown in Equation 2.1.

$$Decoupled_i \sim Bernoulli(p_g) \tag{2.1}$$

$$logit(p_g) = b_g$$

The probability of decoupling in year *i* in the time series block *g* is p_g, which corresponds to a log-odds (or "logit", log(p_g /(1- p_g)) of b_g. I used Bayesian-based Markov chain Monte Carlo (McMC) sampling (Gelman and Rubin, 1992) to generate a full probabilistic estimate for b_g conditioned on the observed binary series. Specifically, for the McMC sampling, I implemented the JAGS ("Just Another Gibbs Sampler") algorithm (Plummer, 2003) with the "R2jags" package (Su and Yajima, 2015) in R. To test whether the decoupling probability p_g increased from the control case due to treatment, I determined the proportion of McMC samples that predict the decoupling probability for each post treatment time period (p_g) to be less than in the pretreatment period ($p_{pretreatment}$). This proportion then corresponds to a "Type-S error" probability, or, the probability of erroneously concluding that $p_{pretreatment} < p_g$, where g ≠ pretreatment (Gelman et al., 2012; Gelman and Tuerlinckx, 2000). I can claim with (1 – pvalue)*100% confidence that the probability of control and treatment annual maximum flows occurring due to independent precipitation events (or different streamflow generating processes) in any given year increases due to treatment.

2.2.5: Flood-Frequency Analysis

Choice of Distribution. I used a Bayesian approach to fit observed annual maximum flow to the generalized extreme value (GEV) distribution, which has the following cumulative distribution function for the annual maximum discharge Q:

$$F(Q;\mu,\sigma,\xi) = \begin{cases} exp\left[-\left(1+\xi\left(\frac{Q-\mu}{\sigma}\right)\right)^{-1/\xi}\right], \xi \neq 0 \\ exp\left[-exp\left(-\left(\frac{Q-\mu}{\sigma}\right)\right)\right], \xi = 0 \end{cases} \tag{2.2}$$

After estimating parameters for Equation 2.2 using McMC, I sampled across different probabilities of occurrence to estimate annual maximum flow magnitudes at given return intervals, as in flood-frequency analysis (Gumbel, 1941). To capture non-stationarities, I developed time-evolving estimates of the location parameter μ (possible range of $-\infty, \infty$) and scale parameter σ (possible range of $0, \infty$). The shape parameter ξ (possible range of $-\infty, \infty$; however, the mean of the GEV $\rightarrow \infty$ for $\xi > 1$) was held stationary due to the narrow range of ξ for which the GEV has a finite (thus physically plausible) mean, and consistent with other nonstationary flood-frequency analyses of paired catchment data (Yu and Alila, 2019). The resulting non-stationary GEV models applied to treatment and control catchments were then compared to detect treatment effects. More details on the selection and fit of GEV models and comparisons to the fit of other candidate extreme value distributions are provided in the Appendix A (Figure A1; including comparison results in Table A1).

Nonstationary Parameter Evolution. Explicitly nonstationary models require a defined form for parameter trends through time (Koutsoyiannis, 2011). In order to capture the alterations in upland forest cover in the catchment experiments, I pose the temporal trend structure shown in Figure 2.2 for the location and scale parameters (μ and σ) of the GEV distribution (Eq. 4). As mentioned earlier, the shape parameter (ξ) for the GEV distribution was held constant in time. Bayesian-based McMC sampling (again with the JAGS algorithm (Plummer, 2003) in the "R2jags" package (Su and Yajima, 2015) in R) was implemented to estimate the hyper-parameters needed for the nonstationary μ and σ (and stationary ξ) models for the treatment and control watersheds (Figure 2.2, and further described below), using maximum flow observations. The advantage of the Bayesian-based McMC approach is that it provides full "posterior" distribution estimates of the hyper-parameters, which incorporate in a statistically consistent way both constraints from the maximum flow observations as well as "prior" information (represented by prior probability distributions) about the hyper-parameters based on previous knowledge of the site and/or physical limitations (Smith and Roberts, 1993).

For S4/S5, the general structure of the nonstationary model for the GEV location and scale parameters (μ and σ) was assumed to follow a piecewise linear trend with time *t* (water year) during its regrowth period, based on breakpoints at the year of complete upland clearcut (t = 1972; 71% of watershed area harvested) and the recovery year (t_r) (Equation 2.3; Figure 2.2a):

$$\begin{bmatrix} \mu(t) \\ \sigma(t) \\ \xi \end{bmatrix} = \begin{bmatrix} \mu_{mature\ aspen} + slope_{\mu} * (t - t_r) * \alpha_t \\ \sigma_{mature\ aspen} + slope_{\sigma} * (t - t_r) * \alpha_t \\ \xi \end{bmatrix} \tag{2.3}$$

with

$$\alpha_t = \begin{cases} 1 & \text{if } t \geq 1972\ and\ t < t_r \\ 0 & otherwise \end{cases}.$$

.

Note that I omitted 1971 from the analysis to avoid complications due to only partial upland clearcut conditions in that year. Bayesian-based McMC sampling was used to estimate ξ, $t_{recovery}$, $\mu_{matureaspen}$, $slope_{\mu}$, $\sigma_{matureaspen}$,and $slope_{\sigma}$ (Equation 2.3).

In previous assessments, recovery of peak flow characteristics for post-harvest aspen regeneration have been hypothesized to occur ~16 years after harvest (Sebestyen et al., 2011c; Verry, 2004, 1986; Verry et al., 1983). The 16-year recovery has been based on considerations of aspen growth rate and crown formation (Perala and Verry, 2011), and previous discharge regression analyses at MEF showing that snowmelt-associated peaks increased for 15 years after harvest (Verry, 2004). Thus, my McMC calculations included a moderately informative prior distribution for the $t_{recovery}$, consisting of a discrete approximation of a normal distribution centered on the 16th year after harvesting (1988) with a standard deviation of two years. A discrete approximation of the normal distribution was used to represent the recovery year to an integer year post-harvest, because the time step of the input data was one year. The shape parameter was constrained between 0 and 1 (as discussed in 2.3.3: Choice of Distribution), and all other prior distributions were set as noninformative. For more information on choice of prior distributions, see Appendix A.

For the S2/S6 experiment, I modeled the location and scale parameters (μ and σ) of the GEV distribution with a piecewise linear model with time *t* (calendar year) that includes stationary values in the pretreatment time period (1976-1979), different stationary values for the years following upland clearcut when the uplands were grazed (1981-1983), decreasing values through time after conifer planting (1984 until the recovery year t_r), and yet another set of stationary values associated with canopy closure of the conifer forest after the recovery year, ~ 2000. (Equation 2.4; Figure 2.2b):

$$\begin{bmatrix} \mu(t) \\ \sigma(t) \\ \xi \end{bmatrix} = \begin{bmatrix} \mu_{pre} + \mu_o * a_t + slope_\mu * (t - 1984) * b_t + slope_\mu * (t_r - 1984) * c_t \\ \sigma_{pre} + \sigma_o * a_t + slope_\sigma * (t - 1984) * b_t + slope_\sigma * (t_r - 1984) * c_t \\ \xi \end{bmatrix} \quad (2.4)$$

and

$$a_t = 1 \; for \; t \geq 1981, else \; 0$$

$$b_t = 1 \; for \; t > 1984, else \; 0$$

$$c_t = 1 \; for \; t \geq t_r, else \; 0$$

Note that I omitted 1980 from the analysis to avoid complications due to only partial upland clearcut conditions in that year. Analogous to the S4/S5 experiment, I applied Bayesian-based McMC sampling to estimate the stationary shape (ξ) parameter, μ_{pre} and σ_{pre}, the slope of the location and scale parameters as the conifer forest grows ($slope_\mu$ and $slope_\sigma$), the effect of harvesting on the location and scale parameters (μ_o and σ_o), and the recovery year t_r (Equation 2.4).

Similar to the approach for estimating the recovery time for the S4/S5 experiment, I included a moderately informative prior distribution in the McMC calculations that is a discrete approximation of a normal distribution centered on 17 years after harvesting (2000), when the canopy is likely to have closed based on previous work (Sebestyen et al. 2011b), and a two-year standard deviation. For information on the noninformative prior distributions used for all other hyperparameters, see Appendix A.

Treatment Effects. Using observations during the pre-treatment time, I generated a linear regression equation for calculating the annual maximum flow series in the treatment catchment based on the annual maximum flow series in the control catchment similar to (Alila et al., 2009). Assuming that this regression equation isolates the non-climatic biophysical differences between the two catchments without treatment, I then applied it to the control catchment annual maximum flow during the post-treatment time

(C_{postT}) in order to predict the expected annual maximum flow series in the treatment catchment during that time had the treatment not occurred ($\tilde{T}_{postT}$):

$$\tilde{T}_{postT,i} = b_0 + b_1 * C_{postT,i} \tag{2.5}$$

where i is the time index during the post-treatment period, and b_0 and b_1 are coefficients estimated using pre-treatment time observations. The full time series of annual maximum flow in the treatment catchment had the treatment not occurred, from the pre-treatment time through the post-treatment time period, is then represented by the concatenation of the pre-treatment observations and $\tilde{T}_{postT,i}$, and I refer to this full time series as $\tilde{T}_i$.

To acknowledge uncertainty in the coefficient estimates and for consistency with the probabilistic treatment of other parameter estimates, b_0 and b_1 in equation 2.5 were determined using Bayesian-based McMC sampling (again with the JAGS package in R). Seventy McMC samples of b0 and b1, representing 70 possible parameter sets given the observed maximum flows, were used to generate 70 possible series of $\tilde{T}_i$ as an uncertainty range of the expected annual maximum flow on the treatment catchment, had treatment not occurred. Each of these 70 series of expected annual maximum flow were then used as data to fit the same form of the nonstationary GEV distributions that were used for the treatment catchments (Equations 2.3 and 2.4), and comparisons of the results for the expected no-treatment cases and for the observed with-treatment case were used to draw inferences about harvesting and regrowth effects. This utilizes the catchment pairing to control for climate covariates. I note that the number of series examined was limited to 70 because of the computational burden of fitting each of the nonstationary GEV models to the "data" using McMC. The calibration regression (Eqn. 2.5) occasionally predicted negative annual maximum discharges for S6 (on average over the 70 series, 2-3 years within the 40-year series), which I replaced with 0 cfs.

To rigorously test my hypothesis that annual maximum flow increases with treatments across different return intervals, it is necessary to report probabilities of occurrence. To reveal differences across the GEV cumulative distribution function (Equation 2.2), random samples from the posterior densities for location (μ), scale (σ), and shape (ξ) parameters in the time periods of interest were taken to construct 100,000 cumulative distribution functions for the expected and observed GEV model fits (Eqns. 2.3 and 2.4). For S4/S5, the effect of upland clearcut harvesting was inferred by comparing cumulative distribution functions from the observed (with treatment) and expected (no treatment) models (Eqn. 2.3) for the year 1972, which is the year for which the treatment effect of harvesting was largest (e.g., for the effect of forest harvesting for S4: μ = $\mu_{matureaspen} +$, etc.). For the S2/S6 experiment, the effect of upland clearcut harvesting was inferred through a similar comparison during the stationary period 1981-1983, immediately after upland clearcutting and during grazing. Further, the effect of conifer conversion was inferred through comparing observed and expected model results during the stationary period after conifer canopy closure on the treatment catchment. Expected (control) and observed (treatment) cumulative distribution functions for return intervals N = 1.5 to 50 years were compared through finding the proportion of the treatment cumulative distribution functions that are greater than (less than) the expected cumulative distribution functions as a “Type S” error probability for each return interval (Gelman and Tuerlinckx 2000), which is the chance of incorrectly concluding that the N-year peak flow has increased (decreased) when they have in fact decreased (increased) or stayed the same.

2.3: RESULTS

2.3.1: ANCOVA, GLS

The ANCOVA results for the S4/S5 Experiment did not show any post-treatment slopes (b0) or intercepts (b1) statistically different than the pretreatment time period (all $p > 0.10$), including in the decade immediately following upland harvesting ($p = 0.47$ for intercept, $p = 0.26$ for slope) (Figure 2.3a). In general, no slopes or intercepts were significantly different than another according to a Type-II ANOVA (Langsrud, 2003), with slopes $p = 0.36$ and intercepts $p = 0.38$ (Figure 2.3a). A GLS regression was also used because the ordinary least squares (OLS) regression detected some outliers. The GLS results also indicated there were no statistical differences of slopes (b0) or intercepts (b1) in the post-treatment time periods compared to the pretreatment time period (all $p > 0.25$).

The ANCOVA results for the S2/S6 experiment showed a significant decrease in regression slopes (b1) for the "Growing Forest" and "Closed Canopy" conifer conditions compared to the pretreatment time period ($p = 0.001$ and 0.004, respectively), but no significant difference between the open/young forest and pretreatment time periods (Figure 2.3b). This decrease supports previous work that has found decreases in peak flows after conversion to conifer species (Sebestyen et al., 2011c). However, there were outliers according to residuals versus leverage plots, and all significant effects of treatment groups were not apparent when using GLS. The regression slopes (b1) corresponding to the "Growing Forest" and "Closed Canopy" time periods were no longer significantly different from pretreatment ($p = 0.15$ and $p = 0.46$, respectively). The GLS regression was a better fit according to diagnostic plots such as residuals versus fitted and residuals versus leverage plots.

2.3.2: Coupling Analysis

Harvest induced a greater probability of the annual maximum flow being due to different independent events (> 7 days apart) on control and treatment catchments. The decoupling is captured in the logistic regression results for S4/S5 and S2/S6 (Table 2.2; Figure 2.4a and 2.4c). The same general trend is seen in both experiments, but I was only confident for the S4/S5 experiment. Furthermore, harvest induced a greater probability of process-decoupling in the S4/S5 experiment, such that annual maximum flows occurred due to different streamflow generating processes on control and treatment catchments (Figure 2.4b, Table 2.2). For eleven of the twelve times that different streamflow generating processes caused the annual maximum flow on control and treatment catchments in a given year, S4 had a rainfall peak (occurring in June or beyond), and S5 had a snowmelt peak (occurring in March or April). Streamflow generating process decoupling was rarely observed for the S2/S6 experiment (only two times in the 41-year record), so process decoupling analysis was not implemented for the S2/S6 experiment.

2.3.3: S4/S5 Flood Frequency Analysis

Expected annual maximum discharge in the absence of treatment was determined based on post-treatment timeframe annual maximum discharges on the control catchment using the 70 McMC samples of the estimated parameter distributions for the pretreatment-period calibration phase (Figure 2.5a). In the pretreatment calibration regression (Equation 2.5), expected annual maximum discharge on S4 given the annual maximum flow on S5 had an intercept estimate of 0.695 (95% credible interval: -0.108 to 1.475) and a slope estimate of 1.288 (95% credible interval: -0.311 to 1.752). For reference, the r^2 value between the annual maximum discharge on the treatment catchment, using the posterior density means for b_0 and b_1 (Equation 2.5), and the control catchment annual maximum discharge in the calibration phase was 0.32.

The N-year discharge increased due to upland clearcutting on the treated catchment compared to expected conditions without treatment in the first year after clearcutting when the effect of harvesting was highest according to my model (1972) (Figure 2.6). I had between 80-85% confidence in discharge increases for return intervals greater than 10 years (Type-S $p < 0.20$), whereas I had only 30% confidence for an increase in the 1.5-year discharge (Figure 2.6b). These results indicated a greater treatment effect for larger discharges. Averaged across all return intervals, I had 80% confidence that annual maximum flows increased, with increasing confidence for increases at larger return intervals ($p = 0.16$ for the 50-year annual maximum flow). Further, the increases in annual maximum flows for each return interval stemmed largely from an increase in the scale (σ; $p = 0.27$) and shape (ξ; $p = 0.19$) parameters due to harvesting (Table 2.3). The shape parameter controls the “heavy-tailedness” of the distribution of annual maximum flows; for the entire record on the treatment watershed S4, the shape parameter equaled 0.40, versus 0.20 on the entire record of the expected conditions, indicating that treatment induced greater probability of very high annual maximum flows. The shape parameter was modeled as a constant value throughout the entire record within each individual GEV model (one for the treatment data, seventy for the expected data). The shape parameter on the treatment catchment, throughout the entire record, was greater than the shape parameter on the entire record of the calibrated control catchment discharges that represented the annual maximum flows that I would have expected on the treatment catchment in the absence of treatment. Because the same annual maximum flow series was used for both expected and observed model fits, this difference in shape parameter between expected and observed model fits can be attributed to harvesting treatment. Even after recovery of the location and scale parameters to pretreatment values on the treatment catchment, the larger shape parameter for the treatment catchment caused larger annual maximum flows, with ~88% confidence, from the 10-year to the 50-year annual maximum flow, than what was expected in the absence of treatment. These results indicated that post-harvest changes in annual maximum flows may be driven largely by changes to the variability of annual maximum flows, as the location parameter (related to mean flow) potentially even decreased ($p = 0.33$) whereas I am more confident in increases to the scale parameter (related to variance; $p = 0.26$), and the shape parameter, related to the probability and variance of very large annual maximum flows ($p = 0.19$). For expected and observed posterior densities for location, scale, and shape, see Figure A2.

The recovery year for location and scale parameters was relatively unchanged from my moderately informative prior distribution. Based on model results, I was 90% confident that recovery of the location and scale parameters to pretreatment conditions occurred between 12 and 18 years after harvest. The shape parameter was held stationary within each model fit (Eqn. 2.3). However, I obtained different shape values when GEV models were fit for expected versus observed time series ($p = 0.19$; Eqn. 2.3). The difference in expected and harvested catchment shape parameters indicates that the shape parameter may have been altered with forest harvesting, and was nonstationary. Thus, I do not know when overall recovery happened because I only assumed location and scale were nonstationary within each individual model, so I have no means of testing when the shape parameter returned to what I would expect in the absence of treatment. My results indicate high confidence (~88%) that annual maximum peak flows were higher on the treatment catchment than what would be expected in the absence of treatment even after recovery of the location and scale parameters. There is no way to investigate when recovery of the shape parameter occurred, if at all, within this modeling framework.

2.3.4: S2/S6 Flood Frequency Analysis

Post-treatment annual maximum discharges on the control catchment were adjusted according to the calibration regression (Figure 2.5b), which had an intercept of -0.120 (95% credible interval: -0.649 to 0.409) and a slope of 1.324 (95% credible interval: 1.106 to 1.550). For reference, the r^2 value using the posterior density means for b0 and b1 was 0.99.

I did not find an increase for which I was confident for the annual maximum flow in the first year after clearcutting when the treatment effect should be highest based on Equation 2.4 (Figure 2.7a, 2.7b). Across the cumulative distribution function, all p-values were between 0.35 and 0.45 up to the 50-year return interval (Figure 2.7b). Further, location, scale, and shape parameters stayed the same (Table 2.3; Figure A3).

There was also no effect of conifer conversion on the annual maximum flow for the S6 catchment (Figure 2.7c, 2.7d). Here, testing for a hypothesized decrease in annual maximum flows, I was not confident in any of the modeled decreases in the annual maximum flow across return intervals up to the 50-year event, with p being about 0.35 for low discharge events, but going up to 0.5 for larger discharge events, indicating that I have no more confidence that flows decreased than I do that flows increased due to conifer conversion (Figure 2.7d). Location, scale, and shape parameters stayed the same; unlike for S4/S5, I do not have evidence that the shape parameter was nonstationary (Table 2.3).

The recovery of the location and scale parameters to a new stationary state after replanting with conifers was heavily influenced by my semi-informative prior which centered the recovery when canopy closure occurred, which was 17 years after conifer planting. However, because no effects of upland clearcutting or canopy conversion were found, recovery year had little meaning.

2.4: DISCUSSION

Based on the ANCOVA and GLS regression analyses, no significant increases were found for annual maximum flows in the time periods directly after upland clearcut harvest when the uplands were in open/young forest conditions, compared to the pretreatment time period (Figure 2.3). My linear model results contrast with previous ANCOVA analyses that have found significant effects of harvesting on snowmelt and rainfall-caused peaks for the S4 experiment (Verry et al., 1983). There were several factors that may explain this discrepancy between past studies and these results, based upon differences in analyses including a longer time period of record (additional 10 years of data used here), my use of the total annual maximum discharge on S4 (compared to previous analyses based only on the S4 north gauge), and my examination of the annual maximum discharge including both rainfall and snowmelt events.

I observed significant decoupling between the event which causes the annual maximum flow on control and treatment catchments, as well as decoupling between the type of event, rain or snowmelt, on the S4/S5 pair in a given year. Decoupling likely accounted for differences between my results and those of previous studies. Annual maximum discharge from the catchments is not the same as individual examinations of snowmelt and rainfall-caused peaks that have been analyzed previously (Verry et al., 1983; Sebestyen et al., 2011b). In my analysis, peak discharge on control and treatment watersheds was not always due to the same event, hence not chronologically paired. Previous ANCOVA analysis of paired-catchment data, at the MEF and elsewhere, relied on chronological pairing of events, such that peaks generated during the same event were compared on control and treatment catchments. The significant event- and process-decoupling I found in the S4/S5 catchment pair calls the appropriateness of chronological pairing for the investigation of annual maximum flows into question. As early as the pre-treatment period, catchment pairs had a non-zero probability of event-decoupling (Table 2.2). Event-decoupling was not dependent on the vegetation type but more linked to open vs forest condition. After an initial increase in event decoupling post-harvest in both the S4/S5 and S6/S2 catchment pairs, the incidence of event decoupling decreased towards preharvest levels as forest cover regrew for both the deciduous-regeneration in the S4 catchment and the conifer conversion in the S6 catchment (Figure 2.4a, 2.4c; Table 2.2). The incidence of event decoupling for S6 with closed-canopy conifer uplands, compared to deciduous cover on S2 during the same time period, was no greater than in the pretreatment time period when both S2 and S6 had deciduous cover ($p = 0.563$). Thus, canopy conversion from deciduous to coniferous did not cause event decoupling.

The S4/S5 experiment showed evidence of process-decoupling where S4 was more likely to have a rainfall-caused annual maximum flow while S5 was more likely to be a snowmelt-caused annual maximum flow (Figure A4). In the first decade following harvest, seven of ten of the S4 annual maximum flows were rainfall-caused, while only three of ten were rainfall-caused on S5. Process decoupling was not observed significantly on S2/S6: only two of the forty years of record had process decoupling, which was too few instances upon which to fit a logistic regression. The process decoupling of S4/S5 was possibly due to internal subtle differences between the treatment (S4) and control (S5) catchments that were exacerbated by disturbance. For example, S5 has 5 small satellite wetlands within the upland rim that act as distributed catchment storage other than the central peatland; S4 does not have these upland wetlands. This difference may cause S4 to be more responsive to summer rainfall events than S5. Harvest may have exacerbated these preexisting differences in catchment processing of flood peaks. Catchment size could have also influenced my results. S4 and S5 have significantly larger area than S2 and S6 (>50 ha for S4 and S5, < 10 hectares for S6 and S2). Thus, physiographic variation between S4 and S5 are more likely than between S2 and S6 due to increasing heterogeneity and complexity at larger scales (Blöschl, 2006; Rogger et al., 2017).

The nonstationary flood-frequency analysis indicated increases in annual maximum flows up to the 50-year return interval within the S4 catchment in the first year after harvest, with the effect size of forest harvesting increasing with increasing return interval (1972: Figure 2.6). The effect of upland clearcutting on annual maximum flow was predicted to be greatest in the first year after harvest for S4 (Eqn. 2.3), so this was the year for which the effect was assessed. Broadly, the increases in annual maximum flows were consistent with previous results that showed increases in snowmelt-caused peak discharges for 15 years and rainfall-caused peak discharges for 7 years after harvesting for the S4 experiment (Verry 2004; Sebestyen et al. 2011b). Further, when Verry et al. (1983) compared stationary flood-frequency distributions for pre- versus post-treatment rainfall peaks for S4 versus S5, they found the 10-year return interval annual maximum rainfall-caused discharge increased more than the 2-year discharge in the decade after harvesting. The process-decoupling between S4 and S5, discussed above, helps explain the increases found in Verry et al.'s (1983) frequency analysis. When only rainfall peaks were compared, the annual maximum from S5, which tended to be snowmelt-caused, was not included.

I found an increasing effect size of forest harvesting for events of increasing return interval, which was similar to previous MEF work (Verry et al. 1983) but opposite the trend elsewhere in North America (e.g., Thomas & Megahan, 1998; Buttle, 2011). My results indicated that in the first year after harvest, the 2-year discharge was effectively the same on the harvested S4 catchment versus expected conditions: 2.98 cfs versus 3.08 cfs, while the 50-year discharge approximately doubled from 16.49 cfs to 32.43 cfs. Despite increasing uncertainty at larger return intervals, my confidence in the presence of an effect on peak flows remained relatively constant from the 10-year even up to the 50-year discharge, at about 80-85% (Figure 2.6b). Thus, my results do not match the paradigm of decreasing effect size with increasing return interval that has been largely derived from paired-catchment studies in western North America catchments with very different landscapes and ecosystems (e.g., Thomas & Megahan, 1998; Buttle, 2011). For the first year after harvest (Figure 2.6), I had between 80-86% confidence in the flow increases due to forest harvesting. However, my confidence in flow increases due to treatment is closer to 88% for large discharge events after recovery of the location and scale parameters recover due to an increased shape parameter. Further, the results of increasing effect size with increasing return interval was consistent with recent flood-frequency analyses of paired catchment data in western North America (Alila et al., 2009; Green & Alila, 2012; Yu & Alila, 2019), and was consistent with the flood-frequency analysis of rainfall peaks at the MEF done by Verry et al. (1983).

The effect of harvest apparent for large return-interval events was heavily influenced by the difference in the GEV model shape parameter on the treatment catchment. This shape parameter was held constant within each GEV model of annual maximum flow. However, when fit to the annual maximum flow series on S4 (treatment), it was larger than when fit to the 70 series of expected conditions had treatment not occurred. The difference in shape parameter value for expected versus observed treatment models caused the increases in annual maximum peak flows to be present in the first year after harvesting. Further, increases in the annual maximum flow after the recovery of location and scale parameters on S4 are evident with high confidence (~88%), even after recovery of the nonstationary location and scale parameters. It should be noted that three of the four largest discharge events on S4 (in 1999, 2002, and 2011) occurred after the hypothesized 16-year recovery estimate for location and scale parameters, and were all in response to rainfall in June or July. Of these three peaks that occurred greater than 16 years after harvest, two were above the 90% credible interval for the expected value based on the pretreatment calibration (1999 and 2011: Figure 2.5). Shape parameters, related to the tail of the annual maximum flow distribution that controls the highest flow events, may thus be nonstationary and sensitive to forest harvesting, contrary to my initial assumption and that of others (Yu and Alila, 2019). However, fitting a nonstationary structure to all three parameters on 54 years of data would rapidly increase the ratio of parameters per data point, decreasing the usefulness of such models.

It is noteworthy that the flood-frequency analysis indicated high confidence for an effect of harvest for the S4/S5 experiment, but not for the S2/S6 experiment (where my confidence in annual maximum flow changes largely ranged between 55-65%). However, the investigation of the S2/S6 experiment was hindered by a short preharvest time period (4 years), which may have been inadequate for detecting a difference due to harvesting and conversion (Loftis et al., 2001; Sebestyen et al., 2011c). Further, the annual maximum flow record for S2/S6 was shorter than for S4/S5, and because S6 was grazed after upland harvesting before forest cover was allowed to regenerate, more parameters were necessary to model S2/S6 compared to S4/S5 (Figure 2.2). Fitting more parameters resulted in greater uncertainty for individual parameter estimates. I also consider the possibility that there truly was no effect of harvesting or conversion. Unlike for S4, I did not have strong evidence of streamflow generating process decoupling for the S2/S6 experiment due to harvesting, which may indicate that S4 passed some flood-generation threshold due to disturbance while S6 did not. Nonlinear and threshold processes have been observed in northern headwater catchments, in which there are disproportional runoff responses to forcing inputs (Ali et al., 2015) and have been invoked for explaining increases in large peak flows and a sensitive upper tail for extreme value distributions

(Alila et al., 2009). Further, S6 has an elongated shape, in contrast to S4, which is more circular and has two outlets (Figure 2.1). More elongated watersheds tend to have relatively lower peak flows (Black, 1972). The peatland is also more centrally located within the catchment in S6 than S4 (Figure 2.1), which could contribute to its ability to dampen peak flows out of the catchment. Finally, catchment differences between individual pairs may have contributed to the different flood-frequency findings in each experiment, as harvesting was found to exacerbate preexisting differences in these catchments via streamflow generating process decoupling. For example, the control catchment S5 includes 5 small satellite wetlands within the uplands in addition to its central peatland. The preexisting differences in S4/S5 that may have contributed to my findings were not present with the S2/S6 pair.

No effect of canopy conversion from deciduous to coniferous upland species on the annual maximum flow was found in the flood-frequency analysis of the S2/S6 experiment. Uncertainty with low pretreatment sample size and number of parameters versus number of datapoints apply similarly to these results. Given this, I note that the observed cumulative distribution function tended to decrease across all return intervals, which was the hypothesized direction of effect (i.e., conifer cover decreases flood peaks) (Figure 2.7c, 2.7d). The ANCOVA analysis supported significant decreases in peak flows while the conifer forest grew and after canopy closure, but once the effects of high-flow outliers were dampened using GLS regression, the significance of these decreases disappeared. The annual maximum flow on both S2 and S6 was relatively low for the last decade of record (2006-2016), reflecting a prolonged period of relatively low flow (Figure 2.5). This period of low flow coinciding roughly with conifer canopy closure did not offer much data on how larger or medium-sized peak flows responded to canopy conversion for a bulk of the closed-canopy conifer conditions, and caused larger flows in that period to exert stronger influence on the regression as outliers.

Limitations in my study included inherent factors in the paired-catchment design (e.g. past harvest treatment, pairings, etc.) and my focus only on annual maximum flow. Both experiments were partial clearcuts (~75% of catchment area) on only the upland portion of the catchments. The unharvested forested wetlands, which tend to attenuate flooding effects (Detenbeck et al., 2005) occupy substantial catchment area. Substantial portions of the harvests were also in the winter on frozen soils to reduce soil impacts and erosion. Furthermore, catchments were rapidly revegetated, leaving few years of "open" conditions on the uplands from which to derive inferences about the effects of open canopy conditions on peak flows. For example, the S4 clearcut was staggered between 1970 and 1972, and before the upland clearcut on S4 was complete, on the portion of the uplands cut the year before there were 41,000 stems/ha, and these were 2 meters tall (Verry et al., 1983). It may take several years for altered hydrology to equilibrate to a new stationary state after conversion to open conditions (Brown et al., 2005). Thus, there are potentially only several years of a transient state in between mature forest and recovery conditions for investigating these effects. The transient state of the effect of forest cover change was reflected in the large uncertainty bounds in the nonstationary models.

Use of a calibration period was another source of uncertainty. Because of the relatively short calibration periods (< 10 years) when applied to the 30+ year post-treatment control catchment flows, I assumed that the relationship between the control and treatment catchments would have been stationary if the treatment not occurred. Additionally, some "expected" values were extrapolated from the pretreatment calibration regression, despite uncertainty about how the calibration regressions may apply to these larger, extrapolated discharges. The selection and appropriateness of a pretreatment calibration regression controlling for the biophysical differences in control and treatment catchments across the range of observed climatic conditions is a large tenant in the paired catchment study design. This tenant of the paired catchment design has been debated through the years, both criticized (Renne, 1967; Zégre et al., 2010) and defended (Hewlett et al., 1969; Neary, 2016). To incorporate my uncertainty about the calibration regressions, I sampled across 70 different slopes and intercepts fit with the calibration regressions. This incorporation of uncertainty in the calibration period is a considerable improvement to remedy issues of calibration uncertainty, but some uncertainty about the calibration, and how it applies for high flow regimes, remains by virtue of the paired catchment study design.

2.5: IMPLICATIONS FOR ANALYSIS OF PAIRED-CATCHMENT STUDIES

Several important ramifications for paired-catchment studies of the forest-peak flow relationship were revealed by this study. As disagreement about how forest cover affects flooding often stems from the statistical "lens" used to look at the question, it is critical to be absolutely clear about the benefits and limitations of various methods, to clearly define the inference space for which the methods are valid, and how this statistical inference space corresponds to a physical inference space. First, the importance of utilizing methods that incorporate the probabilistic nature of peak flows, for example in the nonstationary flood-frequency framework in my study, are critical for finding differences in peak flows. Increased use of probabilistic flood-frequency methods allows researchers to explicitly make inferences about effects of forest harvesting across multiple return intervals, which is not possible for traditional ANOVA/ANCOVA analyses. Next, ANCOVA is highly sensitive to high-flow outliers, which is not adequately remedied through relaxing the constant residual variance assumption in the GLS analysis. Because my flood-frequency model of S4/S5 indicated that flow increases after forest harvesting can manifest as a change in occurrence probability for very large flows (i.e., increase in shape parameter), it is critical to use a method that is robust to high-flow outliers and associated uncertainties, such as a probabilistic framework.

The results of the "coupling analysis" revealed an important peak flow variable that was not captured within ANCOVA *or* flood-frequency analysis; however, the decoupling does not violate the requirements or assumptions of the flood-frequency analysis. These confounding factors indicated that care is needed in the analysis of paired-catchment data, and that simply assuming because the catchments are similar in size and even adjacent does not necessarily mean that their peak flow generation is strongly paired. Methods robust to potential changes in pairing relationships should be developed when analyzing paired-catchment data. The decoupling analysis illustrates the importance of analyzing the probabilistic distribution of peak flows as well as subtle changes in generating process may constitute a threshold change, and can manifest as large changes at the tails of extreme value distributions.

The "coupling analysis" also highlighted the importance of chronological pairing as an underlying assumption in ANCOVA-based methods. In some catchments, for example mountain catchments that reliably have snowmelt-derived peaks every year (Alila et al., 2009), this chronological pairing of annual maximum peaks may be possible. However, I found that harvesting may induce or enhance an alteration in the individual event and, in some cases, the event type that produces the annual maximum flow. I further hypothesize this could be due to the landscape and climate of the MEF, which calls into question the pairing. The lack of chronological-pairing likely explains the poor relationships between annual maximum flows on control and treatment catchments in my ANCOVA/GLS analyses.

2.6: CONCLUSION

No significant effect of forest harvesting on annual maximum flows was found using ANCOVA/GLS or nonstationary flood-frequency model of S2/S6, for which there were only 4 years of pretreatment data. However, increases in annual maximum flows across all return intervals were supported with high confidence (80-85%, i.e, ~6:1 odds that flows increased) for the S4 clearcut and aspen regeneration experiment according to nonstationary flood-frequency analysis. ANCOVA-based methods were not adequate to fully investigate the effect of forest harvesting because annual maximum flows “decoupled” after harvest and tended to occur due to different streamflow generating processes. Thus, a critical conclusion is that even if flood magnitude and frequency may or may not be changed by harvesting, the precipitation event that drives the annual maximum flow may change. My study demonstrated the value of using a probabilistic framework to investigate changes in peak flows. This method can support inferences about harvesting effects for specific return intervals, instead of being limited to differences in means (i.e., linear models). Increases in annual maximum flows after forest harvesting increased with increasing return interval for the S4/S5 experiment, which indicates that if this effect truly occurred, it was not limited to small discharge events, as is the typical paradigm. More investigation is needed, particularly pairing computational, physically based models with Bayesian parameter estimation methods to minimize uncertainty about the form of nonstationarity introduced by harvesting, and to gain more physically based insight into this effect.

CHAPTER 3:

Investigating the effects of forest disturbances on streamflow for a mesoscale postglacial catchment using remotely sensed datasets: a case study

3.1: INTRODUCTION

The effect of forest cover change on water quantity has been widely studied and debated (Alila et al., 2009; Bathurst et al., 2020; Bosch and Hewlett, 1982; Stednick, 1996; Zon, 1927). Small (< 10 km^2) catchment studies have provided the foundation for much of the current knowledge in forest hydrology (Andréassian, 2004). The catchment approach involves the study of hydrological processes with boundaries determined by landscape topography (i.e., surface water drainages), using streamflow as a diagnostic signal of the entire catchment processing of water (Likens, 2001). The catchment approach has historically focused on spatial scales of < 10 km^2 because hydrological fluxes are more easily quantified at these scales, and with greater accuracy than in larger basins with heterogeneous weather and drainage patterns (Andréassian, 2004; Hewlett et al., 1969; Likens, 2001; Loftis et al., 2001). Analysis at the catchment unit integrates many micro-scale processes into a macroscale manifestation of an easily measurable variable: e.g., streamflow and its constituents, aggregating the landscape hydrological and biogeochemical signal of the internal catchment processes.

Despite the dominance of the catchment approach in the modern study of forest hydrology (Andréassian, 2004; Likens, 2001), other methods have also been popular. The catchment approach has several key limitations, including difficulty closing the water balance due to groundwater leakage, unrepresentativeness, and (when the *paired catchment* approach in particular is used) assumptions necessary when deriving pairing relationships (see Chapter 2; also Hewlett et al., 1969). Alternative methods utilized to remedy these weaknesses and support inferences about hydrological processes in working forested watersheds have included controlled plot-scale studies (Pierson et al., 2007), meta-analysis of catchment studies across regions (Ali et al., 2015), and using mathematical models, either physically-based, statistical, or combination (Zégre et al., 2010).

At larger catchment scales, emergent streamflow generation and landscape attributes undermine some of the basic benefits of the catchment approach. The most important differences in catchment processes at a larger scale than the traditional catchment approach include the importance of regional groundwater, increasing catchment heterogeneity, and the importance of large-scale climate variability. These factors influence the generation of streamflow (water quantity), and the waterborne constituents carried by streamflow (water quality).

The changes in catchment processing at larger scales can be conceptualized in critical zone framework. The critical zone (CZ), is defined as the layer of earth from the bottom of groundwater to the top of the tree canopy (Banwart et al., 2013). Streamflow generation depends on the structure and function of a catchment's critical zone – what are the primary biophysical attributes and how do they relate to one another (structure), and what purpose do these structures perform in generating streamflow (function; Jackisch et al., 2017). New CZ structure and function emerge at larger scales. Deeper levels of the critical zone are activated as driving streamflow as streams flow down gradient, representing a vertical axis of critical zone connectivity as spatial scale goes from headwaters to mouth (Figure 3.1a). Thus, structures in deeper layers of the CZ perform an increasingly important role in generating streamflow at larger scales. Regional groundwater increases in importance for generating streamflow at large scales, and as streams increase in size, the dominant processes by which streams thus internally process and exchange water and biogeochemical fluxes change nonlinearly (Figure 3.1b; Laudon and Sponseller, 2018). The benefits of being able to easily quantify inputs and outputs for catchments diminishes at larger spatial scales where regional aquifers are disjoint with surface water drainages, because catchments are defined as surface water drainages.

Small catchments can lack representativeness for their larger counterparts both in the climate signals they filter, and in their landscape attributes. First, regional scale climatic variability occurs at large spatial scales (>100 km^2), driving drainage development and streamflow. Further, the level of heterogeneity in catchment physical characteristics increases with increasing scale. The interaction of many diverse landscape units represents a horizontal axis of connectivity in the critical zone processing of water as catchment size grows from hectares to thousands of square kilometers (Figure 3.1a). Although the streamflow from headwater streams of many catchment studies integrate the characteristics of the contributing area, geologic deposits and bedrock vary at a much larger spatial magnitude than the traditional small catchment study. For example, the average size of a surficial geologic unit in Minnesota is 200 km^2 (Hobbs and Goebel, 1982) – multiple orders of magnitude larger than the catchment studies at the Marcell Experimental Forest in north-central Minnesota (0.1-0.5 km^2). Not only do distinct geological units behave differently between within units, but the boundaries of geological deposits serve as important flow structures as well, such as preferential groundwater flow along some fault boundaries (Bense et al., 2013). As small streams combine at larger spatial scales, different landscape units of geology, cover type, land use, and soils are aggregated in the streamflow signal. The horizontal axis of CZ change as basin scale increases represents how more diverse landscape units each contribute via different processes to streamflow, and how the relationship between landscape units can also drive hydrological behavior at these larger scales (Figure 3.1a).

By virtue of their spatial scale, the streamflow response to forest cover disturbance at larger scales will depend on 1) climate variability, 2) dynamics of vertical and horizontal critical zone generation of streamflow (Figure 3.1a), and 3) the spatial and temporal scale and intensity of the disturbance. This includes how deep the disturbance affects hydrological processing and the effect of disturbance on landscape level heterogeneity and physical characteristics in relation to one another. In this chapter, my objective is to quantify the effect of forest cover disturbance on the way that low-relief glaciated catchments process water and generate streamflow, aggregated as water yield and peak flows, at larger (> 10 km^2) spatial scales than the traditional catchment study, using a case study approach. To accomplish this objective, I plan to test the following hypothesis:

Hypothesis. A spatial threshold exists in low-relief, glaciated catchments below which forest disturbance effects are detectable on surface water hydrology (e.g. annual water yield and peak flow). Above this spatial threshold, land cover effects are negligible among signals of regional groundwater, climate, and water storage.

3.1.2: Emergent Hydrological Drivers beyond the scale of the Catchment Approach

Regional Climate Variability. Forest land cover change is a local phenomenon (e.g., forest harvests in Minnesota are typically < 1 km^2 (Rossman et al., 2016)), whereas climate variation occurs at larger spatial scales (>100+ km^2 (Rogger et al., 2017)). Variability in streamflow is expected to be predominantly explained by climate variation at these larger spatial scales. For example, regional groundwater and lake levels in the Great Lakes fluctuates on a decadal period, possibly driven by large-scale atmospheric circulation patterns across the Pacific Ocean (Watras et al., 2014). Although localized water table fluctuations are closely related to forest cover type (Urie, 1977), climate drives long-term behavior at large scales. However, large-scale land cover changes can be co-dominant with climate in controlling streamflow and waterborne materials: climate change and forest harvesting are expected to be co-dominant drivers of DOC concentrations in large Swedish catchments (Oni et al., 2015).

Increasing Regional Groundwater. As catchment spatial scale increases, streamflow is influenced by increasing basin heterogeneity and regional groundwater interaction (Creed et al., 2015; Laudon and Sponseller, 2018; Oni et al., 2015). This is due to the fact that larger rivers and water bodies serve as local base levels and discharge areas for regional groundwater drainage. Smaller headwater streams are often “perched” above the regional aquifer, while deeper rivers intersect the regional groundwater drainage (Figure 3.1). For example, the headwater peatland catchments at the Marcell Experimental Forest lose, on average, 40% of annual precipitation to deep groundwater seepage (Nichols and Verry, 2001). However, leakage from headwater catchments may be an important component of flow for the parent basins in which they occupy, termed a “groundwater subsidy” (Ameli et al., 2018). In one study, shallow subsurface sources of baseflow decreased dramatically throughout a 5 km^2 catchment, replaced by groundwater in fractured bedrock (Egusa et al., 2016). In boreal Swedish catchments, groundwater was identified as a dominant driver of streamflow and organic carbon with increasing basin size (Laudon et al., 2016; Laudon and Sponseller, 2018; Lidman et al., 2016; Tiwari et al., 2017). Despite these several studies suggesting increasing deep groundwater at larger scales, and the theoretical basis for the interaction, it remains unclear where the relevant "bottom" is for catchments across spatial scales, with different answers among different scientific communities (Condon et al., 2020; Ward and Packman, 2018).

Increasing Catchment Heterogeneity. Catchment characteristics and their relative importance at larger scales is unclear. For example, increasing heterogeneity in land cover and catchment soils, bedrock, and vegetation cover have been widely hypothesized to buffer the peak flow effect of land cover disturbance (Alaoui et al., 2018; Rogger et al., 2017). Some have posited that as headwater catchments join and mix, there is a particular spatial scale (a "representative elementary area", or REA) beyond which local heterogeneities mix to become an emergent large-catchment signal (Asano and Uchida, 2010). Beyond this REA, catchment responses to climate and land cover are self-similar across scales (Asano and Uchida, 2010; Shaman et al., 2004; Woods et al., 1995; Blöschl et al., 1995). For example, overland flow on bedrock outcrops may cause very high peak flows compared to a similarly sized catchment with deeper soils (Burns et al., 2001). Local heterogeneities like bedrock outcrops create varied responses at small scales, but catchment behavior "averages out" and may be self-similar beyond a scale of several square kilometers (Asano and Uchida, 2010). Decreasing importance of local heterogeneities is complementary to the idea that any single disturbance parcel has decreasing effect as catchment size increases. However, there may be new processes that are not simply the additive and averaged effects of many small catchments (Shaman et al., 2004), but rather new scale-dependent processes at work (Blöschl et al., 2007). Thus, there can be considerable difficulty positing self-similar behavior once a REA is reached, and the spatiotemporal scales for which the REA concept is applicable or even reflective of the actual physical condition of catchments is unclear (Fan and Bras, 1995).

As catchment size increases, so does the diversity of landscape characteristics – bedrock, soils, vegetation, and land cover. Catchment storage can also increase, especially in wetland-rich areas. At large scales, the broader geologic history of the area determines the location of different bedrock types, bedrock faults and fractures, and the locations of lakes and wetlands. The physical landscape is not a random repetition of smaller scale features, but rather there are large-scale mechanisms associated with geology and climatology that determine modern landscape features.

Scale and Intensity of Disturbance. Although land cover is expected to decrease in importance for describing streamflow variability at larger scales (Viglione et al., 2016), it is unclear at which threshold climate overtakes land cover as a driver of streamflow. Self-similar behavior of larger catchments has been found at catchment sizes as small as 3 km^2, but effects of land cover change on streamflow have been found at very large scales (e.g., the Minnesota River Basin, >40,000 km^2). The scale and intensity of the disturbance in land cover, as well as the geophysical characteristics of the catchment, determine how streamflow responds to land cover change. Further, changes in climate can interact with changes in land cover in multiple ways, causing emergent discharge trends and interact in nonlinear ways, such as inducing threshold changes and feedback loops. For example, precipitation has increased in the Minnesota River Basin, USA, while at the same time widespread agricultural ditching and tile drainage has homogenized a once-diverse and wetland-rich catchment into largely uniform systems of upland crop fields and channelized ditches (Foufoula-Georgiou et al., 2015; Kelly et al., 2016; Kumar et al., 2018). These changes in precipitation and agricultural practices have increased the ability for the catchment to deliver large amounts of water quickly to the outlet, affecting streamflow aggregated at daily, monthly, and annual timescales. Thus, even large catchments (>>1000 km^2) can exhibit altered streamflow due to land cover drivers, and land cover signals may even be dominant drivers of altered streamflow at this scale. However, the Upper Midwest agricultural landscape is an example of an intensive alteration of multiple levels of the critical zone, including surface vegetation (e.g., corn and soybeans), surface drainage patterns (ditching), soil structure (compaction, cultural inputs), and subsurface drainage (tile drainage). With increasing precipitation due to climate change, this makes for changes to each term of the water budget, including runoff, groundwater recharge and soil moisture storage, and ET (Kelly et al., 2016). Despite other glaciated catchments in the area sourcing most streamflow from groundwater sources, some streams in the Minnesota River basin show most discharge from tile drain sources (Magner and Alexander, 2002). Streamflow changes at large scales in the Minnesota River Basin, then, are due to a cumulative set of related disturbances resulting in a structural change in the critical cone, rather than an isolated disturbance on one aspect of the water balance (e.g., *only* ET).

The effect of forest harvesting on streamflow will depend on the basin critical zone, as well as disturbance severity, and their interaction. Trees contribute significantly to determining the structure and hydrology of the critical zone (Brantley et al., 2017). This includes not only partitioning water between runoff and ET, but also influencing the physical and chemical weathering rates of bedrock, hillslope-scale hydrologic connectivity, and creating preferential flowpaths between soil layers (Brantley et al., 2017).

Forest cover change can occur due to fast disturbances such as harvest, wind blowdowns, and fire. Forest harvesting affects hydrology mainly through decreases in ET, but the forest road and skid trail network can interrupt and alter infiltration and lateral flow paths. For example, forest road runoff can deliver large amounts of water during the rising limb of hydrographs and increase peak flows (Buttle, 2011; Wemple and Jones, 2003). Wind blowdown also affects hydrology through alterations to ET. Further, root-throw mound and pit microtopography can have basin-scale effect on infiltration and water retention capacity of the uplands (Valtera and Schaetzl, 2017). Finally, fire affects streamflow through changes in ET after tree death, but streamflow changes also depend on changes in catchment flowpaths. Changes in flowpaths after wildfire can occur because of the heating of the soil (e.g., creation of hydrophobic conditions), but hydrophobic conditions are not always created by wildfire (Beatty and Smith, 2013). The creation and temporal persistence of hydrophobic soil conditions as infiltration rates recover is spatially heterogeneous depending on localized burn intensity and soil characteristics. Wildfire can create overland flow pathways to the stream over hydrophobic soils, and alters stream geomorphology and the partitioning of water in catchments. Fire increases peak flows that change channel dimensions and sediment yield (Helvey, 1980; Moody and Martin, 2001), and can alter channel dimensions through loss of bank stability associated with riparian forests (Eaton et al., 2010). After wildfire, increases in peak flows are common and more pronounced than after forest harvesting due to altered flowpaths and the increased importance of overland flow (Scott, 1997). This is a contrast to forest harvesting, in which the infiltration capacity of soils is not dramatically altered (as long as site infrastructure is properly managed), which primarily affects streamflow through augmentations to water yield and base flow via increased catchment wetness (Hornbeck et al., 1997; Verry et al., 2000). However, the hydrological effects of forest harvesting versus fire have been primarily investigated in small catchments; it is unclear how these effects would manifest at the large basin scale. It is expected that effects of fire decrease with increasing spatial scale due to increased opportunities for water storage and increasing basin heterogeneity (Stoof et al., 2012). Slow forest disturbance, such as insect/parasite infestation or disease outbreak, also can affect catchment hydrology (Bladon et al., 2019). However, in this chapter I focus on fast disturbances to investigate more clear potential cause-effect relationships between forest disturbance and streamflow, with forest disturbance not confounded with other time-varying variables.

<u>3.2: METHODS</u>

3.2.1: Study Site

Geographical Setting. This case study focused on the Kawishiwi River in northern Minnesota. The Kawishiwi River starts in Kawishiwi Lake, and discharges into Basswood Lake, where it joins the Basswood River (Figure 3.2). The Basswood River then drains to the Rainy River that forms the border between the US and Canada, ultimately draining to Hudson Bay. Where the Kawishiwi discharges into Basswood Lake, the drainage area is 3500 square kilometers. My case study focused on the Upper Kawishiwi basin, which is the furthest upstream USGS-gaged watershed on the

Kawishiwi river – with an area of 650 square kilometers (Figure 3.2). This is an order of magnitude smaller than most HUC-08 watersheds (MN average for HUC-08 is 2700 km^2), yet 1-2 orders of magnitude larger than traditional paired catchment studies in the region (e.g., watersheds at the Marcell Experimental Forest range from ~0.1-0.5 km^2). Catchments were delineated using USGS Streamstats v.4 (USGS, 2016), which delineates catchments based on a 10 meter resolution elevation model. The Upper Kawishiwi River is almost completely in the Boundary Waters Canoe Area Wilderness (Figure 3.2). The USGS gage record begins in June of 1966. The passage of the Wilderness Act in 1964 limited many extractive activities in the watershed, but some logging was still allowed in the BWCA. Then, the passage of the Boundary Waters Canoe Area Wilderness Area Act in 1978 prohibited logging the BWCA. Other disturbances have occurred during the span of stream gaging, such as wind blowdown events, but have all been limited to less than 2% of the watershed area in any given year (Vogeler et al., 2020). In August of 2011, a lightning strike ignited the Pagami Creek Fire, which burned about 30% of the catchment area of the Upper Kawishiwi basin (200 km^2).

Critical Zone. Bedrock is largely < 1 m from the soil surface, although deeper peat deposits and deep lakes in bedrock depressions are common. Bedrock is composed of crystalline formations of the Duluth Complex – predominantly Duluth Complex anorthositic rocks (Figure 3.3a; Jirsa et al., 2011). The bedrock is largely massive, but some lineaments associated with faulting and large fractures sometimes cross watershed boundaries. Hydraulic conductivity for the Duluth Complex has been estimated as ranging between 10^{-8} to 10^{-4} cm/s (Barr Engineering, 2014). Further, estimated transmissivity has been hypothesized to be higher close to mapped lineaments (Stark, 1977, reported in Barr Engineering, 2014). Saprolite may be present within large fractures, but was stripped from the bedrock surface by glaciation (Kaleb Wagner, Minnesota Geological Survey, personal communication).

Soils are generally poorly formed and coarse-grained, formed in quaternary glacial till and outwash, with Entisols and Inceptisols in the uplands and Histosols in the lowlands (Figure 3.3b; Prettyman, 1978). However, clay layering and soils developed in lacustrine deposits are also common; these lacustrine deposits often form confining layers that impede vertical water flow and create perched wetlands. The dominant soil series is Eaglesnest (57%), followed by Conic (6%), Bowstring (5%), Rock outcrops (4%), Aquepts (4%), Merwin (3%), Wahlsten and Insula (~2%), Eveleth, Rifle, and Fluvaquents (~1% apiece). All other series occupy less than 1% of the catchment area.

Approximately 29% of the watershed area in the Upper Kawishiwi Basin is comprised of watershed storage – lakes and wetlands according to the National Wetlands Inventory (Figure 3.3c; cite NWI). About 13% of the watershed area is open-water storage, including Lakes, Freshwater Ponds, and Riverine demarcations in the National Wetlands Inventory (NWI). Another ~16% include emergent, shrub, and forested wetlands. Much of the Kawishiwi River itself is comprised of in-channel lakes, with 82% of the channel (delineated by the MN DNR Hydrography Dataset) demarcated as a "Lake" by the NWI. The Upper Kawishiwi catchment is predominantly forested (Figure 3.3d). Land cover information for both pre-and-post fire can be found in Table 3.1.

Hydroclimatology. The climate in the Upper Kawishiwi catchment is continental, with moist warm summers and dry, cold winters. Since 1895, the average annual precipitation was 693 mm, about 27% of which occurs in the winter. Winter was defined as November through April, because according to a NOAA precipitation gage just west of the catchment boundary, near Winton, MN (record 1966-1995), snowpack lasting at least one week starts, on average, in November; the spring snowmelt often begins in April (NOAA-NCEI, 2020; Menne et al., 2012a; Menne et al., 2012b). Spring was defined as May through June, as a majority of spring freshets occurred in these months (~86%). The annual maximum streamflow for the Upper Kawishiwi gage was most often the spring freshet (84% of years). The average annual hydrograph for the Upper Kawishiwi River gage can be found in Figure B1.

3.2.2: Approach

I utilized a case study approach to identify the primary hydrologic and climatic drivers of water yield and peak flows for mesoscale Canadian Shield basins, using the

Upper Kawishiwi basin. This included 1) identifying the primary climatic drivers of water yield and peak flows via exploratory analyses, 2) assessing the effect of the 2011 Pagami Creek Fire on water yield and peak flows, and 3) conducting a water balance utilizing remote sensing data to identify the basic partitioning of precipitation into streamflow, ET, storage, and groundwater. These analyses will help determine how sensitive catchments on the order of 650 km^2 are to forest cover change for Canadian Shield conditions, and help establish the spatial scale threshold beyond which forest cover change no longer dominantly influences streamflow by providing a detailed and concrete example of either an effect or no effect at this scale. All analyses were conducted in R version 3.6.2 (R Core Team, 2019).

Hydrometric Variables. Streamflow data was daily mean streamflow from the United States Geological Survey (USGS) (USGS, 2020). For water yield in northern Minnesota basins, based on Sebestyen et al. (2011b), I defined a discharge water year as beginning in March (when snowmelt typically starts) and ending in February of the next calendar year. Daily water yield was calculated by multiplying the daily mean streamflow rate by the length of one day, divided by the basin area; then, daily water within each water year was summed to get annual water yield [mm]. The annual maximum peak streamflow was defined as the highest daily yield value in a water year [mm/day]. I assessed effects on peak flow magnitudes and frequencies using the annual maximum discharge series, defined as the highest daily yield in a water year going from March to February.

The precipitation water year used is November of the previous calendar year to October to reflect the accumulation of seasonal snowpack, as in Sebestyen et al. (2011b). Further, I defined winter precipitation as the total November through April precipitation, and the spring precipitation as the total May and June precipitation. All catchment meteorological data were monthly in timestep, and accessed using the PRISM website (PRISM Climate Group, 2020). Meteorological data were aggregated together across a 1km raster cell resampling of the catchment, either through addition (summing annual, winter, spring precipitation), or taking the mean across the entire year (temperature, dew point, etc.). The meteorological variables used to analyze annual water yield and peak flows can be found in Table 3.2.

3.2.3: Exploratory Analysis

Trends in the Discharge Data. First, any general trends in the water yield and annual maximum flow series were assessed using the nonparameteric Mann-Kendall test for monotonic trends (Yue et al., 2002). The climate variables chosen as adequately describing the water yield and annual maximum flows must also meet the requirement of having no trend in the residuals of a relationship between discharge variable and climate variables.

Local Climatic Drivers. I used exploratory linear regression between the hydrological variables of interest and climatic variables in the pre-fire time period (1967-2011). For water yield, this includes regressing annual water yield against annual precipitation, the previous year's runoff ratio (to capture antecedent wetness), average annual temperature, annual average monthly dew point temperature, annual average minimum & maximum vapor pressure deficit, and Thornthwaite potential evapotranspiration (from SPEI package in R). The annual variables were aggregated from monthly data, based on a water year beginning in November of the previous year when snowpack formed to the end of October in the current year. For annual maximum peak flows, I used winter precipitation, spring precipitation, and the average monthly winter temperature as exploratory predictors. I centered all variables around their mean, and scaled them by their standard deviation, to make unitless regressions and avoid spurious significances based on units alone.

Large-Scale Climate Oscillations. To assess for large-scale climatic drivers of the Kawishiwi River peak flows and water yield, I assessed for oscillatory trends in the long-term annually averaged PRISM data going back to 1895 (Table 3.2). I used the Fast Fourier Transform (FFT) to find the dominant periodicity in these data (Fleming et al., 2002; Watras et al., 2014). The FFT results from the local climatic variables were compared to FFT spectral results for large-scale climate oscillations by visually inspecting the spectral plots of the FFT results for all large-scale climate oscillations and the local meteorological variables. The large-scale climate oscillations used included the Atlantic Multidecadal Oscillation (AMO), Pacific Decadal Oscillation (PDO), North Atlantic Oscillation (NAO), and El Niño-Southern Oscillation (ENSO MEI) (Mengistu et al., 2013). Data for the climatic oscillation indices were provided by the NOAA Physical Sciences Laboratory, Boulder, Colorado, USA, from their website at https://psl.noaa.gov/. (NOAA – PSL, 2020). The mean index value for these climate indices within the precipitation water year of November through October was used to represent the large-scale climate oscillations that were analyzed using the FFT.

To select which climate index to include as a predictor for annual water yield and annual maximum peak flow, I assessed how strongly each index was correlated with these streamflow variables. I chose the most strongly correlated climate index to control for large-scale climate oscillations, that also had a statistically significant linear relationship with streamflow metrics ($p < 0.10$), and an apparent spectral signal aligning with local meteorological variables according to the FFT analysis. The final requirement for inclusion of a large-scale climate oscillation index was that, when combined in a linear regression with the local meteorological variables chosen as predictors in the exploratory regression analyses (Table 3.2), the streamflow metric (water yield or peak flows) must no longer have a significant temporal trend in its residuals.

3.2.4: Effects of the Pagami Creek Fire

Water Yield. To assess the effects of the Pagami Creek Fire on water yield, I first constructed an ANCOVA for the pre-fire time period (WY 1967-2010) using the significant variables identified in the exploratory regression, and using the most highly correlated large-scale climate oscillation index, with a clear long-term periodic relationship with local climatic variables as identified in the FFT analysis. The variables chosen as adequately describing annual water yield were the annual precipitation and the annual average AMO index; the AMO was significantly correlated with annual water yield. Further, visually inspecting water yield versus AMO, there appeared to be a piecewise change point at AMO = 0. Distinct catchment signals have been observed based on whether the AMO index was in a positive or negative phase, so I introduced a change-point at AMO = 0, similar to other studies in the area (Mengistu et al., 2013). Thus, the effects of the 2011 fire on water yield were assessed with respect to Equation 3.1:

$$Q_i = b_0 + b_1 * P_i + b_2 * AMO_i + b_3 * \alpha_i + b_4 * AMO_i * \alpha_i + \varepsilon_i \tag{3.1}$$

$$\varepsilon_i \sim Normal(0, \sigma^2)$$

Where Q_i is the annual water yield in year *i* [mm], P_i is the annual precipitation in year *i* [mm], AMO_i is the annual average monthly AMO index value in year *i* [dimensionless], and α_i = 0 when $AMO_i \leq 0$ and α_i = 1 when $AMO_i > 0$. I use Bayesian-based Markov chain Monte Carlo (McMC) sampling (Gelman and Rubin, 1992) to generate a full probabilistic estimate for the parameters conditioned on the observed annual water yield. Specifically, for the McMC sampling, I implemented the JAGS ("Just Another Gibbs Sampler") algorithm (Plummer, 2003) with the "R2jags" package (Su and Yajima, 2015) in R. Goodness of fit was determined via posterior predictive checks on summed-squared residuals (Gelman et al., 1996).

To determine the predicted annual water yield for each year *j* after the Pagami Creek Fire (2012-2019), I sampled across the posterior densities for the parameters in Equation 3.1 to obtain probabilistic estimates of the annual water yield in each year after the fire, incorporating parameter uncertainty as well as the variability about expected values by incorporating the error term ε_i. Then, I compared the observed annual water yield in each year after the fire to the probabilistic estimates of the water yield in that year according to the pre-fire ANCOVA (i.e., the expected annual water yield in the absence of any fire effect). Thus, each year *j* after the fire, there was a distribution of expected annual water yields that represents the range of possibilities for water yield in that year, given no effect of the fire. Through determining the proportion of expected annual water yields in each post-fire year *j* that were smaller than or equal to the observed annual water yield in that year, I calculated a "Type-S" error p-value: the probability that I am mistaken in believing "The annual water yield in year *j* increased due to the fire" (Gelman and Tuerlinckx, 2000). Although no strict threshold for "significance" associated with the Type-S p-value, I rather treated this p-value continuously as the weight of evidence for altered water yield in year *j* (McShane et al., 2019). However, note that a Type-S p-value of 0.5 corresponds to 1:1 odds of the variable of interest either increasing or decreasing (no meaningful support either way); p = 0.2 indicates a 5-to-1 favorite for increasing (or decreasing, depending on the null hypothesis I am investigating); and p = 0.1 indicates 10:1 odds that the variable is increasing (decreasing).

Annual Maximum Flow: ANCOVA. I used two complementary methods to assess for the effects of the Pagami Creek Fire on the annual maximum streamflow on the Kawishiwi River. First, I used an ANCOVA method very similar to that used for annual water yield. This utilized Equation 3.1, but instead of P_i representing the annual precipitation, it represented the winter precipitation (November-April precipitation). The same method of fitting on the pre-fire annual maximum flow, sampling across the posterior densities in post-fire years to develop probabilistic estimates of the annual maximum flow in these years, and calculating Type-S errors remained the same as outlined in the water yield analysis.

Annual Maximum Flow: Flood-Frequency Analysis. The ANCOVA method was used to find how individual peaks may have changed due to the Pagami Creek Fire. However, this does answer how long-term expected behavior could have changed due to the fire: i.e., how the probability of occurrence for certain magnitude peak flows may have changed. To investigate how magnitudes and occurrence probabilities may have changed, I utilized a flood-frequency approach. This involved 1) selecting the proper distribution of annual maximum streamflow; 2) determining how the winter precipitation and AMO index influence the parameters of the extreme value distribution (identified as most important climatic drivers of streamflow in the exploratory analysis); 3) estimating the parameters and hyperparameters of this distribution using McMC sampling via JAGS; 4) estimating the effect of the fire on these parameters; 5) sampling across the posterior densities of the parameters for expected conditions using the parameters estimated on the pre-fire time period and post-fire values of precipitation and AMO to get an expected cumulative distribution function (CDF), to compare to an "observed", effects-adjusted, CDF derived using parameters allowed to shift due to the fire.

The Generalized Extreme Value (GEV) distribution was chosen as the basic distributional form due to it fitting local annual maximum series well (e.g., Chapter 2), and the theoretical considerations of it being a limiting distribution for block maxima (Fisher and Tippett, 1928; Morrison and Smith, 2002). The GEV distribution has three parameters: location (μ), scale (σ), and shape (ξ). However, a special case of the GEV is when the shape parameter equals zero, or the Gumbel distribution (Gumbel, 1958). The shape parameter controls how much of the distribution is concentrated at higher discharge values, or the "heavy-tailedness". Further, it can be notoriously difficult to obtain robust estimates of the shape parameter (Renard et al., 2006; Yu and Alila, 2019). Thus, I quantified if it was necessary to estimate the shape parameter by comparing my relative confidence of two different models of the linearly detrended annual maximum streamflow for the Kawishiwi River: (1) the GEV with nonzero shape, and (2) GEV with zero shape (Gumbel distribution). The detrended data were a simple linear detrending of the annual maximum streamflow series. I compared models (1) and (2) by determining my degree of belief in each model (p_1 versus p_2), determining the most likely parameters conditioned on the data:

$$\begin{gathered}(1)\ Q_{Dmax,i} \sim GEV(\mu_1, \sigma_1, \xi_1 > 0) \\ (2)\ Q_{Dmax,i} \sim GEV(\mu_2, \sigma_2, \xi_2 = 0)\end{gathered} \tag{3.2}$$

$$\begin{gathered}(3)\ Q_{Dmax,i} \sim GEV(\mu_s, \sigma_s, \xi_s) \\ s \sim Cat(p_1, p_2)\end{gathered}$$

Where $Q_{Dmax,i}$ is the detrended annual maximum flow in year *i*; μ_1, σ_1, ξ_1 are location, scale, and shape parameters for the GEV with a shape parameter greater than 0; μ_2, σ_2, ξ_2 are the location, scale, and shape parameters for the GEV with a shape parameter is equal to zero (or, the Gumbel distribution); s is the index for the more likely distribution for a particular set of parameter estimates (1 is nonzero shape GEV, 2 is Gumbel distribution); p_1, p_2 are the probabilities associated with choosing the nonzero-shape GEV versus the Gumbel distribution for a particular set of parameter estimates; and μ_s, σ_s, ξ_s are the most likely parameters describing the annual maximum flow corresponding either to the nonzero-shape GEV versus the Gumbel distribution.

After choosing the most likely form of the extreme value distribution using the linearly detrended annual maximum series, I accounted for nonstationarity in the observed annual maximum daily streamflow according to the drivers identified in the exploratory analysis: the winter precipitation and the annual AMO index. However, it was unclear how these variables drive the parameters of the extreme value distribution. To find the most likely description of the pre-fire annual maximum series, I conducted a similar model selection exercise as outlined in Equation 3.2, fitting all combinations of location and scale to depend on linear equations with winter precipitation and AMO. If the Gumbel distribution was chosen, for example, there would be 16 models to choose from: 2 variables (winter precipitation, AMO index) fit in all combinations with 2 parameters (location and scale), including a completely stationary location and scale model. The "pre-fire model" was chosen as the most likely of these combinations.

The most likely distributional form for the annual maximum flow was the Gumbel distribution (degree of belief = 0.62). After running 16 models including all combinations of linear dependence of Gumbel location and scale on winter precipitation and AMO index, Equation 3.4 was chosen as the most probable model for the 1967-2011 time period, with stationary scale and nonstationary location that varies linearly with AMO index and winter precipitation (degree-of-belief = 0.339; Table B1):

$$Q_{max,i} \sim Gumbel\ (\ \mu_i\ , \sigma_i\ ) \tag{3.4}$$

$$\mu_i = a_1 + a_2 * AMO_i + a_3 * P_i$$

$$\sigma_i = \sigma_{prefire}$$

Where $Q_{max,i}$ is the annual maximum daily discharge in pre-fire year i; μ_i and σ_i are the location and scale parameters in year i, respectively; $\sigma_{prefire}$ is the stationary pre-fire scale parameter; a_1, a_2, and a_3 are hyperparameters describing how μ_i varies with AMO and winter precipitation; AMO_i is the AMO index in year i; and P_i is the winter precipitation in year i.

After fitting Equation 3.4 to the pre-fire years (1967-2011), I assessed the effects of the fire by calculating the expected location and scale parameters in post-fire year j based on Equation 3.4, while also fitting effects hyperparamters to both location and scale, shown in Equation 3.5:

$$Q_{max,j} \sim Gumbel\ (\mu_j, \sigma_j) \tag{3.5}$$
$$\mu_j = a_1 + a_2 * AMO_j + a_3 * P_j + \mu_o$$
$$\sigma_j = \sigma_{prefire} + \sigma_o$$

$$\tilde{Q}_{max,j} \sim Gumbel\ (\tilde{\mu}_j, \tilde{\sigma}_j)$$
$$\tilde{\mu}_j = a_1 + a_2 * AMO_j + a_3 * P_j$$
$$\tilde{\sigma}_j = \sigma_{prefire}$$

Where $Q_{max,j}$ is the annual maximum daily discharge in post-fire year j and $\tilde{Q}_{max,j}$ is the corresponding expected annual maximum daily discharge in post-fire year j had the fire not occurred; μ_j and σ_j are the location and scale parameters in year j, respectively, with $\tilde{\mu}_j$ and $\tilde{\sigma}_j$ the corresponding values for year j had the fire not occurred; a_1, a_2, and a_3 are hyperparameters describing how μ varies with AMO and winter precipitation fit in the pre-fire time period (Equation 3.4); AMO_j is the AMO index in year j; and P_j is the winter precipitation in year j. Then, I sampled across the posterior densities for the parameters in each post-fire year j both with and without the effect term to get the "observed", effects-adjusted, versus "expected" annual maximum flow magnitudes across recurrence intervals up to the 50-year event, and compared these cumulative distributions across recurrence intervals to quantify how annual maximum flow may have changed across the entire probability distribution of annual maximum streamflows. The 50-year event was chosen as the maximum event size because the total streamflow record was ~50 years (1967-2019).

3.2.5: Water Balance

To examine the partitioning of precipitation into streamflow, ET, storage, and groundwater, I conducted a basic monthly water budget for the catchment, assuming provisionally that regional groundwater influxes and outfluxes are equal (Equation 3.3):

$$\Delta S = P - Q - ET + (GW_{in} - GW_{out}) \tag{3.3}$$

Where ΔS is the change in storage in the month, P is monthly precipitation, Q is monthly water yield, ET is monthly ET, GW_{in} is the groundwater inflow, and GW_{out} is the groundwater outflow. Provisionally, I assumed $GW_{in} - GW_{out} = 0$. I assumed this provisionally to explore how the storage term responds given estimates of precipitation, streamflow, and ET, to see whether if modeled storage change was physically plausible given this assumption to test its verity. Technical reports focused on the Duluth Complex in the area finds the bedrock, which is largely < 1 m from the soil surface, is massive with few fractures at depth; fracture density decreases significantly below the top ~12 meters of the bedrock surface (Barr Engineering, 2014). However, large fractures have been reported, and are difficult to map. Some mapped faults cross the catchment boundary (Figure 3.3a). Groundwater flow has been identified as linked with lineament and fault position in Canadian Shield catchments (Gleeson and Novakowski, 2009). Thus, I considered my assumption of net groundwater equal to zero as provisional, influenced by the "open water balance" approach (Kampf et al., 2020). This assessment asked if there were there long term trends in ΔS, or did ΔS remain in a steady state? For mean conditions through time, the ΔS term should approximately equal zero in a steady state (Hudson, 1988; Nichols and Verry, 2001). Further, I visually inspected historical aerial imagery to support or refute any persistent trends in the ΔS term.

I conducted the monthly water balance beginning in September of 1966 and ending in July of 2011 (so effects of the Pagami Creek Fire were not captured). Monthly precipitation was obtained through Oregon State's PRISM dataset (PRISM Climate Group, 2020). Evapotranspiration was calculated using the remotely sensed MODIS-based SSEBop dataset from USGS (Senay and Kagone, 2019; Senay et al., 2013; Senay 2018). However, this dataset begins in January of 2000. I modeled the ET in previous years using the empirical relationship between monthly maximum vapor pressure deficit from PRISM for the entire record, and the SSEBop actual ET value. I used a random forests regression to build a data-driven model to backcast the actual ET in each month between September 1966 and July 2011, based on the monthly maximum vapor pressure deficit from the PRISM data (PRISM Climate Group, 2020; Breiman, 2001; Breiman and Cutler, 2003). In addition to constructing a monthly water budget, I also conducted a mean annual water budget for 1967-2011. For this, I assumed that the long-term $\Delta S = 0$ (Nichols and Verry, 2001), such that a groundwater term could be explicitly calculated, and my monthly water balance assumption of $\mathrm{GW_{in}} - \mathrm{GW_{out}} = 0$ could be assessed.

To help with interpretation of the water yield and peak flow effects of the Pagami Creek Fire assessed using ANCOVA and flood-frequency analysis, I conducted water budgets of each year after the Pagami Creek Fire. I used precipitation data from PRISM (PRISM Climate Group, 2020), actual ET estimates from SSEBop (Senay and Kagone, 2019), and streamflow estimates from the USGS gage (USGS, 2020). I calculated an "error" term here, without attributing this specifically to storage or groundwater terms, leaving the water balance "open" (Kampf et al., 2020). These actual water budget values were compared to "expected" terms, had the fire not occurred. The expected ET was based on predictions from the 2000-2011 (pre-fire) random forests regression between actual ET from SSEBop and the monthly maximum vapor pressure deficit from PRISM. The expected annual water yield was taken from the annual water yield ANCOVA results.

3.3: RESULTS

3.3.1: Exploratory Analysis

Trends in the Discharge Data. Both annual maximum daily streamflow and annual water yield significantly decreased from 1967-2011 ($p < 0.001$) (Figure 3.4).

Local Climatic Drivers. The only significant predictor of annual water yield from Table 3.2 was the annual precipitation ($p < 0.001$); all other $p > 0.10$. Annual precipitation decreased from 1967 to 2011 ($p = 0.067$), but this decrease in annual precipitation did not fully describe the decreasing trend in annual water yield: the residuals from a regression between annual water yield and annual precipitation still significantly decreased ($p < 0.001$). Further, after accounting for all variables in Table 3.2, there was still a decreasing trend in the water yield ($p = 0.075$). Thus, there are other factors driving the decreases in annual water yield.

For annual maximum daily discharge, the only significant variable from Table 3.2 was winter precipitation ($p < 0.001$). P-values for spring precipitation and mean winter temperature were all greater than 0.20. However, winter precipitation was not sufficient for describing the decreases in annual maximum flow: after accounting for winter precipitation, the annual maximum flow was still decreasing through time ($p < 0.001$).

Large-Scale Climate Oscillations. For the annual average values, the Atlantic Multidecadal Oscillation (AMO) had a dominant period between 55 and 82 years (Figure 3.5). The Pacific Decadal Oscillation (PDO) had a dominant period around 60 years, with other noteworthy periods from 20-40 years. The North Atlantic Oscillation (NAO) had about a 35 year periodicity. Many high-frequency spikes were apparent for the El Niño Southern Oscillation (ENSO) Multivariate ENSO Index (MEI) from about 2-13 years, known to have a periodicity of 2-7 years (Mengistu et al), but the dominant period was identified as the entire record of ~70 years. The spectral spike at the period of the entire record was likely due to the fact that I took average annual values and did not detrend the raw time series data. The climate oscillation analyzed with the most clear periodicity dominated by a single period was the AMO, with a clear spike between 55 and 82 years. The period of the AMO according to my spectral analysis was consistent with other literature that has found a periodicity of approximately 60-90 years (Mengistu et al., 2013).

Annual total precipitation, mean monthly dew point temperature, mean minimum and maximum vapor pressure deficits all had a dominant or codominant periodicity of about 60 years (Figure 3.5). The dominant periodicity for average annual temperature was about 5.5 years, but no noteworthy spike was seen at 60 years as in the others.

The AMO was selected to control for large-scale climate oscillations on the Kawishiwi, as it correlated most strongly with water yield and annual maximum flows (-0.39 for yield and -0.41 for annual maximum discharge). The AMO index was significant in a regression against the annual water yield and annual maximum peak streamflow, and had similar periodicity for the long-term climatic variables (precipitation, vapor pressure deficit, and dew point): ~55-80 years. Finally, a regression including the AMO index and the significant precipitation variables identified in the exploratory regression analysis did not leave any temporal trend in the residuals, indicating that trends in the annual water yield and annual maximum discharge were explained by changes in precipitation *and* the AMO. The PDO and NAO indices correlated poorly with water yield and annual maximum flows. The MEI correlated moderately with water yield and annual maximum flow as well (-0.25 and -0.37, respectively), but was not as apparent in the spectral analysis of climatic variables in the Kawishiwi.

Visual inspections of annual water yield versus AMO index, and annual maximum flow versus AMO index, made apparent different behavior when the AMO was in a positive versus negative phase, consistent with other literature from the Canadian Shield region (Mengistu et al., 2013). Thus, I included a change-point at AMO = 0 so there was a piecewise linear relationship between water yield and AMO index, and between annual maximum streamflow and AMO index (Figure 3.6).

The importance of the AMO was apparent as a proxy for climatic trends in the Upper Kawishiwi catchment, as when it was included with precipitation as a linear predictor of annual water yields and annual maximum flow (as in Equation 3.3), there was no significant trend in the residuals ($p > 0.10$). Precipitation and AMO index completely explained the persistent trends in water yield and annual maximum flow; the residual variability is random through time after accounting for these variables (Figure 3.6).

3.3.2: Effects of the Pagami Creek Fire

Water Yield. Expected and observed water yield are shown in Table 3.3. Water yield was elevated in years 2-6 after the fire. However, water yield *decreased* the year after the fire, but only with 82% confidence. I am greater than 90% confident of an increase in water yield in year 2 after the fire (2014). In year 3 after the fire, I was 83% confident in a yield increase. All other years I was neither more than 80% confident in yield increases or in yield decreases.

Annual Maximum Flow: ANCOVA. The ANCOVA results for annual maximum flow show no increases for which I am greater than 90% confident (Table 3.4). However, I was 88% confident that the annual maximum flow increased in year 3 after the fire, and 86% confident that the annual maximum flow decreased in year 5 after the fire.

Annual Maximum Flow: Flood-Frequency Analysis. I had greater confidence that the Gumbel distribution describes the detrended annual maximum daily discharge (Figure B2; degree of belief = p_2 = 0.62), versus the nonzero shape GEV distribution. Thus, I used the Gumbel distribution to describe the annual maximum daily discharge on the Kawishiwi River.

After fitting equations 3.4 and 3.5 and comparing the effects-adjusted versus expected scenarios, there was no effect for which I was confident of the fire on Gumbel distribution location or scale parameters (μ_o = -0.10 ± 0.35 (p = 0.62); σ_o = -0.13 ± 0.31 (p = 0.72)). After sampling across the posterior densities to derive the cumulative distribution functions for the "observed" effects-adjusted post-fire parameters in each post-fire year *j* (μ_j and σ_j) versus the expected parameters in the absence of the fire ($\tilde{\mu}_j$, $\tilde{\sigma}_j$), I found no changes in the annual maximum daily streamflow in any year for which I was greater than 80% confident (i.e., all Type-S p > 0.20; Figure 3.7). Annual maximum flows at any given return interval actually *decreased* relative to what I would expect based on the pre-fire predictions, but I was less than 80% confident in these decreases.

3.3.3: Water Balance

The random forests regression between the actual ET from SSEBop and the PRISM monthly maximum vapor pressure deficit explained 76% of the variance in the actual ET from SSEBop. Using the predicted ET values for monthly ET, the PRISM monthly precipitation, and the USGS streamgage monthly water yield, and given the net groundwater flow was equal to zero, there was a cumulative storage decrease of 3-6 (mean 4.6) meters over the catchment (Figure 3.8). However, aerial imagery indicated that lake and wetland levels in this time period did not substantially decline (Figure B3). Further, soils in the catchment are often < 1m thick over bedrock, and thus do not have 4 meters of storage capacity; this would mean that if storage decreased by this level, lakes and wetlands would have had to decline by a disproportionate amount. There are no lakes or wetlands on which water levels are monitored in the Upper Kawishiwi catchment, but the mean annual lake level for a nearby Canadian Shield flow-through lake 1990-2011 was not significantly changing through time ($p > 0.10$). The weight of evidence by the large persistent decrease in ΔS, despite aerial imagery and a nearby similar lake not indicating these modeled trends, shows the possibility that $\Delta GW = 0$ is not a good assumption in the Upper Kawishiwi catchment, and that groundwater may be a significant part of the water budget.

The importance of groundwater is also implicated in the mean annual water balance. The average annual water balance is shown in Table 3.5, assuming a long-term average $\Delta S = 0$. Outflows via ET and streamflow were greater than the precipitation inputs, indicating that, if $\Delta S = 0$ and our ET estimate was accurate, there must have been a groundwater supplement to streamflow that comes from outside of the catchment to act as a subsidy to streamflow and/or storage.

Using the same relationship between vapor pressure deficit and AET used in the water balance analysis to find expected ET in the post-fire years, the total decrease in ET over the 8 years is 150 mm (Table 3.6). The cumulative increase for the water yield was 115 mm in the post-fire years. Considering error in the ET estimates, for which 80% of estimates are within 20% of flux tower AET estimates (Chen et al., 2016), these values show that the net streamflow accounted for much of the net ET decrease, with the remainder of the ET deficit going towards replenishing storage and/or groundwater seepage. However, in year 1 after the fire, there was a difference between predicted and actual ET of ~200 mm, while water yield actually *decreased* by 51 mm (Table 3.6). This indicates a lagged response between ET deficit and water yield.

3.4: DISCUSSION

My analysis of the Upper Kawishiwi catchment quantifying the dominant climatic drivers of streamflow, the effects of the Pagami Creek Fire on the annual water yield and peak flows, and a long-term water budget has indicated emergent scaling dynamics in streamflow generation and response to forest disturbance in the Upper Kawishiwi River. The lack of a strong effect of forest cover change on water yield and peak flows was due to climate variables comprising a majority of the runoff signal, and the small effects observed were likely attenuated by large-scale basin storage capacity in lakes and wetlands. Finally, the long-term water balance, in the absence of any forest cover change effect, implicates regional-scale groundwater as potentially a significant portion of the water budget in the catchment.

These results supported my hypothesis that there is a spatial scale in low-relief glaciated catchments beyond which the effects of forest cover change are substantially less compared to the effects of climate, catchment storage, and regional groundwater flow, and that the 650 km^2 Upper Kawishiwi basin is beyond that threshold. The Upper Kawishiwi forms an upper bound, below which is the spatial scale where forest cover change substantially drives streamflow. However, with only one specific case study, there is still considerable uncertainty about the location of this threshold. However, it is clear that ET changes due to forest cover change have little effect on annual water yield and annual maximum flow distributions at scales relevant for water management, such as the >1000 km^2 HUC-08 catchment scale.

Importance of Climate. Climatic trends – in precipitation and in the AMO index – were identified as dominant drivers of both water yield and annual maximum flow. The variability in post-fire annual water yield was dominated by climate drivers – annual precipitation and AMO index. In all 8 post-fire years, the climate variables accounted for 58% of the variability in post-fire water yield. There were only three years where water yield increased more than 10mm after the fire: years 2-4. Thus, water yield recovered to pre-fire conditions within ~5 years of the fire: the hydrologic effect relative to surface water was short-lived.

Climatic drivers were much more apparent than forest cover drivers for peak flows as well: while the effect of the fire on the location parameter for the Gumbel distribution was ~ -0.11, a change in the AMO index of one standard deviation of that observed 1967-2019 changed the location parameter by 0.33. In a year with average winter precipitation (195 mm), and the AMO was at the minimum observed 1967-2019, the 1.5-year annual maximum flow was 3.46 mm/day, versus when AMO was at a maximum it is 2.24 mm/day, causing a difference of over 1 mm/day (> 50% difference). However, when the AMO was at its mean value for 1967-2019, as is winter precipitation, the 1.5-year flow on the burned catchment was 2.73 mm/day, versus an expected (i.e., projected based on pre-fire relationships) 2.83 mm/day, a difference of only ~ - 4%.

The dominance of climate factors was also apparent via the ANCOVA results for annual maximum flows. The winter precipitation and AMO index accounts for 32% of the variability in post-fire annual maximum flows. Although this is less than half, annual maximum flows were much more variable even in the pre-fire time period, with a residual standard error of 1.1 mm/day. After the fire, the residual standard error between the predicted values based on climate alone and the observed values according to the ANCOVA had a residual standard error of 0.80 mm/day, indicating similar ability in pre-and-post fire time periods for climatic drivers to adequately explain streamflow. The high level of variability is due to the temporal scale of aggregation for peak flows versus water yield. Despite this variability, climate trends via winter precipitation and AMO index were detectable and significant for describing the annual maximum flow. The 2011 fire, although perhaps increasing the annual maximum flow in year 3 after the fire ($p = 0.12$)

and/or decreasing the annual maximum flow in year 5 after the fire ($p = 0.14$), largely was not a detectable signal in the annual maximum flow series.

The importance of long-term climatic oscillations on hydrological fluxes of surface water and groundwater resources in the broader Great Lakes – Canadian Shield area is well documented (Fortin and Lamoureux, 2009; Mengistu et al., 2013; Watras et al., 2014). The Atlantic Multidecadal Oscillation, in particular, has been shown to heavily influence streamflow in the region (Fortin and Lamoureux, 2009; Mengistu et al., 2013; Sutton and Hodson, 2005). These studies have found AMO to be inversely correlated with water yield and precipitation, and correlated with evaporation. The AMO index in this case study was loosely correlated with precipitation, and thus was more likely a proxy for alterations in evaporative, storage, and deep groundwater fluxes in the Upper Kawishiwi catchment. The importance of the AMO in determining non-precipitation trends in the water balance was indicated by similar periodicity of the AMO, mean dew point temperatures, and vapor pressure deficit (Figure 3.5). The AMO index served as a proxy that represents complex feedbacks: for example, in the Upper Kawishiwi catchment, changes in lake evaporation affect not only the ET flux of the water balance, but also the storage capacity of the catchment. Future study of the catchment should include more assessment of by what mechanisms the AMO drives the trends in the annual water balance.

Importance of Catchment Characteristics. The lagged water yield and peak flow response to the 2011 fire indicates a streamflow response strongly modulated by catchment storage dynamics (Table 3.6). Water yield did not significantly increase until year 2 after the fire (by 82 mm). Further, *if* peak flows were affected by the fire, I was most confident in an effect on the annual maximum peak in year 3 after the fire. The time lag for increases in water yield and peak flow increases after the fire likely represent a response to the Pagami Creek Fire modulated by catchment storage buffering. Catchment storage needed to be “refilled” after the 2010-2011 drought before increased water yield could manifest as increased water yield and peak flows. The two driest years on record since streamgaging began in 1966 were 2010 and 2011 – the year before and the year of the fire. These dry conditions contributed to the large extent of the fire and the difficulty in extinguishing the Pagami Creek Fire (Kolka et al., 2014; Srock et al., 2018). Thus, there was likely a storage deficit that had to be replenished before the extra water in the catchment could be discharged as streamflow.

Cumulative ET deficit was not correlated well with the water yield change in the matching year (cor = 0.06), but was most strongly correlated with the water yield change 2 years in advance (correlation = 0.57) (Table 3.6). The offset correlation indicates a storage lag for excess water compared to pre-fire conditions to make it to the catchment outlet. The lag for excess water to drain past the streamgage is likely related to catchment storage capacity and recharging the storage deficit from the 2010-2011 drought, but also by virtue of the catchment's size. Catchment transit times increase with the depth of the hydrologically active layer (Asano and Uchida, 2012). Thus, where regional groundwater can be a substantial portion of flow at large scales, long transit times are expected. Finally, travel time through lakes and reservoirs serve as natural water storage and can slow transit times. However, to adequately characterize transit times in the catchment, isotopic tracer studies and transit-time distribution modeling would be a good next step to further interpret these observations.

Some of the stored water not discharged as streamflow in years 1 and 2 after the fire may have contributed to wet antecedent conditions for a higher peak flow in year 3 after the fire. Further, the lowest precipitation year of the post-fire time period was year 4 after the fire (657 mm), which may have contributed to a storage deficit that decreased the annual maximum flow in year 5 after the fire (Table 3.6). Even though ET had a cumulative deficit compared to expected conditions of 176 mm in year 4 after the fire, water yield had transported 120 mm of this extra water out of the catchment already in year 4. Thus, storage reserves may have been low enough to cause the apparent decrease in annual maximum streamflow compared to expected conditions in year 5 after the fire. If this is the case, then this decrease in annual maximum streamflow in year 5 is not *per se* attributable to the 2011 fire and is influenced by variability in catchment storage conditions, indicating once again the importance of climate and catchment characteristics at large scale. However, the year 3 increase in annual maximum peak flow, for which I was more confident (88% confidence), was likely attributable to increased catchment wetness in the burned sub-portion of the catchment and full storage reserves throughout the catchment replenished by average to high precipitation in years 1-2 after the fire. Even here, it was apparent that catchment characteristics such as storage capacity are highly important for the timing and magnitude of changes to water yield, and especially peak flows, at this scale.

The hydrological role of catchment storage (i.e., lakes and wetlands) in the drainage network depends on their hydrologic connectivity in the broader system (Roulet, 1990). The Upper Kawishiwi catchment has a much of its storage in the stream course of the Kawishiwi River as lakes (open water is ~13% of catchment area). Further, there are peatlands and forested wetlands distributed throughout the catchment (~16% catchment area: Figure 3.3b). However, without any lakes monitored for storage change in the catchment, the hypothesized importance of storage modulating the water yield and peak flow response remains unquantified. In boreal Canadian Shield lake-dominated headwater catchments, lake storage deficit has been found to be a co-dominant driver of streamflow along with climate (Mielko and Woo, 2006; Spence, 2000), but it is unclear how this relationship scales spatially – particularly within the broader boreal-temperate transition region with complex and varied relationships between groundwater and surface water. In swales filled with deeper unconsolidated glacial deposits, wetland storage is often present. Surface inflow must fill storage deficits of wetlands and the deeper soil matrix; this "fill and spill" process causes sometimes disconnected surface flow, and there is often seepage loss to regional groundwater along the system (Spence and Woo, 2003). Peat wetlands that are disconnected from regional flow through massive bedrock, etc., have different levels of connection to the uplands based on the depth of glacial material in the catchment, with deeper till (1-3 meters vs < 1 m) sustaining connection throughout the year (Devito et al., 1996). Further, catchment storage allows more opportunity for evaporative losses in lakes: evaporation losses from lakes throughout the Canadian Shield were found to average close to 18% of their inflow, with values of evaporation/inflow between 8 and 28% for individual sampling blocks throughout the region. The highest values in the study were noted for lakes just across the US/Canadian border from the BWCAW (Gibson et al., 2017).

Importance of Regional Groundwater. Regional groundwater that likely follows landscape-scale patterns of bedrock fracturing and faulting was implicated in maintaining streamflow and/or catchment storage because modeled changes in catchment storage are infeasible (Figure 3.8, Table 3.5). The water balance 1967-2011, which showed a persistent decrease in cumulative storage by approximately 4-5 meters in the catchment from 1967-2011 if the ΔGW term was assumed to be zero, indicates that the ΔGW term is likely *not* zero. Soils in the catchment are largely < 1m thick, so would not be able to support this storage deficit. Pervasive lakes and wetlands would have had to disproportionately "draw down" to reflect this storage deficit. A large storage drawdown was not supported by a visual inspection of aerial imagery (Figure B3).

The annual runoff ratio significantly decreased ($p < 0.001$). Thus, through time, a higher proportion of precipitation did not run off as streamflow. Thus, this "extra" precipitation must either satisfy increased evaporative demands, replenish deep groundwater, or go into storage. Decreasing streamflow through time, not explained entirely by trends in precipitation, would indicate that storage was *increasing* through time; however, this was not supported by aerial imagery (Figure B3), nor was it supported by the long-term water balance. Further, there was no trend in the back-cast ET, based on PRISM vapor pressure deficit values ($p = 0.91$). However, pre-2000 ET values were based on the assumption that the relationship between maximum vapor pressure deficit and actual ET in 1967-2000 is the same as that relationship 2000-2011, which may not be true if the AMO changes climatic variables other than maximum vapor pressure deficit that also affect ET. Even after the 2011 Pagami Creek Fire, although there were marked declines in ET compared to expected conditions in some years (Table 3.6), there was no significant trend in actual minus expected ET ($p = 0.536$). Thus, it is unclear when "recovery" to pretreatment ET conditions occurred, based on the 8 years of post-fire data. However, ET is notoriously difficult to quantify, and more work is needed through the integration of different remote sensing ET products to better quantify uncertainty in the ET estimates used to make any strong claims about specific values of ET, groundwater, and storage, instead of the general trends discussed here.

While ET was provisionally assumed to be relatively constant in the record 1967-2011, precipitation was declining ($p = 0.067$). If ET maintains a relatively constant level and precipitation declines, a higher fraction of the precipitation would be used as ET, explaining the decreasing runoff ratios. The proportion of annual yield that is baseflow (Nathan and McMahon, 1990) was increasing through time ($p = 0.07$), indicating possibly more reliance on slow flowpaths (which include groundwater) as inputs for streamflow through time.

The Duluth Complex bedrock in the Upper Kawishiwi catchment is crystalline and generally has low hydraulic conductivity, estimated as ranging between 10^{-8} to 10^{-4} cm/s (Barr Engineering, 2014). Lineaments are common in the area, and large-scale faulting crosses the catchment boundary in several locations (Figure 3.3a). In a study on the influence of bedrock lineaments on groundwater flow in the Canadian Shield, lineaments were found to significantly influence regional groundwater flow, including acting as a barrier to flow across the lineament (Gleeson and Novakowski, 2009). However, fault zones and lineaments, depending on structure, bedrock type, and the process by which they were formed, can exhibit vastly different hydrogeological characteristics, including acting as flow barriers (Gleeson and Novakowski, 2009), create barrier-conduit system where flow across the fault zone is limited but flow parallel to the fault is preferential (Bense and Person, 2006), and can act as flow conduits (Bense et al., 2013). Further, some previous work in the area has found sampled hydraulic conductivity values to be higher near lineaments (Stark 1977, quoted in Barr Engineering, 2014). Preferential flow in the damaged rock zone associated with faults could carry water from outside of the catchment to maintain lake levels and support a streamflow subsidy. Additionally, catchments in wetland complexes are notoriously difficult to delineate, even for very small catchments and ground-based survey crews (Verry et al., 2011). Thus, the surface water catchment delineated at 10m resolution may not fully capture the effective catchment even for the unconsolidated deposits, let alone potential regional-scale flow in the fractured bedrock aquifer. Further, catchment boundaries may change year-to-year based on antecedent wetness. Despite the low hydraulic conductivity of the Duluth Complex, there is indication in my analysis that the groundwatershed that may discharge into the Kawishiwi River at the upper gage may be distinct in space and not follow the catchment boundaries. The implication of regional-scale groundwater is another manifestation of emergent scaling dynamics.

Groundwater drainage patterns likely have strong relationships with catchment storage in lakes as well. Lakes in the catchment are often bedrock-lined, forming in bedrock depressions. Thus, lakes in the catchment could serve as "hot spots" where groundwater is either replenished via seepage, or is discharged, serving as a subsidy to streamflow. Further, if there is negligible groundwater exchange, as I initially assumed in this study, and catchment storage *did* decline substantially, this would be possible due to the large scale of the catchment: there are many unique storage reservoirs throughout the catchment that would make a change like this possible. However, without more precise quantification of uncertainty of the ET estimates used, as well as measurements of lake levels and catchment storage, it is unclear how exactly water partitions between ET, groundwater, and storage.

3.5: CONCLUSION

Precipitation metrics and the Atlantic Multidecadal Oscillation were dominant drivers of streamflow as water yield and annual maximum streamflow in the Upper Kawishiwi catchment. These drivers remained more influential in determining water yield and peak flows in the 8 years after a wildfire burned ~1/3 of the catchment area in 2011. My ANCOVA analysis of water yield effects indicated, however, that water yield 1) had a lagged response to post-fire ET decreases because of the necessity to fill catchment storage reserves before discharging excess water available for streamflow, and 2) water yield can increase by up to 30% after 1/3 of the surface area of a large catchment is burned, but the effect is short-lived. Water yields remained elevated by greater than 10mm only for years 2-4 after the fire. ANCOVA analysis of annual maximum flow events shows that 1) the effect of the fire on peak flows was limited if any effect did occur due to inherent variability in peak flows, and 2) peak flows may have increased in year 3 after the fire, also representing a lagged effect due to catchment storage. A peak flow decrease for which I had similar confidence in year 5 after the fire, but also after the lowest post-fire precipitation year, calls into question whether the peak flow changes observed were due to the fire, antecedent moisture and catchment characteristics, or a combination of fire and storage effects. The flood-frequency analysis indicated that even if individual peak flows changed, average behavior of peak flows responding to forest disturbance over the long run is not expected to change significantly. Finally, my long-term water balance implicated the groundwater term of the water balance as a potentially significant driver of hydrology in the Upper Kawishiwi catchment, that likely contributes to hydrology in the Upper Kawishiwi catchment but from a spatially distinct contributing area, but more uncertainty quantification in the ET estimates used is needed. Regional groundwater flow in the area is likely influenced by heterogeneous regional-scale bedrock fracturing and faulting that crosses the surface water catchment boundaries. However, the degree to which regional groundwater flow contributes to streamflow in the area is still unclear, without more uncertainty estimation for the ET metric used as well as data on catchment storage and lake levels.

The hydrology of the Kawishiwi River in its uppermost gaged basin (650 km^2) exhibited emergent scaling dynamics via registering signals of large-scale climate patterns, diverse sources of catchment storage throughout the landscape, and potential regional groundwater flow. Forest disturbance, defoliating 1/3 of the catchment area via wildfire, demonstrated negligible effect in driving the hydrometric variables of water yield and annual maximum flow.

CONCLUSION

This investigation revealed that forest cover loss significantly affects streamflow and sediment yield, affecting the partitioning of water throughout catchments at a range of sizes. I have elucidated dominant drivers of elevated sediment yield due to forest harvesting using a new, holistic conceptual model that identifies the direct and indirect processes by which sediment yield is elevated after harvesting (Chapter 1). Additionally, I have addressed both original hypotheses about how streamflow in low-relief glaciated catchments responds to forest cover change:

Hypothesis 1

My nonstationary flood-frequency analysis of annual maximum peak streamflow at the Marcell Experimental Forest showed that clearcutting the entire upland of a small snowmelt-dominated upland-peatland watershed can increase annual peak flows across all return intervals compared to preharvest mature forest conditions. Forest regrowth of the upland decreased annual peak flows across all return intervals compared to the initial increase, but the recovery time to pre-harvest annual maximum flow distributions was unclear. Changes to the distribution of annual maximum peak flows manifested primarily as an increased probability for very large events.

Several important ramifications for the analysis of peak flows in small experimental catchments were discussed. The most noteworthy ramification for the paired catchment approach of my work at the MEF was the ability for catchment pairs to "decouple" their streamflow generating process for the annual maximum flow, to switch between snowmelt-dominated and rainfall-dominated. Chapter 2 highlighted the methodological benefits to adding probabilistic flood-frequency analysis methods in addition to traditional ANCOVA methods. Probabilistic methods account for both changes in the magnitude and probability of flood occurrence, answering the question "do we get bigger floods *more often* after forest harvesting?" Further, probabilistic flood-frequency methods can account for continuous nonstationarity in distributions of peak flows as the forest regrows, and are robust to changing coupling relationships for catchment pairs. This is because a strong pairing assumption is not necessary within these methods, as in traditional linear models.

Hypothesis 2

My case study analysis of the Upper Kawishiwi catchment supported the existence of a spatial scale at which land cover effects are negligible among signals of regional groundwater, climate, and water storage. Water yield and peak flows corresponded primarily to precipitation and large-scale climate fluctuations in the Atlantic Multidecadal Oscillation, even after a large-scale wildfire that burned 30% of a 650 km^2 catchment. Effects of the 2011 Pagami Creek Fire were detectable, but small, in the water yield of the Upper Kawishiwi catchment. At its largest, this was a 30% increase in annual water yield compared to expected conditions. However, the effect of the fire on water yield persisted less than 7 years, and I was only greater than 90% confident that there was *any* effect on water yield in year 2 after the fire: a short-lived effect, and an effect that was attenuated by catchment storage in lakes and wetlands. Finally, despite bedrock that is often assumed to be relatively competent and impermeable, my analysis questioned this common assumption about where the “bottom” of the catchment is located. The long-term water balance indicated regional groundwater influxes possibly exist to maintain streamflow, but more work in quantifying uncertainty in remotely sensed ET estimates is needed.

Synthesis

In summary, although an effect of forest canopy loss was found for peak flows in small catchments, this effect was not observed at a larger scale. The catchment approach, in which basin inputs and outputs are easily quantifiable, has historically been focused on the small spatial scale, such as the experimental catchments at the Marcell Experimental Forest for the Lake States region. The catchment approach has provided a foundation for most of the modern knowledge in forest hydrology. The application of catchment approach methods (water balance, traditional statistical analysis of streamflow hydrometric variables, etc.) to a larger drainage basin in the Kawishiwi case study was possible through the development of accurate remotely-sensed data products such as the

PRISM model from Oregon State, and USGS' SSEBop ET dataset. The catchment approach at larger scales is promising because of the availability and accuracy of these products.

My research advanced our knowledge of 1) how forest harvesting can affect stream sediment yield through multiple processes, including those mediated by hydrological changes as investigated in Chapters 2 and 3 (increases in peak flows and total streamflow); 2) how forest harvesting can affect peak flows across the range of occurrence probabilities; and 3) how forest canopy loss (via wildfire) can affect peak flows and water yields for large (650 km^2) catchments, and what the dominant hydrological processes that generate streamflow are at this scale. However, important questions remain. For example, distributed physically-based hydrological modeling studies would be good complements to the statistical approach I have taken to investigate the primary flowpath changes that may have occurred in the MEF and Kawishiwi catchments. Although the statistical analyses have given insight into the physical hydrology of these catchments, more detailed process-based modeling would allow for the investigation of particular sub-processes of interest (for example, using a routing model to help explain why the increased water yield after the Pagami Creek Fire did not manifest until the second year after the fire). Another excellent example would be to model regional groundwater flow in the Boundary Waters Canoe Area Wilderness, and couple this groundwater flow model with surface water observations and modeling. Groundwater and surface water are one resource, even in areas with supposedly "impermeable" layers, and future water management will depend on our increased understanding of these coupled systems.

Changing climate and land use/land cover patterns necessitate developing and conducting analyses that account for variability and nonstationarity. I have done this by accounting for land cover change explicitly in my flood-frequency models at the small scale, and by exploring climate indices such as the Atlantic Multidecadal Oscillation (AMO) to help explain trends in water yield and peak flows at the large scale. The effects of "short" (< 50 years) gaging records affect our ability to make robust inferences, and may even lead us to misattribute trends and correlations that only occur due to chance, or the fact that we are only looking at a small subset of a long-term trend. To adequately attribute trends, I used my physical knowledge of the catchment, such as at the MEF where land cover was well known, and explored correlations with long-term deterministic trends such as the AMO.

The ability to make inferences truly reflective of physical processes involves using both our prior physical knowledge *and* statistical frameworks that can adequately account for both this prior knowledge and uncertainty given the data. My physico-statistical approach has illustrated real advantages over traditional statistical tests with difficult-to-interpret "significance thresholds", or overparameterized physically based models, while retaining commitment to revealing objective order in nature. Advantages included the ability for the method of peak flow analysis to more closely represent physical conditions on the catchment through *a priori* nonstationarity structures informed by physical knowledge and previous work at the MEF. Further, uncertainty was presented as a "Type-S" p-value in both chapters 2 and 3, as we are often more interested in the question "did flows get larger or smaller than what we would expect", rather than testing a physically implausible "null hypothesis" of *exactly* zero change in flows. Further, this "Type-S" value represents an easy to interpret "degree-of-belief". The selection of an arbitrary significance threshold was unnecessary in a framework that allows for uncertainty to be communicated on a continuous scale. In summary, I have made both methodological and conceptual advances with this thesis, but more work remains necessary. The low-relief glaciated region of the Upper Midwest provides an exemplary area for developing new methods and new hypotheses about hydrological response to forest cover change and climate change.

TABLES

Table 1.1 (pages 107-114): Key paired-watershed studies relating forest harvesting to streamflow and stream sediment response in the reviewed regions. Rubric for "Discussion of indirect effects" – Yes = explicitly distinguished indirect versus direct effects and discussed both ; No = all increases in stream sediment attributed to direct effects without explicitly quantifying indirect effects ; Mentioned in discussion = indirect effects were mentioned somewhere in the paper as a potential driver of increased stream sediment, but without further quantification; Unclear = indirect effects were alluded to but not discussed.

Study	Region	Physiographic Section	Paper Type	Sediment Response Variable to Forest Harvesting (+, -, inconclusive)	Discharge Response to Forest Harvesting (+, -, inconclusive)	Discussion of indirect effects?	Comments
Lewis et al., 2001	Pacific Mountain System	California Coast Ranges	Paired-watershed analysis	Storm suspended sediment loads (+)	Storm peaks (+); storm runoff volume (+)	Yes	Caspar Creek: Increases in storm sediment loads attributed to increased volume of streamflow
Gomi et al., 2005	Pacific Mountain System	Entire Pacific Mountain System	Literature Review	Dependent on studies reviewed	Dependent on studies reviewed	Yes	"…an issue that cannot be definitively answered based on existing studies relates to the relative roles of hydrologic changes versus changes in sediment supply

							from external sources after harvesting." (pg. 893)
Moore and Wondzell, 2005	Pacific Mountain System	Entire Pacific Mountain System	Literature Review	Dependent on studies reviewed	Dependent on studies reviewed	Mentioned in discussion	Some reviewed studies related peak flow increases to increases in sediment yield, but drivers of sediment response not discussed in detail
Hassan et al., 2006	Pacific Mountain System	Entire Pacific Mountain System	Literature Review	Dependent on studies reviewed	Dependent on studies reviewed	Yes	Dominant drivers of harvest-related direct versus indirect effects importance not discussed in detail
Reiter et al., 2009	Pacific Mountain System	Middle Cascade Mtns/Puget Trough	Time-series analysis	Turbidity (+)	Not quantified	Unclear	Flow-adjusted turbidity decreases are attributed to improvements in road construction and maintenance
Reid et al., 2010	Pacific Mountain System	California Coast Ranges	Paired-watershed analysis	Suspended sediment yield based on Lewis et al., 2001 (+);	See Lewis et al., 2001	Yes: explicitly investigated	Caspar Creek: 28% increase in drainage density after logging; in-channel sources within logged area and

				Gully incidence and erosion rates (+)			downstream, and increased hillslope-channel connectivity, implicated in elevated sediment yields
Klein et al., 2012	Pacific Mountain System	Klamath Mountains, California Coast Ranges	Multiple-basin analysis	Turbidity	Not quantified	Unclear	Legacy effects indicated but in-stream sediment sources not discussed
Bywater-Reyes et al., 2017	Pacific Mountain System	Oregon Coast Range	Paired-watershed analysis	Suspended sediment yield (+)	Not quantified	Mentioned in discussion	Changes in sediment rating curves in given years encapsulate both direct and indirect effects
Bywater-Reyes et al., 2018	Pacific Mountain System	Middle Cascade Mountains	Paired-watershed analysis	Suspended sediment yield (inconclusive)	Not quantified	Mentioned in discussion	H.J. Andrews Experimental Forest: Results could indicate increasing in-stream sourced sediment with drainage area
Hatten et al., 2019	Pacific Mountain System	Oregon Coast Range	Paired-Watershed Analysis	Suspended sediment yield (no effect)	Not quantified	No effect on sediment yield	Alsea Watershed Study: Revisited

Safeeq et al., 2020	Pacific Mountain System	Middle Cascade Mountains	Paired-watershed analysis	Total sediment yield (+): suspended (+) and bedload (+)	Water Yield (+); small peaks (+); large peaks (unchanged)	Yes: explicitly investigated	H.J. Andrews Experimental Forest: Both direct and indirect effects were found and attributed using modeling of sediment rating curves; direct effects substantially more important (20 times more)
Alexander et al., 1985	Intermountain West	Southern Rocky Mtns	Paired-watershed analysis	Sediment yield (+)	Water Yield (+); Peak flows (+ or unchanged)	No	Multiple paired-watershed experiments at Fraser Experimental Forest reviewed
Karwan et al., 2007	Intermountain West	Northern Rocky Mtns	Paired-watershed analysis	Total suspended solids (+)	Not quantified	Mentioned in discussion	Mica Creek Experimental Watershed: Increase in suspended load not attributable only to hillslope or road erosion due to only marginal increases in concentration
Swank et al., 2014	Southeast		Paired-watershed analysis	Sediment yield (+) (based on	Water Yield (+); baseflow	Mentioned in discussion	Coweeta Hydrologic Laboratory: Only minor instances of streambank

		Southern Blue Ridge		weir pond collection)	(+); peaks (small +)		erosion derived from cross-section measurements (Swank et al. 2001; unpublished data). Sediment yield measured above and below road crossings found much of the sediment yield was sourced from forest roads. One large storm caused a large influx of sediment that continues to serve as an in-stream sediment source.
Beasley and Granillo, 1988	Southeast	Mississippi Alluvial Plain	Paired-watershed analysis	Stormflow total suspended sediment (+)	Water Yield (+)	Mentioned in discussion	Water yield discussed as a driver of sediment yield but not separated from increases in sediment concentration.
McBroom et al., 2008	Southeast	West Gulf Coastal Plain	Paired-watershed analysis	Sediment yield (+ on watersheds <10ha; no effect or + on	Stormflow (+ on watersheds <10ha, no difference on large	Mentioned in discussion	Only marginal increases in sediment concentration interpreted as supporting in-channel versus upland supply source for sediment

				watersheds >50ha)	watersheds >50ha)		
Terrell et al., 2011	Southeast	East Gulf Coastal Plain	Paired-watershed analysis	Total Suspended Solids Yield (+)	Water Yield (+); peaks (no change)	Mentioned in discussion	Bank erosion and failures observed in both treatment and control watersheds
Fraser et al., 2012	Southeast	Piedmont Upland	Paired-watershed analysis	Total Suspended Solids: Concentration (no effect), Yield (+)	Water Yield (+); peak flows (+)	Yes: explicitly investigated	Assessed bed composition and streambank condition to attribute increased sediment yield to increased flows
Boggs et al., 2016	Southeast	Piedmont	Paired-watershed analysis	Total suspended sediment (+)	Water Yield (+); peak flows (+); stormflow (+)	Mentioned in discussion	Post-harvest increases in sediment yields attributed to in-stream sources and mobilization of legacy sediment
Aubertin and Patric, 1974	Southeast/North east	Allegheny Mtns.	Paired-watershed analysis	Turbidity (+)	Water Yield (+); most increases in the growing season	Mentioned in discussion	Fernow: "…It is quite probable that most of the increased turbidity observed during storm periods resulted from channel extension or channel scour, or both…" (pg. 248)

Kochenderfer & Hornbeck, 1999	Southeast/North east	Allegheny Mtns.	Paired-watershed analysis	Sediment yield (+), Turbidity (+)	Water Yield (+); Some peak flows (+)	Mentioned in discussion	Fernow Experimental Forest
Martin et al. 2000	Northeast	White Mtns.	Paired-watershed analysis	Annual sediment yield (+); note this was sediment collected in weir pond	Water Yield (+, mostly during growing season); Peaks (+ moderately)	Mentioned in discussion	Hubbard Brook: Small impacts on peak flows interpreted as having minimal effect on stream and channel scour
Verry et al., 1972	Western Lake States	Central Lowland: Western Lake	Paired-watershed analysis	Not collected	Water yield (+); small to moderate peak flows (+)	No	Marcell Experimental Forest: "Sediment losses were not measured because they were expected to be small due to the low relief and rapid regrowth of herbaceous plants, shrubs, and trees." (pg. 283).
Merten et al., 2010	Western Lake States	Central Lowland: Western Lake	Paired-plot analysis on the stream-reach scale	Geomorphic assessment of reaches: streambed	Not collected	Mentioned in discussion	Increases in streamflow discussed and implicated as a potential driver, but discharge was not measured

surficial fine sediments (+), residual pool depth (-), embeddedness (+), depth of refusal (+), and proportion unstable banks (+)

Table 2.1: Stationary blocks used in the analysis of peak flows in Sebestyen et al., 2011b.

S4/S5 Experiment		S2/S6 Experiment	
1962-1970	Pretreatment	1976-1980	Pretreatment
1971-1979	Open/Young Forest	1981-1989	Open/Young Forest
1980-1989	Growing Forest	1990-1999	Growing Forest
1990-1999	Mid-Life Forest	2000-2016	Closed-Canopy
2000-2016	Mature Forest		

Table 2.2: Probability of decoupling in the stationary time periods defined in Table 1 for both experiments. In parentheses are the probabilities of incorrectly stating that the decoupling probability in that time period is greater than the decoupling probability in the pretreatment time period. * = Type-S error rate less than 0.10

	S4/S5: p_g ($P[p_g \leq p_{pretrt}]$)		S2/S6: p_g ($P[p_g \leq p_{pretrt}]$)
Time Period	p_g = probability that AM flow on S4 and S5 occur > 7 days apart	p_g = probability that AM flow on S4 and S5 occur due to different streamflow generating processes	p_g = probability that AM flow on S2 and S6 occur > 7 days apart
Pretreatment	0.111	0.110	0.249
Open/Young Forest	0.556 (0.013)*	0.436 (0.035)*	0.405 (0.245)
Growing Forest	0.296 (0.120)	0.297 (0.128)	0.199 (0.546)
Mid-Life Forest	0.300 (0.123)	0.202 (0.255)	NA
Mature Forest	0.297 (0.103)	0.119 (0.431)	NA
Closed Canopy	NA	NA	0.178 (0.563)

Table 2.3: Type S error probabilities for alterations in the location, scale, and shape parameters in observed versus expected models of annual maximum flow for both harvesting experiments. Most noteworthy is the shape (ξ) parameters for the S4/S5 experiment, for which I have the most confidence of an increase (i.e., the smallest p-value).

	S4/S5	S2/S6	
Parameter	P[harvest year 1 parameter ≤ expected parameter]	P[harvest year 1 parameter ≤ expected parameter]	P[mature conifer parameter ≥ expected aspen parameter]
μ	0.677	0.357	0.346
σ	0.263	0.514	0.252
ξ	0.187	0.357	0.643

Table 3.1: Land cover in the Upper Kawishiwi catchment, pre and post fire, in percent (according to NLCD 2011: Homer et al., 2015).

Land Cover	Open Water	Deciduous Forest	Evergreen Forest	Mixed Forest	Woody Wetlands	Other	Burned Land
Pre-Fire	13.7	14.0	27.7	17.5	23.8	3.3	0
Post-Fire	13.7	12.3	15.8	12.7	16.5	2.0	27.0

Table 3.2: Exploratory regression variables. Variables with a * represent variables for which I assessed oscillatory trends as well.

Annual Water Yield	Data Source	Data Citation	Annual Maximum Daily Streamflow	Data Source
Annual precipitation*	PRISM	PRISM Climate Group, 2020	Winter precipitation	PRISM Climate Group, 2020
Previous year's runoff ratio (to capture antecedent wetness)	USGS discharge record, PRISM	USGS, 2016; PRISM Climate Group, 2020	Spring precipitation	PRISM Climate Group, 2020
Annual average monthly temperature*	PRISM	PRISM Climate Group, 2020	Average monthly winter temperature	PRISM Climate Group, 2020
Annual average monthly dew point temperature*	PRISM	PRISM Climate Group, 2020		
Annual average minimum monthly vapor pressure deficit*	PRISM	PRISM Climate Group, 2020		
Annual average maximum monthly vapor pressure deficit*	PRISM	PRISM Climate Group, 2020		
Thornthwaite PET	PRISM, SPEI package in R	PRISM Climate Group, 2020 SPEI package in R (Beguería & Vicente-Serrano, 2017)		

Table 3.3: Water yield increases on the Upper Kawishiwi catchment, N years after the fire. (sd) = standard deviation

Years after the fire	1	2	3	4	5	6	7	8
Expected (sd) [mm]	263 (58)	274 (58)	312 (59)	175 (59)	309 (64)	346 (66)	256 (56)	295 (58)
Observed [mm]	212	356	367	210	312	351	251	286
p	0.810	0.078	0.171	0.270	0.480	0.465	0.537	0.560

Table 3.4: ANCOVA-based annual maximum flows. (sd) = standard deviation

Years after the fire	1	2	3	4	5	6	7	8
Expected (sd) [mm/day]	2.88 (1.16)	3.27 (1.16)	3.57 (1.19)	2.36 (1.19)	4.76 (1.39)	3.87 (1.33)	2.11 (1.17)	3.69 (1.17)
Observed [mm/day]	2.90	3.56	4.97	2.25	3.31	3.35	2.01	3.16
p	0.491	0.404	0.116	0.534	0.856	0.652	0.538	0.678

Table 3.5: Average annual water balance for the Upper Kawishiwi catchment, 1967-2011, assuming long-term average $\Delta S = 0$.

Water Balance Term	Average annual value [mm]
Precipitation	717
Streamflow	257
Evapotranspiration	564
Net Groundwater	104 [inflow]

Table 3.6: Open water balance for each post-fire year, both observed (with fire) and expected (had fire not occurred). The "Groundwater and/or Storage" term is signed to represent the directionality: positive sign indicates a combination of increased catchment storage and/or groundwater outflow; negative sign indicates decreased catchment storage and/or groundwater inflow.

Year after the fire	Component	Observed [mm]	Expected [mm]	Cumulative Observed – Expected [mm]
1	Precipitation	785	785	
	ET	461	662	-201
	Streamflow	212	263	-51
	Groundwater and/or Storage	113	-139	252
2	Precipitation	802	802	
	ET	552	502	-151
	Streamflow	356	274	31
	Groundwater and/or Storage	-106	26.1	120
3	Precipitation	850	850	
	ET	524	451	-77
	Streamflow	367	313	85
	Groundwater and/or Storage	-42	87	-8
4	Precipitation	657	657	
	ET	493	592	-176
	Streamflow	210	175	120
	Groundwater and/or Storage	-46	-110	56
5	Precipitation	863	863	
	ET	522	575	-229
	Streamflow	312	309	124
	Groundwater and/or Storage	28	-22	105
6	Precipitation	912	912	
	ET	532	471	-168
	Streamflow	351	346	129
	Groundwater and/or Storage	29	95	39
7	Precipitation	773	773	
	ET	481	488	-175
	Streamflow	251	256	124
	Groundwater and/or Storage	42	30	51
8	Precipitation	828	828	
	ET	546	523	-152
	Streamflow	286	295	116
	Groundwater and/or Storage	-5	10	36

FIGURES

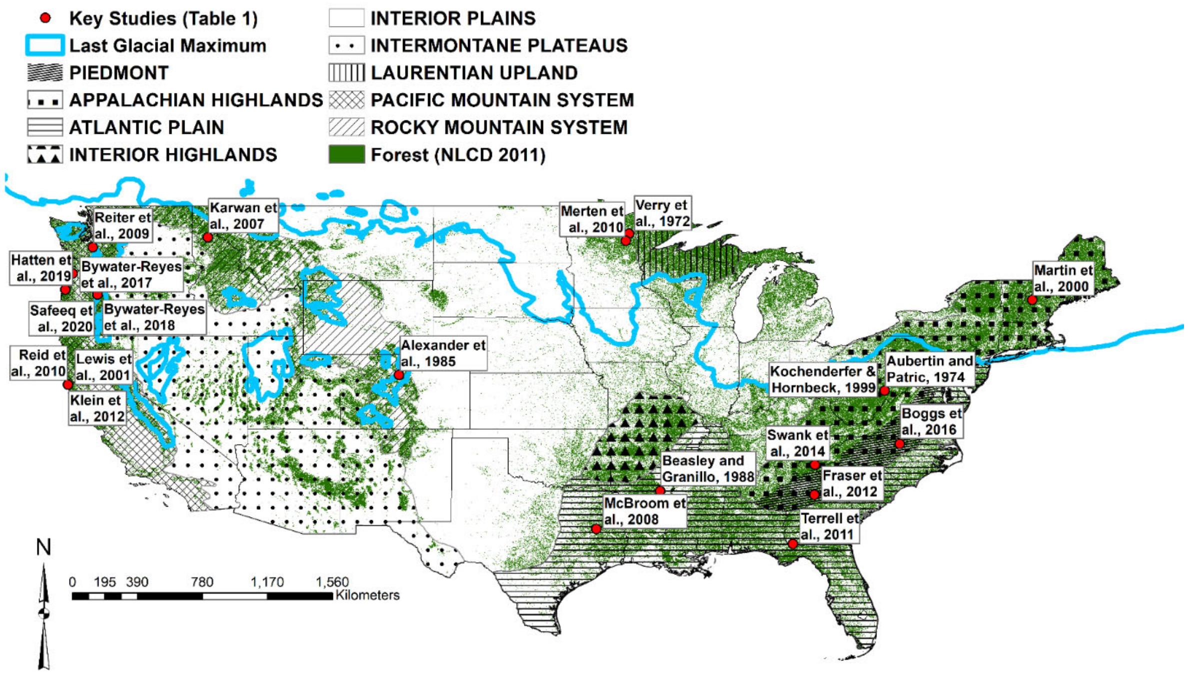

Figure 1.1: Contiguous United States with physiographic divisions (Fenneman and Johnson, 1946) and US states. The regional review is based on landscape and management characteristics: Northeast (Appalachian Highlands, Piedmont, and Coastal Plain north of Maryland), western Lake States (Laurentian Highlands and surrounding areas in Minnesota, Wisconsin, and Michigan), Southeast (Appalachian Highlands, Piedmont, and Coastal Plain south of Maryland), intermountain West (Rocky Mountain System), and Pacific Mountain System (Pacific Mountain System). State boundaries modified from National Weather Service 1999. Forest cover is shown from the NLCD 2011 (Homer et al., 2015), and the last glacial maximum is shown in light blue (Ehlers, Gibbard, and Hughes (eds), 2011).

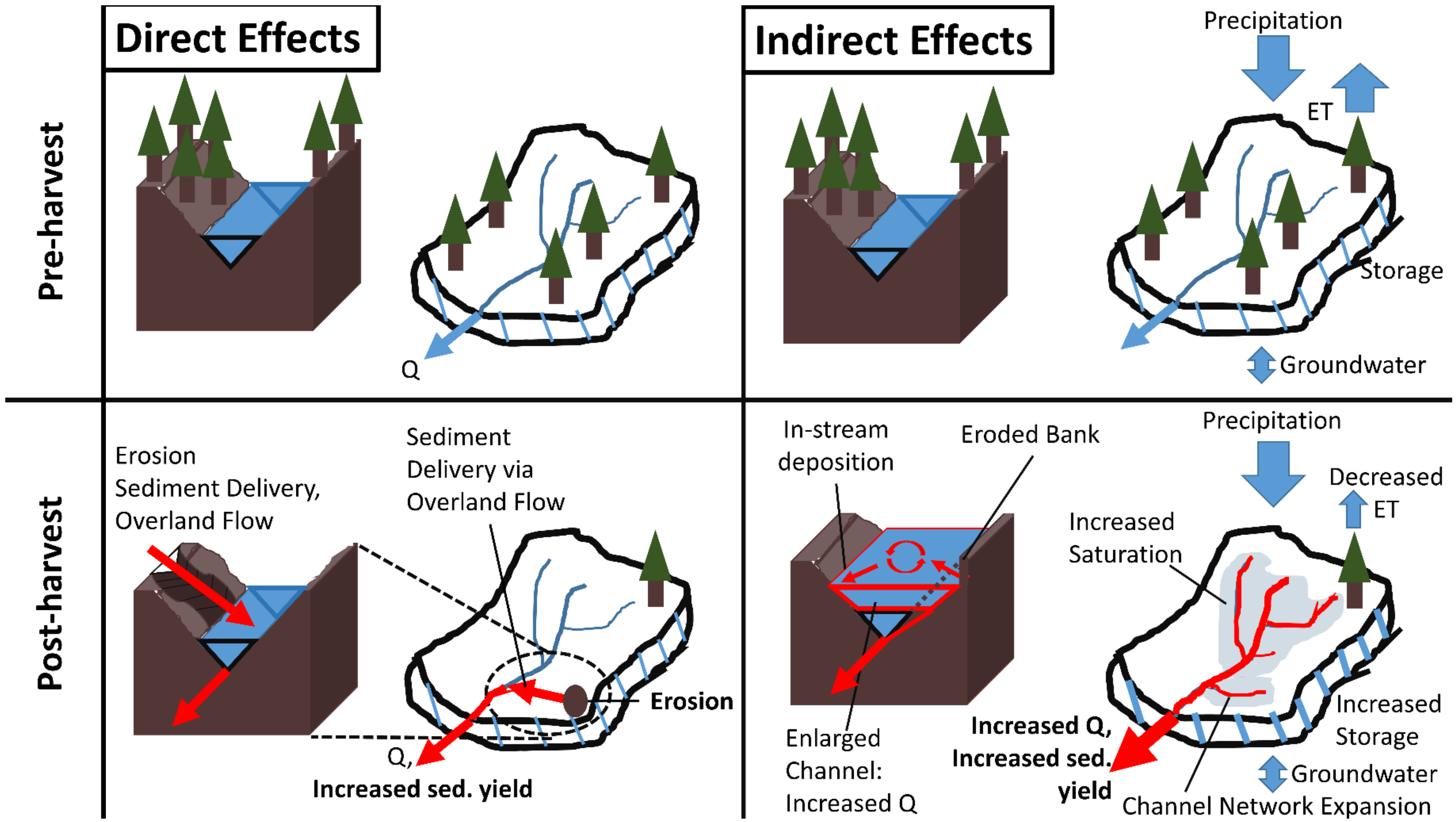

Figure 1.2: Conceptual model of direct and indirect effects of forest harvesting on sediment yield in temperate forested watersheds. Sediment movement and transport is illustrated in red. Note that for direct effects, sediment connectivity (red) is congruous with overland hydrologic connectivity (represented by red sediment delivery arrow). For indirect effects, hydrologic connectivity (light blue) is large throughout the watershed but sediment connectivity (red) is primarily within and near the fluvial network.

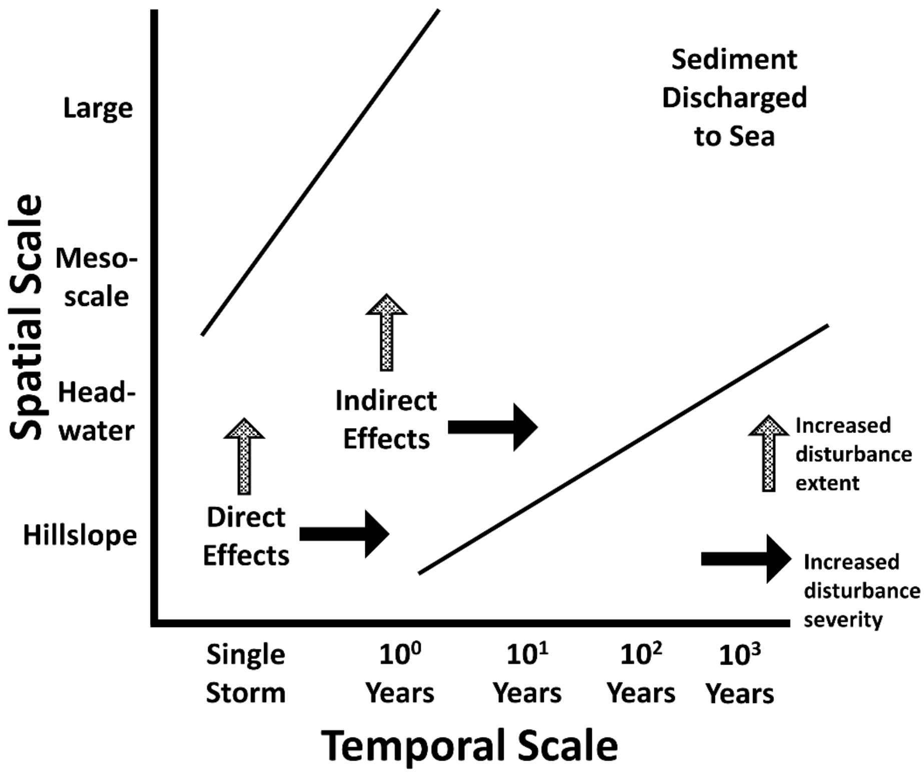

Figure 1.3: Space-time diagram for direct and indirect effects (based on Figure 2.3 in National Research Council, 1988). Direct effects are defined at the hillslope spatial scale and single storm temporal scale; indirect effects are defined in reference to catchment-scale changes in the water balance and thus occur at the scale of (generally small) catchments. Increased disturbance severity that limits soil and hydrologic recovery can cause direct and indirect effects to persist longer in time, and increased spatial extent of disturbance can cause direct and indirect effects to be significant at larger spatial scales. Discharge of sediment deposited in streams due to direct or indirect effects can take > 1000 years depending on local geomorphic and hydrologic conditions.

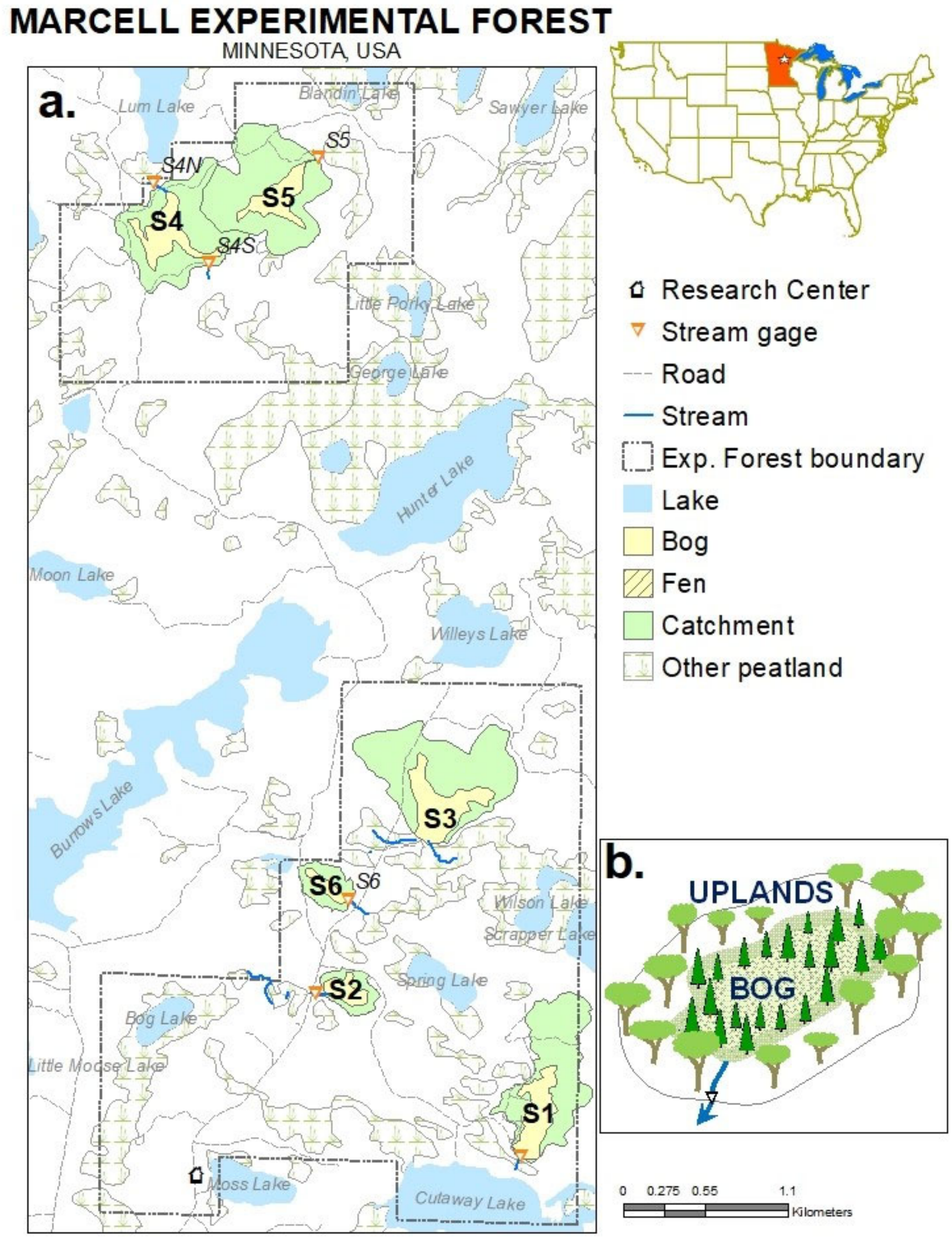

Figure 2.1: a) Marcell Experimental Forest. b) a typical upland-peatland watershed such as those found at the MEF. Thank you to Stephen Sebestyen, USDA Forest Service, for this figure.

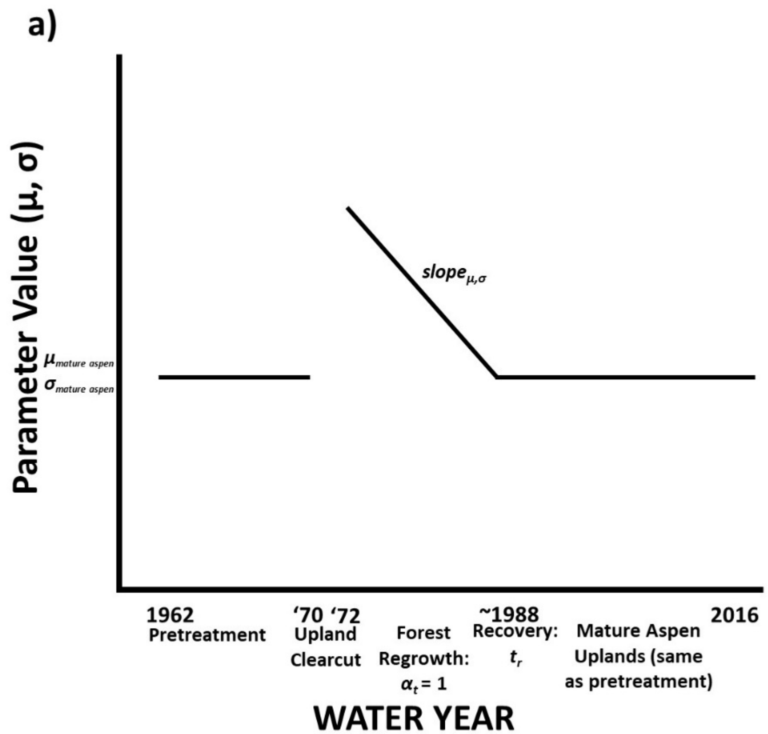

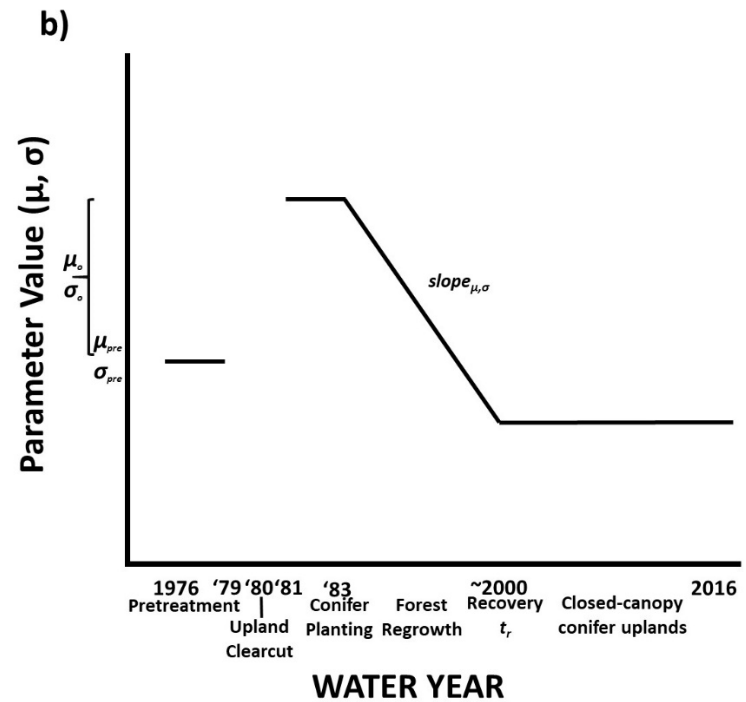

Figure 2.2: Nonstationary parameter evolution for the location and scale parameters for the a) S4 and b) S6 catchments.

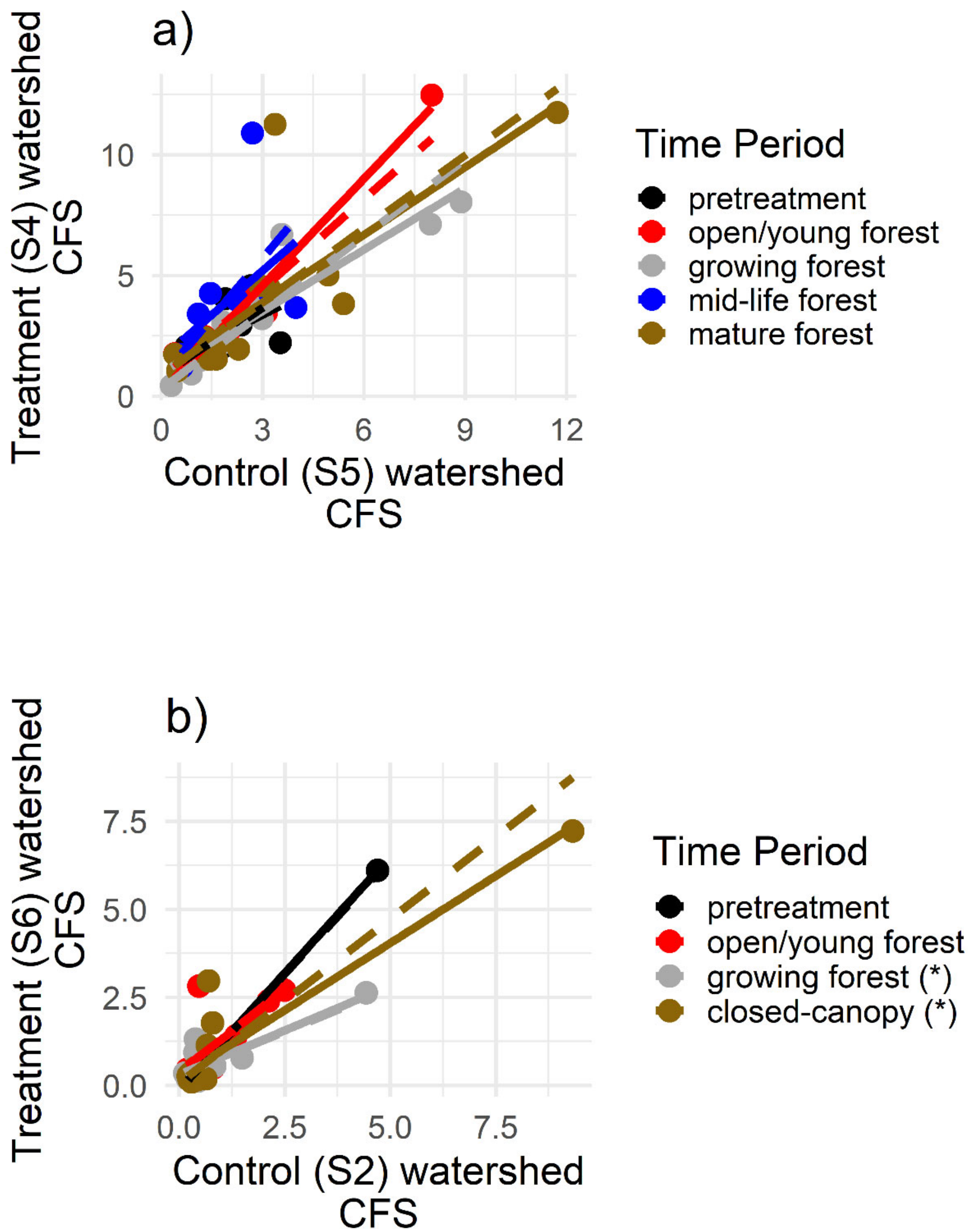

Figure 2.3: a) S4 experiment ANCOVA (solid line) and GLS (dashed line) analyses of annual maximum flows. No significant differences in slopes or intercepts for the ANCOVA regression, nor for the GLS regression. b) S6 experiment ANCOVA (solid line) and GLS (dashed line) analyses of annual maximum flows. Significantly different regression slopes according to ANCOVA are indicated by (*). There were no significant treatment effects according to the GLS analysis.

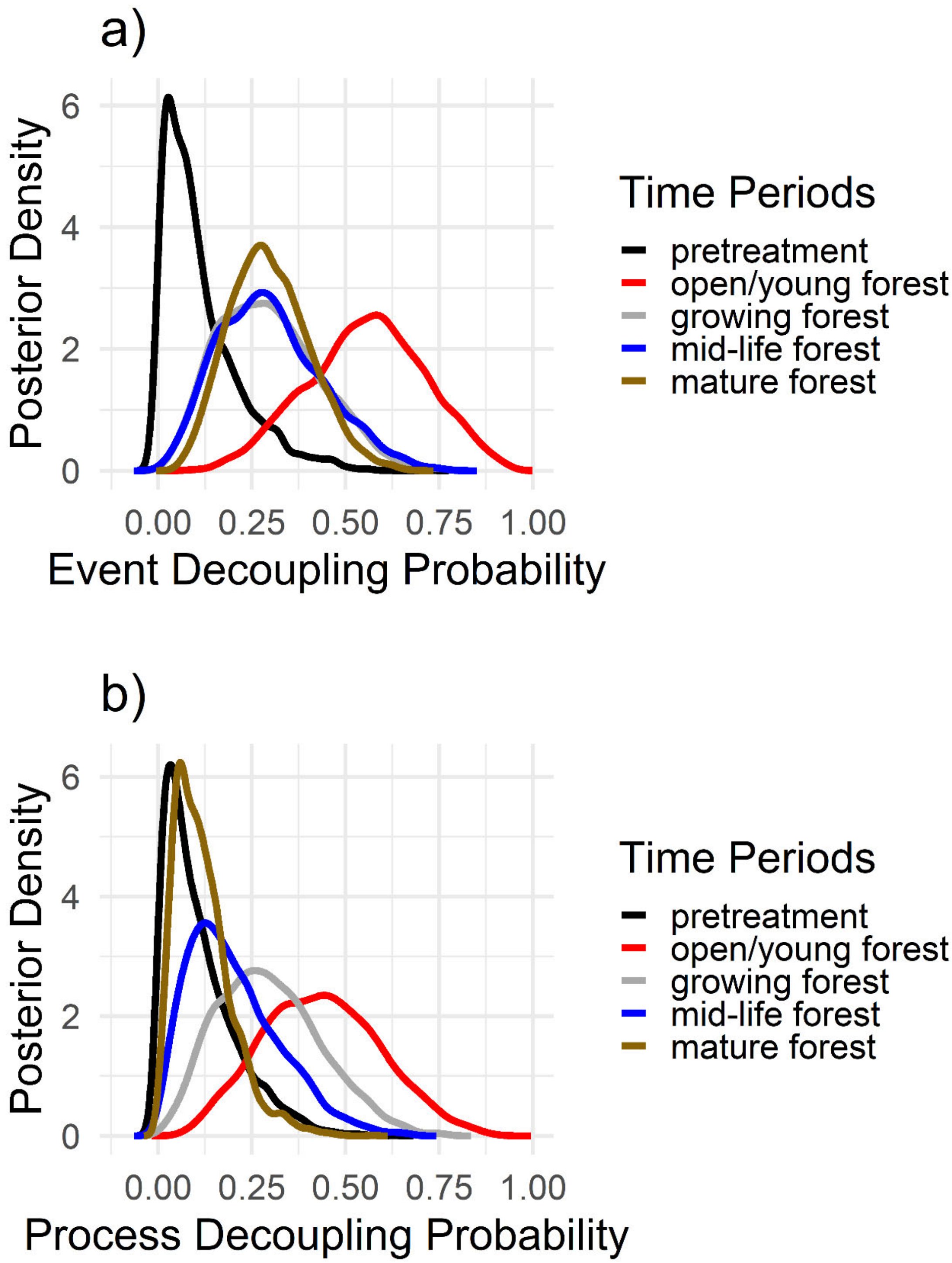

Figure 2.4: Caption on page 131.

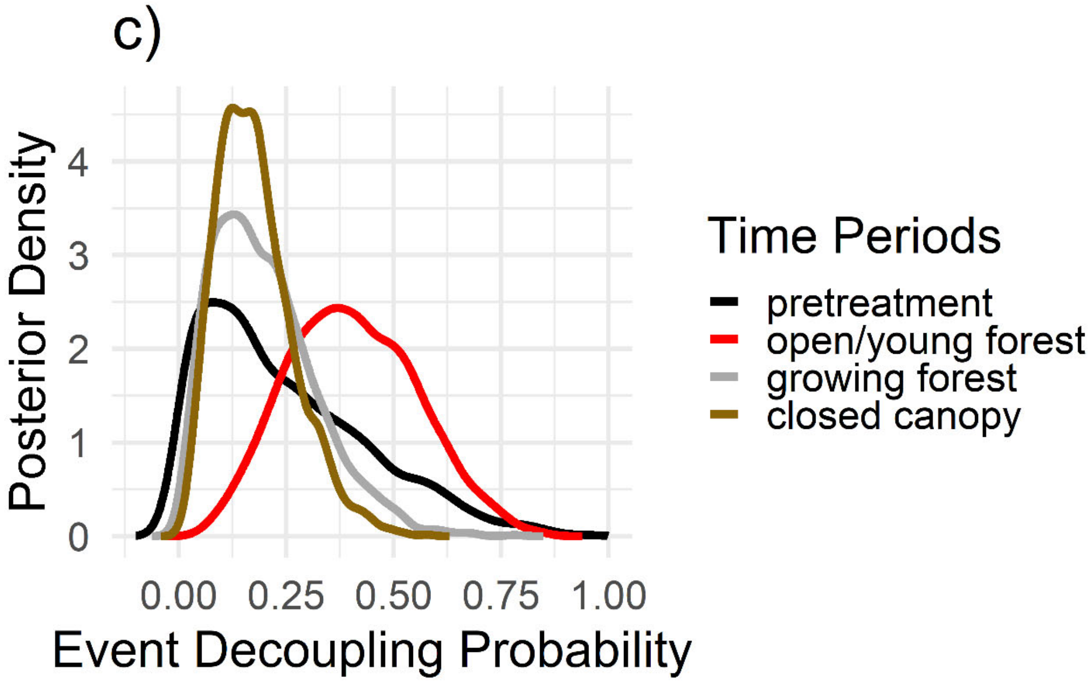

Figure 2.4: a) Event decoupling probabilities for the S4/S5 experiment, from the logistic regression. b) Streamflow generating process decoupling probabilities for the S4/S5 experiment. c) Event decoupling probabilities for the S2/S6 experiment. P-values for differences in all decoupling probabilities with respect to pretreatment are in Table 2.2.

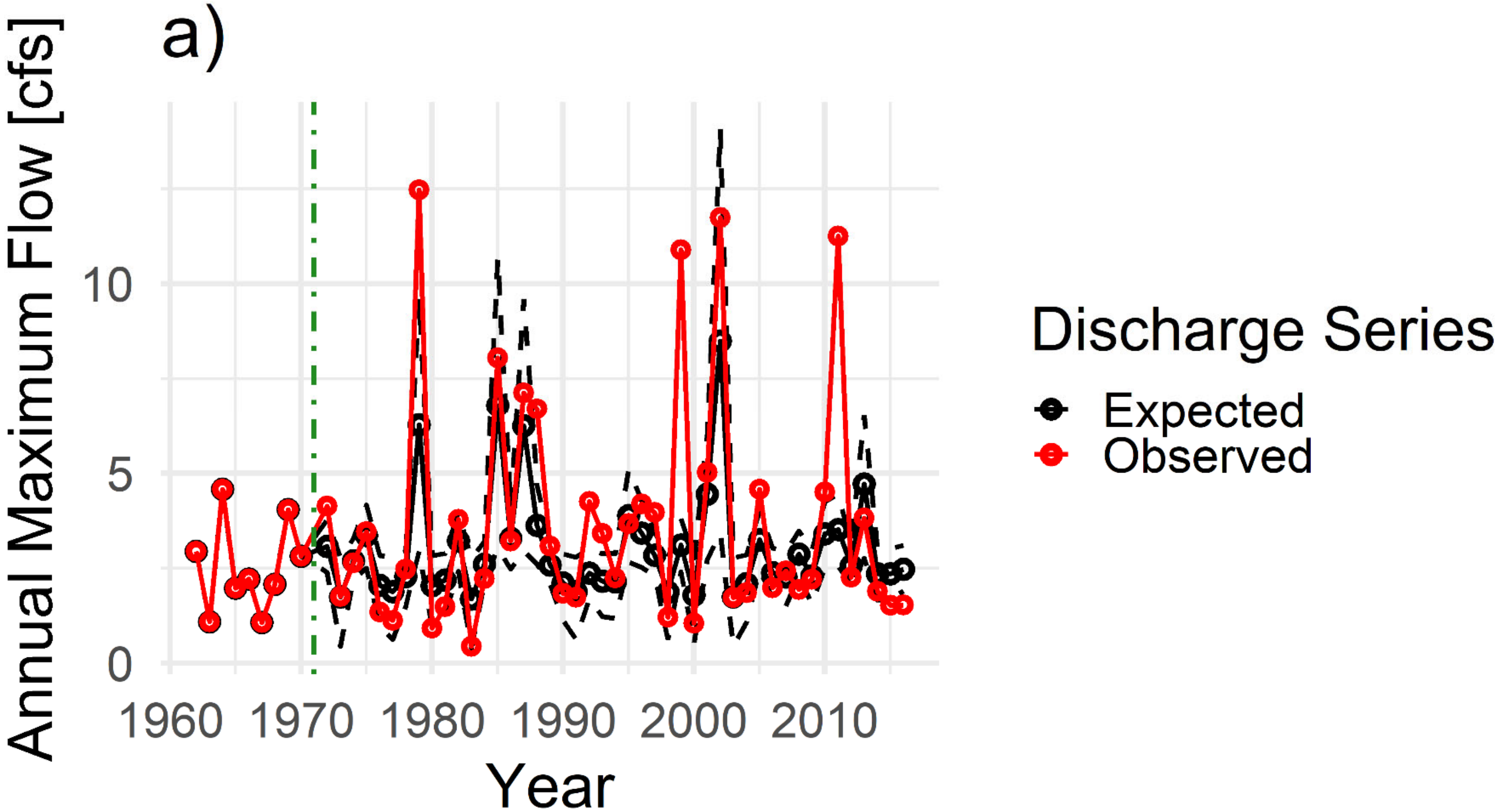

Figure 2.5a: Expected and observed series' for a) S4 and b) S5, plus uncertainty of the expected series shown as a 90% credible interval based on 70 expected series fit from the calibration regressions (dashed lines). The year of upland clearcut harvesting for each catchment is represented by a dashed green line.

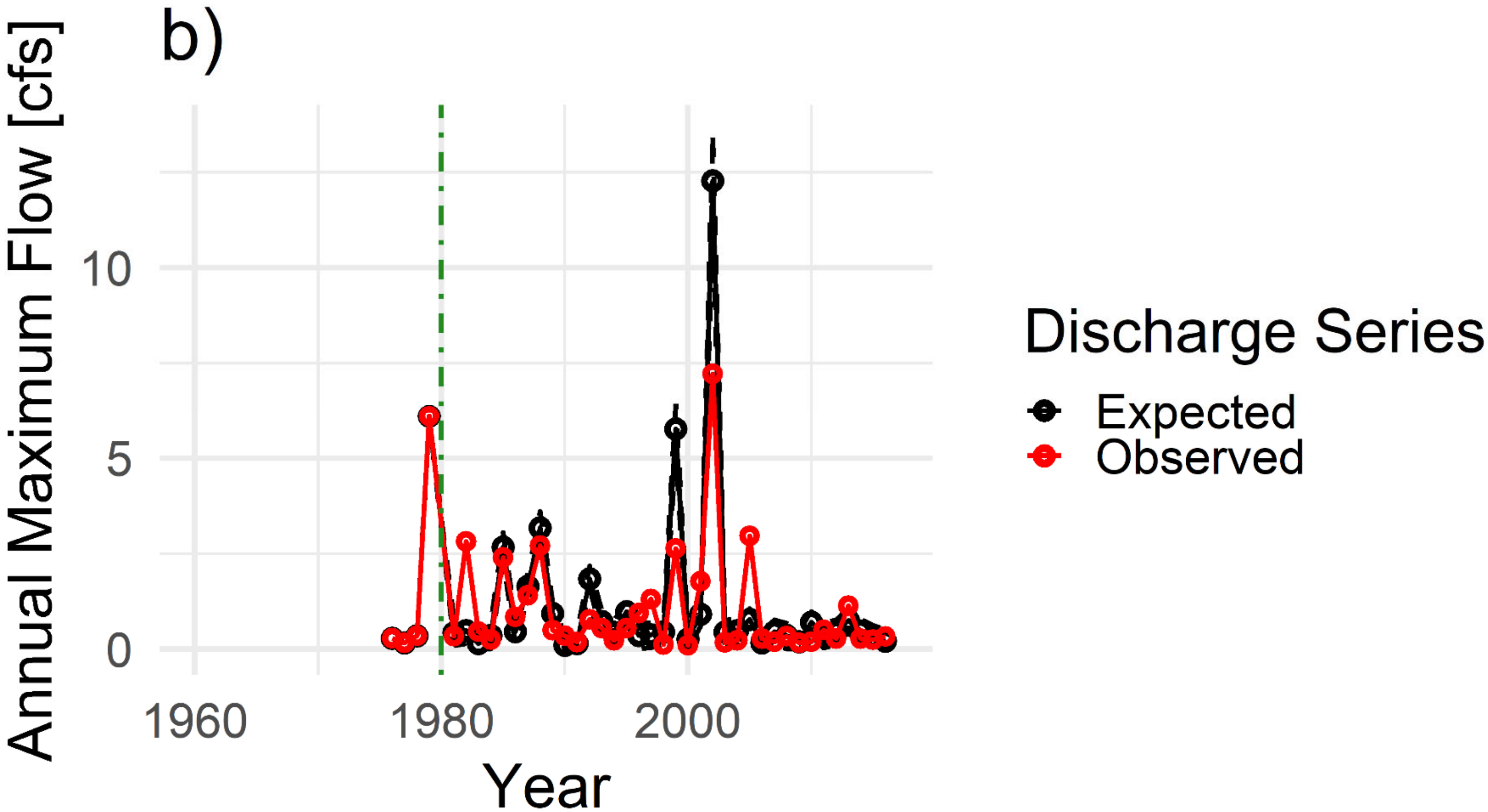

Figure

Figure 2.5b: Expected and observed series' for a) S4 and b) S5, plus uncertainty of the expected series shown as a 90% credible interval basd on 70 expected series fit from the calibration regressions (dashed lines). The year of upland clearcut harvesting for each catchment is represented by a dashed green line.

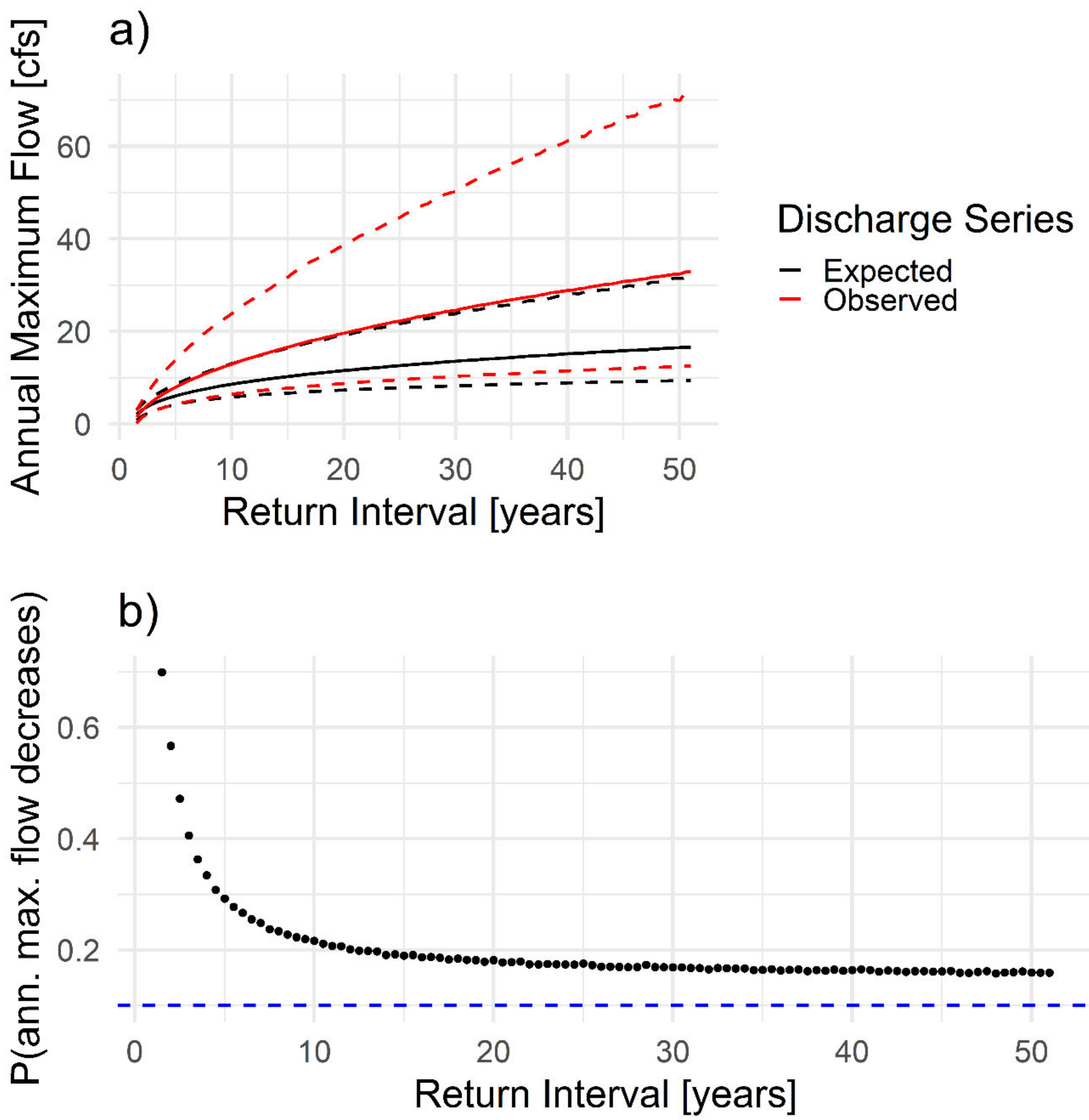

Figure 2.6: a) S4 cumulative distribution for the first year after upland clearcut, compared to expected conditions derived from the calibration regression. Pictured with 90% credible intervals. b) Probability that I am incorrectly concluding that the N-year annual maximum flow is increasing, across return intervals up to N=50. A dashed line is shown at p = 0.10 for reference.

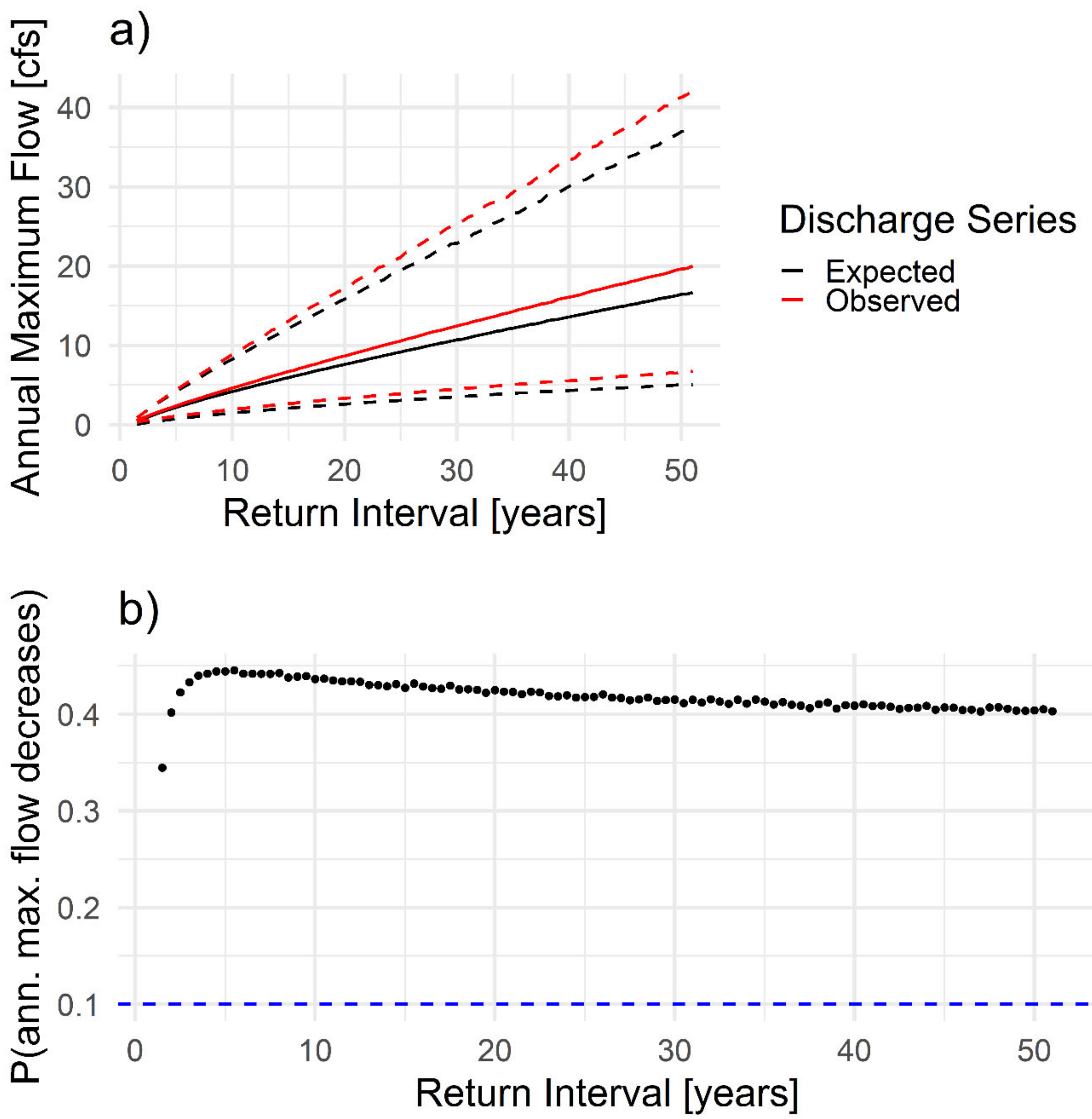

Figure 2.7: a) S6 cumulative distribution for immediately after upland forest harvesting, compared to the expected values derived from the control watershed adjusted to the calibration regression. b) S6 probabilities that I am incorrect in stating that the N-year annual maximum flow decreased due to upland harvesting. (c) and (d) are on page 136.

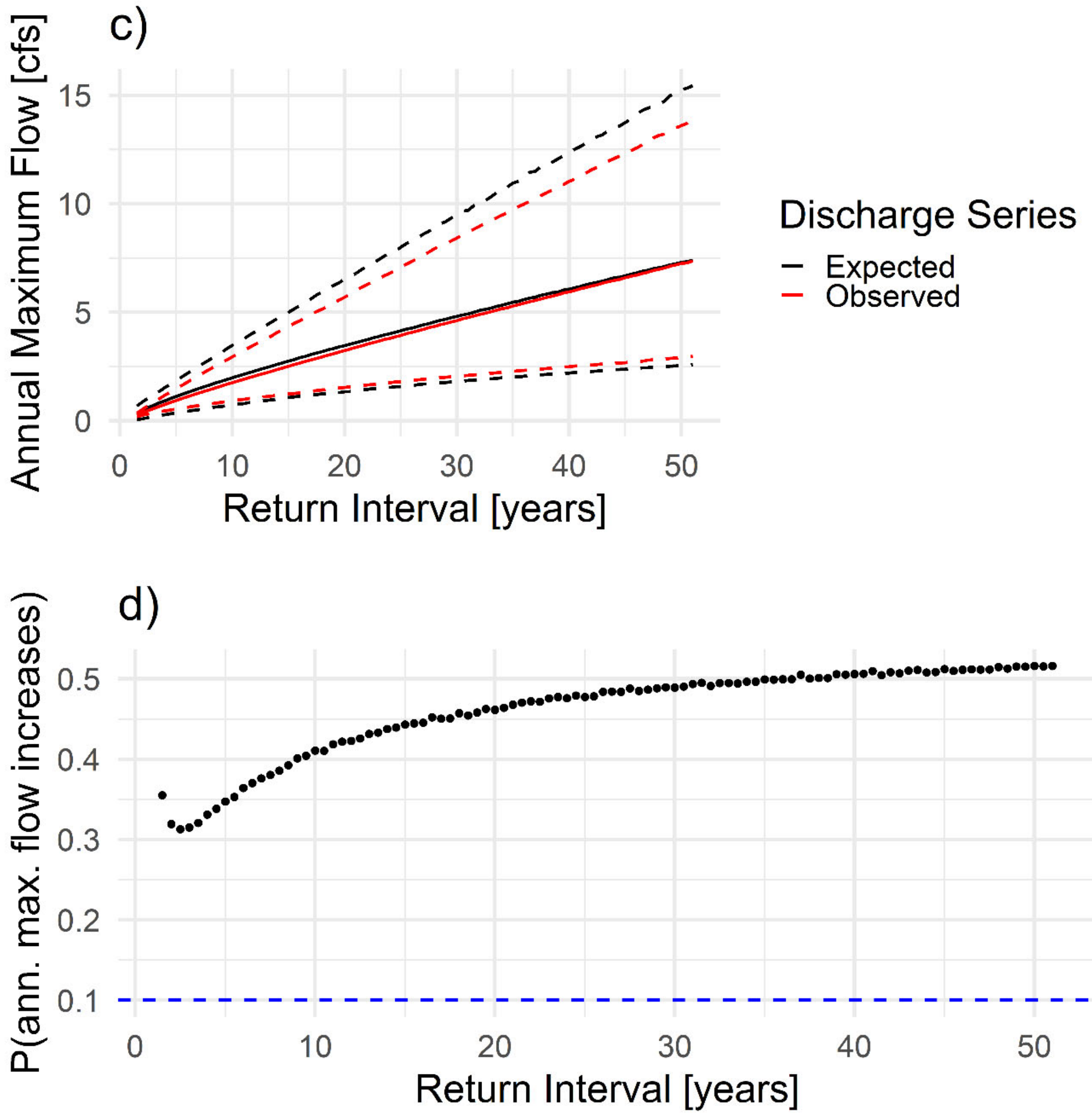

Figure 2.7: (a) and (b) are on page 135. c) S6 cumulative distribution for when S6 had a closed-canopy conifer forest, compared to the expected values derived from the control watershed d) S6 probabilities that I am incorrect in stating that the N-year annual maximum flow increased due to conversion from deciduous to coniferous species.

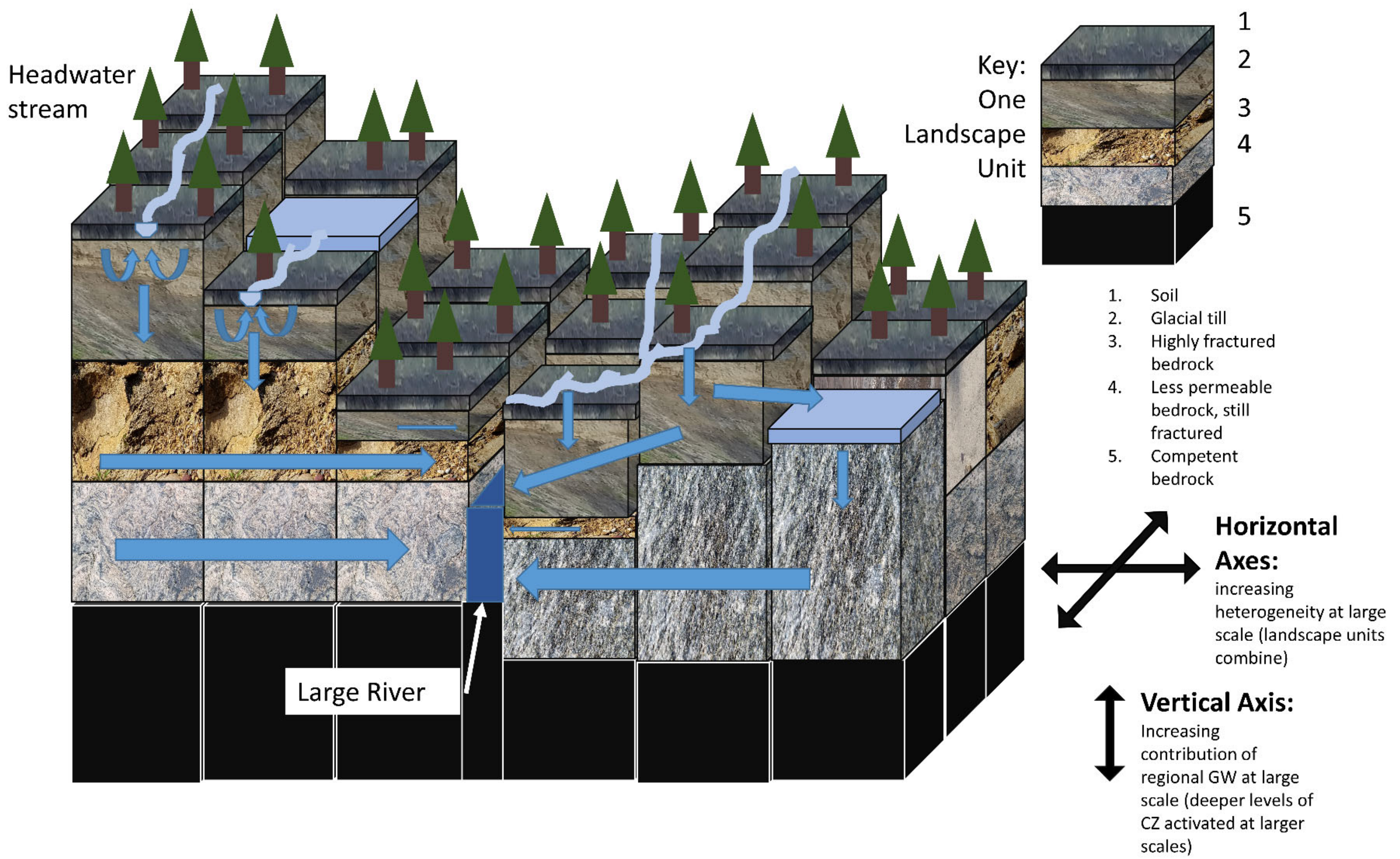

Figure 3.1a: a) A subset of the critical zone for a large river. For larger streams, more diverse landscape units combine to produce streamflow than in the smaller streams illustrated, corresponding to a horizontal axis of CZ change as catchments get larger. Further, deeper levels of the CZ are activate in producing streamflow for larger rivers, representing a vertical axis of CZ change as catchments get larger. (b) on page 138.

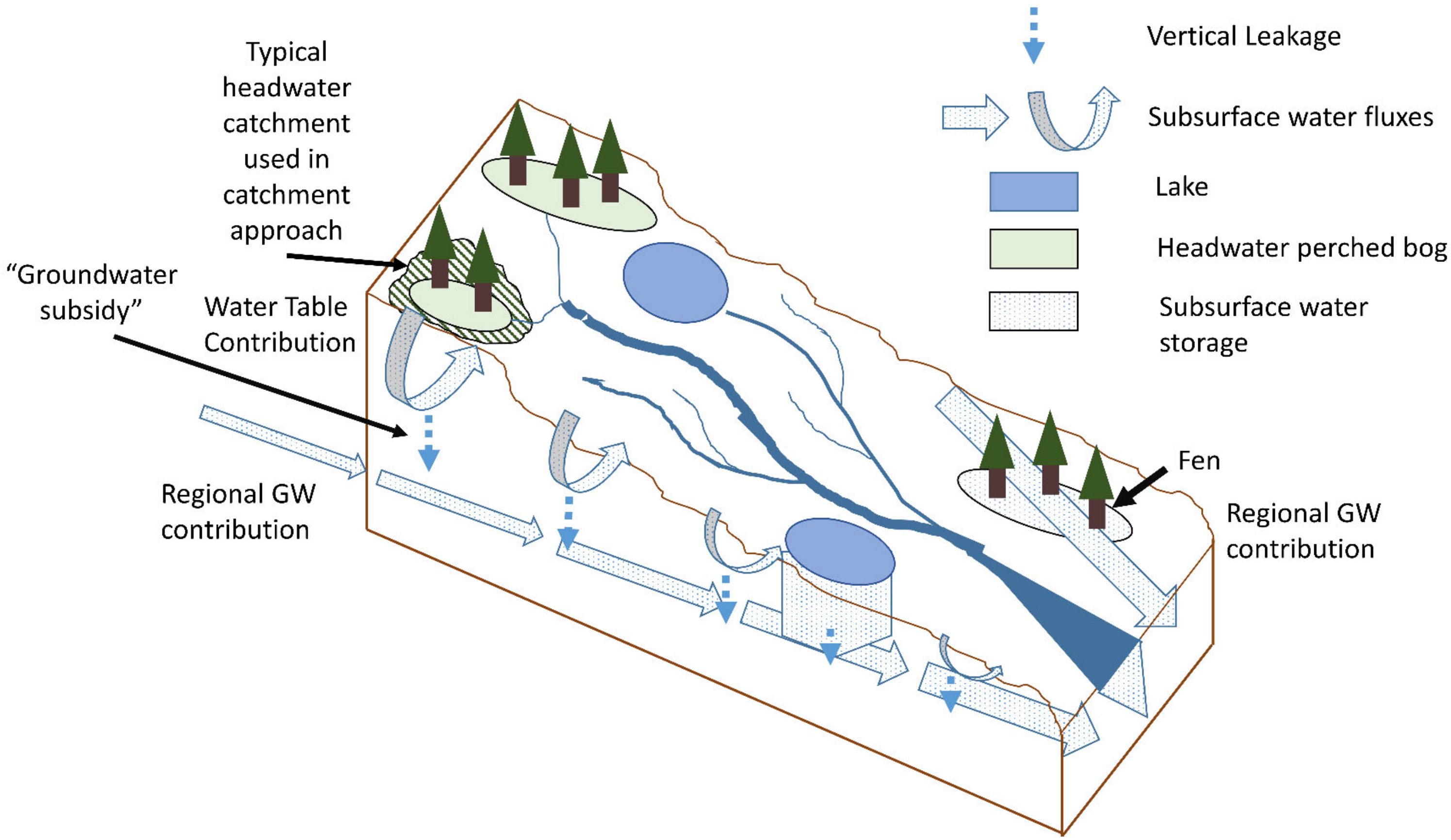

Figure 3.1b: b) Conceptual model for increasing importance of regional GW contribution at larger scales. Based on Figure 6 in Tiwari et al., 2017. Note the typical headwater catchment used in the catchment approach represents only one particular set of processes for groundwater exchange (water table influx to stream, deep seepage to regional groundwater flow). These "perched" conditions are also illustrated by the small lake near the headwaters, whereas the lake further downstream (and the downstream fen) is driven by regional groundwater.

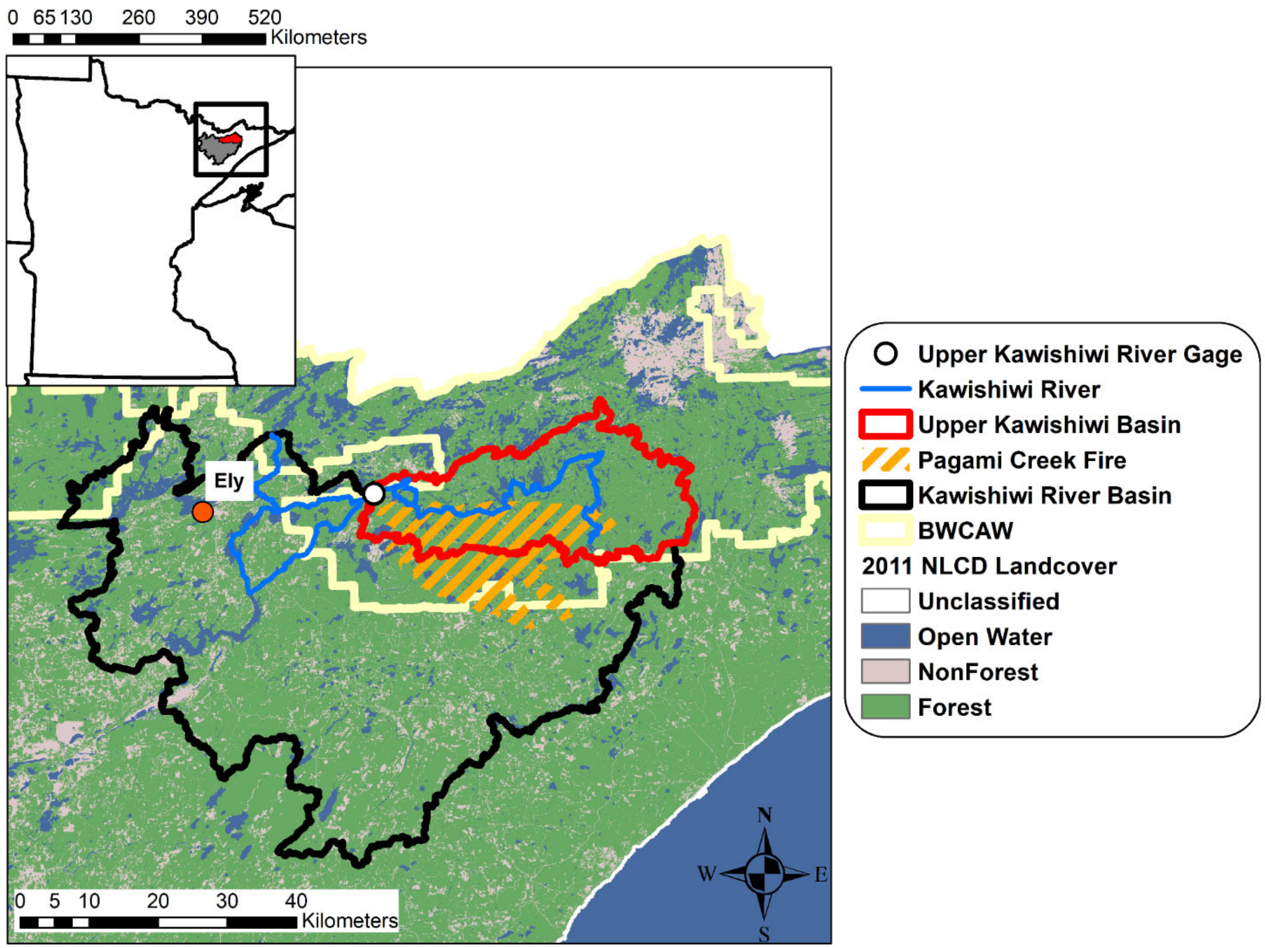

Figure 3.2: Kawishiwi River in northern Minnesota, USA.

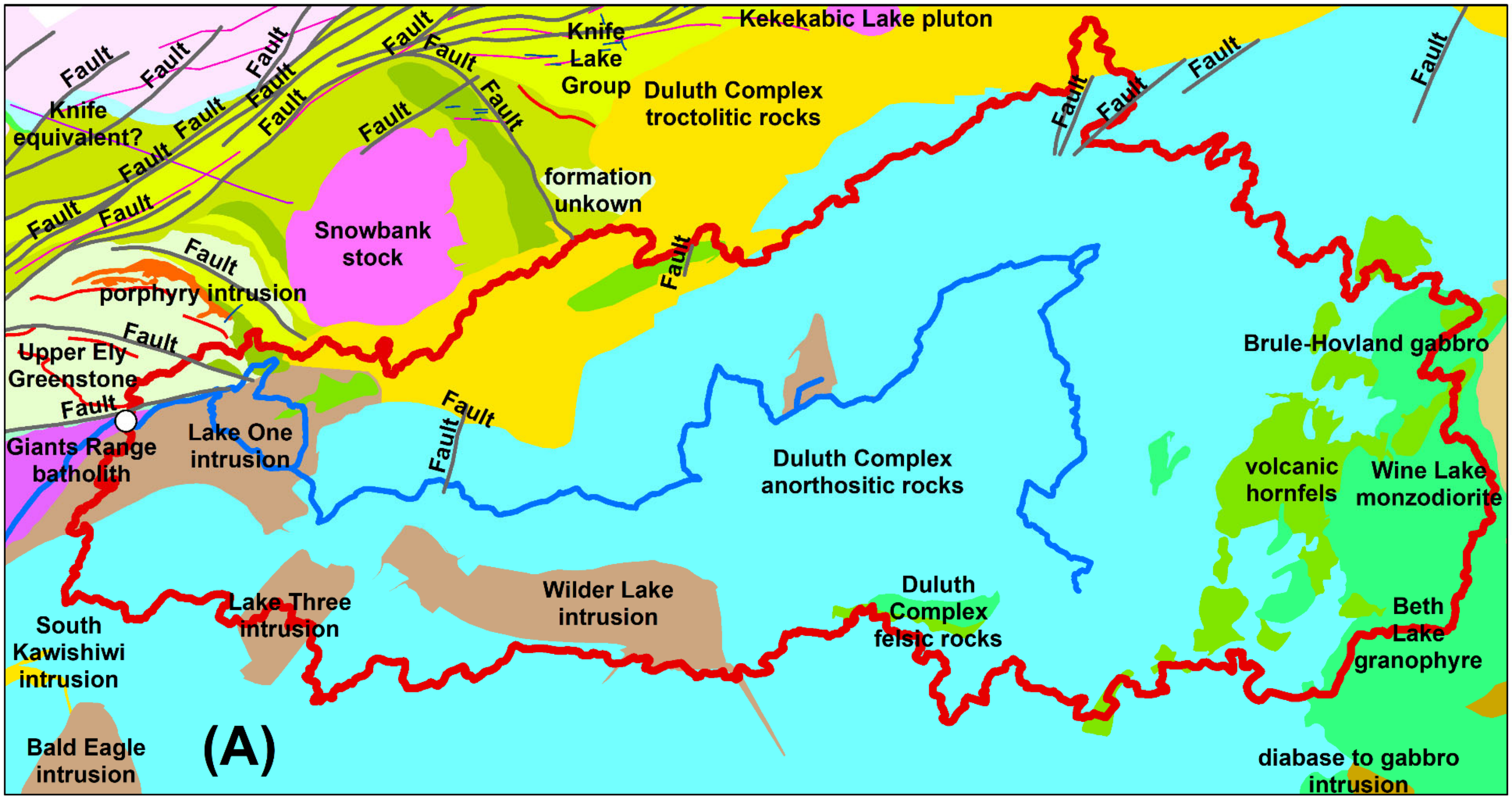

Figure 3.3a: Upper Kawishiwi catchment bedrock geology. Bedrock geology map from (Jirsa et al., 2011).

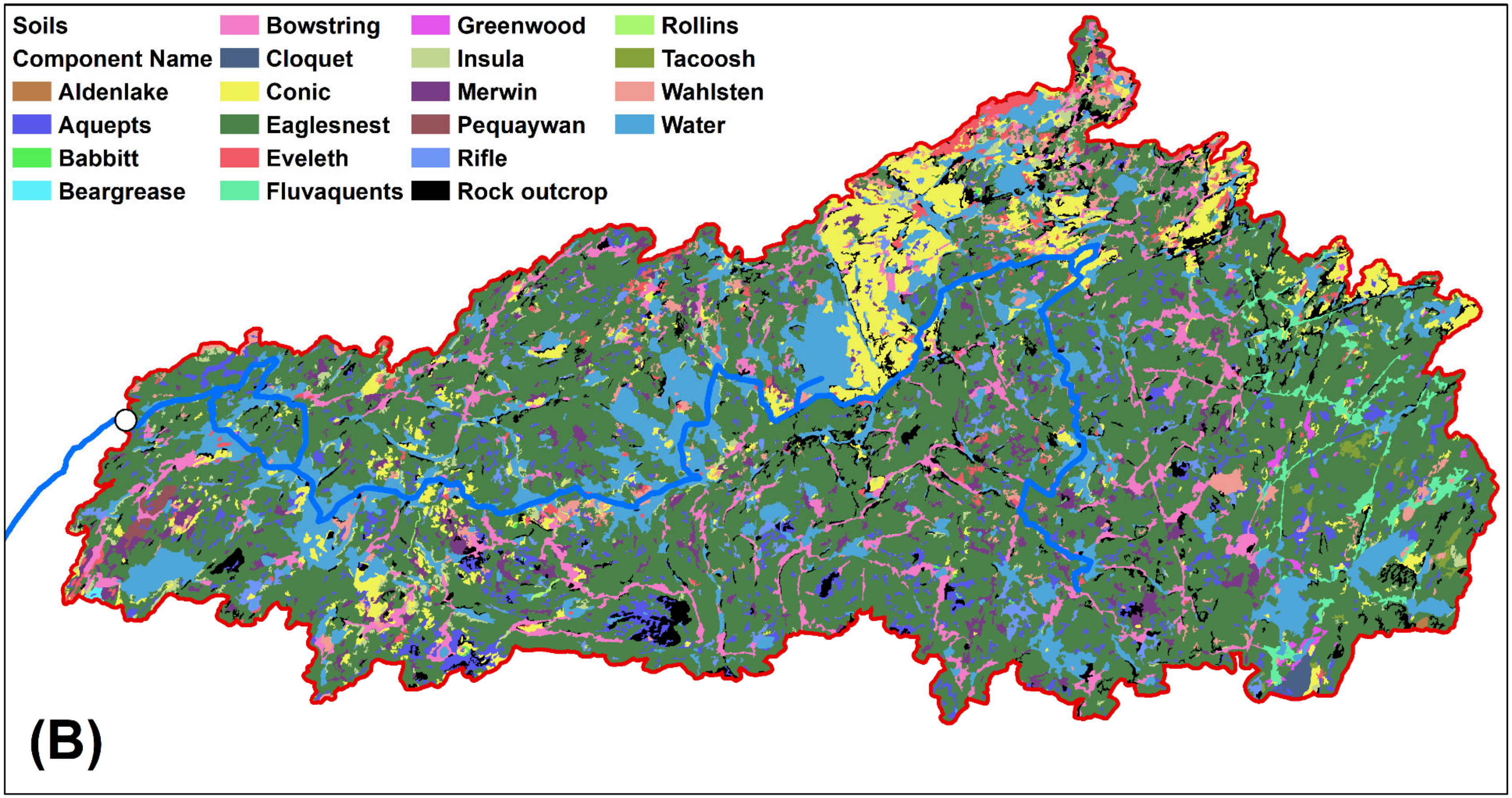

Figure 3.3b: Soil components in the Upper Kawishiwi catchment, dominated by Eaglesnest series. Soil map from GSSURGO (Soil Survey Staff, 2020).

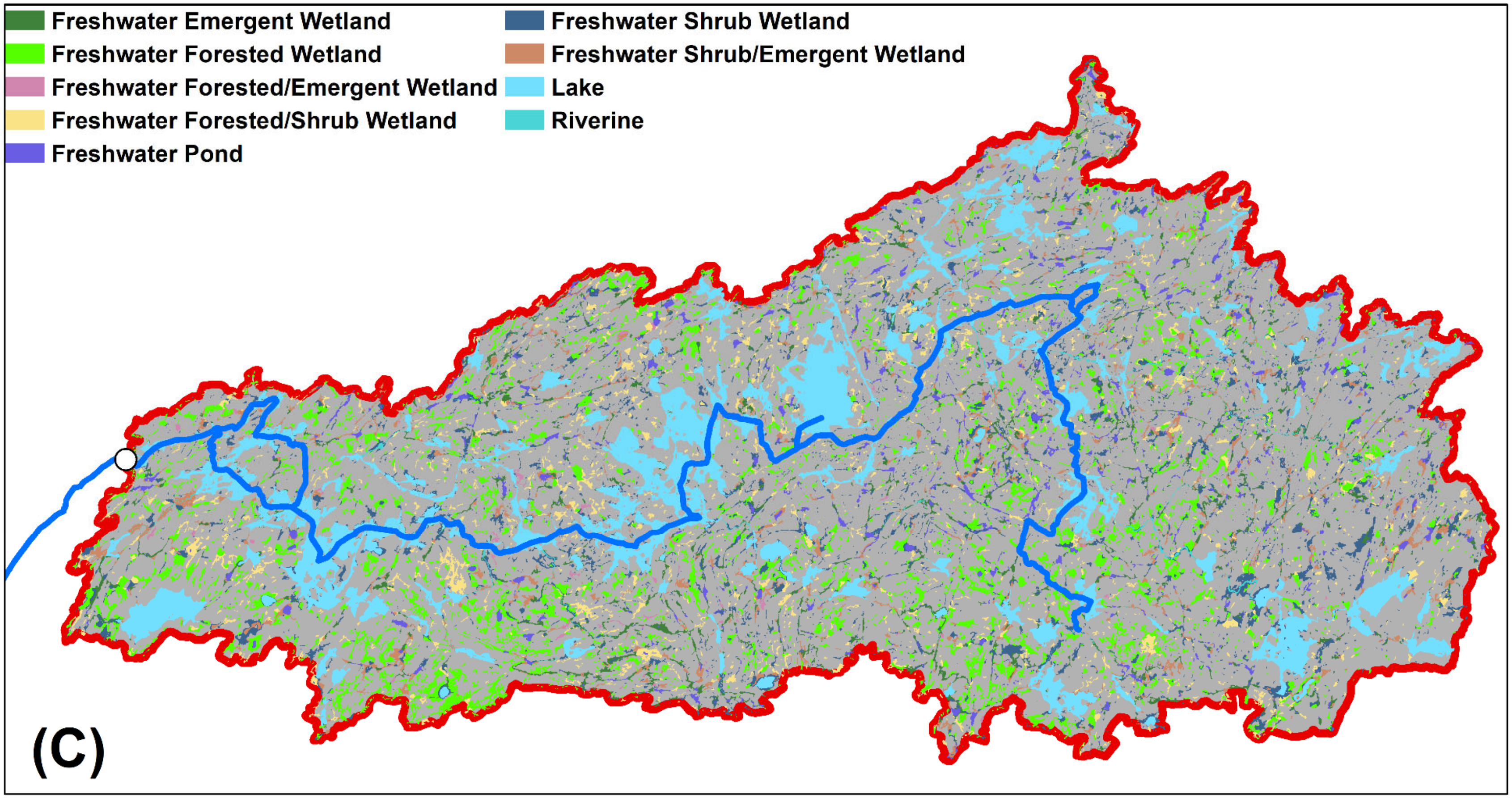

Figure 3.3c: Wetlands in the Upper Kawishiwi catchment. From the Minnesota National Wetlands Inventory (2019).

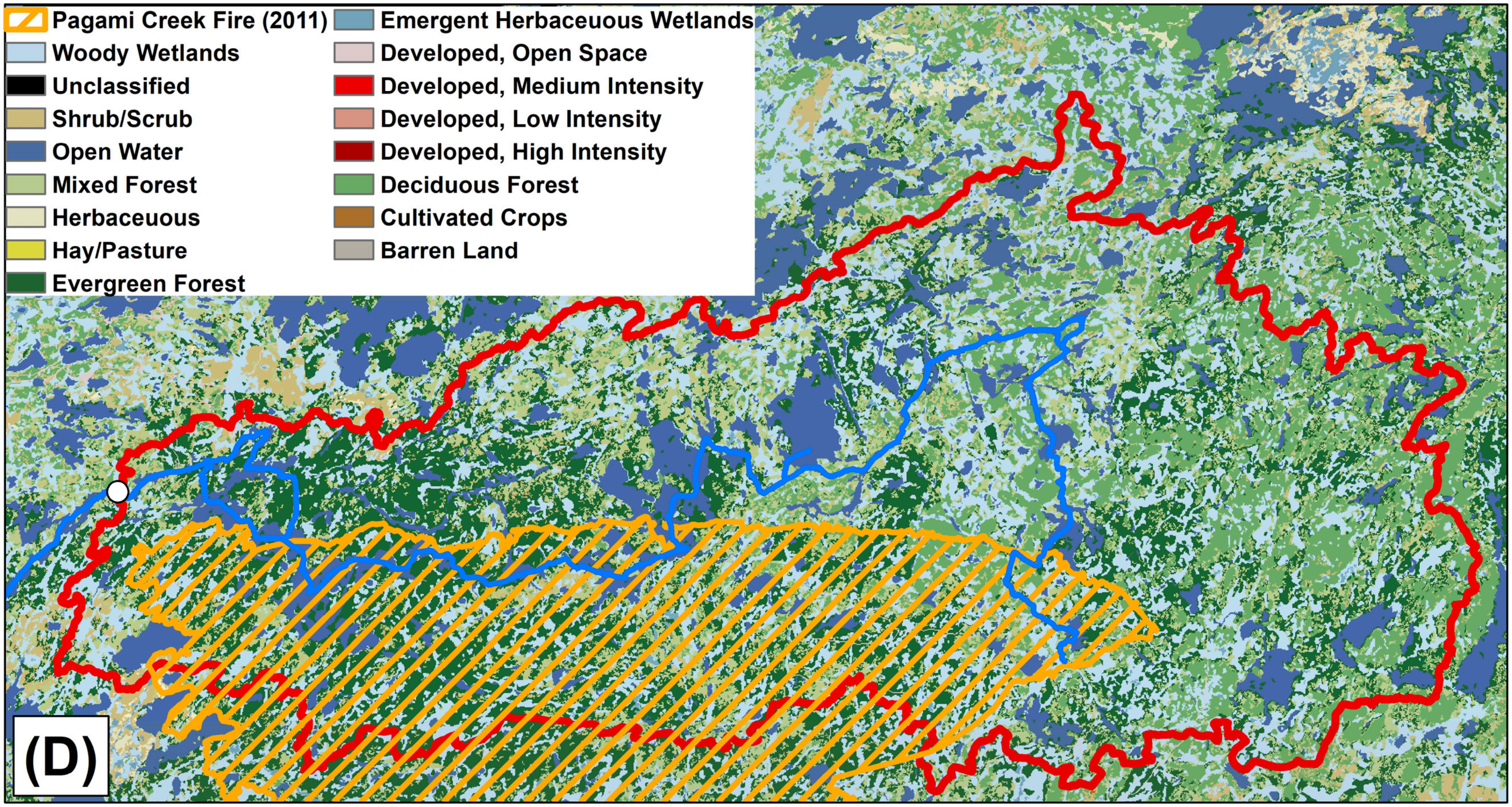

Figure 3.3d: Land cover in the Upper Kawishiwi catchment, from the 2011 NLCD (Homer et al., 2015). Perimeter of the 2011 Pagami Creek Fire is from USDA Forest Service National Forest System Lands GIS and Fire personnel (2020)

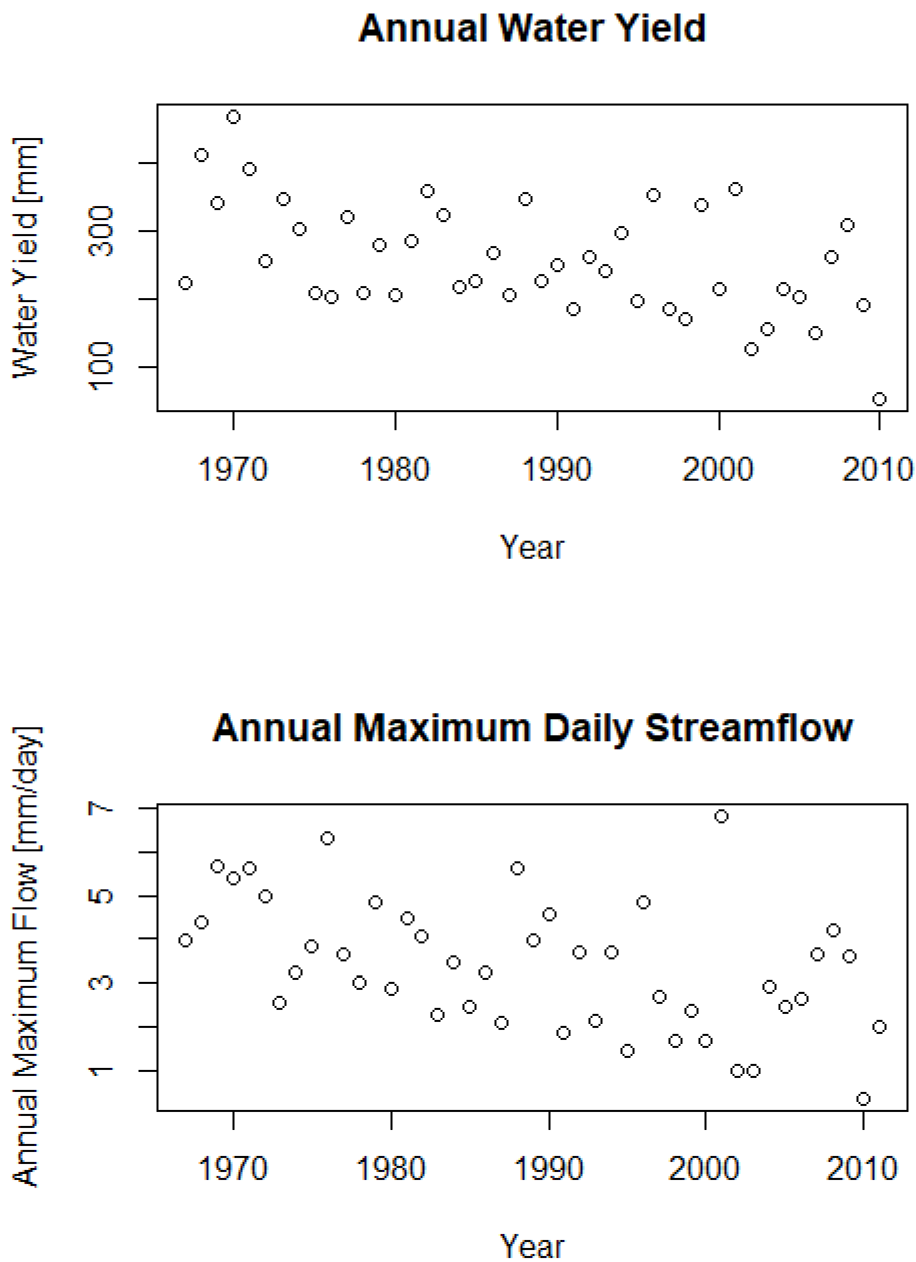

Figure 3.4: a) Annual water yield, and b) annual maximum daily streamflow are both significantly declining ($p < 0.001$).

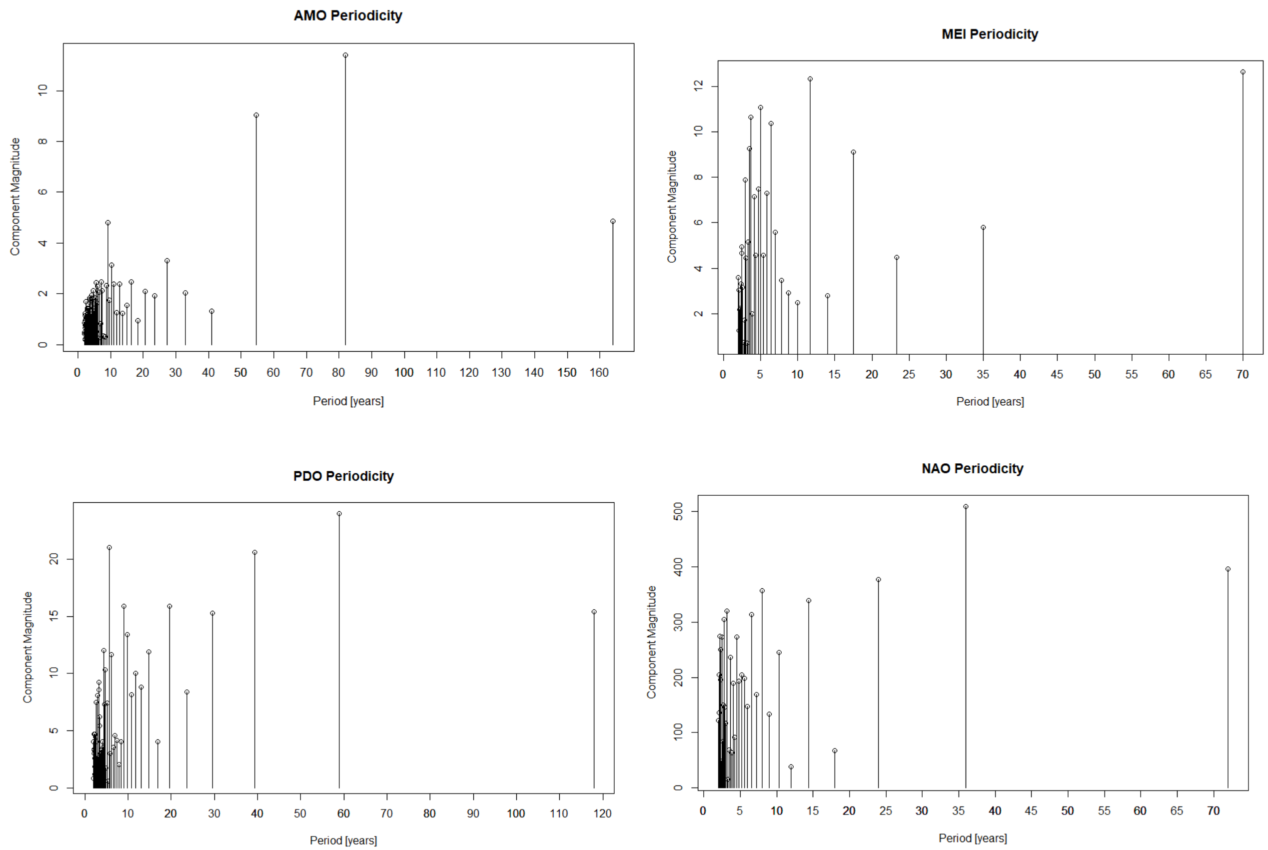

Figure 3.5: FFT spectral results for AMO, NAO, PDO, and MEI (this page), alongside FFT results from precipitation, dew point, minimum and maximum vapor pressure deficit, and temperature (page 146).

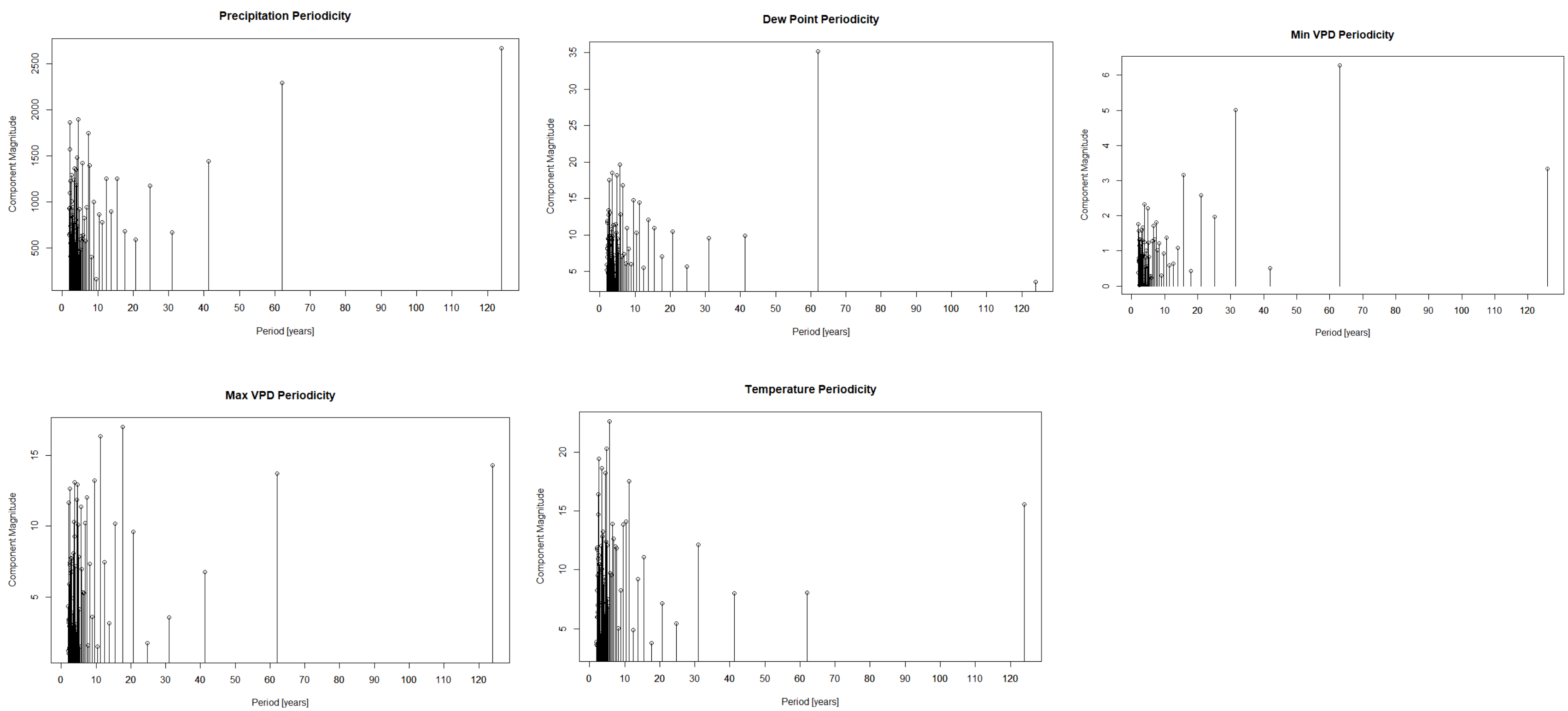

Figure 3.5, continued: FFT spectral results for AMO, NAO, PDO, and MEI (page 145), alongside FFT results from annual precipitation, annual average monthly dew point, annual average minimum and maximum monthly vapor pressure deficit, and annual average temperature (this page).

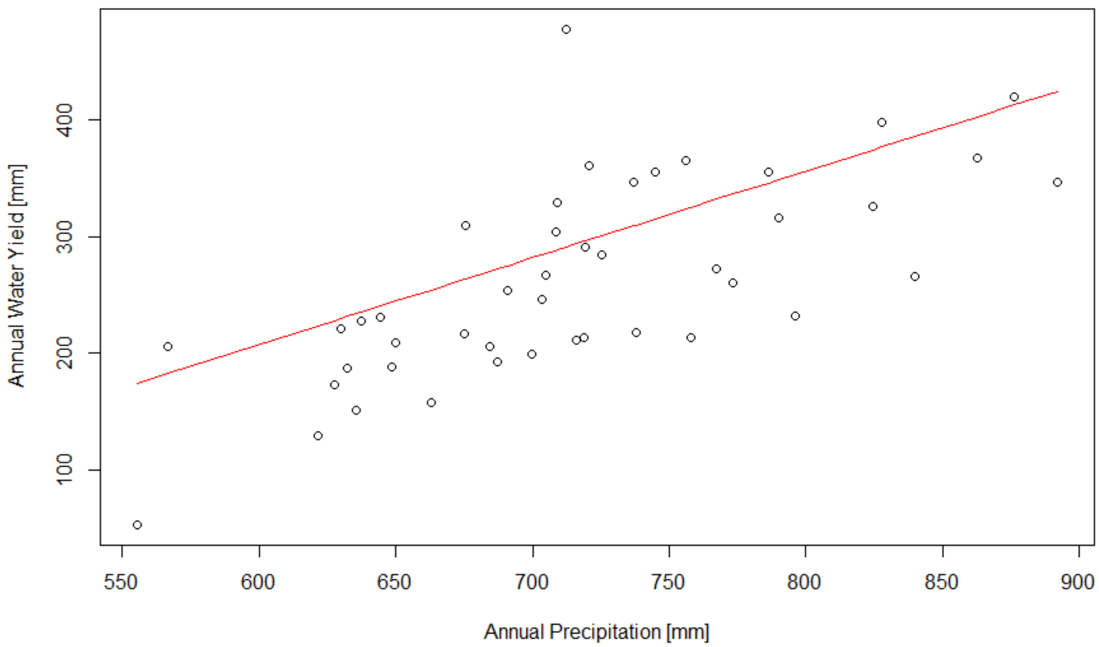

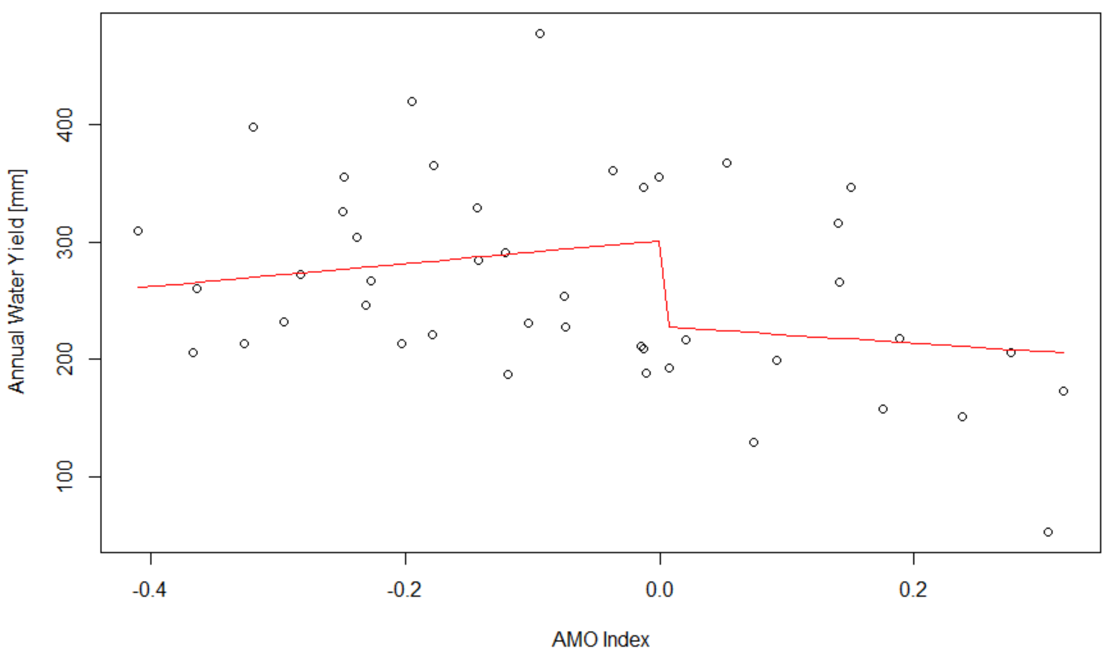

Figure 3.6: Linear regressions for (top to bottom): a) Annual water yield versus annual precipitation, at the mean AMO index for the period of record; b) annual water yield versus AMO index, at the mean value of precipitation; (figure continued on next page)

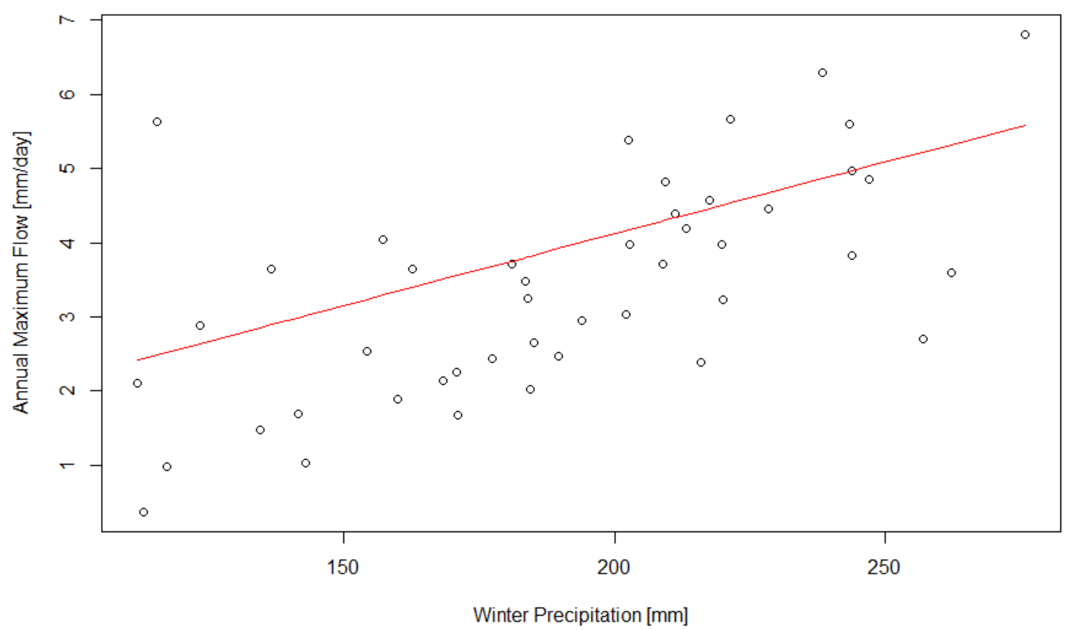

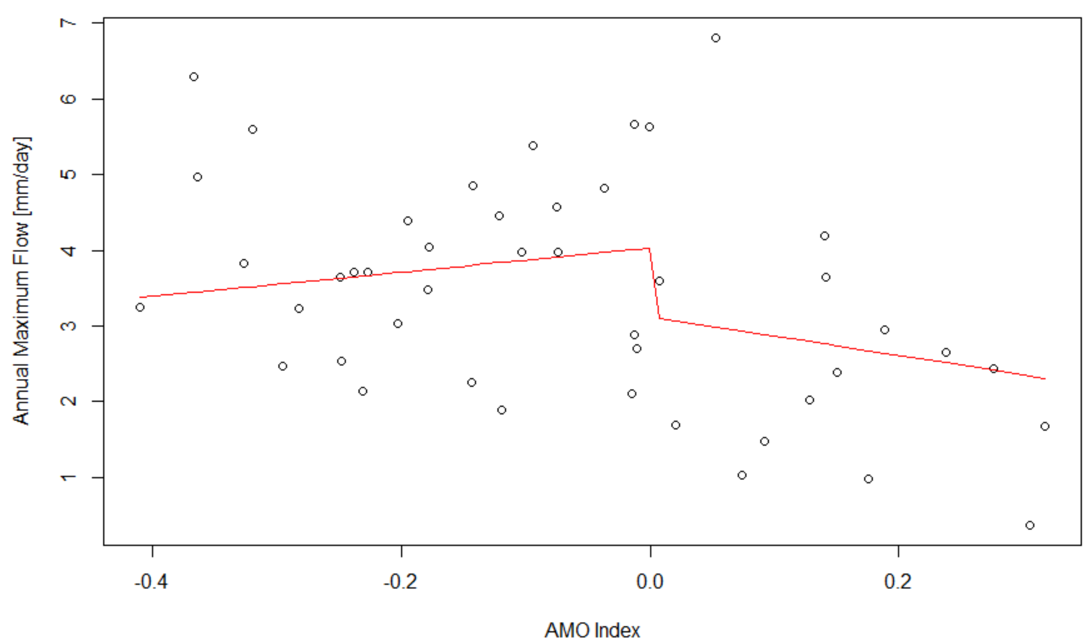

Figure 3.6: (continuation from previous page): c) annual maximum flow versus winter precipitation, at the mean AMO index; d) annual maximum flow versus AMO index, at the mean value of winter precipitation.

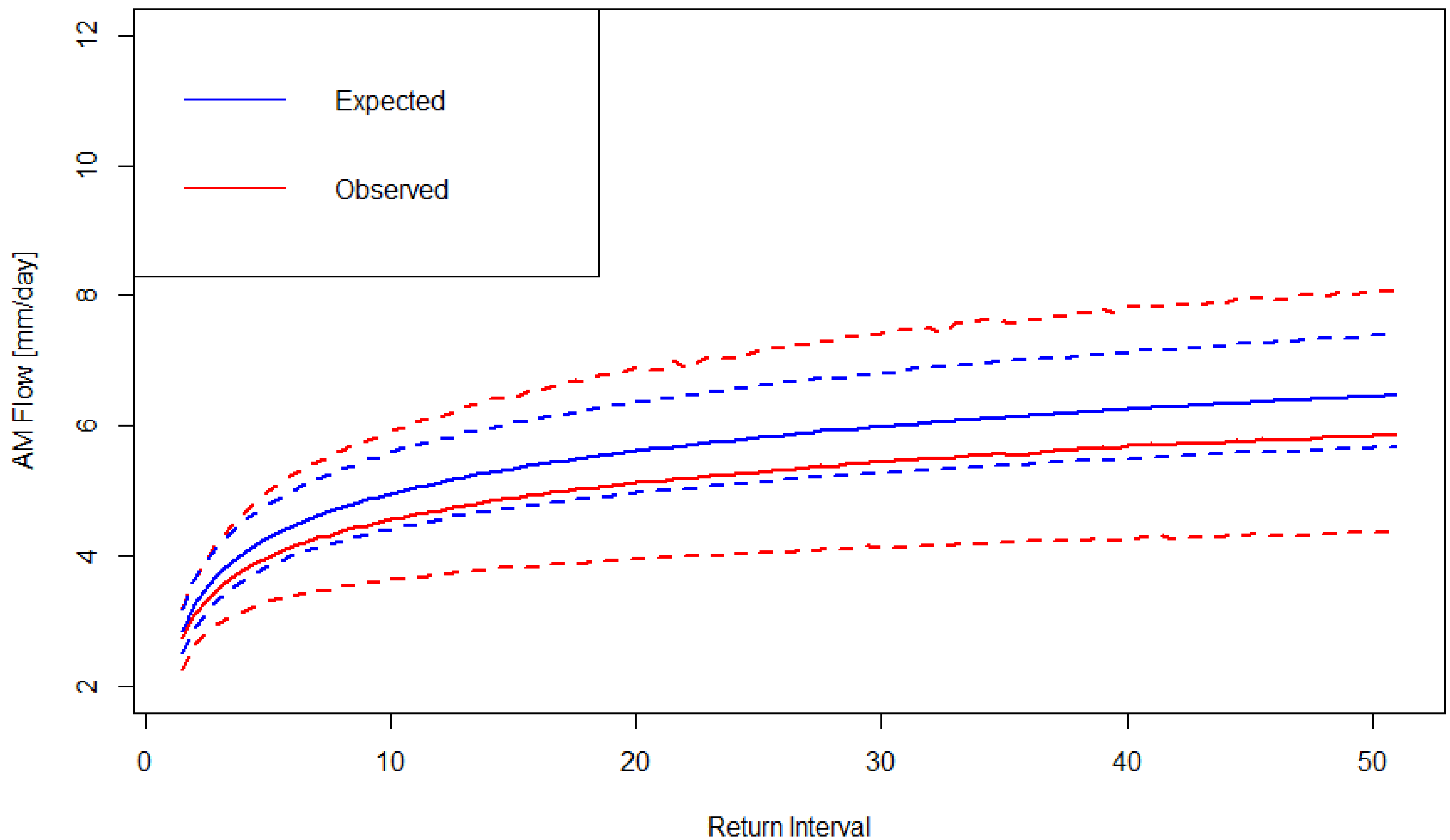

Figure 3.7: Cumulative distribution functions for expected and observed conditions for a representative post-fire year, shown with 90% credible intervals.

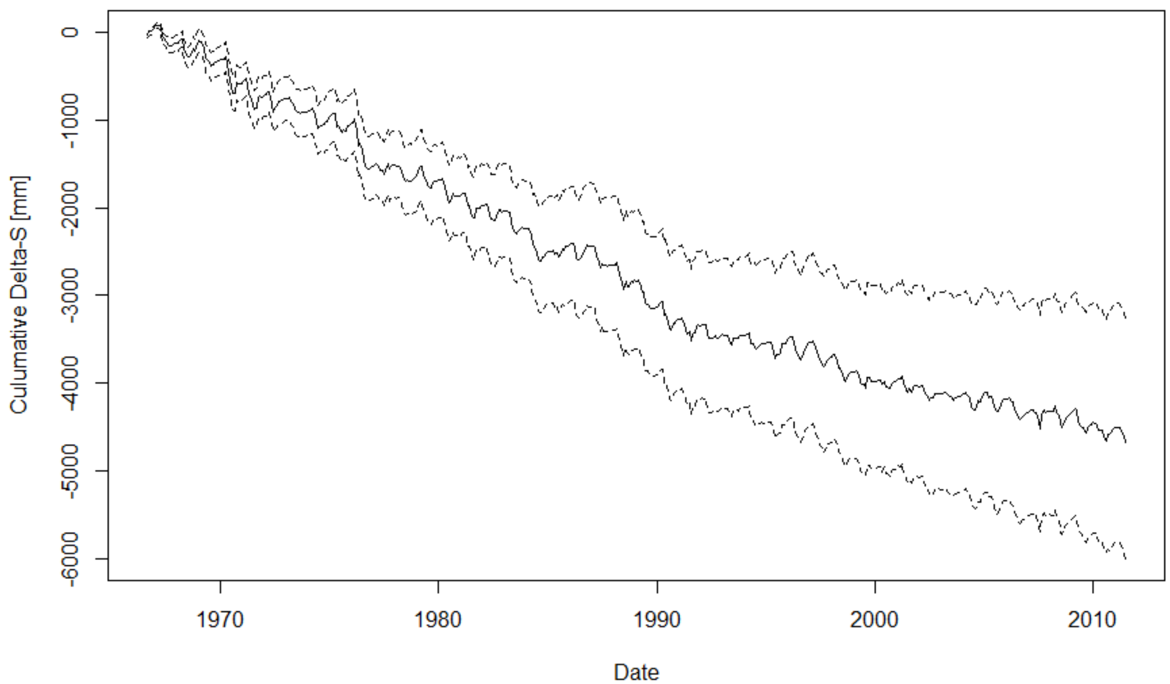

Figure 3.8: Cumulative ΔS for the Kawishiwi catchment using ET back-cast using SSEBop values for 2000-2011 and their relation with monthly maximum vapor pressure deficit.

BIBLIOGRAPHY

Advisory Committee for Vermont FPR, 2015. Voluntary Harvesting Guidelines for Landowners in Vermont.

Alaoui, A., Rogger, M., Peth, S., Blöschl, G., 2018. Does soil compaction increase floods? A review. J. Hydrol. 557, 631–642. https://doi.org/10.1016/j.jhydrol.2017.12.052

Alexander, R.R., Troendle, C.A., Kaufmann, M.R., Shepperd, W.D., Crouch, G.L., Watkins, R.K., 1985. The Fraser Experimental Forest, Colorado: research program and published research 1937-1985. Gen. Tech. Rep. - US Dep. Agric. For. Serv. https://doi.org/10.5962/bhl.title.99529

Ali, G., Tetzlaff, D., Mcdonnell, J.J., Soulsby, C., Carey, S., Laudon, H., McGuire, K., Buttle, J., Seibert, J., Shanley, J., 2015. Comparison of threshold hydrologic response across northern catchments. Hydrol. Process. 29, 3575–3591. https://doi.org/10.1002/hyp.10527

Alila, Y., Green, K.C., 2014. Reply to comment by Birkinshaw on "a paradigm shift in understanding and quantifying the effects of forest harvesting on floods in snow environments." Water Resour. Res. 50, 2769–2774. https://doi.org/10.1002/2013WR014198

Alila, Y., Kuraś, P.K., Schnorbus, M., Hudson, R., 2009. Forests and floods: A new paradigm sheds light on age-old controversies. Water Resour. Res. 45, W08416, 1–24. https://doi.org/10.1029/2008WR007207

Anderson, C.J., Lockaby, B.G., 2011. Research gaps related to forest management and stream sediment in the United States. Environ. Manage. 47, 303–313. https://doi.org/10.1007/s00267-010-9604-1

Andréassian, V., 2004. Waters and forests: From historical controversy to scientific debate. J. Hydrol. 291, 1–27. https://doi.org/10.1016/j.jhydrol.2003.12.015

Angel, J., Swanston, C., Boustead, B.M., Conlon, K.C., Hall, K.R., Jorns, J.L., Kunkel, K.E., Lemos, M.C., Lofgren, B., Ontl, T.A., Posey, J., Stone, K., Takle, G., Todey, D., 2018. Midwest, in: Reidmiller, D.R., Avery, C.W., Easterling, D.R., Kunkel, K.E., Lewis, K.L.M., Maycock, T.K., Stewart, B.C. (Eds.), Impacts, Risks, and Adaptation in the United States: Fourth National Climate Assessment, Volume II2. U.S. Global Change Research Program, Washington, D.C., pp. 872–940. https://doi.org/10.7930/NCA4.2018.CH21

Arno, S.F., Harrington, M.G., Fiedler, C.E., Carlson, C.E., 1995. Restoring Fire-Dependent Ponderosa Pine Forests in Western Montana. Restor. Manag. Notes 13, 32–36. https://doi.org/10.3368/er.13.1.32

Asano, Y., Uchida, T., 2012. Flow path depth is the main controller of mean base flow transit times in a mountainous catchment. Water Resour. Res. 48, 8. https://doi.org/10.1029/2011WR010906

Asano, Y., Uchida, T., 2010. Is representative elementary area defined by a simple mixing of variable small streams in headwater catchments? Hydrol. Process. 24, 666–671. https://doi.org/10.1002/hyp.7589

Aubertin, G.M., Patric, J.H., 1974. Water Quality After Clearcutting a Small Watershed in West Virginia. J. Environ. Qual. 3, 243–249. https://doi.org/10.2134/jeq1974.00472425000300030012x

Auerswald, K., Geist, J., 2018. Extent and causes of siltation in a headwater stream bed: Catchment soil erosion is less important than internal stream processes. L. Degrad. Dev. 29, 737–748. https://doi.org/10.1002/ldr.2779

Aust, W.M., Blinn, C.R., 2004. Forestry Best Management Practices for Timber Harvesting and Site Preparation in the Eastern United States : an Overview of Water Quality and Productivity Research During the Past 20 Years (1982-2002). Water, Air, Soil Pollut. Focus 4, 5–36.

Aust, W.M., Bolding, M.C., Barrett, S.M., 2015. Best Management Practices for Low-Volume Forest Roads in the Piedmont Region. Transp. Res. Rec. J. Transp. Res. Board 2472, 51–55.

https://doi.org/10.3141/2472-06

Azevedo, J.C., Williams, J.R., Messina, M.G., Fisher, R.F., 2005. Impacts of the Sustainable Forestry Initiative Landscape Level Measures on Hydrological Processes. Water Resour. Manag. 19, 95–110. https://doi.org/10.1007/s11269-005-1503-5

Bahuguna, D., Mitchell, S.J., Miquelajauregui, Y., 2010. Windthrow and recruitment of large woody debris in riparian stands. For. Ecol. Manage. 259, 2048–2055. https://doi.org/10.1016/j.foreco.2010.02.015

Balascio, N.L., Kaste, J.M., Meyer, M.G., Renshaw, M., Smith, K., Chambers, R.M., 2019. A high-resolution mill pond record from eastern Virginia (USA) reveals the impact of past landscape changes and regional pollution history. Anthropocene 25, 1–14. https://doi.org/10.1016/j.ancene.2019.100190

Banwart, S.A., Chorover, J., Gaillardet, J., Sparks, D., White, T., Anderson, S., Aufdenkampe, A., Bernasconi, S., Brantley, S.L., Chadwick, O., Dietrich, W.E., Duffy, C., Goldhaber, M., Lehnert, K., Nikolaidis, N.P., Ragnarsdottir, K. V, 2013. Sustaining Earth's Critical Zone: Basic Science and Interdisciplinary Solutions for Global Challenges. University of Sheffield, Sheffield, UK.

Barr Engineering, 2014. Hydrogeology of Fractured Bedrock in the Vicinity of the NorthMet Project Hydrogeology of Fractured Bedrock in the Vicinity of the NorthMet Project.

Bathurst, J.C., 2014. Comment on '"A paradigmshift in understanding and quantifying the effects of forest harvesting on floods in snow environments"' by K. C. Green and Y. Alila. Water Resour. Res. 50, 2756–2758. https://doi.org/10.1002/2013WR013613

Bathurst, J.C., Fahey, B., Iroumé, A., Jones, J., 2020. Forests and floods: Using field evidence to reconcile analysis methods. Hydrol. Process. 34, 3295–3310. https://doi.org/10.1002/hyp.13802

Bathurst, J.C., Iroumé, A., Cisneros, F., Fallas, J., Iturraspe, R., Novillo, M.G., Urciuolo, A., Bièvre, B. de, Borges, V.G., Coello, C., Cisneros, P., Gayoso, J., Miranda, M., Ramírez, M., 2011. Forest impact on floods due to extreme rainfall and snowmelt in four Latin American environments 1: Field data analysis. J. Hydrol. 400, 281–291. https://doi.org/10.1016/j.jhydrol.2010.11.044

Beasley, R.S., Granillo, A.B., 1988. Sediment and Water Yields from Managed Forests on Flat Coastal Plain Sites. Water Resour. Bull. 24, 361–366.

Beatty, S.M., Smith, J.E., 2013. Dynamic soil water repellency and infiltration in post-wildfire soils. Geoderma 192, 160–172. https://doi.org/10.1016/j.geoderma.2012.08.012

Belmont, P., Gran, K.B., Schottler, S.P., Wilcock, P.R., Day, S.S., Jennings, C., Lauer, J.W., Viparelli, O.E., Willenbring, J.K., Engstrom, D.R., Parker, G., 2011. Large Shift in Source of Fine Sediment in the Upper Mississippi River. Environ. Sci. Technol. 45, 8804–8810. https://doi.org/10.1021/es2019109

Bense, V.F., Gleeson, T., Loveless, S.E., Bour, O., Scibek, J., 2013. Fault zone hydrogeology. Earth-Science Rev. 127, 171–192. https://doi.org/10.1016/j.earscirev.2013.09.008

Bense, V.F., Person, M.A., 2006. Faults as conduit-barrier systems to fluid flow in siliciclastic sedimentary aquifers. Water Resour. Res. 42, 1–18. https://doi.org/10.1029/2005WR004480

Bent, G.C., 2001. Effects of forest-management activities on runoff components and ground-water recharge to Quabbin Reservoir , central Massachusetts. For. Ecol. Manage. 143, 115–129. https://doi.org/10.1016/S0378-1127(00)00511-9

Beschta, R.L., 1999. Forest Hydrology in the Pacific Northwest: Additional Research Needs. J. Am. Water Resour. Assoc. 34, 729–741. https://doi.org/10.1111/j.1752-1688.1998.tb01511.x

Beschta, R.L., 1978. Long-Term Patterns of Sediment Production Following Road Construction and Logging in the Oregon Coast Range. Water Resour. Res. 14, 1011–1016.

Beschta, R.L., Pyles, M.R., Skaugset, A.E., Surfeet, C.G., 2000. Peakfow responses to forest practices in the western cascades of Oregon, USA. J. Hydrol. 233, 102–120. https://doi.org/10.1016/S0022-1694(00)00231-6

Binkley, D., Brown, T.C., 1993. Forest Practices as Nonpoint Sources of Pollution in North America. Water Resour. Bull. 29, 729–740.

Birkinshaw, S.J., 2014. Comment on '"A paradigmshift in understanding and quantifying the effects of forest harvesting on floods in snow environments"' by Kim C. Green and Younes Alila. Water Resour. Res. 50, 2765–2768. https://doi.org/doi:10.1002/2013WR013586

Black, P.E., 1972. Hydrograph Responses to Geomorphic Model Watershed Characteristics and Precipitation Variables. J. Hydrol. 17, 309–329. https://doi.org/10.1016/0022-1694(72)90090-X

Bladon, K.D., Bywater-reyes, S., Leboldus, J.M., Keriö, S., Segura, C., Ritóková, G., Shaw, D.C., 2019. Increased streamflow in catchments affected by a forest disease epidemic. Sci. Total Environ. 691, 112–123. https://doi.org/10.1016/j.scitotenv.2019.07.127

Blom, A., Arkesteijn, L., Chavarrías, V., Viparelli, E., 2017. The equilibrium alluvial river under variable flow and its channel-forming discharge. J. Geophys. Res. Earth Surf. 122, 1924–1948. https://doi.org/10.1002/2017JF004213

Blöschl, G., 2006. Hydrologic synthesis: Across processes, places, and scales. Water Resour. Res. 42, 3. https://doi.org/10.1029/2005WR004319

Blöschl, G., Ardoin-bardin, S., Bonell, M., Dorninger, M., Goodrich, D., Gutknecht, D., Matamoros, D., Merz, B., Shand, P., Szolgay, J., 2007. At what scales do climate variability and land cover change impact on flooding and low flows? Hydrol. Process. 21, 1241–1247. https://doi.org/10.1002/hyp

Blöschl, G., Grayson, R.B., Sivapalan, M., 1995. On the representative elementary area (REA) concept and its utility for distributed rainfall-runoff modelling. Hydrol. Process. 9, 313–330. https://doi.org/10.1002/hyp.3360090307

Boggs, J., Sun, G., Domec, J.C., McNulty, S., Treasure, E., 2015. Clearcutting upland forest alters transpiration of residual trees in the riparian buffer zone. Hydrol. Process. 29, 4979–4992. https://doi.org/10.1002/hyp.10474

Boggs, J., Sun, G., McNulty, S., 2016. Effects of Timber Harvest on Water Quantity and Quality in Small Watersheds in the Piedmont of North Carolina. J. For. 114, 27–40. https://doi.org/10.5849/jof.14-102

Bolstad, P. V., Swank, W.T., 1997. Cumulative impacts of landuse on water quality in a southern Appalachian watershed. J. Am. Water Resour. Assoc. 33, 519–533. https://doi.org/10.1111/j.1752-1688.1997.tb03529.x

Bonniwell, E.C., Matisoff, G., Whiting, P.J., 1999. Determining the times and distances of particle transit in a mountain stream using fallout radionuclides. Geomorphology 27, 75–92. https://doi.org/10.1016/S0169-555X(98)00091-9

Bosch, J.M., Hewlett, J.D., 1982. A Review of Catchment Experiments to Determine the Effect of Vegetation Changes on Water Yield and Evapotranspiration. J. Hydrol. 55, 3–23. https://doi.org/10.1016/0022-1694(82)90117-2

Bracken, L., Turnbull, L., Wainwright, J., Bogaart, P., 2015. Sediment connectivity: a framework for understanding sediment transfer at multiple scales. Earth Surf. Process. Landforms 40, 177–188. https://doi.org/10.1002/esp.3635

Bracken, L., Wainwright, J., 2006. Geomorphological equilibrium: myth and metaphor ? Trans. Inst. Br. Geogr. 31, 167–178.

Bradford, J.B., Kastendick, D.N., 2010. Age-related patterns of forest complexity and carbon storage in pine and aspen-birch ecosystems of northern Minnesota, USA. Can. J. For. Res. 40, 401–409. https://doi.org/10.1139/X10-002

Bradshaw, C.J., Sodhi, N.S., Peh, K.S.-H., Brook, B.W., 2007. Global evidence that deforestation amplifies flood risk and severity in the developing world. Glob. Chang. Biol. 13, 2379–2395. https://doi.org/10.1111/j.1365-2486.2007.01446.x

Brantley, S.L., Eissenstat, D.M., Marshall, J.A., Godsey, S.E., Balogh-Brunstad, Z., Karwan, D.L., Papuga, S.A., Roering, J., Dawson, T.E., Evaristo, J., Chadwick, O., McDonnell, J.J., Weathers, K.C., 2017. Reviews and syntheses: on the roles trees play in building and plumbing the critical zone. Biogeosciences 14, 5115–5142. https://doi.org/10.5194/bg-14-5115-2017

Breiman, L., 2001. Random forests. Mach. Learn. 45, 5–32. https://doi.org/10.1023/A:1010933404324

Breiman, L., Cutler, A., 2003. Setting Up, Using, and Understanding Random Forests. https://doi.org/10.1017/CBO9781107415324.004

Briggs, R.D., Cormier, J., Kimball, A., 1998. Compliance with Forestry Best Management Practices in Maine. North. J. Appl. For. 15, 57–68. https://doi.org/10.1093/njaf/15.2.57

Brown, A.E., Zhang, L., McMahon, T.A., Western, A.W., Vertessy, R.A., 2005. A review of paired catchment studies for determining changes in water yield resulting from alterations in vegetation. J. Hydrol. 310, 28–61. https://doi.org/10.1016/j.jhydrol.2004.12.010

Bull, W.B., 1997. Discontinuous ephemeral streams. Geomorphology 19, 227–276. https://doi.org/10.1016/S0169-555X(97)00016-0

Buongiorno, J., Zhu, S., Raunikar, R., Prestemon, J.P., 2012. Outlook to 2060 for World Forests and Forest Industries: A Technical Document Supporting the Forest Service 2010 RPA Assessment. USFS Gen. Tech. Rep.

Buras, A., Menzel, A., 2018. Projecting Tree Species Composition Changes of European Forests for 2061-2090 Under RCP 4.5 and RCP 8.5 Scenarios. Front. Plant Sci. 9, 20. https://doi.org/10.3389/fpls.2018.01986

Burns, D.A., McDonnell, J.J., Hooper, R.P., Peters, N.E., Freer, J.E., Kendall, C., Beven, K., 2001. Quantifying contributions to storm runoff through end-member mixing analysis and hydrologic measurements at the Panola Mountain Research Watershed (Georgia, USA). Hydrol. Process. 15, 1903–1924. https://doi.org/10.1002/hyp.246

Butler, B.J., Hewes, J.H., Dickinson, B.J., Andrejczyk, K., Butler, S.M., Markowski-Lindsay, M., 2016. Family Forest Ownerships of the United States, 2013: Findings from the USDA Forest Service's National Woodland Owner Survey. J. For. 114, 638–647. https://doi.org/10.5849/jof.15-099

Buttle, J.M., 2011. The Effects of Forest Harvesting on Forest Hydrology and Biogeochemistry, in: Levia, D.F., Carlyle-Moses, D., Tanaka, T. (Eds.), Forest Hydrology and Biogeochemistry: Synthesis of Past Research and Future Directions. Springer, Dordrecht, pp. 659–677. https://doi.org/10.1007/978-94-007-1363-5_33

Bywater-Reyes, S., Segura, C., Bladon, K.D., 2017. Geology and geomorphology control suspended sediment yield and modulate increases following timber harvest in temperate headwater streams. J. Hydrol. 548, 74–83. https://doi.org/10.1016/j.jhydrol.2017.03.048

Calder, I.R., Smyle, J., Aylward, B., 2007. Debate over flood-proofing effects of planting forests. Nature 450, 945. https://doi.org/10.1038/450945b

Caldwell, P. V., Jackson, C.R., Miniat, C.F., Younger, S.E., Vining, J.A., McDonnell, J.J., Aubrey, D.P., 2018. Woody bioenergy crop selection can have large effects on water yield: A southeastern United States case study. Biomass and Bioenergy 117, 180–189. https://doi.org/10.1016/j.biombioe.2018.07.021

Caldwell, P. V., Miniat, C.F., Elliott, K.J., Swank, W.T., Brantley, S.T., Laseter, S.H., 2016. Declining water yield from forested mountain watersheds in response to climate change and forest mesophication. Glob. Chang. Biol. 22, 2997–3012. https://doi.org/10.1111/gcb.13309

Cannon, S.H., Degraff, J., 2009. The Increasing Wildfire and Post-Fire Debris-Flow Threat in Western USA, and Implications for Consequances of Climate Change, in: Sassa, K., Canuti, P. (Eds.), Landslides - Disaster Risk Reduction. Springer-Verlag, Berlin, pp. 177–190.

Cannon, S.H., Gartner, J.E., Rupert, M.G., Michael, J.A., Rea, A.H., Parrett, C., 2010. Predicting the probability and volume of postwildfire debris flows in the intermountain western United States. Bull. Geol. Soc. Am. 122, 127–144. https://doi.org/10.1130/B26459.1

Chanasyk, D.S., Whitson, I.R., Mapfumo, E., Burke, J.M., Prepas, E.E., 2003. The impacts of forest harvest and wildfire on soils and hydrology in temperate forests: A baseline to develop hypotheses for the Boreal Plain. J. Environ. Eng. Sci. 2, S51–S62. https://doi.org/10.1139/s03-034

Chen, M., Senay, G.B., Singh, R.K., Verdin, J.P., 2016. Uncertainty analysis of the Operational Simplified Surface Energy Balance (SSEBop) model at multiple flux tower sites. J. Hydrol. 536, 384–399. https://doi.org/10.1016/j.jhydrol.2016.02.026

Church, M., 2002. Geomorphic thresholds in riverine landscapes. Freshw. Biol. 47, 541–557. https://doi.org/10.1046/j.1365-2427.2002.00919.x

Church, M., Ryder, J.M., 2010. Physiography of British Columbia, in: Pike, R.G., Redding, T.E., Moore, R.D., Winkler, R., Bladon, K.D. (Eds.), Compendium of Forest Hydrology and Geomorphology in British Columbia: Vol. 1. B.C. Min. For. Range, For. Sci. Prog., Victoria, B.C. and FORREX Forum for Research and Extension in Natural Resources, Kamloops, B.C., Canada, pp. 17–46.

Clayton, J.L., Megahan, W.F., 1997. Natural erosion rates and their prediction in the Idaho Batholith. J. Am. Water Resour. Assoc. 33, 689–703.

Collins, B.J., Rhoades, C.C., Battaglia, M.A., Hubbard, R.M., 2012. The effects of bark beetle outbreaks on forest development, fuel loads and potential fire behavior in salvage logged and untreated lodgepole pine forests. For. Ecol. Manage. 284, 260–268. https://doi.org/10.1016/j.foreco.2012.07.027

Collins, T.K., 2008. Debris flows caused by failure of fill slopes: Early detection, warning, and loss prevention. Landslides 5, 107–120. https://doi.org/10.1007/s10346-007-0107-y

Condon, L.E., Markovich, K.H., Kelleher, C.A., McDonnell, J.J., Ferguson, G., McIntosh, J.C., 2020. Where Is the Bottom of a Watershed? Water Resour. Res. 56, 9. https://doi.org/10.1029/2019WR026010

Cowie, R.M., Knowles, J.F., Dailey, K.R., Williams, M.W., Mills, T.J., Molotch, N.P., 2017. Sources of streamflow along a headwater catchment elevational gradient. J. Hydrol. 549, 163–178. https://doi.org/10.1016/j.jhydrol.2017.03.044

Cristan, R., Aust, W.M., Bolding, M.C., Barrett, S.M., Munsell, J.F., Schilling, E., 2016. Effectiveness of forestry best management practices in the United States: Literature review. For. Ecol. Manage. 360, 133–151. https://doi.org/10.1016/j.foreco.2015.10.025

Croke, J., Hairsine, P., Fogarty, P., 2001. Soil recovery from track construction and harvesting changes in surface infiltration, erosion and delivery rates with time. For. Ecol. Manage. 143, 3–12. https://doi.org/10.1016/S0378-1127(00)00500-4

Croke, J., Hairsine, P.B., 2006. Sediment delivery in managed forests: a review. Environ. Rev. 14, 59–87. https://doi.org/10.1139/a05-016

Croke, J., Mockler, S., 2001. Gully initiation and road-to-stream linkage in a forested catchment, southeastern Australia. Earth Surf. Process. Landforms 217, 205–217. https://doi.org/10.1002/1096-9837(200102)26:2<205::AID-ESP168>3.0.CO;2-G

Czapowskyj, M.M., Safford, L.O., 1993. Site preparation, fertilization, and 10-year yields of hybrid poplar on a clearcut forest site in eastern Maine, USA. New For. 7, 331–344.

D'Amato, A.W., Bolton, N.W., Blinn, C.R., Ek, A.R., 2009. Current Status and Long-term Trends of Silvicultural Practices in Minnesota : A 2008 Assessment. Univ. Minnesota Dep. For. Resour. Staff Pap. 205, 58.

Detenbeck, N.E., Brady, V.J., Taylor, D.L., Snarski, V.M., Batterman, S.L., 2005. Relationship of stream flow regime in the western Lake Superior basin to watershed type characteristics. J. Hydrol. 309, 258–276. https://doi.org/10.1016/j.jhydrol.2004.11.024

Dethier, E., Magilligan, F.J., Renshaw, C.E., Nislow, K.H., 2016. The role of chronic and episodic disturbances on channel–hillslope coupling: the persistence and legacy of extreme floods. Earth Surf. Process. Landforms 41, 1437–1447. https://doi.org/10.1002/esp.3958

Dettinger, M.D., Cayan, D.R., 1995. Large-scale atmospheric forcing of recent trends towards early snowmelt runoff in California. J. Clim. 8, 606–623. https://doi.org/10.1175/1520-0442(1995)008<0606:LSAFOR>2.0.CO;2

Devito, K.J., Hill, A.R., Roulet, N., 1996. Groundwater-surface water interactions in headwater forested wetlands of the Canadian Shield. J. Hydrol. 181, 127–147. https://doi.org/10.1016/0022-1694(95)02912-5

Donovan, M., Miller, A., Baker, M., Gellis, A., 2015. Sediment contributions from floodplains and legacy sediments to Piedmont streams of Baltimore County, Maryland. Geomorphology 235, 88–105. https://doi.org/10.1016/j.geomorph.2015.01.025

Dooge, J.C.I., 1986. Looking for Hydrologic Laws. Water Resour. Res. 22, 46S-58S.

Durgin, P.B., Johnston, R.R., Parsons, A.M., 1988. Causes of erosion on private timberlands in Northern California: Observations of the Interdisciplinary Team. Crit. Sites Eros. Study Tech. Rep. 1, 50.

Dyke, A.S., Andrews, J.T., Clark, P.U., England, J.H., Miller, G.H., Shaw, J., Veillette, J.J., 2002. The Laurentide and Innuitian ice sheets during the Last Glacial Maximum. Quat. Sci. Rev. 21, 9–31. https://doi.org/10.1016/S0277-3791(01)00095-6

Eaton, B.C., Moore, R.D., Giles, T.R., 2010. Forest fire, bank strength and channel instability: The "unusual" response of Fishtrap Creek, British Columbia. Earth Surf. Process. Landforms 35, 1167–1183. https://doi.org/10.1002/esp.1946

Edwards, P.J., Williard, K.W.J., 2010. Efficiencies of Forestry Best Management Practices for Reducing Sediment and Nutrient Losses in the Eastern United States. J. For. 108, 245–249. https://doi.org/10.1093/jof/108.5.245

Ehlers, Gibbard, Hughes (eds.). 2011. Quaternary Glaciations - Extent and Chronology Volume 15. http://booksite.elsevier.com/9780444534477/. GIS data downloaded via https://crc806db.uni-koeln.de/layer/show/6. Accessed 11-15-19.

Eisenbies, M.H., Vance, E.D., Aust, W.M., Seiler, J.R., 2009. Intensive Utilization of Harvest Residues in Southern Pine Plantations: Quantities Available and Implications for Nutrient Budgets and Sustainable Site Productivity. BioEnergy Res. 2, 90–98. https://doi.org/10.1007/s12155-009-9036-z

Ensign, S.H., Mallin, M.A., 2001. Stream water quality changes following timber harvest in a coastal plain swamp forest. Water Res. 35, 3381–3390. https://doi.org/10.1016/S0043-1354(01)00060-4

Fan, Y., Bras, R.L., 1995. On the concept of a representative elementary area in catchment runoff. Hydrol. Process. 9, 821–832. https://doi.org/10.1002/hyp.3360090708

Fenneman, N.M., Johnson, D.W., 1946. Physiographic Divisions of the Conterminous United States.

Finney, M.A., Mchugh, C.W., Grenfell, I.C., Riley, K.L., Short, K.C., 2011. A simulation of probabilistic wildfire risk components for the continental United States. Stoch. Environ. Res. Risk Assess. 25, 973–1000. https://doi.org/10.1007/s00477-011-0462-z

Fisher, R.A., Tippett, L.H.C., 1928. Limiting forms of the frequency distribution of the largest or smallest number of a sample. Proc. Camb. Philol. Soc. 24, 180–190.

Flannigan, M.D., Stocks, B.J., Wotton, B.M., 2000. Climate change and forest fires. Sci. Total Environ. 262, 221–229. https://doi.org/10.1016/S0048-9697(00)00524-6

Fleming, S.W., Lavenue, A.M., Aly, A.H., Adams, A., 2002. Practical applications of spectral analysis to hydrologic time series. Hydrol. Process. 16, 565–574. https://doi.org/10.1002/hyp.523

Fletcher, J.E., Huber, A.L., Farmer, E.E., McLaughlin, K.R., Rector, J., Schmidt, L.J., 1981. Precipitation Characteristics of Summer Storms at Straight Canyon Barometer Watershed, Utah. Intermt. For. Range Exp. Stn. Res. Pap. INT-274, 11.

Ford, C.R., Elliott, K.J., Clinton, B.D., Kloeppel, B.D., Vose, J.M., 2012. Forest dynamics following eastern hemlock mortality in the southern Appalachians. Oikos 121, 523–536. https://doi.org/10.1111/j.1600-0706.2011.19622.x

Ford, C.R., Laseter, S.H., Swank, W.T., Vose, J.M., 2011. Can forest management be used to sustain water-based ecosystem services in the face of climate change? Ecol. Appl. 21, 2049–2067. https://doi.org/10.1890/10-2246.1

Fortin, D., Lamoureux, S.F., 2009. Multidecadal hydroclimatic variability in northeastern North America since 1550 AD. Clim. Dyn. 33, 427–432. https://doi.org/10.1007/s00382-008-0422-6

Foufoula-Georgiou, E., Takbiri, Z., Czuba, J.A., Schwenk, J., 2015. The change of nature and the nature of change in agricultural landscapes: Hydrologic regime shifts modulate ecological transitions. Water Resour. Res. 51, 6649–6671. https://doi.org/10.1002/2015WR017637

Fraser, N., Jackson, R., Radcliffe, D., 2012. A paired watershed investigation of silvicultural best management practices revisited: B.F. Grant Memorial Forest, Georgia. For. Sci. 58, 652–662. https://doi.org/10.5849/forsci.09-101

Gavin, D.G., Hallett, D.J., Feng, S.H., Lertzman, K.P., Prichard, S.J., Brown, K.J., Lynch, J.A., Bartlein, P., Peterson, D.L., 2007. Forest fire and climate change in western North America: Insights from sediment charcoal records. Front. Ecol. Environ. 5, 499–506. https://doi.org/10.1890/060161

Gellis, A.C., 2013. Factors influencing storm-generated suspended-sediment concentrations and loads in four basins of contrasting land use , humid-tropical Puerto Rico. Catena 104, 39–57. https://doi.org/10.1016/j.catena.2012.10.018

Gelman, A., Hill, J., Yajima, M., 2012. Why We (Usually) Don't Have to Worry About Multiple Comparisons. J. Res. Educ. Eff. 5, 189–211. https://doi.org/10.1080/19345747.2011.618213

Gelman, A., Meng, X., Stern, H., 1996. Posterior Predictive Assessment of Model Fitness via Realized Discrepancies. Stat. Sin. 6, 733–807.

Gelman, A., Rubin, D.B., 1992. Inference from Iterative Simulation Using Multiple Sequences. Stat. Sci. 7, 457–511.

Gelman, A., Tuerlinckx, F., 2000. Type S error rates classical and Bayesian single and multiple compparison procedures. Comput. Stat. 15, 373–390. https://doi.org/10.1007/s001800000040

Gibson, J.J., Birks, S.J., Jeffries, D., Yi, Y., 2017. Regional trends in evaporation loss and water yield based on stable isotope mass balance of lakes : The Ontario Precambrian Shield surveys. J. Hydrol. 544, 500–510. https://doi.org/10.1016/j.jhydrol.2016.11.016

Gleeson, T., Novakowski, K., 2009. Identifying watershed-scale barriers to groundwater flow: Lineaments in the Canadian shield. Bull. Geol. Soc. Am. 121, 333–347. https://doi.org/10.1130/B26241.1

Godsey, S.E., Kirchner, J.W., 2014. Dynamic, discontinuous stream networks: hydrologically driven variations in active drainage density, flowing channels and stream order. Hydrol. Process. 28, 5791–5803. https://doi.org/10.1002/hyp.10310

Gomi, T., Moore, R.D., Hassan, M. a., 2005. Suspended sediment dynamics in samll forest streams of the Pacific Northwest. J. Am. Water Resour. Assoc. 41, 877–898.

Goode, J.R., Luce, C.H., Buffington, J.M., 2012. Enhanced sediment delivery in a changing climate in semi-arid mountain basins: Implications for water resource management and aquatic habitat in the northern Rocky Mountains. Geomorphology 139–140, 1–15. https://doi.org/10.1016/j.geomorph.2011.06.021

Grace, J.. I., 2005. Forest Operation and Water Quality in the South. Trans. ASAE 48, 871–880.

Gran, K.B., Belmont, P., Day, S.S., Finnegan, N., Jennings, C., Lauer, J.W., Wilcock, P.R., 2011. Landscape evolution in south-central Minnesota and the role of geomorphic history on modern erosional processes. GSA Today 21, 7–9. https://doi.org/10.1130/G121A.1

Grant, G.E., Swanson, F.J., Wolman, M.G., 1990. Pattern and origin of stepped-bed morphology in high-gradient streams, Western Cascades, Oregon. GSA Bull. 102, 340–352.

Grant, G.E., Wolff, A.L., 1991. Long-term patterns of sediment transport following timber harvest, Western Cascade Mountains, Oregon, USA, in: Sediment and Streamwater Quality in a Changing Environment: Trends and Explanation (Proceedings of the Vienna Symposium, August 1991). pp. 31–41.

Green, K.C., Alila, Y., 2012. A paradigm shift in understanding and quantifying the effects of forest harvesting on floods in snow environments. Water Resour. Res. 48, W10503, 1–21. https://doi.org/10.1029/2012WR012449

Griffiths, N.A., Jackson, C.R., Bitew, M.M., Fortner, A.M., Fouts, K.L., Mccracken, K., Phillips, J.R., 2017. Water quality effects of short-rotation pine management for bioenergy feedstocks in the southeastern United States. For. Ecol. Manage. 400, 181–198. https://doi.org/10.1016/j.foreco.2017.06.011

Grigal, D.F., 2000. Effects of extensive forest management on soil productivity. For. Ecol. Manage. 138, 167–185. https://doi.org/10.1016/S0378-1127(00)00395-9

Grizzel, J.D., Wolff, N., 1995. Occurrence of Windthrow in Forest Buffer Strips and its Effect on Small Streams in Northwest. Northwest Sci. 72, 214–223.

Guardiola-Claramonte, M., Troch, P.A., Breshears, D.D., Huxman, T.E., Switanek, M.B., Durcik, M., Cobb, N.S., 2011. Decreased streamflow in semi-arid basins following drought-induced tree die-off: A counter-intuitive and indirect climate impact on hydrology. J. Hydrol. 406, 225–233. https://doi.org/10.1016/j.jhydrol.2011.06.017

Guertin, D.P., Barten, P.K., Brooks, K.N., 1987. The Peatland Hydrologic Impact Model: Development and Testing. Hydrol. Res. 18, 79–100. https://doi.org/10.2166/nh.1987.0007

Guillemette, F., Plamondon, A.P., Prévost, M., Lévesque, D., 2005. Rainfall generated stormflow response to clearcutting a boreal forest: peak flow comparison with 50 world-wide basin studies. J. Hydrol. 302, 137–153. https://doi.org/10.1016/j.jhydrol.2004.06.043

Gumbel, E.J., 1958. Statistics of Extremes. Columbia University Press, New York.

Gumbel, E.J., 1941. The Return Period of Flood Flows. Ann. Math. Stat. 12, 163–190.

Harvey, A.M., 2007. Geomorphic instability and change – Introduction: Implications of temporal and spatial scales. Geomorphology 84, 153–158. https://doi.org/10.1016/j.geomorph.2006.03.008

Hassan, M.A., Church, M., Lisle, T.E., Brardinoni, F., Benda, L., Grant, G.E., 2006. Sediment transport and channel morphology of small, forested streams. J. Am. Water Resour. Assoc. 41, 853–876. https://doi.org/10.1111/j.1752-1688.2005.tb03774.x

Hatten, J.A., Segura, C., Bladon, K.D., Hale, V.C., Ice, G.G., Stednick, J.D., 2018. Effects of contemporary forest harvesting on suspended sediment in the Oregon Coast Range: Alsea Watershed Study Revisited. For. Ecol. Manage. 408, 238–248. https://doi.org/10.1016/j.foreco.2017.10.049

Hayes, J.P., Schoenholtz, S.H., Hartley, M.J., Murphy, G., Powers, R.F., Berg, D., Radosevich, S.R., 2005. Environmental Consequences of Intensively Managed Forest Plantations in the Pacific Northwest. J. For. 103, 83–87. https://doi.org/10.1093/jof/103.2.83

Heede, B.H., 1991. Response of a stream in desequilibrium to timber harvest. Enviromental Manag. 15, 251–255.

Helvey, J.D., 1980. Effects of a North Central Washington Wildfire on Runoff and Sediment Production. Water Resour. Bull. 16, 627–634. https://doi.org/10.1111/j.1752-1688.1980.tb02441.x

Hershfield, D.M., 1961. Rainfall Frequency Atlas of the United States, for Durations from 30 Minutes to 24 Hours and Return Periods from 1 to 100 Years. Tech. Pap. No. 40 65.

Hewlett, J.D., 1982. Forests and floods in the light of recent investigation, in: Proceedings of the Canadian Hydrology Symposium - Associate Committee on Hydrology.

Hewlett, J.D., Doss, R., 1984. Forests, Floods, and Erosion: A Watershed Experiment in the Southeastern Piedmont. For. Sci. 30, 424–434. https://doi.org/doi.org/10.1093/forestscience/30.2.424

Hewlett, J.D., Helvey, J.D., 1970. Effects of Forest Clear-Felling on the Storm Hydrograph. Water Resour. Res. 6, 768–782. https://doi.org/10.1029/WR006i003p00768

Hewlett, J.D., Lull, H.W., Reinhart, K.G., 1969. In Defense of Experimental Watersheds. Water Resour. Res. 5, 306–316. https://doi.org/10.1029/WR005i001p00306

Hewlett, J.D., Post, H.E., Doss, R., 1984. Effect of Clear-Cut Silviculture on Dissolved Ion Export and Water Yield on the Piedmont. Water Resour. Res. 20, 1030–1038. https://doi.org/10.1029/WR020i007p01030

Hobbs, H.C., Goebel, J.E., 1982. Geologic Map of Minnesota - Quaternary Geology. MGS Map S-1.

Hodgkins, G.A., Dudley, R.W., Huntington, T.G., 2003. Changes in the timing of high river flows in New England over the 20th Century. J. Hydrol. 278, 244–252. https://doi.org/10.1016/S0022-1694(03)00155-0

Homer, C.G., Dewitz, J.A., Yang, L., Jin, S., Danielson, P., Xian, G., Coulston, J., Herold, N.D., Wickham, J.D., Megown, K., 2015. Completion of the 2011 National Land Cover Database for the conterminous United States-Representing a decade of land cover change information. Photogramm. Eng. Remote Sensing 81, 345–354.

Hornbeck, J.W., 1973. Storm Flow from Hardwood-Forested and Cleared Watersheds in New Hampshire. Water Resour. Res. 9. https://doi.org/10.1029/WR009i002p00346

Hornbeck, J.W., Adams, M.B., Corbett, E.S., Verry, E.S., Lynch, J.A., 1993. Long-term impacts of forest treatments on water yield : a summary for northeastern U S A. J. Hydrol. 150, 323–344. https://doi.org/10.1016/0022-1694(93)90115-P

Hornbeck, J.W., Leak, W.B., 1992. Ecology and Management of Northern Hardwood Forests in New England. USFS Gen. Tech. Rep. NE-159, 1–41.

Hornbeck, J.W., Martin, C.W., Eagar, C., 1997. Summary of water yield experiments at Hubbard Brook Experimental Forest , New Hampshire. Can. J. For. Res. 27, 2043–2052. https://doi.org/10.1139/x97-173

Hudson, J.A., 1988. The contribution of soil moisture storage to the water balances of upland forested and grassland catchments. Hydrol. Sci. J. 33, 289–309. https://doi.org/10.1080/02626668809491249

Huntington, T.G., Richardson, A.D., McGuire, K.J., Hayhoe, K., 2009. Climate and Hydrological Changes in the Northeastern United States: Recent Trends and Implications for Forested and Aquatic Ecosystems. Can. J. For. Res. 39, 199–212. https://doi.org/10.1139/X08-116

Hupp, C.R., 2000. Hydrology, geomorphology, and vegetation of Coastal Plain rivers in the south-eastern USA. Hydrol. Process. 14, 2991–3010. https://doi.org/10.1002/1099-1085(200011/12)14:16/17<2991::AID-HYP131>3.0.CO;2-H

Hupp, C.R., Woodside, M.D., Yanosky, T.M., 1993. Sediment and Trace Element Trapping in a Forested Wetland, Chickahominy River, Virginia. Soc. Wetl. Sci. 13, 95–104.

Inamdar, S., Johnson, E., Rowland, R., Warner, D., Walter, R., Merritts, D., 2018. Freeze–thaw processes and intense rainfall: the one-two punch for high sediment and nutrient loads from mid-Atlantic watersheds. Biogeochemistry 141, 333–349. https://doi.org/10.1007/s10533-017-0417-7

Jackisch, C., Angermann, L., Allroggen, N., Sprenger, M., Blume, T., Tronicke, J., Zehe, E., 2017. Form and function in hillslope hydrology: in situ imaging and characterization of flow-relevant structures. Hydrol. Earth Syst. Sci. 21, 3749–3775. https://doi.org/10.5194/hess-21-3749-2017

Jackson, C.R., Batzer, D.P., Cross, S.S., Haggerty, S.M., Sturm, C.A., 2007. Headwater Streams and Timber Harvest: Channel, Macroinvertebrate, and Amphibian Response and Recovery. For. Sci. 53, 356–370. https://doi.org/10.1093/forestscience/53.2.356

Jackson, C.R., Martin, J.K., Leigh, D.S., West, L.T., 2005. A southeastern piedmont watershed sediment budget: Evidence for a multi-millennial agricultural legacy. J. Soil Water Conserv. 60, 298–310.

Jakob, M., Bovis, M., Oden, M., 2005. The significance of channel recharge rates for estimating debris-flow magnitude and frequency. Earth Surf. Process. Landforms 30, 755–766. https://doi.org/10.1002/esp.1188

James, L.A., 2013. Legacy sediment: Definitions and processes of episodically produced anthropogenic sediment. Anthropocene 2, 16–26. https://doi.org/10.1016/j.ancene.2013.04.001

Jefferson, A.J., Mcgee, R.W., 2013. Channel network extent in the context of historical land use, flow generation processes, and landscape evolution in the North Carolina Piedmont. Earth Surf. Process. Landforms 38, 601–613. https://doi.org/10.1002/esp.3308

Jennings, C.E., Johnson, M.D., 2011. The Quaternary of Minnesota, in: Ehlers, J., Gibbard, P.L., Hughes, P.D. (Eds.), Developments in Quaternary Sciences, Volume 15: Quaternary Glaciations - Extent and Chronology. Elsevier Inc., Amsterdam, pp. 499–511. https://doi.org/10.1016/B978-0-444-53447-7.00038-6

Jirsa, M.A., Boerboom, T.J., Chandler, V.W., Mossler, J.H., Runkel, A.C., Setterholm, D.R., 2011. S-21 Geologic Map of Minnesota-Bedrock Geology.

Johnson, A.C., Edwards, R.T., Erhardt, R., 2007. Ground-Water Response to Forest Harvest: Implications for Hillslope Stability. J. Am. Water Resour. Assoc. 43, 134–147. https://doi.org/10.1111/j.1752-1688.2007.00011.x

Johnson, E.A., Dils, R.E., 1956. Outline for Compiling Precipitation, Runoff, and Ground Water Data from Small Watersheds. Stn. Pap. No. 68.

Johnson, K.M., Snyder, N.P., Castle, S., Hopkins, A.J., Waltner, M., Merritts, D.J., Walter, R.C., 2019.

Legacy sediment storage in New England river valleys : Anthropogenic processes in a postglacial landscape. Geomorphology 327, 417–437. https://doi.org/10.1016/j.geomorph.2018.11.017

Jones, J.A., Grant, G.E., 1996. Peak flow responses to clear cutting and roads in small and large basins, western Cascades, Oregon. Water Resour. Res. 32, 959–974. https://doi.org/10.1029/95WR03493

Jones, J.A., Perkins, R.M., 2010. Extreme flood sensitivity to snow and forest harvest, western Cascades, Oregon, United States. Water Resour. Res. 46, 21. https://doi.org/10.1029/2009WR008632

Jurmu, M.C., Andrle, R., 1997. Morphology of a wetland stream. Environ. Manage. 21, 921–941. https://doi.org/10.1007/s002679900077

Kampf, S.K., Burges, S.J., Hammond, J.C., Bhaskar, A., Covino, T.P., Eurich, A., Harrison, H., Lefsky, M., Martin, C., Mcgrath, D., Puntenney-Desmond, K., Willi, K., 2020. The Case for an Open Water Balance: Re - envisioning Network Design and Data Analysis for a Complex , Uncertain World Water Resources Research. Water Resour. Res. 56, 1–19. https://doi.org/10.1029/2019WR026699

Karwan, D.L., Gravelle, J.A., Hubbart, J.A., 2007. Effects of timber harvest on suspended sediment loads in Mica Creek, Idaho. For. Sci. 53, 181–188.

Kelly, S.A., Takbiri, Z., Belmont, P., Foufoula-Georgiou, E., 2016. Human amplified changes in precipitation-runoff patterns in large river basins of the Midwestern United States. Hydrol. Earth Syst. Sci. 1–43. https://doi.org/10.5194/hess-2016-571

Kirchner, J.W., 2006. Getting the right answers for the right reasons: Linking measurements, analyses, and models to advance the science of hydrology. Water Resour. Res. 42, 1–5. https://doi.org/10.1029/2005WR004362

Kirchner, J.W., Finkel, R.C., Riebe, C.S., Granger, D.E., Clayton, J.L., King, J.G., Megahan, W.F., 2001. Mountain erosion over 10 yr, 10 k.y., and 10 m.y. time scales. Geology 29, 591–594. https://doi.org/10.1130/0091-7613(2001)029<0591:MEOYKY>2.0.CO;2

Klein, R.D., Lewis, J., Buffleben, M.S., 2012. Logging and turbidity in the coastal watersheds of northern California. Geomorphology 139–140, 136–144. https://doi.org/10.1016/j.geomorph.2011.10.011

Klos, P.Z., Link, T.E., Abatzoglou, J.T., 2014. Extent of the rain-snow transition zone in the western U.S. under historic and projected climate. Geophys. Res. Lett. 41, 4550–2568. https://doi.org/10.1002/2014GL060500

Kluth, C.F., Coney, P.J., 1981. Plate tectonics of the Ancestral Rocky Mountains. Geology 9, 10–15. https://doi.org/10.1130/0091-7613(1981)9<10:PTOTAR>2.0.CO;2

Kochenderfer, J.N., Hornbeck, J.W., 1999. Contrasting Timber Harvesting Operations Illustrate the Value of BMPs, in: Stringer, J.W., Loftis, D.L. (Eds.), Proceedings, 12th Central Hardwood Forest Conference. USDA Forest Service Southern Research Station, Lexington, KY, pp. 128–136.

Kolka, R., Sturtevant, B., Townsend, P., Miesel, J., Wolter, P., Fraver, S., DeSutter, T., 2014. Post-Fire Comparisons of Forest Floor and Soil Carbon, Nitrogen, and Mercury Pools with Fire Severity Indices. Soil Sci. Soc. Am. J. North Am. For. Soils Conf. Proc. 78, S58–S65. https://doi.org/10.2136/sssaj2013.08.0351nafsc

Kolka, R.K., Steber, A., Brooks, K., Perry, C.H., Powers, M., 2012. Relationships between Soil Compaction and Harvest Season, Soil Texture, and Landscape Position for Aspen Forests. North. J. Appl. For. 29, 21–25. https://doi.org/10.5849/njaf.10-039

Koutsoyiannis, D., 2011. Hurst-Kolmogorov Dynamics and Uncertainty. J. Am. Water Resour. Assoc. 47, 481–495. https://doi.org/10.1111/j.1752-1688.2011.00543.x

Kumar, P., Le, P.V.V., Papanicolaou, A.N.T., Rhoads, B.L., Anders, A.M., Stumpf, A., Wilson, C.G., Bettis III, E.A., Blair, N., Ward, A.S., Filley, T., Lin, H., Keefer, L., Keefer, D.A., Lin, Y.-F., Muste, M., Royer, T. V., Foufoula-Georgiou, E., Belmont, P., 2018. Critical transition in critical zone of intensively managed landscapes. Anthropocene 22, 10–19. https://doi.org/10.1016/j.ancene.2018.04.002

Kuraś, P.K., Alila, Y., Weiler, M., 2012. Forest harvesting effects on the magnitude and frequency of peak flows can increase with return period. Water Resour. Res. 48, W01544, 1–19. https://doi.org/10.1029/2011WR010705

Kurz, W.A., Dymond, C.C., Stinson, G., Rampley, G.J., Neilson, E.T., Carroll, A.L., Ebata, T., Safranyik, L., 2008. Mountain pine beetle and forest carbon feedback to climate change. Nature 452, 987–990. https://doi.org/10.1038/nature06777

Lang, A.J., Aust, W.M., Bolding, M.C., Barrett, S.M., Mcguire, K.J., Lakel, W.A., 2015. Streamside Management Zones Compromised by Stream Crossings, Legacy Gullies, and Over-Harvest in the Piedmont. J. Am. Water Resour. Assoc. 51, 1153–1164. https://doi.org/10.1111/jawr.12292

Lang, A.J., Aust, W.M., Bolding, M.C., Mcguire, K.J., Schilling, E.B., 2018. Best Management Practices Influence Sediment Delivery from Road Stream Crossings to Mountain and Piedmont Streams. For. Sci. 64, 682–695. https://doi.org/10.1093/forsci/fxy019

Langbein, W.B., Leopold, L.B., 1964. Quasi-Equilibrium States in Channel Morphology. Am. J. Sci. 262, 782–794.

Langsrud, Ø., 2003. ANOVA for unbalanced data: Use Type II instead of Type III sums of squares. Stat. Comput. 13, 163–167. https://doi.org/10.1023/A:1023260610025

Larson, G.J., 2011. Ice-margin Fluctuations at the End of the Wisconsin Episode, Michigan, USA, in: Developments in Quaternary Sciences, Volume 15: Quaternary Glaciations - Extent and Chronology. Elsevier Inc., pp. 487–497. https://doi.org/10.1016/B978-0-444-53447-7.00037-4

Laudon, H., Sponseller, R.A., 2018. How landscape organization and scale shape catchment hydrology and biogeochemistry: insights from a long-term catchment study. WIREs Water 5, 15. https://doi.org/10.1002/wat2.1265

Laurance, W.F., 2007. Forests and floods. Nature 449, 409. https://doi.org/10.1038/449409a

Lewis, J., Mori, S.R., Keppeler, E.T., Ziemer, R.R., 2001. Impacts of logging on storm peak flows, flow volumes and suspended sediment loads in Caspar Creek, California, in: Wigmosta, M.S., Burges, S.J. (Eds.), Land Use and Watersheds: Human Influence on Hydrology and Geomorphology in Urban and Forest Areas. Water Science and Application Volume 2. American Geophysical Union, Washington, D.C., pp. 85–125.

Lewis, J., Reid, L.M., Thomas, R.B., 2010. Comment on "forest and floods: A new paradigm sheds light on age old controversies" by Younes Alila et al. Water Resour. Res. 46, 1–4. https://doi.org/10.1029/2009WR008766

Likens, G.E., 2001. Biogeochemistry, the watershed approach: Some uses and limitations. Mar. Freshw. Res. 52, 5–12. https://doi.org/10.1071/MF99188

Litschert, S.E., MacDonald, L.H., 2009. Frequency and characteristics of sediment delivery pathways from forest harvest units to streams. For. Ecol. Manage. 259, 143–150. https://doi.org/10.1016/j.foreco.2009.09.038

Loftis, J.C., MacDonald, L.H., Streett, S., Iyer, H.K., Bunte, K., 2001. Detecting cumulative watershed effects: The statistical power of pairing. J. Hydrol. 251, 49–64. https://doi.org/10.1016/S0022-1694(01)00431-0

Lu, S.-Y., 1994. Forest Harvesting Effects on Streamflow and Flood Frequency in the Northern Lake States. University of Minnesota Ph.D. Thesis.

Luce, C.H., Black, T., 1999. Sediment production from forest roads in western Oregon. Water Resour. Res. 35, 2561–2570. https://doi.org/10.1029/1999WR900135

Lynch, J.A., Corbett, E.S., 1990. Evaluation of best management practices for controlling nonpoint pollution from silvicultural operations. Water Resour. Bull. 26, 41–52. https://doi.org/10.1111/j.1752-1688.1990.tb01349.x

MacDonald, L.H., 2000. Evaluating and managing cumulative effects: Process and constraints. Environ. Manage. 26, 299–315. https://doi.org/10.1007/s002670010088

MacDonald, L.H., Hoffman, J.A., 1995. Causes of Peak Flows in Northwestern Montana and Northeastern Idaho. Water Resour. Bull. 31, 79–95. https://doi.org/10.1111/j.1752-1688.1995.tb03366.x

Madej, M.A., 2001. Erosion and sediment delivery following removal of forest roads. Earth Surf. Process. Landforms 26, 175–190. https://doi.org/10.1002/1096-9837(200102)26:2<175::AID-ESP174>3.0.CO;2-N

Magner, J.A., Alexander, S.C., 2002. Geochemical and Isotopic Tracing of Water in Nested Southern Minnesota Corn-Belt Watersheds Geochemical and isotopic tracing of water in nested southern Minnesota corn-belt watersheds. Water Sci. Technol. 45, 37–42. https://doi.org/10.2166/wst.2002.0199

Magner, J.A., Brooks, K.N., 2008. Predicting stream channel erosion in the lacustrine core of the upper Nemadji River, Minnesota (USA) using stream geomorphology metrics. Environ. Geol. 54, 1423–1434. https://doi.org/10.1007/s00254-007-0923-3

Maine Forest Service, 2013. Maine Forestry Best Management Practices (BMP) Use and Effectiveness - Data Summary 2013 1–47.

Malutta, S., Kobiyama, M., Chaffe, P.L.B., Bonumá, N.B., 2020. Hysteresis analysis to quantify and qualify the sediment dynamics: state of the art. Water Sci. Technol. In Press, 1–17. https://doi.org/10.2166/wst.2020.279

Mao, D., Cherkauer, K.A., 2009. Impacts of land-use change on hydrologic responses in the Great Lakes region. J. Hydrol. 374, 71–82. https://doi.org/10.1016/j.jhydrol.2009.06.016

Marks, D., Kimball, J., Tingey, D., Link, T., 1998. The sensitivity of snowmelt processes to climate conditions and forest cover during rain-on-snow: a case study of the 1996 Pacific Northwest Food. Hydrol. Process. 12, 1569–1587.

Martin, C.W., Hornbeck, J.W., Likens, G.E., Buso, D.C., 2000. Impacts of intensive harvesting on hydrology and nutrient dynamics of northern hardwood forests. Can. J. Fish. Aquat. Sci. 57, 19–29.

Masek, J.G., Huang, C., Wolfe, R., Cohen, W., Hall, F., Kutler, J., Nelson, P., 2008. North American forest disturbance mapped from a decadal Landsat record. Remote Sens. Environ. 112, 2914–2926. https://doi.org/10.1016/j.rse.2008.02.010

McBroom, M.W., Beasley, R.S., Chang, M., Gowin, B., Ice, G.G., 2003. Runoff and sediment losses from annual and unusual storm events from the Alto Experimental Watersheds, Texas: 23 years after silvicultural treatments. Fac. Publ. 7, 607–613.

McBroom, M.W., Beasley, R.S., Chang, M., Ice, G.G., 2008. Storm runoff and sediment losses from forest clearcutting and stand re-establishment with best management practices in East Texas, USA. Hydrol. Process. 22, 1509–1522. https://doi.org/10.1002/hyp.6703

McCarney-Castle, K., Childress, T.M., Heaton, C.R., 2017. Sediment source identification and load prediction in a mixed-use Piedmont watershed , South Carolina. J. Environ. Manage. 185, 60–69. https://doi.org/10.1016/j.jenvman.2016.10.036

McDonnell, J.J., Sivapalan, M., Vache, K., Dunn, S., Grant, G., Haggerty, R., Hinz, C., Hooper, R., Kirchner, J., Roderick, M.L., Selker, J., Weiler, M., 2007. Moving beyond heterogeneity and process complexity : A new vision for watershed hydrology. Water Resour. Res. 43, 1–6. https://doi.org/10.1029/2006WR005467

McEachran, Z.P., Slesak, R.A., Karwan, D.L., 2018. From skid trails to landscapes: Vegetation is the dominant factor influencing erosion after forest harvest in a low relief glaciated landscape. For. Ecol. Manage. 430, 299–311. https://doi.org/10.1016/j.foreco.2018.08.021

Mckinley, R., Radcliffe, D., Mukundan, R., 2013. A streamlined approach for sediment source fingerprinting in a Southern Piedmont watershed, USA. J. Soils Sediments 303, 1754–1769. https://doi.org/10.1007/s11368-013-0723-1

McShane, B.B., Gal, D., Gelman, A., Robert, C., Tackett, J.L., 2019. Abandon Statistical Significance. Am. Stat. 73, 235–245. https://doi.org/10.1080/00031305.2018.1527253

Megahan, W.F., 1972. Logging, Erosion, Sedimentation - Are They Dirty Words? J. For. 403–407.

Megahan, W.F., Kidd, W.J., 1972. Effects of logging and logging roads on erosion and sediment deposition from steep terrain. J. For. 70, 136–141. https://doi.org/10.1016/0022-4898(73)90177-8

Megahan, W.F., King, J.G., 2004. Erosion, sedimentation, and cumulative effects in the Northern Rocky Mountains, in: Ice, G.G., Stednick, J.D. (Eds.), A Century of Forest and Wildland Watershed Lessons. pp. 201–222.

Megahan, W.F., Wilson, M., Monsen, S.B., 2001. Sediment production from granitic cutslopes on forest roads in Idaho, USA. Earth Surf. Process. Landforms 26, 153–163. https://doi.org/10.1002/1096-9837(200102)26:2<153::AID-ESP172>3.0.CO;2-0

Mengistu, S.G., Creed, I.F., Kulperger, R.J., Quick, C.G., 2013. Russian nesting dolls effect – Using wavelet analysis to reveal non-stationary and nested stationary signals in water yield from catchments on a northern forested landscape. Hydrol. Process. 27, 669–686. https://doi.org/10.1002/hyp.9552

Menne, M.J., Durre, I., Vose, R.S., Gleason, B.E., Houston, T.G., 2012. An overview of the global historical climatology network-daily database. J. Atmos. Ocean. Technol. 29, 897–910. https://doi.org/10.1175/JTECH-D-11-00103.1

Menne, M.J., I. Durre, B. Korzeniewski, S. McNeal, K. Thomas, X. Yin, S. Anthony, R. Ray, R.S. Vose, B.E.Gleason, and T.G. Houston, 2012: Global Historical Climatology Network - Daily (GHCN-Daily), Version 3.26. NOAA National Climatic Data Center. http://doi.org/10.7289/V5D21VHZ Accessed December 2019.

Merten, E.C., Hemstad, N.A., Kolka, R.K., Newman, R.M., Verry, E.S., Vondracek, B., 2010. Recovery of sediment characteristics in moraine, headwater streams of Northern Minnesota after forest harvest. J. Am. Water Resour. Assoc. 46, 733–743. https://doi.org/10.1111/j.1752-1688.2010.00445.x

Mielko, C., Woo, M.K., 2006. Snowmelt runoff processes in a headwater lake and its catchment, subarctic Canadian Shield. Hydrol. Process. 20, 987–1000. https://doi.org/10.1002/hyp.6117

Milly, P.C.D., Betancourt, J., Falkenmark, M., Hirsch, R.M., Zbigniew, W., Lettenmaier, D.P., Stouffer, R.J., 2008. Stationarity Is Dead: Whither Water Management? Science (80-.). 319, 573–575. https://doi.org/10.1126/science.1151915

Minnesota DNR, 2019. Minnesota National Hydrography Dataset. Available at https://resources.gisdata.mn.gov/pub/gdrs/data/pub/us_mn_state_dnr/water_dnr_hydrography/metadata/metadata.html. Accessed 06/05/2020.

Minnesota Forest Resources Council, 2012. Sustaining Minnesota Forest Resources: Voluntary Site-Level Forest Management Guidelines for Landowners, Loggers and Resource Managers.

Minnesota National Wetlands Inventory. 2019. Available at https://gisdata.mn.gov/dataset/water-natwetlands-inv-2009-2014. Accessed 06/18/2020.

Mitchell, N., Kumarasamy, K., Cho, S.J., Belmont, P., Dalzell, B., Gran, K., 2018. Reducing High Flows and Sediment Loading through Increased Water Storage in an Agricultural Watershed of the Upper Midwest, USA. Water 10, 1053. https://doi.org/10.3390/w10081053

Mogollón, B., Frimpong, E.A., Hoegh, A.B., Angermeier, P.L., 2016. An empirical assessment of which inland floods can be managed. J. Environ. Manage. 167, 38–48. https://doi.org/10.1016/j.jenvman.2015.10.044

Montgomery, D.R., 1994. Road surface drainage, channel initiation, and slope instability. Water Resour. Res. 30, 1925–1932. https://doi.org/10.1029/94WR00538

Moody, J.A., Martin, D.A., 2001. Initial hydrologic and geomorphic response following a wildfire in the Colorado front range. Earth Surf. Process. Landforms 26, 1049–1070. https://doi.org/10.1002/esp.253

Moore, R.D., Wondzell, S.M., 2005. Physical hydrology and the effects of forest harvesting in the Pacific Northwest: A review. J. Am. Water Resour. Assoc. 41, 763–784. https://doi.org/10.1111/j.1752-1688.2005.tb04463.x

Moores, A., Puettmann, K., Maguire, D., 2007. The Focus of Intensive Silvicultural Research on Coastal Douglas-Fir Over the Last 20 Years. West. J. Appl. For. 22, 21–28.

Morrison, J.E., Smith, J.A., 2002. Stochastic modeling of flood peaks using the generalized extreme value distribution. Water Resour. Res. 38, 41-1-41–12. https://doi.org/10.1029/2001WR000502

Motha, J.A., Wallbrink, P.J., Hairsine, P.B., Grayson, R.B., 2003. Determining the sources of suspended sediment in a forested catchment in southeastern Australia. Water Resour. Res. 39, 1056. https://doi.org/10.1029/2001wr000794

Mukundan, R., Radcliffe, D.E., Ritchie, J.C., 2011. Channel stability and sediment source assessment in streams draining a Piedmont watershed in Georgia, USA. Hydrol. Process. 25, 1243–1253. https://doi.org/10.1002/hyp.7890

Murray, C.D., Buttle, J.M., 2003. Impacts of clearcut harvesting on snow accumulation and melt in a northern hardwood forest. J. Hydrol. 271, 197–212. https://doi.org/10.1016/S0022-1694(02)000352-9

Nathan, R.J., McMahon, T.A., 1990. Evaluation of Automated Techniques for Base Flow and Recession Analyses. Water Resour. Res. 26, 1465–1473.

National Oceanic and Atmospheric Administration – National Centers for Environmental Information (NOAA-NCEI) (2020). Weather data for Winton Power Plant, Station # USC00219101, Period of Record 1966-1995. Accessed via https://www.ncdc.noaa.gov/cdo-web/datasets on 12/19/2019.

National Oceanic and Atmospheric Administration – Physical Sciences Laboratory (NOAA-PSL) (2020). Atlantic Multidecadal Oscillation data. Accessed from https://psl.noaa.gov/data/timeseries/AMO/ on 07/07/2020.

National Oceanic and Atmospheric Administration – Physical Sciences Laboratory (NOAA-PSL) (2020). Multivariate El Niño Southern Oscillation (ENSO) Index (MEI) data. Accessed from https://www.psl.noaa.gov/enso/mei.old/table.html on 07/07/2020.

National Oceanic and Atmospheric Administration – Physical Sciences Laboratory (NOAA-PSL) (2020). North Atlantic Oscillation data. Accessed from https://psl.noaa.gov/data/timeseries/daily/NAO/ on 07/07/2020.

National Oceanic and Atmospheric Administration – Physical Sciences Laboratory (NOAA-PSL) (2020). Pacific Decadal Oscillation data. Accessed from https://psl.noaa.gov/pdo/ on 07/07/2020.

National Research Council, 1988. Earth System Science: A New Approach to Global Change, in: Earth

System Science: A Closer View. NASA, Washington, D.C., pp. 22–33. https://doi.org/10.17226/19088

National Research Council (NRC), 2008. Hydrologic Effects of a Changing Forest Landscape.

Naylor, S., Letsinger, S.L., Ficklin, D.L., Ellett, K.M., Olyphant, G.A., 2016. A hydropedological approach to quantifying groundwater recharge in various glacial settings of the mid-continental USA. Hydrol. Process. 30, 1594–1608. https://doi.org/10.1002/hyp.10718

Neary, D.G., 2016. Long-Term Forest Paired Catchment Studies: What Do They Tell Us That Landscape-Level Monitoring Does Not? 7, 15. https://doi.org/10.3390/f7080164

Neary, D.G., Ice, G.G., Jackson, C.R., 2009. Linkages between forest soils and water quality and quantity. For. Ecol. Manage. 258, 2269–2281. https://doi.org/10.1016/j.foreco.2009.05.027

Negron, F., Smith, J.M., Schoennagel, T., Veblen, T.T., 2012. Effects of Mountain Pine Beetle on Fuels and Expected Fire Behavior in Lodgepole Pine Forests, Colorado, USA. PLoS One 7. https://doi.org/10.1371/journal.pone.0030002

Nichols, D.S., Verry, E.S., 2001. Stream flow and ground water recharge from small forested watersheds in north central Minnesota. J. Hydrol. 245, 89–103. https://doi.org/10.1016/S0022-1694(01)00337-7

Noe, G.B., Cashman, M.J., Skalak, K., Gellis, A.C., Hopkins, K.G., Moyer, D., Webber, J., Benthem, A., Maloney, K., Brakebill, J., Sekellick, A., Langland, M., Zhang, Q., Shenk, G., Keisman, J., Hupp, C., 2020. Sediment dynamics and implications for management: State of the science from long-term research in the Chesapeake Bay watershed, USA. WIREs Water 7, 28. https://doi.org/10.1002/wat2.1454

Nyberg, P.R., 1987. Soil Survey of Itasca County, Minnesota.

O'Loughlin, C.L., 1985. The Effects of Forest Land Use on Erosion and Slope Stability. Final Rep. based Pap. Present. a Semin. held East-West Center, Honolulu, HI, 7-11 May 1984 26.

Orr, W.N., Orr, E.L., 2002. Cornerstones of Pacific Northwest Geology, in: Geology of the Pacific Northwest. Waveland Press, Long Grove, IL, pp. 1–18.

Patric, J.H., 1976. Soil Erosion in the Eastern Forest. J. For. 74, 671–677. https://doi.org/10.1093/jof/74.10.671

Perala, D., Verry, E., 2011. Forest Management Practices and Silviculture. Peatl. Biogeochem. Watershed Hydrol. Marcell Exp. For. 371–400. https://doi.org/10.1201/b10708-13

Pfeiffer, A.M., Finnegan, N., 2018. Regional Variation in Gravel Riverbed Mobility , Controlled by Hydrologic Regime and Sediment Supply. Geophys. Res. Lett. 45, 3097–3106. https://doi.org/10.1002/2017GL076747

Pfeiffer, A.M., Finnegan, N.J., Willenbring, J.K., 2017. Sediment supply controls equilibrium channel geometry in gravel rivers. Proc. Natl. Acad. Sci. United States Am. 114. https://doi.org/10.1073/pnas.1612907114

Phillips, C.B., Jerolmack, D.J., 2019. Bankfull Transport Capacity and the Threshold of Motion in Coarse-Grained Rivers. Water Resour. Res. 55, 11316–11330. https://doi.org/10.1029/2019WR025455

Phillips, C.B., Jerolmack, D.J., 2016. Self-organization of river channels as a critical filter on climate signals. Science (80-.). 352, 694–698. https://doi.org/10.1126/science.aad3348

Phillips, J.D., 1992a. Nonlinear dynamical systems in geomorphology: revolution or evolution? Geomorphology 5, 219–229. https://doi.org/10.1016/0169-555X(92)90005-9

Phillips, J.D., 1992b. The end of equilibrium? Geomorphology 5, 195–201. https://doi.org/10.1016/0169-555X(92)90002-6

Phillips, R.T.J., Desloges, J.R., 2015. Glacial legacy effects on river landforms of the southern Laurentian Great Lakes. J. Great Lakes Res. 41, 951–964. https://doi.org/10.1016/j.jglr.2015.09.005

Phillips, R.T.J., Desloges, J.R., 2014. Glacially conditioned specific stream powers in low-relief river catchments of the southern Laurentian Great Lakes. Geomorphology 206, 271–287. https://doi.org/10.1016/j.geomorph.2013.09.030

Pierson, F.B., Bates, J.D., Svejcar, T.J., Hardegree, S.P., 2007. Runoff and erosion after cutting western juniper. Rangel. Ecol. Manag. 60, 285–292. https://doi.org/10.2111/1551-5028(2007)60[285:RAEACW]2.0.CO;2

Pizzuto, J., Neal, M.O., Stotts, S., 2010. On the retreat of forested, cohesive riverbanks. Geomorphology 116, 341–352. https://doi.org/10.1016/j.geomorph.2009.11.008

Pizzuto, J., O'Neal, M., 2009. Increased mid-twentieth century riverbank erosion rates related to the Increased mid-twentieth century riverbank erosion rates related to the demise of mill dams, South River, Virginia. Geology 37, 19–22. https://doi.org/10.1130/G25207A.1

Pizzuto, J., Schenk, E.R., Hupp, C.R., Gellis, A., Noe, G., Williamson, E., Karwan, D.L., O'Neal, M., Marquard, J., Aalto, R., Newbold, D., 2014. Characteristic length scales and time-averaged transport velocities of suspended sediment in the mid-Atlantic Region, USA. Water Resour. Res. 50, 790–805. https://doi.org/10.1002/2013WR014485

Plummer, M., 2003. JAGS: A program for analysis of Bayesian graphical models using Gibbs sampling. Proc. 3rd Int. Work. Distrib. Stat. Comput. (DSC 2003) 20–22. https://doi.org/10.1.1.13.3406

Poff, N.L., 2002. Ecological response to and management of increased flooding caused by climate change. Philos. Trans. R. Soc. 360, 1497–1510. https://doi.org/10.1098/rsta.2002.1012

Poff, N.L., Allan, J.D., Bain, M.B., Karr, J.R., Prestegaard, K.L., Richter, B.D., Sparks, R.E., Stromberg, J.C., 1997. Natural Flow Regime. Bioscience 47, 769–784. https://doi.org/10.2307/1313099

Poff, N.L., Bledsoe, B.P., Cuhaciyan, C.O., 2006. Hydrologic variation with land use across the contiguous United States: Geomorphic and ecological consequences for stream ecosystems. Geomorphology 79, 264–285. https://doi.org/10.1016/j.geomorph.2006.06.032

Pomeroy, J.W., Granger, R.J., 1997. Sustainability of the western Canadian boreal forest under changing hydrological conditions. I. Snow accumulation and ablation, in: Sustainability of Water Resources under Increasing Uncertainty (Proceedings of the Rabat Symposium S1, April 1997). pp. 237–242.

Pomeroy, J.W., Granger, R.J., Pietroniro, A., Elliot, J.E., Toth, B., Hedstrom, N., 1994. Hydrological Pathways in the Prince Albert Model Forest, Final Report Submitted to the Prince Albert Model Forest Association. NHRI Contrib. Ser. No. CS-97004.

Prettyman, D.H., 1978. Soil Survey of Kawishiwi Area, Minnesota: Parts of Lake and Cook Counties in Superior National Forest.

Price, K., 2011. Effects of watershed topography, soils, land use, and climate on baseflow hydrology in humid regions: A review. Prog. Phys. Geogr. 35, 465–492. https://doi.org/10.1177/0309133311402714

Price, K., Leigh, D.S., 2006. Comparative water quality of lightly- and moderately-impacted streams in the southern Blue Ridge Mountains, USA. Environ. Monit. Assess. 120, 269–300. https://doi.org/10.1007/s10661-005-9060-1

PRISM Climate Group (2020), Oregon State University, http://prism.oregonstate.edu, created 4 Feb 2004. Most recent update: 07/15/2020. Accessed 07/18/2020.

R Core Team, 2019. R: A language and environment for statistical computing.

Radbruch-Hall, D.H., Colton, R.B., Davies, W.E., Lucchitta, I., Skipp, B.A., Varnes, D.J., 1982. Landslide overview map of the coterminous United States, USGS Professional Paper 1183. https://doi.org/10.3133/pp1183

Rashin, E.B., Clishe, C.J., Loch, A.T., Bell, J.M., 2006. Effectiveness of Timber Harvest Practices for Controlling Sediment Related Water Quality Impacts. J. Am. Water Resour. Assoc. 42, 1307–1327. https://doi.org/10.1111/j.1752-1688.2006.tb05303.x

Reid, L.M., Dewey, N.J., Lisle, T.E., Hilton, S., 2010. The incidence and role of gullies after logging in a coastal redwood forest. Geomorphology 117, 155–169. https://doi.org/10.1016/j.geomorph.2009.11.025

Reid, L.M., Dunne, T., 1984. Sediment Production from Forest Road Surfaces. Water Resour. Res. 20, 1753–1761. https://doi.org/10.1029/WR020i011p01753

Reiter, M., Heffner, J.T., Beech, S., Turner, T., Bilby, R.E., 2009. Temporal and spatial turbidity patterns over 30 years in a managed forest of Western Washington. J. Am. Water Resour. Assoc. 45, 793–808. https://doi.org/10.1111/j.1752-1688.2009.00323.x

Renard, B., Lang, M., Bois, P., 2006. Statistical analysis of extreme events in a non-stationary context via a Bayesian framework: case study with peak-over-threshold data. Stoch. Environ. Res. Risk Assess. 21, 97–112. https://doi.org/10.1007/s00477-006-0047-4

Renard, K.G., 1997. Predicting soil erosion by water: a guide to conservation planning with the Revised Universal Soil Loss Equation (RUSLE). United States Government Printing.

Renne, R.R., 1967. Research Guidelines to Sound Watershed Development. J. Irrig. Drain. Div. ASCE 92, 53–58.

Rice, R.M., Lewis, J., 1991. Estimating Erosion Risks Associated With Logging and Forest Roads in Northwestern California. Water Resour. Bull. 27, 809–818. https://doi.org/10.1111/j.1752-1688.1991.tb01479.x

Richards, C., Johnson, L.B., Host, G.E., 1996. Landscape-scale influences on stream habitats and biota. Can. J. Fish. Aquat. Sci. 53, 295–311. https://doi.org/10.1139/f96-006

Richards, R.P., 1990. Measures of Flow Variability and a New Flow-Based Classification of Great Lakes Tributaries. J. Great Lakes Res. 16, 53–70. https://doi.org/10.1016/S0380-1330(90)71398-6

Riedel, M.S., Verry, E.S., Brooks, K.N., 2005. Impacts of land use conversion on bankfull discharge and mass wasting. J. Environ. Manage. 76, 326–337. https://doi.org/10.1016/j.jenvman.2005.02.002

Rivenbark, B.L., Jackson, C.R., 2004. Concentrated flow breakthroughs moving through silvicultural streamside management zones: southeastern peidmont, USA. J. Am. Water Resour. Assoc. 40, 1043–1052. https://doi.org/10.1111/j.1752-1688.2004.tb01065.x

Roberts, R.G., Church, M., 1986. The sediment budget in severely disturbed watersheds, Queen Charlotte Ranges, British Columbia. Can. J. For. Res. https://doi.org/10.1139/x86-189

Rogger, M., Agnoletti, M., Alaoui, A., Bathurst, J.C., Bodner, G., Borga, M., Chaplot, V., Gallart, F., Glatzel, G., Hall, J., Holden, J., Holko, L., Horn, R., Kiss, A., Quinton, J.N., Leitinger, G., Lennartz, B., Parajka, J., Peth, S., Robinson, M., Salinas, J.L., Santoro, A., Szolgay, J., Tron, S., Viglione, A., 2017. Land use change impacts on floods at the catchment scale: Challenges and opportunities for future research. Water Resour. Res. 53, 5209–5219. https://doi.org/10.1002/2017WR020723.Received

Rose, L.A., Karwan, D.L., Godsey, S.E., 2018. Concentration – discharge relationships describe solute and sediment mobilization , reaction, and transport at event and longer timescales. Hydrol. Process. 32, 2829–2844. https://doi.org/10.1002/hyp.13235

Roulet, N., 1990. The hydrological role of peat-covered wetlands. Can. Geogr. 34, 82–83. https://doi.org/10.1111/j.1541-0064.1990.tb01073.x

Safeeq, M., Grant, G.E., Lewis, S.L., Hayes, S.K., 2020. Disentangling effects of forest harvest on long-term hydrologic and sediment dynamics, western Cascades, Oregon. J. Hydrol. 580, 124259. https://doi.org/10.1016/j.jhydrol.2019.124259

Sahin, V., Hall, M.J., 1996. The effects of afforestation and deforestation on water yields. J. Hydrol. 178, 293–309.

Santiago Beguería and Sergio M. Vicente-Serrano (2017). SPEI: Calculation of the Standardised Precipitation-Evapotranspiration Index. R package version 1.7. https://CRAN.R-project.org/package=SPEI

Schenk, E.R., Hupp, C.R., 2009. Legacy effects of colonial millponds on floodplain sedimentation, bank erosion, and channel morphology, Mid-Atlantic, USA. J. Am. Water Resour. Assoc. 45, 597–606. https://doi.org/10.1111/j.1752-1688.2009.00308.x

Schnackenberg, E.S., MacDonald, L.H., 1998. Detecting cumulative effects on headwater streams in the Routt National Forest, Colorado. J. Am. Water Resour. Assoc. 34. https://doi.org/10.1111/j.1752-1688.1998.tb04162.x

Schnorbus, M., Alila, Y., 2013. Peak flow regime changes following forest harvesting in a snow-dominated basin : Effects of harvest area, elevation, and channel connectivity. Water Resour. Res. 49, 517–535. https://doi.org/10.1029/2012WR011901

Schomberg, J.D., Host, G., Johnson, L.B., Richards, C., 2005. Evaluating the influence of landform, surficial geology, and land use on streams using hydrologic simulation modeling. Aquat. Sci. 67, 528–540. https://doi.org/10.1007/s00027-005-0785-2

Schuler, J.L., Briggs, R.D., 2000. Assessing Application and Effectiveness of Forestry Best Management Practices in New York. North. J. Appl. For. 17, 125–134. https://doi.org/10.1093/njaf/17.4.125

Scott, D.F., 1997. The contrasting effects of wildfire and clearfelling on the hydrology of a small catchment 11, 543–555.

Sebestyen, S.D., Dorrance, C., Olson, D.M., Verry, E.S., Kolka, R.K., Elling, A.E., Kyllander, R., 2011a. Long-term monitoring sites and trends at the Marcell Experimental Forest, in: Peatland Biogeochemistry and Watershed Hydrology at the Marcell Experimental Forest. CRC Press, Boca Raton, pp. 15–71. https://doi.org/10.1201/b10708-3

Sebestyen, S.D., Dorrance, C., Olson, D.M., Verry, E.S., Kolka, R.K., Elling, A.E., Kyllander, R., 2011b. Long-Term Monitoring Sites and Trends at the Marcell Experimental Forest, in: Kolka, R.K., Sebestyen, S.D., Verry, E.S., Brooks, K.N. (Eds.), Peatland Biogeochemistry and Watershed Hydrology at the Marcell Experimental Forest. CRC Press, Boca Raton, pp. 15–72.

Sebestyen, S.D., Verry, E.S., Brooks, K.N., 2011c. Hydrological Responses to Changes in Forest Cover on Uplands and Peatlands, in: Peatland Biogeochemistry and Watershed Hydrology at the Marcell Experimental Forest. CRC Press: Taylor & Francis Group, LLC, Boca Raton, FL, pp. 401–432.

Seibert, J., McDonnell, J.J., 2010. Land-cover impacts on streamflow: a change-detection modelling approach that incorporates parameter uncertainty approach that incorporates parameter uncertainty. Hydrol. Sci. J. 55, 316–332. https://doi.org/10.1080/02626661003683264

Senay, G. B., S. Bohms, R. K. Singh, P. H. Gowda, N. M. Velpuri, H. Alemu, and J. P. Verdin. 2013. Operational Evapotranspiration Mapping Using Remote Sensing and Weather Datasets: A New Parameterization for the SSEB Approach. Journal of the American Water Resources Association 49 (3):577-591. https://doi.org/10.1111/jawr.12057

Senay, G. 2018. Satellite Psychrometric Formulation of the Operational Simplified Surface Energy Balance (SSEBop) Model for Quantifying and Mapping Evapotranspiration. Applied Engineering in Agriculture 34 (3):555-566. https://doi.org/10.13031/aea.12614

Senay, G. B. and Kagone, S., 2019, Daily SSEBop Evapotranspiration: U. S. Geological Survey Data Release, https://doi.org/10.5066/P9L2YMV

Seyfried, M., Lohse, K., Marks, D., Flerchinger, G., Pierson, F., Holbrook, W.S., 2018. Reynolds creek experimental watershed and critical zone observatory. Vadose Zo. J. 17. https://doi.org/10.2136/vzj2018.07.0129

Shakesby, R.A., Doerr, S.H., 2006. Wildfire as a hydrological and geomorphological agent. Earth-Science Rev. 74, 269–307. https://doi.org/10.1016/j.earscirev.2005.10.006

Shaman, J., Stieglitz, M., Burns, D., 2004. Are big basins just the sum of small catchments? Hydrol. Process. 18, 3195–3206. https://doi.org/10.1002/hyp.5739

Shanley, J.B., Sebestyen, S.D., Mcdonnell, J.J., Mcglynn, B.L., Dunne, T., 2015. Water's Way at Sleepers River watershed – revisiting flow generation in a post-glacial landscape, Vermont USA. Hydrol. Process. 3459, 3447–3459. https://doi.org/10.1002/hyp.10377

Simon, A., 1992. Energy, time, and channel evolution in catastrophically disturbed fluvial systems. Geomorphology 5, 345–372. https://doi.org/10.1016/0169-555X(92)90013-E

Simon, A., Hupp, C.R., 1987. Geomorphic and vegetative recovery processes along modified Tennessee streams: an interdisciplinary approach to distributed fluvial systems, in: Forest Hydrology and Watershed Management: Proceedings of the Vancouver Symposium. pp. 251–262.

Simon, A., Rinaldi, M., 2006. Disturbance, stream incision, and channel evolution: The roles of excess transport capacity and boundary materials in controlling channel response. Geomorphology 79, 361–383. https://doi.org/10.1016/j.geomorph.2006.06.037

Slesak, R.A., Corcoran, J., Rossman, R., 2018. A Holistic Monitoring Approach for Water Quality BMP and Forest Watershed Risk Assessment. J. For. 116, 283–290. https://doi.org/10.1093/jofore/fvy005

Smith, A.F.M., Roberts, G.O., 1993. Bayesian Computation via the Gibbs Sampler and Related Markov Chain Monte Carlo Methods. J. R. Stat. Soc. Ser. B 55, 3–23. https://doi.org/10.1111/j.2517-6161.1993.tb01466.x

Smith, H.G., Dragovich, D., 2009. Interpreting sediment delivery processes using suspended sediment-discharge hysteresis patterns from nested upland catchments, south-eastern Australia. Hydrol. Process. 23, 2415–2426. https://doi.org/10.1002/hyp.7357

Soil Survey Staff. Gridded Soil Survey Geographic (gSSURGO) Database for Minnesota. United States Department of Agriculture, Natural Resources Conservation Service. Available online at https://gdg.sc.egov.usda.gov/. Accessed 06/01/2020. (FY20 official release).

Sørensen, R., Ring, E., Meili, M., Högbom, L., Seibert, J., Grabs, T., Laudon, H., Bishop, K., 2009. Forest Harvest Increases Runoff Most during Low Flows in Two Boreal Streams. AMBIO A J. Hum. Environ. 38, 357–363. https://doi.org/10.1579/0044-7447-38.7.357

Spence, C., 2000. The Effect of Storage on Runoff from a Headwater Subarctic Shield Basin. Arctic 53, 237–247.

Spence, C., Woo, M.K., 2003. Hydrology of subarctic Canadian shield: Soil-filled valleys. J. Hydrol. 279, 151–166. https://doi.org/10.1016/S0022-1694(03)00175-6

Srock, A.F., Charney, J.J., Potter, B.E., Goodrick, S.L., 2018. The Hot-Dry-Windy Index : A New Fire Weather Index. Atmosphere (Basel). 9, 11. https://doi.org/10.3390/atmos9070279

Stark, J. R., 1977. Surficial Geology and Ground-Water Geology of the Babbitt-Kawishiwi Area, Northeastern Minnesota with Planning Implications. [Master of Science thesis]. s.l. : University of Wisconsin-Madison.

Starrs, C.F., Butsic, V., Stephens, C., Stewart, W., 2018. The impact of land ownership , firefighting , and reserve status on fire probability in California. Environ. Res. Lett. 13, 11. https://doi.org/10.1088/1748-9326/aaaad1

Stednick, J.D., 2008. Long-term Streamflow Changes Following Timber Harvesting, in: Stednick, J.D. (Ed.), Hydrological and Biological Responses to Forest Practices: The Alsea Watershed Study. Springer, pp. 139–155.

Stednick, J.D., 1996. Monitoring the effects of timber harvest on annual water yield. J. Hydrol. 176, 79–95. https://doi.org/10.1016/0022-1694(95)02780-7

Stoner, J.D., Lorenz, D.L., Wiche, G.J., Goldstein, R.M., 1993. Red River of the North Basin, Minnesota, North Dakota, and South Dakota. Water Resour. Bull. 29, 575–615. https://doi.org/10.1111/j.1752-1688.1993.tb03229.x

Stoof, C.R., Vervoort, R.W., Iwema, J., Ferreira, A.J.D., Ritsema, C.J., 2012. Hydrological response of a small catchment burned by experimental fire. Hydrol. Earth Syst. Sci. 16, 267–285. https://doi.org/10.5194/hess-16-267-2012

Su, Y.-S., Yajima, M., 2015. R2jags: Using R to Run "JAGS."

Sugden, B.D., Woods, S.W., 2007. Sediment production from forest roads in western Montana. J. Am. Water Resour. Assoc. 43, 193–206. https://doi.org/10.1111⁄j.1752-1688.2007.00016.x

Sun, G., Noormets, A., Chen, J., McNulty, S.G., 2008. Evapotranspiration estimates from eddy covariance towers and hydrologic modeling in managed forests in Northern Wisconsin, USA. Agric. For. Meteorol. 148, 257–267. https://doi.org/10.1016/j.agrformet.2007.08.010

Surfleet, C.G., Tullos, D., 2013. Variability in effect of climate change on rain-on-snow peak flow events in a temperate climate. J. Hydrol. 479, 24–34. https://doi.org/10.1016/j.jhydrol.2012.11.021

Sutton, R.T., Hodson, D.L.R., 2005. Atlantic Ocean Forcing of North American and European Summer Climate. Science (80-.). 309, 115–118. https://doi.org/10.1126/science.1109496

Swank, W.T., Douglass, J.E., 1974. Streamflow Greatly Reduced by Converting Deciduous Hardwood Stands to Pine. Science (80-.). 185, 857–859.

Swank, W.T., Miner, N.H., 1968. Conversion of Hardwood-Covered Watersheds to White Pine Reduces Water Yield. Water Resour. Res. 4, 947–954. https://doi.org/10.1029/WR004i005p00947

Swank, W.T., Vose, J.M., Elliott, K.J., 2001. Long-term hydrologic and water quality responses following commercial clearcutting of mixed hardwoods on a southern Appalachian catchment. For. Ecol. Manage. 143, 163–178. https://doi.org/10.1016/S0378-1127(00)00515-6

Swanson, F.J., Benda, L., Duncan, S.H., Grant, G.E., Megahan, W.F., Reid, L.M., Ziemer, R.R., 1987. Mass failures and other processes of sediment production in Pacific Northwest Forest Landscapes, in: Salo, E., Cundy, T. (Eds.), Streamside Management: Forestry and Fishery Interactions. Proceedings of a Symposium Held at University of Washington, 12-14 February 1986. Contribution No. 57, Institute of Forest Resources, Seattle, Washington. pp. 9–37.

Syverson, K.M., Colgan, P.M., 2011. The Quaternary of Wisconsin: An Updated Review of Stratigraphy, Glacial History, and Landforms, in: Ehlers, J., Gibbard, P.L., Hughes, P.D. (Eds.), Developments in Quaternary Sciences, Volume 15: Quaternary Glaciations - Extent and Chronology. Elsevier, Amsterdam, pp. 537–552.

Terrell, S.B., Summer, W.B., Jackson, C.R., Miwa, M., Jones, D.G., 2011. Harvest, Site Preparation, and

Firebreak Effects on Hydrology and Sediment Transport in Coastal Plain Headwater Streams. Trans. ASABE 54, 2117–2127.

Tetzlaff, D., Buttle, J., Carey, S.K., Mcguire, K., Laudon, H., Soulsby, C., 2015. Tracer-based assessment of flowpaths, storage and runoff generation in northern catchments: a review. Hydrol. Process. 29, 3475–3490. https://doi.org/10.1002/hyp.10412

Tetzlaff, D., Soulsby, C., Buttle, J., Capell, R., Carey, S.K., Laudon, H., McDonnell, J., McGuire, K., Seibert, J., Shanley, J., 2013. Catchments on the cusp? Structural and functional change in northern ecohydrology. Hydrol. Process. 27, 766–774. https://doi.org/10.1002/hyp.9700

Thomas, R.B., Megahan, W.F., 1998. Peak flow responses to clear-cutting and roads in small and large basins, western Cascades, Oregon: A second opinion. Water Resour. Res. 34, 3393–3403. https://doi.org/10.1029/98WR02500

Thompson, C., Devito, K.J., Mendoza, C.A., 2018. Hydrologic impact of aspen harvesting within the subhumid Boreal Plains of Alberta. Hydrol. Process. 32, 3924–3937. https://doi.org/10.1002/hyp.13301

Thompson, G.A., Burke, D.B., 1974. Regional geophysics of the Basin and Range province. Annu. Rev. Earth Planet. Sci. 2, 213–238.

Trimble, S.W., 2008. Man-induced soil erosion on the Southern Piedmont, 1700-1970., 2nd ed. Soil and Water Conservation Society, Ankeny, IA.

Trimble, S.W., 1977. The Fallacy of Stream Equilibrium in Contemporary Denudation Studies. Am. J. Sci. 277, 876–887. https://doi.org/10.2475/ajs.277.7.876

USDA Forest Service National Forest System Lands GIS and Fire personnel. 2020. Final Fire Perimeter, Version 6.2. Available at https://data.fs.usda.gov/geodata/edw/index.php. Accessed 07/06/2020.

U.S. Geological Survey, 2020, National Water Information System data available on the World Wide Web (USGS Water Data for the Nation), accessed July 2020, at URL https://waterdata.usgs.gov/nwis/dv/?site_no=05124480&agency_cd=USGS&referred_module=sw. DOI: http://dx.doi.org/10.5066/F7P55KJN

U.S. Geological Survey, 2016, The StreamStats program, Version 4, online at http://streamstats.usgs.gov, accessed on 09/10/2018.

Urie, D.H., 1977. Ground water differences on pine and hardwood forests of the Udell Experimental Forest in Michigan. USDA For. Serv. Res. Pap. NC-145 1–12.

Valtera, M., Schaetzl, R.J., 2017. Pit-mound microrelief in forest soils: Review of implications for water retention and hydrologic modelling. For. Ecol. Manage. 393, 40–51. https://doi.org/10.1016/j.foreco.2017.02.048

van Dijk, A.I.J.M., van Noordwijk, M., Calder, I.R., Bruijnzeel, S.L.A., Schellekens, J., Chappell, N.A., 2009. Forest – flood relation still tenuous – comment on 'Global evidence that deforestation amplifies flood risk and severity in the developing world' by C. J. A. Bradshaw, N. S. Sodi, K. S.-H. Peh and B. W. Brook. Glob. Chang. Biol. 15, 110–115. https://doi.org/10.1111/j.1365-2486.2008.01708.x

Van Steeter, M.M., Pitlick, J., 1998. Geomorphology and endangered fish habitats of the upper Colorado River 1 . Historic changes in streamflow, sediment load, and channel morphology. Water Resour. Res. 34, 287–302. https://doi.org/10.1029/97WR02766

Varanka, S., Hjort, J., Luoto, M., 2015. Geomorphological factors predict water quality in boreal rivers. Earth Surf. Process. Landforms 40, 1989–1999. https://doi.org/10.1002/esp.3601

Vaughan, A.A., Belmont, P., Hawkins, C.P., Wilcock, P., 2017. Near-Channel Versus Watershed Controls on Sediment Rating Curves. J. Geophys. Res. Earth Surf. 122, 1901–1923.

https://doi.org/10.1002/2016JF004180

Verry, E.S., 2004. Land Fragmentation and Impacts to Streams and Fish in the Central and Upper Midwest, in: Ice, G.G., Stednick, J.D. (Eds.), A Century of Forest and Wildland Watershed Lessons. Society of American Foresters, Bethesda, MD, pp. 129–154.

Verry, E.S., 1986. Forest Harvesting and Water: The Lake States Experience. Water Resour. Bull. 22, 1039–1047.

Verry, E.S., 1972. Effect of an Aspen Clearcutting on Water Yield and Quality in Northern Minnesota, in: Csallany, S.G., McLaughlin, T.G., Striffler, W.D. (Eds.), National Symposium on Watersheds in Transition. American Water Resources Association, Fort Collins, CO, pp. 276–284.

Verry, E.S., Bay, R., Boelter, D., 2011. Establishing the Marcell Experimental Forest: Threads in Time, in: Peatland Biogeochemistry and Watershed Hydrology at the Marcell Experimental Forest: Results from 50 Years of Scientific Research. pp. 1–13.

Verry, E.S., Elling, A.E., Sebestyen, S.D., Kolka, R.K., Kyllander, R., 2018. Marcell Experimental Forest daily streamflow data. For. Serv. Res. Data Arch. https://doi.org/10.2737/RDS-2018-0009

Verry, E.S., Hornbeck, J.W., Todd, A.H., 2000. Watershed Research and Management in the Lake States and Northeastern United States, USDA Forest Service Proceedings RMRS-P-13.

Verry, E.S., Janssens, J., 2011. Geology, Vegetation, and Hydrology of the S2 Bog at the MEF: 12,000 Years in Northern Minnesota, in: Kolka, R.K., Sebestyen, S.D., Verry, E.S., Brooks, K.N. (Eds.), Peatland Biogeochemistry and Watershed Hydrology at the Marcell Experimental Forest. CRC Press: Taylor & Francis Group, LLC, Boca Raton, FL, pp. 93–134.

Verry, E.S., Kolka, R.K., 2003. Importance of wetlands to streamflow generation, in: In: Renard, Kenneth G.; et Al., Eds. 1st Interagency Conference on Research in the Watersheds; 2003 October 27-30; Benson, AZ.: US Department of Agriculture, Agricultural Research Service: 126-132.

Verry, E.S., Lewis, J.R., Brooks, K.N., 1983. Aspen Clearcutting increases Snowmelt and Storm Flow Peaks in North Central Minnesota. Water Resour. Bull. 19, 59–67.

Vidon, P., Karwan, D.L., Andres, A.S., Inamdar, S., Kaushal, S., Morrison, J., Mullaney, J., Ross, D.S., Schroth, A.W., Shanley, J.B., Yoon, B., 2018. In the path of the Hurricane: impact of Hurricane Irene and Tropical Storm Lee on watershed hydrology and biogeochemistry from North Carolina to Maine, USA. Biogeochemistry 141, 351–364. https://doi.org/10.1007/s10533-018-0423-4

Viglione, A., Merz, B., Viet Dung, N., Parajka, J., Nester, T., Blöschl, G., 2016. Attribution of regional flood changes based on scaling fingerprints. Water Resour. Res. 52, 5322–5340. https://doi.org/10.1002/2016WR019036

Villarini, G., Smith, J.A., 2010. Flood peak distributions for the eastern United States. Water Resour. Res. 46, 1–17. https://doi.org/10.1029/2009WR008395

Villarini, G., Smith, J.A., Baeck, M.L., Krajewski, W.F., 2011. Examining Flood Frequency Distributions in the Midwest U.S. J. Am. Water Resour. Assoc. 47, 447–463. https://doi.org/10.1111/j.1752-1688.2011.00540.x

Vinson, J.A., Barrett, S.M., Aust, W.M., Bolding, M.C., 2017a. Evaluation of bladed skid trail closure methods in the ridge and valley region. For. Sci. 63, 432–440. https://doi.org/10.5849/FS.2016-030R1

Vinson, J.A., Barrett, S.M., Aust, W.M., Bolding, M.C., 2017b. Suitability of soil erosion models for the evaluation of bladed skid trail BMPs in the Southern appalachians. Forests 8. https://doi.org/10.3390/f8120482

Vogeler, J.C., Slesak, R.A., Fekety, P.A., Falkowski, M.J., 2020. Characterizing over Four Decades of

Forest Disturbance in Minnesota , USA. Forests 11, 1–18. https://doi.org/10.3390/f11030362 . Associated digital forest disturbance data available at https://gisdata.mn.gov/dataset/env-fast-forest-disturbances. Accessed 07/23/2020.

Walter, R.C., Merritts, D.J., 2008. Natural Streams and the Legacy of Water-Powered Mills. Science (80-.). 319, 299–304. https://doi.org/10.1126/science.1151716

Wang, W.J., He, H.S., Thompson III, F.R., Fraser, J.S., Hanberry, B.B., Dijak, W.D., 2015. Importance of succession, harvest, and climate change in determining future composition in U.S. Central Hardwood Forests. Ecosphere 6, 1–18. https://doi.org/10.1890/ES15-00238.1

Warrick, J.A., 2015. Trend analyses with river sediment rating curves. Hydrol. Process. 29, 936–949. https://doi.org/10.1002/hyp.10198

Watras, C.J., Read, J.S., Holman, H.D., Liu, Z., Song, Y.-Y., Watras, A.J., Morgan, S., Stanley, E.H., 2014. Decadal oscillation of lakes and aquifers in the upper Great Lakes region of North America: Hydroclimatic implications. Geophys. Res. Lett. 41, 456–462. https://doi.org/10.1002/2013GL058679

Watters, J.R., Stanley, E.H., 2007. Stream channels in peatlands: The role of biological processes in controlling channel form. Geomorphology 89, 97–110. https://doi.org/10.1016/j.geomorph.2006.07.015

Wemple, B.C., Jones, J.A., 2003. Runoff production on forest roads in a steep , mountain catchment. Water Resour. Res. 39. https://doi.org/10.1029/2002WR001744

Wemple, B.C., Jones, J.A., Grant, G.E., 1996. Channel Network Extension by Logging Roads in Two Basins, Western Cascades, Oregon. Water Resour. Bull. 32, 1195–1207. https://doi.org/10.1111/j.1752-1688.1996.tb03490.x

Wemple, B.C., Swanson, F.J., Jones, J.A., 2001. Forest roads and geomorphic process interactions, Cascade Range, Oregon. Earth Surf. Process. Landforms 26, 191–204. https://doi.org/10.1002/1096-9837(200102)26:2<191::AID-ESP175>3.0.CO;2-U

Whicker, J.J., Pinder, J.E., Breshears, D.D., 2006. Increased Wind Erosion from Forest Wildfire: Implications for Contaminant-Related Risks. J. Environ. Qual. 35, 468. https://doi.org/10.2134/jeq2005.0112

Wicherski, W., Dethier, D.P., Ouimet, W.B., 2017. Erosion and channel changes due to extreme flooding in the Fourmile Creek catchment, Colorado. Geomorphology 294, 87–98. https://doi.org/10.1016/j.geomorph.2017.03.030

Wieczorek, M.E., LaMotte, A.E., 2010. Attributes for NHDPlus Catchments (Version 1.1) for the Conterminous United States: Mean Annual R-factor, 1971-2000. USGS Digit. Data Ser.

Wilkerson, E., Hagan, J.M., Whitman, A.A., 2010. The effectiveness of different buffer widths for protecting water quality and macroinvertebrate and periphyton assemblages of headwater streams in Maine, USA. Can. J. Fish. Aquat. Sci. 67, 177–190. https://doi.org/10.1139/F09-162

Winter, T.C., 2001. The concept of hydrologic landscapes. J. Am. Water Resour. Assoc. 37, 335–349. https://doi.org/10.1111/j.1752-1688.2001.tb00973.x

Wischmeier, W.H., Smith, D.D., 1978. Predicting rainfall erosion losses: A guide to conservation planning. Agric. Handb. 1–58.

Wohl, E., Goode, J.R., 2008. Wood dynamics in headwater streams of the Colorado Rocky Mountains. Water Resour. Res. 44, 1–14. https://doi.org/10.1029/2007WR006522

Wohl, E., Merritts, D.J., 2007. What Is a Natural River? Geogr. Compass 1, 871–900. https://doi.org/doi:10.1111/j.1749-8198.2007.00049.x

Wolman, M.G., Miller, J.P., 1960. Magnitude and Frequency of Forces in Geomorphic Processes. J. Geol. 68, 54–74.

Wondzell, S.M., King, J.G., 2003. Postfire erosional processes in the Pacific Northwest and Rocky Mountain regions. For. Ecol. Manage. 178, 75–87. https://doi.org/10.1016/S0378-1127(03)00054-9

Woods, R., Sivapalan, M., Duncan, M., 1995. Investigating the representative elementary area concept: an approach based on field data. Hydrol. Process. 9, 291–312. https://doi.org/10.1002/hyp.3360090306

Worrell, W.C., Bolding, M.C., Aust, W.M., 2011. Potential Soil Erosion following Skyline Yarding the Appalachian Region of Virginia. South. J. Appl. For. 35, 131–135. https://doi.org/10.1093/sjaf/35.3.131

Young, M.K., Haire, D., Bozek, M.A., 1994. The Effect and Extent of Tie Drives in Streams of Southeastern Wyoming. West. J. Appl. For. 9, 125–130. https://doi.org/10.1093/wjaf/9.4.125

Yu, X.J., Alila, Y., 2019. Nonstationary frequency pairing reveals a highly sensitive peak flow regime to harvesting across a wide range of return periods. For. Ecol. Manage. 444, 187–206. https://doi.org/10.1016/j.foreco.2019.04.008

Yue, S., Pilon, P., Cavadias, G., 2002. Power of the Mann-Kendall and Spearman's rho tests for detecting monotonic trends in hydrological series. J. Hydrol. 259, 254–271. https://doi.org/10.1016/S0022-1694(01)00594-7

Zégre, N., Skaugset, A.E., Som, N.A., McDonnell, J.J., Ganio, L.M., 2010. In lieu of the paired catchment approach: Hydrologic model change detection at the catchment scale. Water Resour. Res. 46, 1–20. https://doi.org/10.1029/2009WR008601

Zenner, E.K., Fauskee, J.T., Berger, A.L., Puettmann, K.J., 2007. Impacts of Skidding Traffic Intensity on Soil Disturbance, Soil Recovery, and Aspen Regeneration in North Central Minnesota. North. J. Appl. For. 24, 177–183. https://doi.org/10.1093/njaf/24.3.177

Zhang, M., Liu, N., Harper, R., Li, Q., Liu, K., Wei, X., Ning, D., Hou, Y., Liu, S., 2017. A global review on hydrological responses to forest change across multiple spatial scales: Importance of scale, climate, forest type and hydrological regime. J. Hydrol. 546, 44–59. https://doi.org/10.1016/j.jhydrol.2016.12.040

Zierholz, C., Prosser, I.P., Fogarty, P.J., Rustomji, P., 2001. In-stream wetlands and their significance for channel filling and the catchment sediment budget, Jugiong Creek, New South Wales. Geomorphology 38, 221–235. https://doi.org/10.1016/S0169-555X(00)00092-1

Zon, R., 1927. Forests and Water in the Light of Scientific Investigation. USDA Forest Service. https://doi.org/10.5962/bhl.title.114941

APPENDIX A: Chapter 2

Notes on Data:

The data were recorded as breakpoint data (Johnson and Dils, 1956) with more frequent stage readings during stormflow, and few readings (i.e., 2 to 4 per day) during baseflow and over the winter when flow often ceases. Because breakpoint data are not recorded at fixed intervals and the timing of flow events varied among catchments, stream stage during stormflow events is highly resolved, yet not at the same date/time stamps among the different stream gages. To add together S4S and S4N, for each recorded data point in each series, and if there was no recorded value at the other gage for that timestep, the two nearest datapoints were used to form a linear interpolation, and the interpolated value was added to the actual value for the other gage to attain a total streamflow record for S4.

There was one water year for which S4N did not have data (1984). However, there was a full record at the S4S gage. The annual maximum flow for S4 in this year was attained through interpolation within least-squares linear regressions between the annual maximum flow on S4 and the annual maximum flow on just S4S in the defined stationary block associated with ANCOVA analyses used in previous work (Table 1; Sebestyen et al., 2011b). The date of the annual maximum flow was also missing. I filled in the date of the annual maximum flow for S4 in the missing year with the date of the annual maximum flow on the control watershed S5. Thus, any significant treatment effects on the relationship between control and treatment watershed peak flow timing will be a conservative estimate, and not due to assumptions about years for which there is no data.

Some years, the highest peak of the year from the breakpoint discharge record was due to weir replacement (i.e., a dam was built upstream during low flow, the weir replaced, then dam breached releasing impounded flow). These peaks were identified using the data completeness report from (Verry et al., 2018), and removed. Thus, all annual maximum peaks used were due to watersheds processing of precipitation or snowmelt inputs.

Special thanks to Stephen Sebestyen, USDA Forest Service, for much of this section on the breakpoint data.

Details on Prior Distributions Used

S4:
For all other hyper-parameters, there is relatively little prior knowledge, so most of their prior distributions were set to generic normal distributions centered on 0 with a standard deviation of 10. The exceptions were the mature aspen scale parameter ($\sigma_{mature\ aspen}$), which must be greater than 0 and was thus represented as a uniform distribution between 0 and 5 for its prior distribution, and the stationary shape parameter (ξ), which based on physically plausible limits (discussed above in *2.3.3: Choice of Distribution*) was represented as a uniform distribution between 0 and 1 for its prior distribution.

S6:
For nearly all other hyper-parameters, prior distributions were set as generic normal distribution centered on 0 with a standard deviation of 1. A smaller prior standard deviation was used compared to the S4/S5 experiment (for which 10 was used) because S2/S6 are smaller catchments than S4/S5, so are more likely to have smaller location and scale parameters (mean annual maximum flow on S2 = 0.86 cfs while for S5 = 2.43 cfs). As with the S4/S5 experiment, exceptions were the pretreatment scale parameter (σ_{pre}), which must be greater than 0 and was

thus set to a prior uniform distribution over 0 to 5, and the shape parameter, which was set to the physically plausible prior uniform distribution over 0 to 1.
Figures:

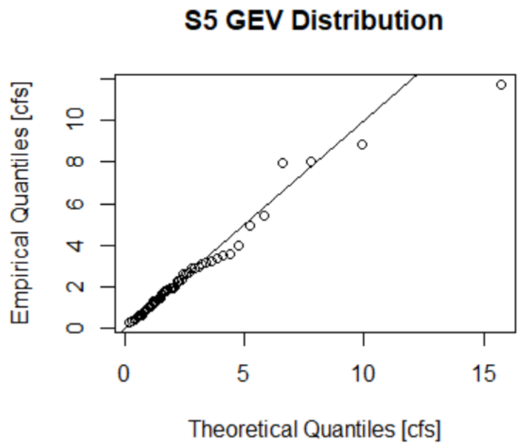

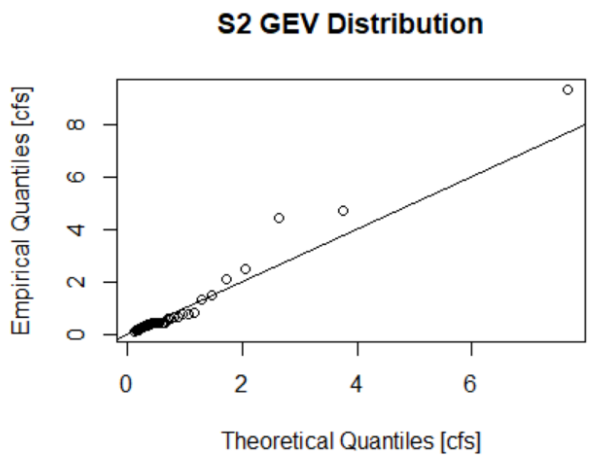

Figure A1: QQ-plots of the observed versus theoretical values for the GEV for both control watersheds, along with the posterior predictive goodness-of-fit test based on them, support the GEV as sufficiently descriptive of the annual maximum series' on these watersheds. Shown with 1:1 lines.

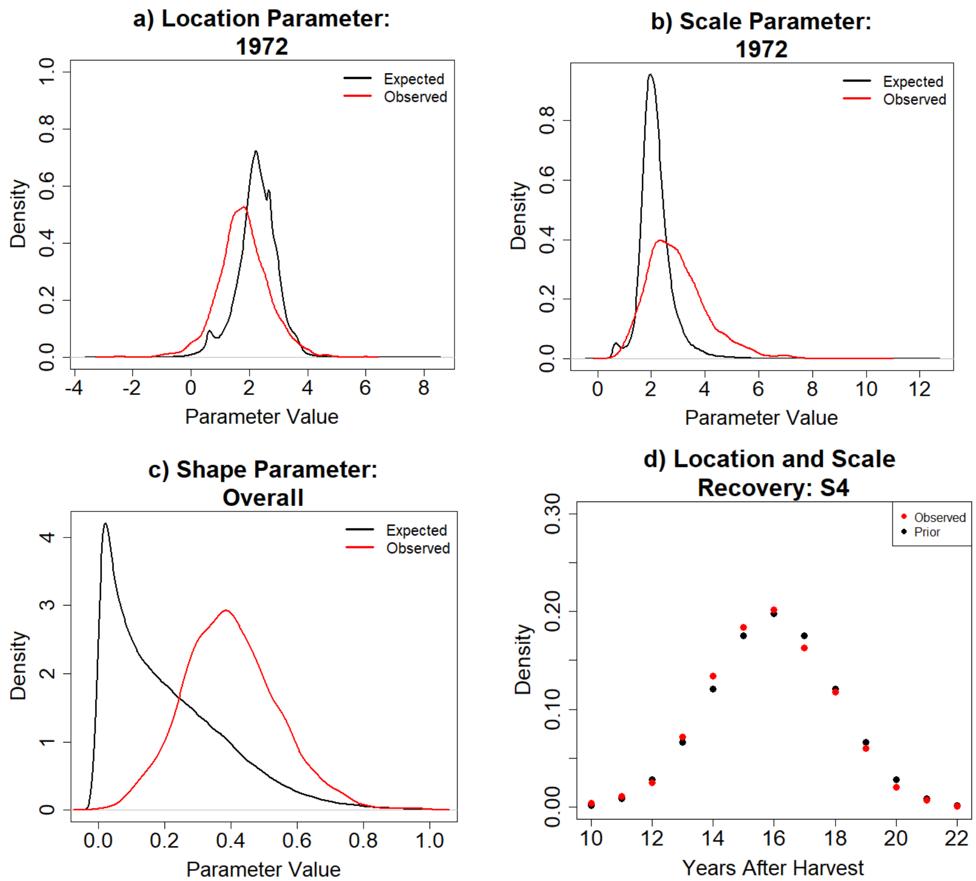

Figure A2: a) Location parameter in first year of upland clearcut for S4, compared to the expected value derived from application of the nonstationary model to the expected series' derived from the calibration regressions. b) Scale parameter in first year of upland clearcut for S4. c) Shape parameter for the observed versus expected model fits. d) Recovery year of the location and scale parameters to pretreatment values from the observed series, compared to the moderately informative prior distribution given this variable. No recovery was inferred of the shape parameter, as it was held constant within each model iteration.

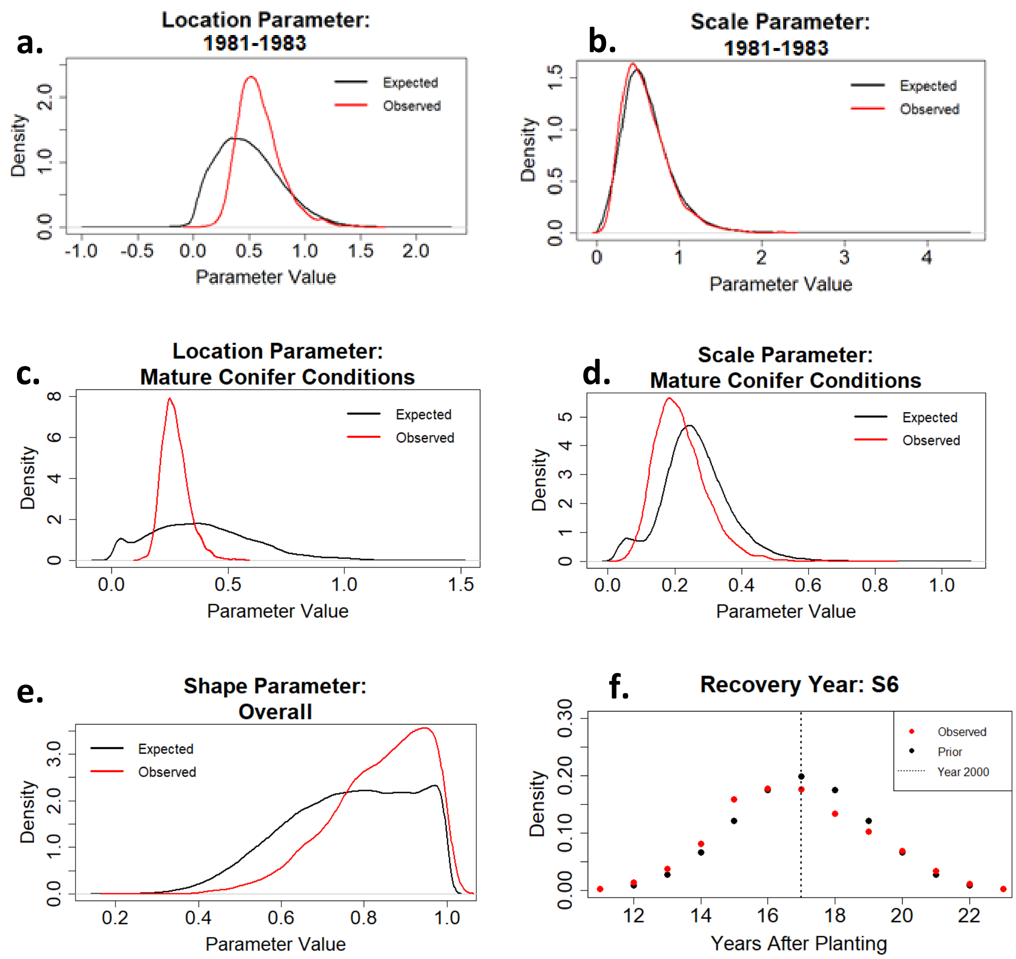

Figure A3: None of the parameters are significantly different between treatment and expected conditions. a) Location parameter when the uplands of S6 had just been clearcut and were grazed, compared to the expected value derived from application of the nonstationary model to the expected series' derived from the calibration regressions. There is a slight rightward shift in location parameter. b) Scale parameter when the uplands of S6 had just been clearcut and were grazed. There is no shift. c) Location parameter for the closed-canopy conifer forest, compared to the expected value which corresponds to the mature aspen forest. There is a left-ward shift of the mean but no significance. d) Scale parameter after conifer canopy closure. There is a non-significant leftward shift. e) Shape parameter for the observed versus expected model fits. Note that the shape parameter was held stationary. f) Recovery year of the location and scale parameters to a new stationary state corresponding to a closed-canopy conifer forest from the observed series, compared to the moderately informative prior distribution given this variable. Note that the posterior for the recovery year is very similar to the prior.

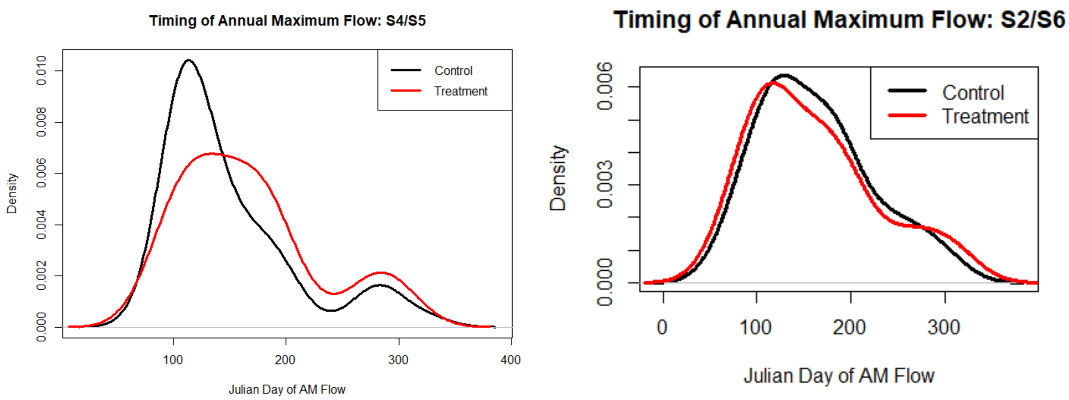

Figure A4: Density plots of the timing of the annual maximum flow for the control and treatment watersheds. Note that the S2/S6 density plots indicate a pretty closely coupled distribution of peak flow timing, whereas the S4/S5 plot indicates that for the duration of the study, there were more annual maximum flows later in the year on the treated (S4) watershed. This supports the decoupling analysis that found a more pronounced decoupling on the S4/S5 pair.

Tables

Table A1: Bayesian p-values for qq-goodness-of-fit posterior predictive checks.

Distribution	S2	S5
Gumbel	0.000	0.015
Generalized Extreme Value	0.580	0.591
Gamma	0.005	0.104
Generalized Gamma	0.046	0.369
Log-Normal	0.073	0.584

APPENDIX B: Chapter 3

Figures

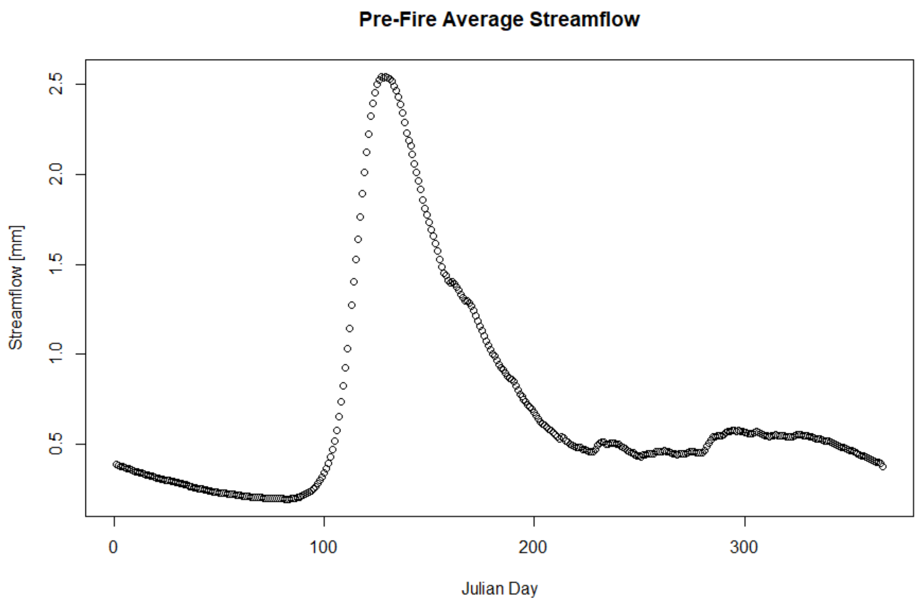

Figure B1: Average calendar-year streamflow hydrograph.

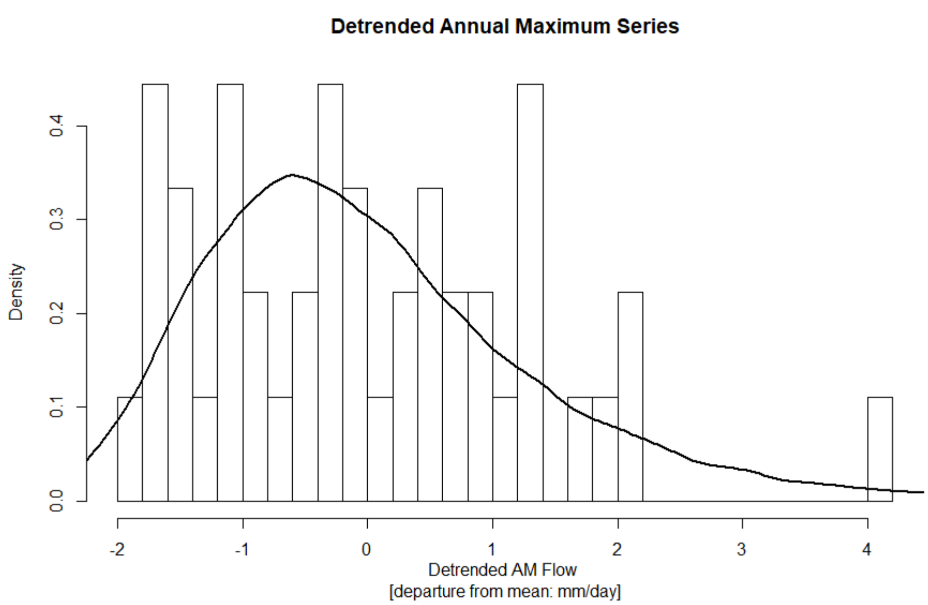

Figure B2: Annual maximum ***detrended*** streamflow, with a stationary Gumbel distribution, showing adequacy of fit for the Gumbel distribution describing annual maximum flows.

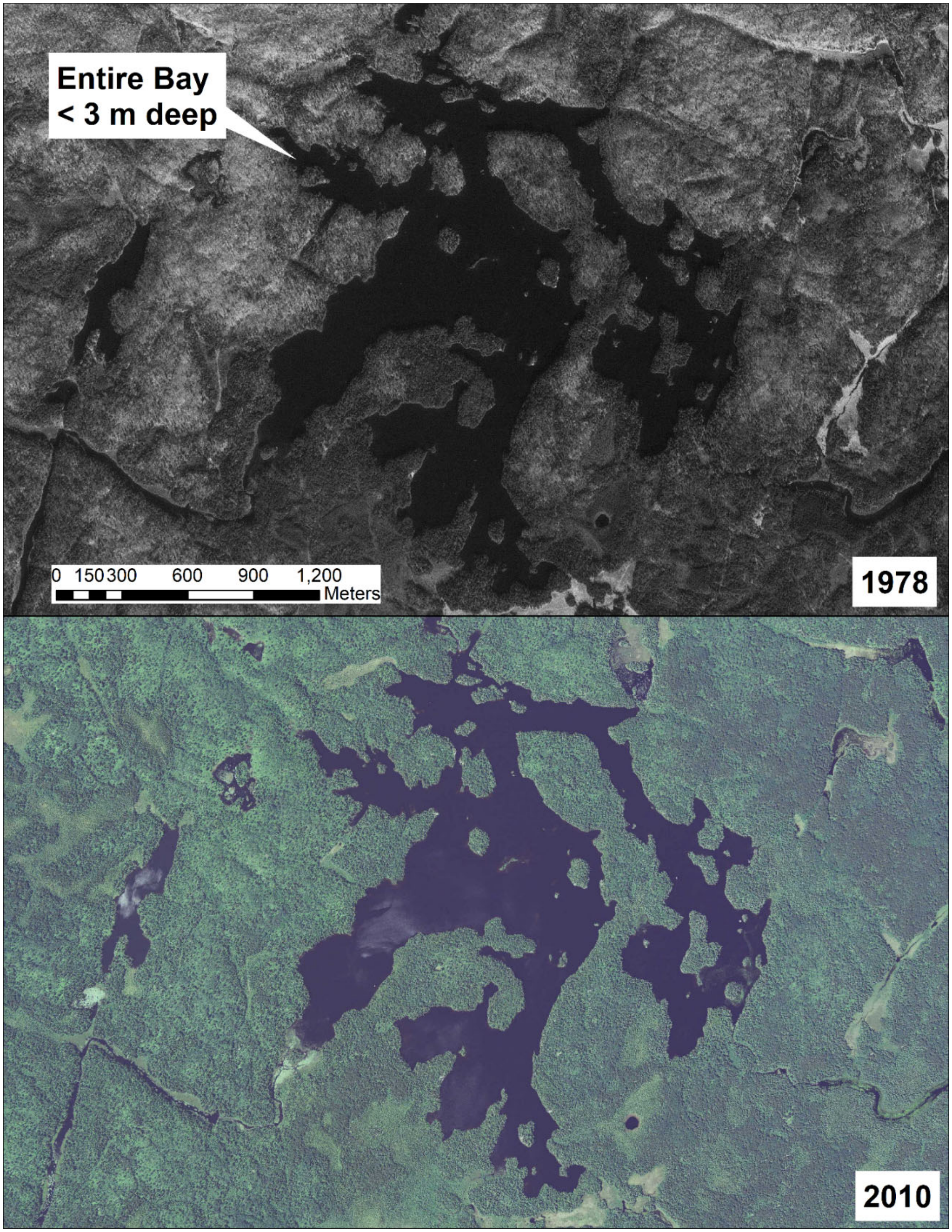

Figure B3: Aerial imagery of Lake Polly, a shallow lake in the Upper Kawishiwi catchment, with surrounding wetlands, indicating no drastic decline in catchment storage in the intervening time period.

Tables

Table B1: Results of the multiple location (μ) and scale (σ) models fit to the pretreatment annual maximum flow (1967-2011). Stationary μ and σ are listed as simply those parameters; in nonstationary models they are fit as linear responses to varying AMO index in water year *i* (AMO_i) and/or winter precipitation in water year *i* (P_i). The selected model is shown with a * in the degree-of-belief column.

Location	Scale	Degree-Of-Belief
μ	σ	0
$\mu(AMO_i, P_i)$	$\sigma(AMO_i, P_i)$	0.155
$\mu(AMO_i, P_i)$	$\sigma(AMO_i)$	0.162
$\mu(AMO_i, P_i)$	$\sigma(P_i)$	0.318
$\mu(AMO_i, P_i)$	σ	0.339*
$\mu(P_i)$	σ	0.006
$\mu(P_i)$	$\sigma(P_i)$	0.004
$\mu(P_i)$	$\sigma(AMO_i)$	0.009
$\mu(P_i)$	$\sigma(AMO_i, P_i)$	0.007
μ	$\sigma(AMO_i, P_i)$	0
μ	$\sigma(AMO_i)$	0
μ	$\sigma(P_i)$	0
$\mu(AMO_i)$	σ	0
$\mu(AMO_i)$	$\sigma(AMO_i)$	0
$\mu(AMO_i)$	$\sigma(P_i)$	0
$\mu(AMO_i)$	$\sigma(AMO_i, P_i)$	0